UTS UNIVERSITY OF TECHNOLOGY SYDNEY

Casting a light on diatom silicification in changing oceans

by Billy FitzGerald-Lowry

Thesis submitted in fulfilment of the requirements for the degree of

Doctor of Philosophy

under the supervision of Assoc. Prof. Katherina Petrou,

Dr Daniel Aagren Nielsen and Prof. Jonathan Webb

University of Technology Sydney
Faculty of Science

August 2024

Certificate of original authorship

I, Billy FitzGerald-Lowry declare that this thesis is submitted in fulfilment of the requirements for the award of Doctor of Philosophy, in the School of Life Science at the University of Technology Sydney.

This thesis is wholly my own work unless otherwise referenced or acknowledged. In addition, I certify that all information sources and literature used are indicated in the thesis.

This document has not been submitted for qualifications at any other academic institution.

This research is supported by the Australian Government Research Training Program.

Signature of Student:

Production Note:
Signature removed
prior to publication.

Date: 27/08/2024

The quote that took me on this journey.

"Give me a half tanker of iron, and I will give you an ice age."

- John Martin, (1988) at Woods Hole

And the one that got me through.

"If you can't have a laugh, what can you have?"

- Johnny Birse, (2010) on the school playground

Thesis Acknowledgement

Words on a page do not feel sufficient for the love and appreciation I have for the people who have helped me get to this point.

To Katherina, thank you for giving me this opportunity and for changing my life. Your enthusiasm for biology is inspiring and has always given me a boost when mine falls short. Your support, guidance and patience has made this experience something I will look back on with joy and I will forever be grateful for helping me see parts of the world I never thought possible. To Daniel, your ability to turn chaos into calm (sometimes diatom related, often my thoughts) has been invaluable. I really appreciate all your help over the years. The strict 'beers at 5pm' rule on Heron Island ready to watch the sunset are some of my fondest memories of this journey. And to the little man, Darwin. It has been a joy to have you around, thank you for brightening up the lab whenever you come by.

A massive thank you to Helen Price. You are an underappreciated superstar and have always had solutions to my endless stream of questions. You deserve a lifetime supply of Joe's ice cream. To Amy, thank you for all your help with microscopy in such a short period of time. Without you, I would still be on the wrong focal plane.

To the people at CSIRO and IMOS, for making two research cruises on RV Investigator possible; Elizabeth, Max and Ruth, thank you so much for your help. I have seen Albatross and aurora australis because of you.

To the titrator. I have loved you and loathed you, but you have given me some great research, so thank you, you POS.

The Petrou Lab family – my home away from home. Georgia, I did not think that letting a lost girl into the building would give me a friend for life. You have been a rock on my hardest days, the laughter needed at 1am in the fish lab and my favourite Mr Chen's dining partner. Certainly, without you I would have given up and quit. I am forever grateful for your friendship and motivation. You mean more to me than I can say. Thanks also to Scott and Kelly for making me feel welcome in the Thompson family. Alyson, thank you for making 36 hour experiments survivable, talking diatom silicification at all hours normal and this journey bearable. There have been many ups and downs for both of us

throughout our time, yet you have persevered, and I am so excited for you to finish soon also! To Bec, thank you so much for saying it how it is and being real. You are an incredible person and an amazing researcher. I am looking forward to seeing where your career goes, even if the photos make me incredibly jealous. Holly, your enthusiasm and ability to make a tough day brighter has been lovely addition. Puppy photos, Vietnamese coffee and heavy metal have been a welcome reprieve. You are about to embark on this journey for yourself and will absolutely ace it – call on me any time you need it. And Lily, the Foram queen, thank you for letting me be a helping hand in your research, I snorkelled on the Great Barrier Reef because of you.

To my dear friends Nine and Matthias. Thank you for your support, coffee breaks, morning surfs and advice. We shall soon be in Norway celebrating and I appreciate you both very much.

I would not be here without the teachers and academics that fostered a deep love of science and biology. Mr Rae and Mr Heffernan for sparking my interest, Mr Rowan for getting me through some tough periods with tough love and Gavin Foster, Mark Moore and Andy Milton for helping me try my hand at research during my Masters.

To my nearest and dearest trio. Jock, you have listened to all my unhinged ideas and seen me at my complete worst yet still drag me for morning swims and make me dinner when I am incapable of being human. Jack, we are different in so many ways, but we complement each other perfectly. You are the nearest thing I have to a brother and your calmness when it matters most is amazing. And Dylan, I cannot thank you enough for making me feel at home in Sydney. Inviting me to Sunday football has kept my mental on track.

To Saja and Maisha, the unsung heroes of this PhD. I am not sure where I would be without you two. Thank you so much.

To my family; Mad, John, Sam, Luke, Janet, Jackie and Sue. Thank you for helping me become the person I am today. In no uncertain terms you have helped me get to where I am, and this PhD is possible because of you. To my mum - I will be eternally grateful for everything you do for me, you have worked so hard so that I can have it easy. You motivate me in moments of self-doubt and your belief in me has been a constant source of strength, and I owe so much of this accomplishment to you. Thank you forever.

To Nana and Luke, my number one fans, we have come a long way from times tables in the living room. Thank you for all your support along the way. To Heather, your calmness and support will forever be appreciated. And to my dad. With a football analogy for everything, we have reached the promised land. Thank you for all the support, for instilling a sense of travel and thinking rationally when I am haywire. I know your father would be so proud of you for helping me achieve all my dreams.

And lastly, I would like to dedicate this to Grandad Peach. Thank you for making wildlife and horticulture a part of my life for as long as I can remember. You let me eat my bodyweight in raspberries and anything else I could get my hands on. You were always intrigued by my work, and I wish you were here to see this. This is for you.

Table of Contents

List of Tables

List of Figures

Abstract

Diatoms are ubiquitous, microscopic photoautotrophs. These hugely diverse phytoplankton dominate marine primary productivity, fixing roughly 40% of the global organic carbon in the oceans annually. This drawdown of carbon dioxide from the atmosphere makes them important in both marine food webs and the biogeochemical cycling of nutrients. What sets them apart from their counterparts, is their requirement for silicic acid, which is deposited to their cell walls, known as frustules. This armour-like structure is thought to have many purposes; defence against predation, photoprotection from light inhibition and UV, photo-focussing of light as a means of transfer to photosystems and buoyancy regulation in the water column. The latter of these is important in the context of marine silicon cycling and carbon sequestration due to their dense frustule structure aiding sinking to the deep ocean. The rate of deposition of silica to the frustule (silicification) is susceptible to environmental influence, therefore any shifts in marine ecosystems due to climate change are likely to have an impact. Studies of warming and stratification influence on diatom silicification are limited, and the influence of ocean acidification (OA) has only just started to be investigated.

The work within this thesis addresses how silicification rates of whole communities and diatom isolates will be affected by changing ocean conditions. **Chapter 2** investigated how the biomolecular composition and silicification rates of *Phaeodactylum tricornutum* and *Thalassiosira weissflogii* change under high and low light (a proxy for mixed layer depth shoaling) at modern and future pCO_2 concentrations. Treatment conditions elicited changes in lipid content for both species however *P. tricornutum* exhibited no significant silicification response under any treatment due to its ability to

grow without silicifying. A significant effect of pCO_2 on silicification rate was however found in *T. weissflogii* under high irradiance, with links to improved photochemical efficiency. It was proposed that increased photosynthetic activity under high pCO_2 may alleviate the need for photoprotection from increased frustule production therefore suggesting a complex energy exchange linking growth, photosynthesis and silica dynamics to optimise cell homeostasis.

To assess whether the reduction in silicification rate due to OA was common across other diatom species, we measured and compared physiological responses of diatom communities exposed to two pH levels (representing current and projected future ocean conditions) (**Chapter 3**). We found that although two diatom species increased cell-specific silicification at low pH, with no effect detected in the other species, OA reduced total diatom biomass by 33% and species diversity by 25% in the natural community. These data suggest that OA may hinder growth rather than directly altering of silicification rate. By undertaking single-cell analysis of the whole community, we were able to distinguish species specific responses and a broad range of phenotypic plasticity amongst diatoms.

Species specific plasticity was also evident within Southern Ocean diatoms when exposed to depth dependent irradiance (**Chapter 4**). Assessing how the interactions of light and water column position impact silicification, we observed non uniform silicification responses to irradiance, suggesting potential light adaptation and energy capture potential differences amongst species which could be used to support silica incorporation. Silicification per cell area was greatest at the surface and declined from 100 to 27 µmol photons m^{-2} s^{-1} when pooling all area specific silicification data, but no change below 27 µmol photons m^{-2} s^{-1} suggesting a minimal light requirement for net

positive silicification. These findings show that diatom silicification at the Southern Ocean Time Series (SOTS) is modulated by light under non-deplete nutrient conditions. With future ocean conditions expected to be warmer and more stratified, causing greater residence times in saturating irradiances, the increase in light may provide energy for greater silicification. It is unclear however if cumulative climate change factors, such as saturating light and OA, will work synergistically to reduce overall diatom fitness.

Taken together, these findings present novel insight into how climate change induced perturbations, specifically light and pCO_2, will impact diatom silicification. The high level of phenotypic plasticity and variability in species specific responses highlights the need for conducting single cell analysis alongside bulk assessments of whole communities. By combining these two methods, we are likely to gain a clearer understanding of how diatoms in changing ocean systems will fair, uncovering both pronounced and more intricate nuanced shifts. The varied responses in silica production presented herein indicate a level of adaptability within diatoms to changing ocean conditions, although the rate of change necessary for survival is yet to be determined.

Chapter 1: General introduction and thesis outline

Introduction

Marine phytoplankton

Phytoplankton, derived from the Greek words *phyton* (plant) and *planktos* (to wander or drift) are an extremely diverse group of microorganisms, often placed into five main functional groups (cyanobacteria, diatoms, coccolithophores, dinoflagellates and green algae). Spanning seven orders of magnitude in cell volume (Cermeño *et al*., 2006) these microalgae exhibit a vast range of shapes (Ryabov *et al*., 2021), elemental requirements (Finkel *et al*., 2010), chemical functions (Ianora *et al*., 2011) and survival strategies (Margalef, 1978). This functional and genetic diversity has afforded them a high degree of adaptability (Malviya *et al*., 2016) and consequently phytoplankton are ubiquitous in our global oceans (Reynolds, 2006). Although they are found in all ocean systems, their distribution is not uniform (**Figure 1.1**) preferentially inhabiting coastal shelf regions and high latitudes (Bopp *et al*., 2005). The biogeography of these organisms is also seasonally dependent, with spring blooms hosting a rapid proliferation of biomass once optimal conditions arise (Brzezinski *et al*., 2001; Kopczyńska *et al*., 2007). Deep winter mixing brings nutrients to the surface (Rigby *et al*., 2020) in time for the arriving increasing temperature and light regimes of Spring (Rumyantseva *et al*., 2019). Bloom formation is often a series of sequential blooms, showing a succession of phytoplankton groups – diatoms can grow rapidly but become limited by silicate, allowing dinoflagellates to succeed them. As nutrient depletion arises (usually nitrogen), deterioration of larger species populations occurs and nanoplankton begin to dominate, able to sustain low but

constant biomass due to their large surface area to volume ratio (Mann & Lazier, 2005; Winder & Cloern, 2010).

Although present throughout the world's oceans, the biogeography of the key functional groups is unique due to their divergent physiological properties and requirements. Diatoms are usually found in cold waters, generally following Bergmann's rule (Bergmann, 1848) and James' rule (James, 1970) which suggest larger species tend to be found at higher latitudes and therefore colder temperatures and intra-specifically the body size of a species will be smaller in warmer temperatures. They also dominate cold core eddies and upwelling regions in coastal system, entraining a cascade of trophic productivity.

Cyanobacteria are often found to dominate tropical, oligotrophic warm waters, preferring high irradiance and more stratified water columns (Rajaneesh *et al.*, 2020). Two dominant cyanobacterial groups are *Prochlorococcus*, the smallest and most abundant photosynthetic cell on the planet (Partensky *et al.*, 1999_a) and *Synechococcus*. There is a general overlap of geographical distribution between the two species between 40°S and 40°N (Partensky *et al.*, 1999_a) with differences observed in *Synechococcus* extending further into polar and high nutrient regions (Partensky *et al.*, 1999_b; Jiao *et al.,* 2005) and *Prochlorococcus* not found in waters colder than 15 °C (Johnson *et al.*, 2006). *Prochlorococcus* is usually present down to 150m, whilst *Synechococcus* does not extend as far in the water column (Flombaum *et al.*, 2013). Together, these two species account for more than 20% of ocean productivity. The other key group within the cyanobacteria are the diazotrophes, including *Trichodesmium*. Diazotrophs are able to fix atmospheric nitrogen into ammonium and utilise dissolved organic carbon release from other species providing symbiotic relationships between this group and/or host

species (Carpenter & Foster, 2002). Recent research however has found a resurgence in cyanobacteria bloom distribution, frequency and duration (Paul, 2008; Paerl *et al*., 2018) due to eutrophication and the freshwater-marine continuum, transporting blooms from riverways to oceans (Zepernick *et al*., 2022).

Dinoflagellates are also a highly abundant and diverse group, with estimates of over 2000 species in marine and freshwater environments (Gómez, 2012). Whilst half the group are photosynthetic, the others are heterotrophic, either free-living or endosymbiotic inhabiting organisms such as corals (Stat *et al*., 2008). Distinct from other phytoplankton groups, these organisms are often associated with toxic algal blooms such as red tides (Lin *et al*., 1981; Grzebyk *et al*., 1997), can produce bioluminescence (Valiadi & Iglesias-Rodriguez, 2013) and persist for long periods in the water column in cyst form (Wall & Dale, 1968; Bravo & Figueroa, 2014). Dinoflagellate theca production can aid in sinking and contribute to the biological pump (Alldredge *et al*., 1998).

Coccolithophores are found in greatest abundances in temperate oceans (Balch *et al*., 2016; Winter *et al*., 2014). They are a key group of calcifying haptophytes, playing a key role in the ocean carbonate pump. The threat of ocean acidification on this group of calcifying organisms, whereby the higher *p*CO2 environment dissolves the coccoliths of coccolithophores by decreasing the aragonite and calcite saturation state (Yamamoto-Kawai *et al*., 2009). These organisms form seasonal phenomena of the great calcite belt, an elevated particulate inorganic carbon (PIC) feature (Smith *et al*., 2017) spanning the major Southern Ocean circumpolar front between 40-60ºS. Seasonal fluctuations of conditions determine diatom or coccolithophore dominance. Usually, diatoms bloom first, utilising available nutrients post winter deep-mixing and irradiance increase (Salter *et al*., 2007) however are eventually limited by silicate availability (and iron) allowing

coccolithophore biomass to increase in post-spring bloom conditions (Bathmann *et al*., 1997; Balch *et al*., 2014). How these dynamics will shift in future ocean conditions is still unclear.

Impressively, phytoplankton make up less than one percent of the earth's photosynthetic biomass yet perform fifty percent of the world's primary production (Field *et al*., 1998). These photoautotrophs form the foundation of many marine food webs and play an important role in biogeochemical cycling whereby phytoplankton derived carbon and other elements are either consumed by higher trophic levels (Fry & Wainright, 1991), remineralised in the water column, or exported to the deep ocean (Tréguer *et al*., 2018). These processes form the basis of the biological carbon pump. Briefly, phytoplankton synthesise organic and inorganic carbon through photosynthesis in sunlit waters (Colman & Rotatore, 1995; Morel *et al*., 2002) and produce carbohydrates, lipids and proteins for cellular function. Once the carbon is fixed, phytoplankton may remain at the surface, being consumed and the carbon (and other nutrients) recycled to form a regenerative loop.

Some particles will move into a second phase and sink through the photic zone to the deep ocean. As these carbon-rich particles sink, they often aggregate, which greatly increases the sinking rate (Alldredge & Gotschalk, 1989; Riebesell, 1989). Some particles will be remineralised by the microbial loop, restoring carbon and other nutrients to the water column. This downward movement transports carbon away from the surface and, ultimately, sequesters it in the deep ocean or sediments for extended periods (Tréguer *et al*., 2018). This process not only helps regulate atmospheric carbon dioxide levels but also influences global climate patterns and ocean chemistry. The efficiency and functioning of the biological carbon pump are affected by factors such as nutrient

availability, water temperature and ocean circulation, making it a dynamic and vital component of Earth's carbon cycle.

As the primary producers of the sea, all phytoplankton are key players in ocean carbon cycling, however, some groups of phytoplankton play large roles in other nutrient cycles too. Diazotrophic cyanobacteria are involved in nitrogen (N) cycling, creating bioavailable nitrogen through N-fixation (Capone *et al.,* 2005). Heterotrophic dinoflagellates have particularly high phosphorus (P) requirements, influencing phosphorus cycles and the sulphur (S) cycle through the production of dimethylsulfoniopropionate (DMSP). Biomineralizing phytoplankton, such as calcifying coccolithophores drive much of the carbonate pump, whilst diatoms regulate the silica (Si) cycle due to their biomineralisation of silicic acid into siliceous cell walls (Sumper & Brunner, 2008). Put together, these organisms, are essential for life on earth to exist. Environmental and/or climate induced shifts in community composition will have far reaching impacts on marine food webs, nutrient transfer, and eventual export (Sanders *et al*., 2014; Nowicki *et al*., 2022).

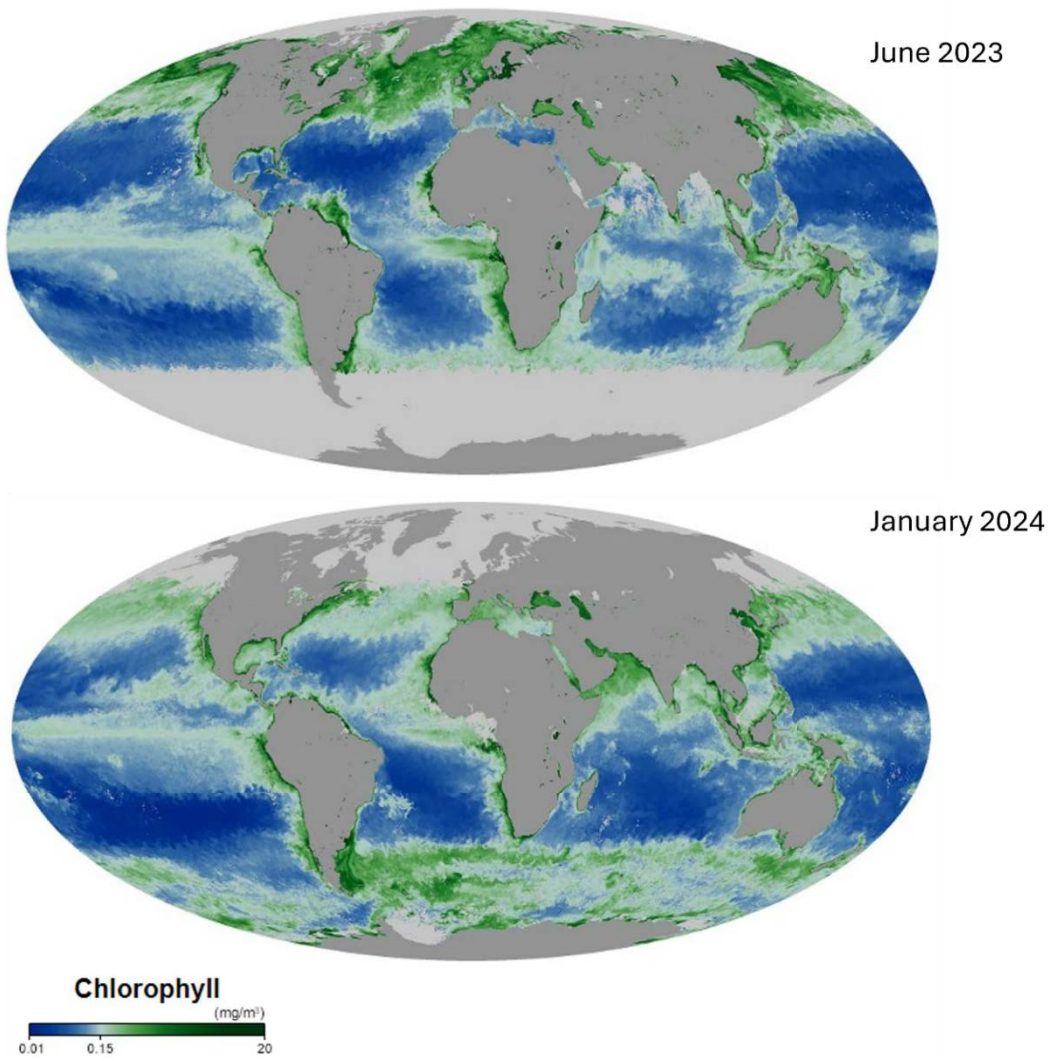

Figure 1. 1 Global distribution of chlorophyll *a* (mg mL^{-3}) in Northern (A) and Southern hemisphere late spring/early summer (B). Darker, blue colours indicate low biomass, with greens indicating high biomass. Dark grey areas show landmass, whilst oceanographic grey depicts areas data could not be collected from due to sea ice, clouds or polar darkness. Data taken from the Moderate Resolution Imaging Spectroradiometer (MODIS), NASA.

Diatom diversity and biogeography

Diatoms (Bacillariophyta) contribute up to 40% of total phytoplankton primary productivity (Nelson *et al.*, 1995). This polyphyletic group of protists are thought to comprise of at least 30,000 extant species, potentially rising to 200,000 (Mann & Vanormelingen, 2013), span three orders of magnitude in size (Hillebrand *et al.*, 1999) and are found in both freshwater and marine environments (Litchman *et al.*, 2009; Nakov

et al., 2019). Their diversity is further highlighted by their highly variable, yet organised morphology (**Figure 1.2**).

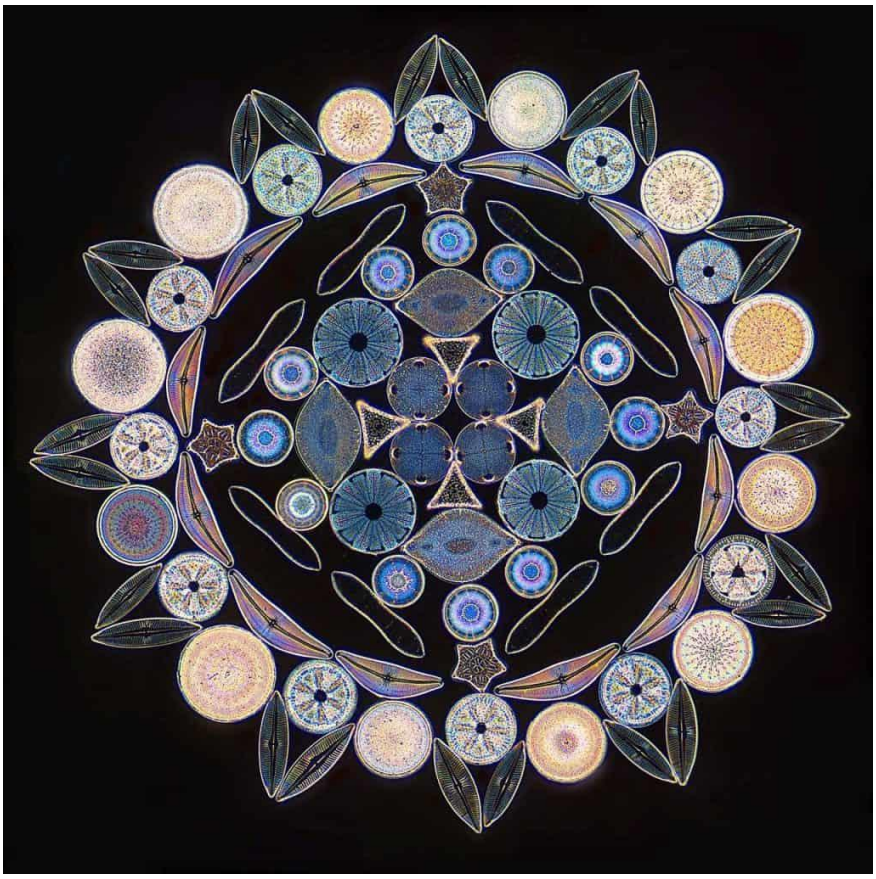

Figure 1. 2 Diatom arrangement by Klaus Kemp shows the diversity of shapes and sizes. "Algae in glass houses."

Diatoms abundance is often determined by nutrient availability, temperature and light exposure (Heil *et al.*, 2007; Edwards *et al.*, 2016). They often found to dominate coastal shelf regions and polar waters (Armbrust, 2009; Malviya *et al.*, 2016; Karlusich *et al.*, 2020), areas which are governed by strong wind patterns, driving ocean currents that bring nutrient rich waters from the deep ocean, through the thermohaline circulation and upwell near continental shelves (García-Reyes & Largier, 2010; Boé *et al.*, 2011; Closset *et al.*, 2021). The composition of diatom communities in these regions are often nutrient dependent (Falkowski *et al.*, 1998; Hoffmann *et al.*, 2008) with different strategies employed for times of prolonged limitation or pulsed inputs (Abelmann *et al.*, 2006; Boyd

et al., 2017). Species in polar regions for example must employ iron (Fe) storage strategies due to iron concentrations being a limiting factor for growth (Timmermans *et al.*, 2001). Aeolian input of iron rich dust is often a precursor for diatom prosperity (Martin & Gordon, 1988; Boyd *et al*., 2000) therefore the Southern Ocean surrounding Antarctica and parts of the North and Equatorial Pacific Ocean are often known as an HNLC (high nitrate, low chlorophyll) regions (Boyd *et al*., 2007). Despite this, there are still healthy diatom populations due to employment of two main strategies for iron storage: the protein ferratin and vacuole storage mechanisms. Genera such as *Thalassiosira* and *Chaetoceros* employ vacuolar strategies whilst *Pseudo-nitzschia* employ greater ferratin accumulation, with the latter group showing comparatively greater iron storage under Fe limitation (Cohen *et al*., 2018). Ferratin appears mostly absent in centric diatoms including some *Thalassiosira* and *Chaetoceros* species, suggesting bloom forming species able to utilise ferratin may be provided an advantage in low Fe regions, and morphological differences governing nutrient utilisation (Kustka *et* al., 2007; Marchetti *et al*., 2009). Diatoms also have a basal requirement for silica, used in formation of siliceous cell walls (De Tommasi *et al*., 2017). Their unique silica-based architecture (frustules) makes them crucial in marine silicon cycling (Yool & Tyrell, 2003; Struyf *et al*., 2009) as the increased density aids their sinking, also making them strong contributors to ocean carbon sequestration (Buesseler, 1998; Dugdale and Wilkerson, 1998; Tréguer *et al*., 2018). Changes to these processes in future oceans may have impacts at the cellular level and whole ocean systems.

Diatom Morphology

Through the acquisition of silicic acid ($Si(OH)_4$), diatoms produce species-specific amorphous silica frustules (Gordon *et al.*, 2009). These frustules, or cell walls, are provide mechanical, optical, and fluido-dynamical functionalities (De Tommasi *et al.*, 2017) and their porous nature allows for the influx and efflux of nutrients from the surrounding environment (Hale & Mitchel, 2001; Losic *et al.*, 2006). The three-dimensional (3D) construct of frustules is also thought to aid physical interactions with the environment (Kopanska *et al.,* 2014*;* Su *et al.*, 2018) such as adhering to smooth surfaces important for species that live and reproduce on surfaces (De Tommasi *et al.*, 2017; Rogato & De Tommasi, 2020). There is also evidence to suggest frustules play important roles in light absorption, carrying out light focussing and photo-selective/protective functions (Fuhrmann *et al.*, 2004; Noyes *et al.*, 2008; Goessling *et al.*, 2019). The largest diatom species, often cylindrical, can range from 2-5 mm down to smaller, fast growing bloom forming species ranging from 2-50 µm (Falkowski & Knoll, 2007; Armbrust, 2009). There is also considerable diversity in the morphology of diatom frustules, with varying scale of features and patterns across the surface. Structural designs however show a distinct commonality within both main classes of diatoms, centric and pennate (**Figure 1.3**). Both frustule morphologies are assembled similar to a petri dish, with two valves overlapping top and bottom, with curved, stacked components on the side known as girdle bands (gbs). The larger epitheca sits atop the smaller hypotheca with gbs providing overlap of the two thecae (**Figure 1.3**). The distinction between the two groups is their difference in symmetry, with centric diatoms possessing radial symmetry, whilst pennate diatoms have bilateral symmetry (Round *et al.*, 1990). Evolutionary timelines show centric diatoms developed first, with bipolar and

multipolar variants developing subsequently, followed by araphid and raphid pennates (Armbrust, 2009). The possession of a raphe is thought to be an elongated slit for mucilage secretion, aiding these diatoms to adhere and glide across surfaces (Pickett-Heaps, 1990).

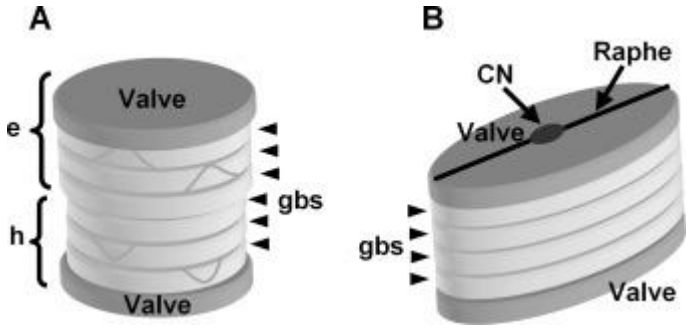

Figure 1. 3 Schematic of the morphological differences between the two major groups. Centric diatom (A) frustule structure displays the epitheca (e) and hypotheca (h) overlapping one another through girdle bands (gbs) extending between the two thecae. Centric diatoms present radial symmetry whilst pennate diatoms (B), also possessing overlapping girdle bands (gbs), are characterised by bilateral symmetry. Some species of these elongated diatoms possess a fissure running the length of the cell (raphe) originating from a central node (CN). Schematic adapted from Hildebrand & Lerch (2015).

Frustule formation plays a key role in diatom reproduction. During asexual reproduction, mother cells undergo cytokinesis whereby the cytoplasm is pinched in two at the cleavage furrow (Pickett-Heaps, 1998) (**Figure 1.4**). Two daughter cells are then formed within the mother cell each forming a new valve. The valves and girdle bands of the daughter cells are produced in the silica deposition vesicle (SDV). The valves constructed in the SDV will form part of the daughter cell's hypotheca whilst the mother's frustule will form the new cell epitheca. Once formed, the new valves are exocytosed to form the new frustule (Pickett-Heaps, 1998). As this process is both energy expensive and results in size reduction for the mother cell, diatoms will extend their girdle width in preparation for exocytosis of the daughter cell (de Haan *et al.*, 2023). As cells continue to reduce in size with every division, eventually, sexual reproduction must occur to restore cell size (Hense & Beckmann, 2015). There is large diversity in

reproductive cycles and strategies amongst diatoms, making it difficult to fit a one-size process. Possible reasons as to why more is not known about the different life cycle strategies are high generation numbers and therefore long-life cycle durations (Mann, 1988), a short time-scale with which to observe division, on the scale of hours and problems identifying the sexual stage (Koester *et* al., 2007; Mann, 2011), need to observe many of these stages in the natural environment. This complexity highlights the need for more advanced methodologies and long-term studies to fully understand diatom reproductive strategies.

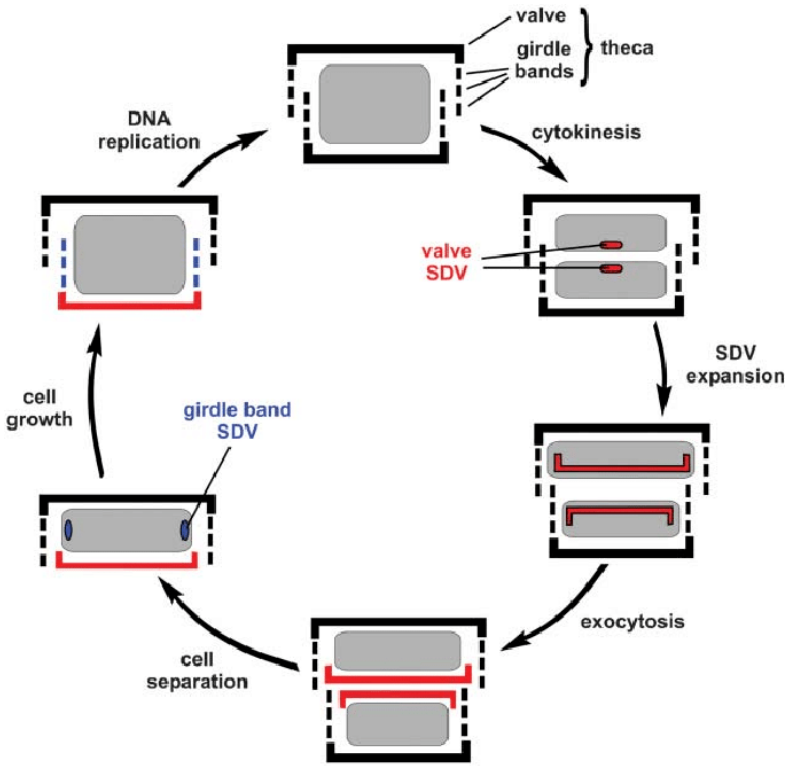

Figure 1. 4 Cross-sectional schematic of diatom cytokinesis. Silica frustule of the mother cell is depicted in black, the new frustule of the daughter cell in red and the girdle bands in blue. Taken from Sumper and Kröger (2004).

Role in Silicon (Si) cycling

Due to their cell composition and global abundance, diatoms play a significant role in biogeochemical cycling of elements through the conversion of inorganic nutrients into

organic carbon and silicon (Dell'Aquila *et al.*, 2017). Their distinctive frustule formation makes them particularly efficient at carbon sequestration (Allen *et al.*, 2005; Smetacek *et al.*, 2012; Tréguer *et al.*, 2018), as their armour-like architecture, thought to have evolved for defence (Hamm *et al.*, 2003), provides ballast, meaning that diatoms sink very effectively, due to silica being denser than seawater (Beinfang *et al.*, 1982). The combination of grazing protection and high density, places them on a pedestal with respect to carbon sequestration in the ocean.

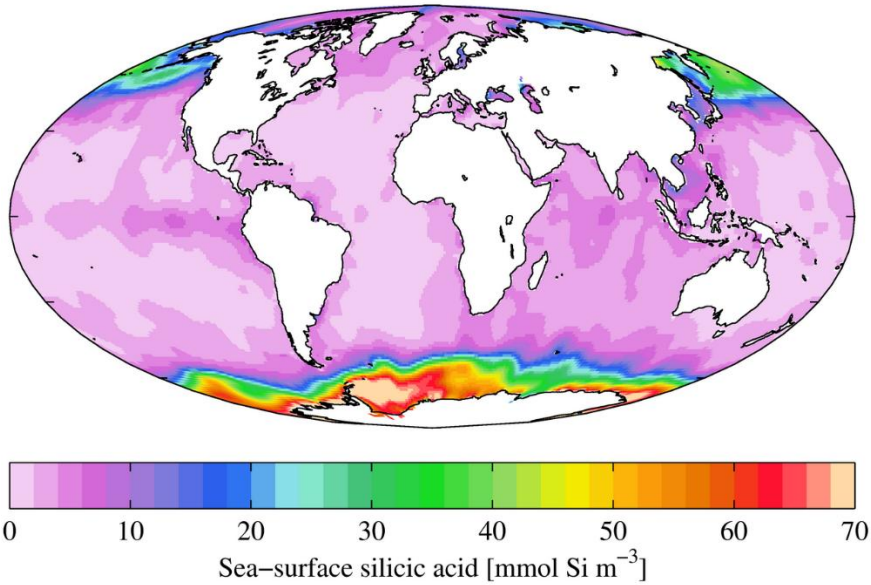

Figure 1. 5 Global distributions of silicic acid (mmol Si m^{-3}) in the surface ocean showing much of the global ocean at low concentrations (pink). Northern hemisphere Pacific gyres show moderate (green) whilst the Southern Ocean surrounding Antarctica shows high concentrations (red). Taken from World Ocean Atlas (Garcia *et al.*, 2006).

The biogeography of silicon (in the form of silicic acid) in the surface ocean is spatially and temporally variable (**Figure 1.5**), however, although seasonal, we generally see high concentrations in cold polar waters, making these regions a veritable nutrient-rich soup for diatoms. The biomineralisation of silicon into opal or silica by diatoms influences silicon cycling across the ocean, where biogenic silica is either recycled in the photic zone or exported to depth, where it may dissolve on descent or accumulate intact on the sea floor (Tréguer *et al.*, 2018). Predation is highest in the upper two hundred metres, with

only large diatom shells remaining intact through this zone, therefore making them the greatest exporters of silicate (Salter *et al*., 2007). Stoke's Law suggests there is a direct link between cell size and sinking speed; large, silicified diatoms will reach the sea floor more readily than smaller less silicified diatoms. This remains true if density remains constant. This is also true of carbon export – highly species specific however, silica and carbon export are often decoupled (**Figure 1.6**). Fast growing, bloom forming diatoms usually possessing thinner frustules, undergo mass mortality and sink in aggregates, removing significant amounts of carbon but little silica (Assmy *et al*., 2013; Leblanc *et al*., 2018). In contrast, heavily silicified large diatoms (more resistant to grazing) can remain in the photic zone for longer (Salter *et al*., 2007). When they sink, they sequester ample silica but little carbon (Assmy *et al*., 2013). This highlights species composition as the principal factor in sequestration of silica and carbon due to difference in growth, silicification, size and grazing resistance (Baines *et* al., 2010; Abrantes *et al*., 2016). As such, the need to differentiate species and their ecophysiologies is important for understanding biogeochemical patterns and processing in the ocean.

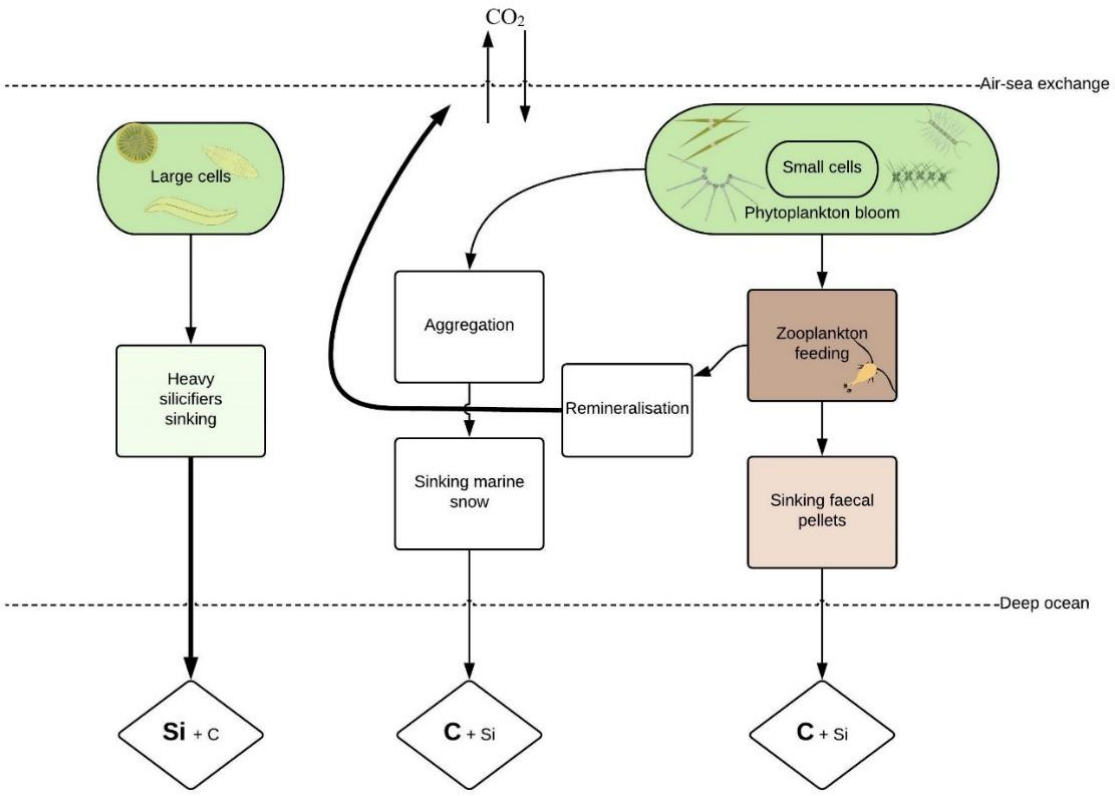

Figure 1. 6 Conceptual model of carbon and silica deposition. The model highlights (in bold) greater silica deposition through larger cell sinking whilst greater carbon sequestration occurs via small cells and marine snow deposition.

Climate change in our oceans

Physical drivers

Anthropogenic carbon emissions are changing our atmosphere and consequently our oceans. The carbon dioxide (CO_2) emitted diffuses into our ocean, with an equilibration time of roughly eight months (Gattuso & Hansson, 2011). This injection of CO_2 causes perturbations in seawater chemistry by increasing the partial pressure of CO_2 and lowering pH (Orr *et al.*, 2005). These changes are happening on a global scale, with world ocean monitoring sites reporting increased pCO_2 concentrations, some as much as four percent increase in $[H^+]$ annually (Jiang *et al.*, 2019). Representative emissions pathways (RCP's) show surface ocean pH decreasing in all future predictions by the end of the 21st century (**Figure 1.7A-B**). RCP2.6 model scenario predictions suggest surface ocean pH

to decrease by 0.06 to 0.07 units (15 to 17% increase in acidity) while for the worst-case scenario, RCP8.5, pH will likely decline by 0.30 to 0.32 units (100 to 109%). This process, known as ocean acidification (OA), is one of the most salient, pan-oceanic threats to marine organisms.

The release of carbon emissions is concurrent with global warming due to the greenhouse effect of these gasses (Lashof & Ahuja, 1990). Both our atmosphere and our oceans are warming (Sarmiento *et al.*, 2004) with the threshold of 1.5 °C fast approaching. This value was set to limit global mean temperature to below 1.5 °C above pre-industrial levels, suggested to minimise impacts on human, terrestrial, freshwater and oceanic systems by the Paris agreement (Armstrong McKay *et al.*, 2022). There is some variability in the magnitude and rate of change for both OA and global warming, however some areas are experiencing faster declines in pH and sea surface temperature (SST) than others (Wernberg *et al.*, 2011; Hobday & Pecl, 2014). Western boundary current regions have warmed 2-3 times the global sea surface temperature average (Wu *et al.*, 2012) and therefore many of these areas are termed 'ocean hotspots,' Nearshore, coastal habitats, such as those around the Tasman Sea, are such areas, and therefore are likely to feel the effects of ocean acidification and warming sooner (Lenton *et al.*, 2015).

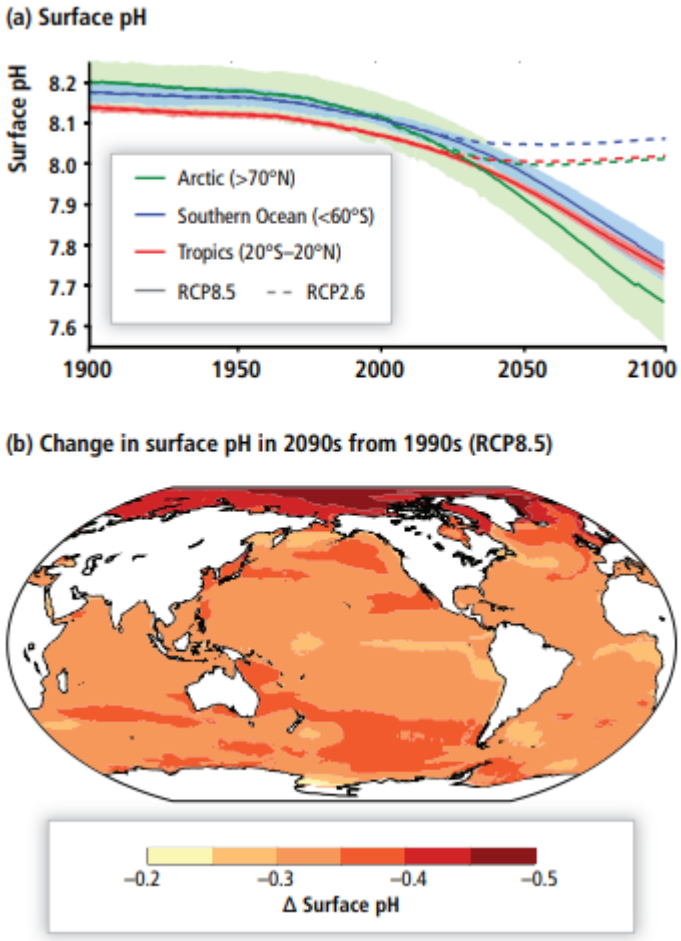

Figure 1. 7 Change in ocean surface pH. Time series (a) of surface pH in RCP 8.5 shown as the mean (solid line) with model ranges (shaded area) with RCP 2.6 shown as dashed lines. (b) Map of the median model surface ocean pH change from 1990 to 2090. Figure taken from (IPCC, 2018).

Earth System Model predictions at Port Hacking, a National Reference Station (NRS) and long-standing oceanographic time series mooring close to Sydney, are already showing ocean warming trends well above global averages (**Figure 1.8A**), having warmed > 0.7ºC in the last few decades (**Figure 1.8A**) and mean annual pH below global trends (**Figure 1.8B**), earning it the title of a global change 'hotspot' (Piontek *et al.*, 2014; Hemming *et al.*, 2023). Port Hacking is situated in the East Australian Current, a marine carriageway from the Coral Sea in northeastern Australia down to Tasmania. The greatest increase in sea surface temperature in the EAC is found between Maria Island and Port Hacking due to changes in wind forcing and eddy development (Malan *et al.*, 2021) resulting in the

region warming 30-50% faster than the global mean increase (Rohde & Hausfather, 2020). Sampling depth profiles at the Port Hacking monitoring site have revealed variations in warming rates at different depths (**Figure 1.8A**). There has been significant warming at the surface and at depths from 77-100 m since 1990 (Hemming *et al.*, 2023), with greater increases in the warmest temperature anomalies compared to the lowest temperature anomalies (**Figure 1.8A**). This extension of temperature ranges throughout the water column could have huge implications for community structure and function, with particular impacts for the sessile members of the marine community and increased tropicalisation, whereby tropical species move down into temperate regions (Wernberg *et al.*, 2013; Vergés *et al.*, 2014). A multitude of ecological and evolutionary consequences may arise from the occurring rapid warming and lowered pH, through influencing individual species physiology and behaviour, as well as altering community composition, consequent shifts in trophic web dynamics and potential whole ecosystem regime shifts (Zarzyczny *et al.*, 2024).

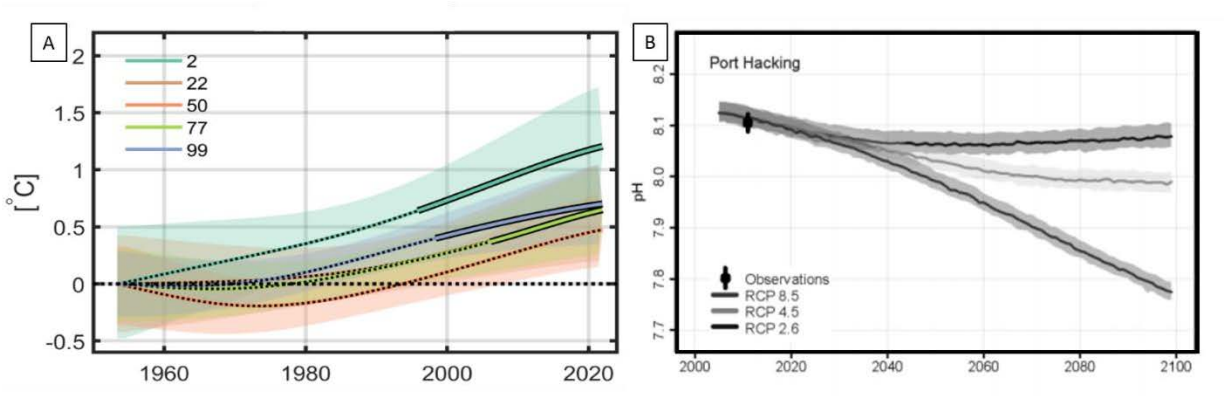

Figure 1. 8 (A) Historical temperature ensemble empirical mode decompositions (EEMD) trend at Port Hacking showing changes of the mean from expected. The five coloured lines represent depth level (metres) with uncertainty for each depth shaded using a downsampling method. Insignificant periods of temperature change are outlined by dashed lines, with significant periods of warming represented as filled lines with black outlines (depths 2, 22 and 50m post 1990), adapted from Hemming *et al*., (2023). 8B shows pH projections for National Reference Station (NRS) Port Hacking, NSW, Australia. Median changes (solid line) with upper and lower percentile range (10^{th} and 90^{th} shaded) are shown for RCP 2.6, 4.5 and 8.5. In-situ observations from NRS PH are represented by the 10^{th} and 90^{th} percentile. Adapted from Lenton *et al*., (2015). Note the different time scales on the x axis.

Structural changes

Anomalous warming of surface waters alters the structure of the upper ocean by changing vertical density gradients (Sarmiento *et al*., 2004). Water columns are naturally separated, often with warmer waters sitting on top of dense, cooler waters, a process known as ocean stratification (Li *et al*., 2020). Increases in SST results in a shallowing and/or reduction in the amplitude of the surface mixed layer (Yamaguchi & Suga, 2019; Li *et al*., 2020), thereby exacerbating thermal stratification. Dampening of mixing potential can become a barrier to vertical exchange, impeding processes such as nutrient entrainment or organism migration (Cermeño *et al*., 2008) although species specific responses are more likely better than use of current broad-sweeping mandals (Kemp & Villareal, 2018). Much like pH, worst-case scenario predictions (CMIP6 SSP5-8.5) also suggest vast changes, with the mixed layer depth (MLD) predicted to shoal by up to 20 metres in many parts of the ocean (Kwiatkowski *et al*., 2020). These structural

and subsequent physico-chemical changes to the euphotic zone can have cascading effects on the biology; whereby in shrinking physical space and reduced input of nutrients from the deep ocean to the surface may increase resource competition (Litchman *et al.*, 2006; Moore *et al.*, 2013), higher light availability and warmer temperatures result in increased metabolic activity of the primary producers, causing further changes to food web dynamics (Taucher & Oschlies, 2011; Capitani *et al.*, 2022) and biogeochemical cycling.

Biological impacts

For organisms living in the surface waters, their plasticity and ability to adjust to new conditions will determine their survivability. For diatoms, future ocean conditions such as OA and warming could prove beneficial through CO_2 fertilisation for greater photosynthesis (Gao & Campbell, 2014) and warming increasing metabolic activity (Jabre *et al.*, 2021). These stimulating effects have often been found in isolation of other factors under favourable conditions, however more realistic future scenarios encompass multi factor stressors. Compounding effects could therefore increase pressure on diatom plasticity to overcome rapidly changing environments, with the rate of change necessary for survival not possible (Edwards & Richardson, 2004; Zhong *et al.*, 2021; Li *et al.*, 2018). Despite the potential benefits at the cellular level, such as greater metabolic rate, the warming necessary for such change also subsequently results in stratification, meaning prolonged exposure and residence time in high irradiance under nutrient stress (Cermeño *et al.*, 2008; Gao *et al.*, 2012), which has been shown to decrease net primary productivity due to increased competition for resources and photoinhibition (Chen & Gao, 2011; Gao *et al.,* 2012; Roxy *et al.*, 2016; Gao *et al.*, 2019). Equally, while ocean acidification has generally been seen as driving positive increases

in diatom productivity (Gao & Campbell, 2014), structural change to the diatom assemblages have been observed, with mesocosm studies finding small diatoms to outcompete larger ones in some regions (Brussaard *et* al., 2013; Davidson *et al.*, 2016), while other studies have found the opposite, whereby OA favours larger diatoms (Feng *et* al., 2010; Bach & Taucher, 2019). Only recently have studies started looking into how OA might influence diatoms biomineralisation (Milligan & Morel, 2002; Herve *et al.,* 2012; Petrou *et al.,* 2019). In this way, any changes to the euphotic zone, structurally and/or chemically, will exert strong influence on ocean productivity (Tréguer *et al.*, 2018). Whilst the magnitude of decline is dependent on the light, temperature and pH tolerances of individual phytoplankton species, coupled with top-down pressure exerted from grazing, ocean productivity is expected to shift with ocean warming.

Knowledge gaps

Our oceans are experiencing unprecedented changes due to anthropogenic carbon emission release. How our oceans will respond, and if the marine organisms within them can adapt in time, is an ongoing debate. Many questions are still to be answered on vastly different scales, such as basin-wide carbon export potential, community composition shifts and trophic web transformation, down to physiological responses, biomolecular composition and genetic drift in individual cells under ocean acidification and warming. The breadth and complexity of these questions make answering them hugely difficult, as the answer to each question within each broader question, provides only a small piece of an incredibly large puzzle. Furthermore, conducting research in ecologically relevant environmental settings, under realistic conditions is challenging, despite it being the only genuine way of producing results that are relevant for extrapolating to global systems.

Ocean acidification differentially affects phytoplankton

One of the many impending threats to marine phytoplankton is ocean acidification. Current research shows positive (Levitan *et al*., 2007; Tortell *et al*., 2008; Wu *et al*., 2010; Schaum *et al*., 2013; Wu *et al*., 2014; Dutkiewicz *et al*., 2015), neutral (Burkhardt *et al*., 1999; Tortell *et al*., 2002) and negative responses (Riebesell *et al*., 2013; Sala *et al*., 2016; Petrou *et al*., 2019) to OA highlighting an inherent variability amongst phytoplankton. When looking at diatom specific responses to OA, most of the research is limited to its effect on community composition, growth or productivity (Tatters *et* al., 2013; Davidson *et* al., 2016; Schulz *et al*., 2017; Deppeler *et al*., 2018; Bach *et al*., 2019). There is however a paucity of research on the impact OA will play on silica frustule formation, the aspect which differentiates diatoms from their phytoplankton counterparts. Research has shown that diatom silicification varies with other environmental condition changes, such as iron limitation, increasing temperature and light (Martin *et* al., 1990; Hutchins & Bruland, 1998; Boyd & Law, 2001; Durkin et al. 2013; Baines *et al*., 2010; Javaheri *et al*., 2015; Baker *et al*. 2016; Gleich *et al*., 2020; Sheehan et al 2020), yet we have a limited understanding of how increasing oceanic pH will affect frustule synthesis and even less information on potential synergistic or antagonistic effects of multiple stressors. The few studies available have looked at the mechanistic relationship between pH and frustule silicification (Milligan & Morel, 2002; Hervé *et al*., 2012) and how environmental pH shifts influence diatom silicification rates (Milligan *et al*., 2004; Sugie & Yoshimura, 2016). **This highlights a distinct lack of knowledge surrounding frustule morphogenesis considering this pan-oceanic threat.** Should we find OA negatively impacts diatom

silicification, we may see changes to diatom sinking capacity and predator defence with further reaching impacts on biogeochemical cycling and carbon export.

Phylogenetic diversity and multiple stressors negate universal assumption

Elucidating responses to climate change are further complicated by the phylogenetic diversity of the diatoms. These organisms span many orders of magnitude in size, present numerous different shapes, and are found in a multitude of habitats. It is therefore entirely plausible that climate change will induce species-specific responses and even within species phenotypic variability. Because of their convenience, laboratory experiments utilising a small number of taxa, usually readily culturable species, are still the norm. This method, although offering some merits, negates within, across and muti-species interactions. Several studies have highlighted the variability within and between species responses to environmental change (Nicotra *et al*., 2010; Franks & Hoffmann, 2012; Ajani *et al*., 2021), thereby suggesting that single-cell analysis, within a relevant ecological setting could provide a unique and somewhat more realistic insight into a species and/or community response. The addition of including the entire microbial community, something often left out of laboratory single strain experiments, provides potentially critical information of among and between species and trophic level responses. **Increasing work on the importance of inter-species interactions and species-specific response diversity, highlights the need for studies to broaden the taxonomic coverage of their investigations into climate change impacts.**

Going beyond the laboratory-style study model

Artificial conditions under which lab and some field studies are performed could also be problematic for determining underlying responses. In many cases, amended seawater conditions could be masking potential effects, altering our understanding of climate change impacts to diatom physiology and ecology. For example, in the majority of culture studies and even some mesocosm or natural community studies, high additions of macronutrients are applied. This unnaturally high nutrient availability may provide cells with resources that enable coping strategies that wouldn't be present under natural conditions, thus limiting potential detrimental effects of increasing pCO_2, hindering our understanding of how in-situ diatoms will respond. Commonly used media for culture work such as F/2 (Guillard & Ryther, 1962), have nearly 100 times higher concentration of N, P and Si than natural seawater. While useful to negate nutrient limitation, it may alter the response to C enrichment in the absence of other nutrients, by enabling continued growth rather than investigating the cellular responses under stoichiometric imbalances. There is also the added complication of stress responses vs acclimation response. Surplus nutrient availability could alleviate detrimental effects on short time scales which, if they were experienced for extended periods in realistic nutrient conditions, may provide more realistic responses, reminiscent of natural scenarios. **Therefore, if we are to fully comprehend environmental change impacts on diatoms, we need to start using natural seawater conditions or at least testing for interactive effects of nutrient enrichment with other climate change stressors.**

The problem of multiplicity

In the way that natural communities are multi-specious, climate change is also multifaceted. Ocean acidification and the intrusion of anthropogenic CO_2 is one issue; however, sea surface temperature (SST) rise due to the greenhouse effect of emissions release which promotes stratification of surface waters and consequently increases residence time in high irradiance are also happening concurrently (Gao *et al.*, 2019). How then do we truly ascertain a species or community response without considering two or more factors. Previous research has shown increasing irradiance and pCO_2 independently of each other can be beneficial for productivity (Riebesell & Tortell, 2011; Gao & Campbell, 2014) however when combined, to saturating and predicted future oceanic CO_2 concentrations, they synergically decline the health of the diatom (Gao *et al.*, 2012). Conversely, one or more of these climate change factors might compensate for another, dampening the detrimental effects. **Without expanding our experimental designs to encompass multiple changing variables and look past sole indicators for response, we cannot fully understand how diatoms will respond to climate change both physiologically and ecologically.** Ultimately, the clearest picture will be garnered through multi factor, multi species and multi trait experiments performed under realistic conditions, a challenge that is yet to be undertaken.

Combining community-level response with individual single-cell analysis

The scale at which we decipher environmental change also has its challenges. Assessment of an entire community response through bulk analysis shows gross changes under an induced condition, however individual species contributions, phenotypic responses and taxonomic shifts may be overlooked. Conversely, single

strain culture experiments offer insight into individual species-specific responses, yet extrapolating these data in the assumption that other phytoplankton will respond similarly is fraught with limitation. Further still, within and across species, plus multi-species interactions are also neglected. Given that several studies have shown large within and between species variability in responses to environmental change (Godhe & Rynearson, 2017; Anderson & Rynearson, 2020) we need to start combining these two levels of analyses. In that way, we can start to reap the benefits of community-based bulk change and species-specific responses to better understand ecosystem level change. **Disentangling individual cell responses from within a community in an ecologically relevant setting (Havenhand *et al.*, 2010) will provide new knowledge on how diatoms may respond as a group and reveal the phenotypic variability at the species level, highlight potential floristic shifts and delivering a more nuanced understanding of who the 'winners and losers' might be in future ocean scenarios.**

These gaps in our understanding leave many unanswered questions on how diatoms will be affected by climate change. Focusing on silicification by diatoms and of specific relevance to the work in this thesis, the key questions of interest underpinning the aims of my thesis included:

1. Does the negative effect of OA on Antarctic diatom silicification translate to other regions of the ocean? – specifically-
    a. What effect does OA have on coastal temperate diatom silicification?
    b. Are the responses species-specific?
    c. How do silicification rates vary in polar, sub-Antarctic and sub-tropical waters?

2. How will shallowing of the mixed layer in a future acidified oceans influence diatom physiology and silicification?
    a. What effect does OA in combination with light have on diatom silicification?
    b. Is this effect species specific?
3. Do changes in light alone influence diatom silica production rates?
4. Can potential light-induced changes in silicification be linked to buoyancy regulation?

Thesis Aims, Objectives and Outline

The overarching aim of my PhD project was to assess how climate change induced perturbations to marine ecosystems, namely ocean acidification and higher light regimes, influence diatom silicification. I set out to deliver quantitative data on diatom responses to lowered pH, higher irradiance and a combination of both pH and light, seeking to better understand how physical changes to the euphotic zone, like ocean shoaling and ocean acidification may independently and interactively influence diatom physiology. I did this using a mixture of culture strain studies and mixed natural community studies that looked at both bulk and individual species responses, in both laboratory and field settings. My key aim was to elucidate morphological, physiological, metabolic and biomolecular responses to these environmental perturbations and their interactive effect. My work herein, is represented by three specific aims.

1. Ocean acidification and mixed layer depth shoaling, as a product of ocean warming, are happening concurrently and have already been shown as synergistically detrimental to diatom productivity, posing further questions about their impact on diatom

silicification. Therefore, aim 1 was to: **determine how changes in light and pH, simulating ocean shoaling under OA conditions, will alter diatom growth, morphology, silicification and biomolecular composition in two 'model diatoms' (Chapter 2).** This work was done on two diatom species, often used in culture work (model diatoms). These taxa were chosen to provide data that could be compared with previous research and to contrast the physiologies and responses of two commonly studied diatoms, with a subsequent goal to establish whether such species provide a reasonable benchmark for discussing global diatom responses.

2. Despite ocean acidification being a pan-oceanic threat to marine life, certain areas are more susceptible than others. 'Global change hotspots' describe environments that are experiencing climate change more rapidly than the global mean and coastal marine habitats around the southeast coast of Australia are considered as such. To elucidate floristic shifts under ocean acidification, it is crucial to assess communities at the single cell level, thereby alleviating broad stroke averages which could mask potential outliers and novel species interactions. Therefore aim 2 was to: **assess how elevated CO_2 affects silicification rates of natural coastal communities and whether individual diatom taxa within the community are differentially affected – who are the winners and losers? (Chapter 3).**

3. Much of the Southern Ocean is considered a high nitrate, low chlorophyll (HNLC) region yet still sequesters a disproportionate amount of anthropogenic CO_2 compared to other basins. The biological influence on carbon export is imperative for its continuation as a carbon sink. With increased residence time in higher irradiance expected for

diatoms in the pelagic zone, understanding the role light plays on diatom silicification in these cold waters is critical, as frustule density is strongly tied to diatom export capacity. Therefore aim 3 was to: **characterise how light influences pelagic diatom silicification and uncover potentially distinct ecotypes at different depths (Chapter 4).**

Cumulatively, these three research aims explored in the following chapters provide new insight into species-specific diatom silicification under variable environmental conditions and cover a range of complexities from multi-factorial to multi-species. Understanding the plasticity of diatoms and gaining insight into their physiological responses will help elucidate the winners and losers in a future ocean. Furthermore, combining single strains and multiple species studies may afford us the greatest coverage of physiological and ecological responses for predicting future ocean diatom prosperity or decline. This knowledge is presented in subsequent **Chapters 2, 3** and **4**, and synthesised in **Chapter 5** presenting the key findings, the research summarised, and future directions proposed for further inquiry.

Author contributions

Each chapter is my own work with involvement and contributions from my supervisors, collaborators and fellow research students. I am grateful for all their contributions and the opportunity to collaborate with such a wonderful group of people.

Chapter 1 (Introduction) and **Chapter 5** (Synthesis) are my own work with editorial feedback from my primary supervisor. I do not intend to publish this work.

Chapter 2: This chapter is in review with *Limnology and Oceanography* as:

FitzGerald-Lowry B, Aagren Nielsen D, Duncan RJ, Theseira AM, Thompson G, Petrou K (2024) Multi-trait responses in two marine diatoms to ocean acidification and mixed layer depth reveals interactive effect of light and pCO2, mediated by silicification

- Contributions as listed in the publication

Chapter 3: Disentangling species-specific physiological and morphological responses to ocean acidification in a coastal diatom community

- Conceptualisation: KP, BF-L; methodology: KP, DAN; investigation: BF-L, DAN, AMT, AB, GT, KP; formal analysis: BF-L, DAN; visualisation: BF-L; writing—original draft: BF-L; Writing—review and editing: all authors; Funding acquisition: KP; Supervision: KP, DAN.

Chapter 4: Uncovering how light modulates diatom silicification in a Southern Ocean community

- Conceptualisation: KP, BF-L; methodology: KP, DAN; investigation: BF-L, DAN, AMT, AB, RE, ES, KP; formal analysis: BF-L, DAN; visualisation: BF-L; writing—original draft: BF-L; Writing—review and editing: all authors; Funding acquisition: KP; Supervision: KP, DAN.

Signatures of contributors

Production Note:
Signature removed prior
to publication.

B. FitzGerald-Lowry

Production Note:
Signature removed prior
to publication.

RJ. Duncan

Production Note:
Signature removed prior
to publication.

G. Thompson

Production Note:
Signature removed prior
to publication.

AM. Theseira

Production Note:
Signature removed prior
to publication.

A. Bottomley

Production Note:
Signature removed prior
to publication.

DA. Nielsen

Production Note:
Signature removed prior
to publication.

K. Petrou

Chapter 2: Multi-trait responses in two marine diatoms to pH and irradiance reveals interactive effect of light and acidification, mediated by silicification

This chapter is in review with *Limnology and Oceanography* as:

FitzGerald-Lowry B, Aagren Nielsen D, Duncan RJ, Theseira AM, Thompson G, Petrou K (2024) Multi-trait responses in two marine diatoms to ocean acidification and mixed layer depth reveals interactive effect of light and pCO2, mediated by silicification

Author contributions

Conceptualisation: KP, BF-L; methodology: KP, DAN; investigation: BF-L, DAN, RJD, AMT, GT, KP; formal analysis: BF-L, DAN; visualisation: BF-L, RJD; writing—original draft: BF-L, KP; Writing—review and editing: all authors; Funding acquisition: KP, DAN; Supervision: KP, DAN.

Keywords: climate change, biogenic silica, *Phaeodactylum tricornutum*, *Thalassiosira weissflogii*, shoaling, pCO_2

Running header: Influence of light and pH on diatom silicification

Abstract

Ocean ecosystem shifts in response to anthropogenic climate change are impacting marine organisms, including phytoplankton. Ocean acidification and warming represent two key threats to marine phytoplankton causing significant changes to the upper mixed layer of the ocean, reshuffling their distribution, and reorganising their physiology and metabolism. In this study, we investigated changes in biomolecular composition and silicification rates of the two 'model' diatom species *Phaeodactylum tricornutum* and *Thalassiosira (Conticribra) weissflogii* under low (~350) and projected future (~800) pCO_2 concentrations with low (20 µmol photons m^{-2} s^{-1}) and high (200 µmol photons m^{-2} s^{-1}) light, simulating expected climate change-induced impacts of ocean shoaling and acidification. Specifically, our study conditions elicited changes in lipid and protein content in both species. We also found a negative effect of pCO_2 on silica production under high light in *T. weissflogii* that was linked to improved photochemical efficiency. This interactive effect between light and pCO_2 with silica production, suggests a potential controlling role of the frustule in diatom photosynthesis and photoprotection (energy balance). Based on these data, ocean shoaling and acidification have the potential to influence the nutritional value and biogeochemical role of diatoms through its effect on diatom frustule synthesis and photobiology.

Introduction

Since the industrial revolution, roughly 40% of total anthropogenic carbon emissions have been absorbed by the oceans (DeVries, 2014), causing perturbations in ocean chemistry; the partial pressure of CO_2 steadily increasing, lowering seawater pH (Orr *et al.*, 2005). As atmospheric CO_2 concentrations continue to rise, end-of-century and 2150 projections suggest seawater pH could decline by 0.5 units, equivalent to an acidity

increase of up to 150% (Gattuso *et al*., 2015). This process, known as ocean acidification (OA), is one of the most salient threats currently facing marine ecosystems.

A direct consequence of elevated atmospheric CO_2 is warming, which is occurring rapidly across the globe. In the ocean, warming alters vertical density gradients in the upper layers, forcing shoaling (a shallowing and/or a reduction in amplitude) of the surface mixed layer (Yamaguchi & Suga, 2019; Li *et al*., 2020). This natural separation, whereby warmer water sits on top of more dense, cold water, is known as ocean stratification. With surface ocean waters predicted to continue warming, mixing potential is dampened and can become a barrier to vertical exchange. Recent projections based on the worst-case CO_2 emission scenario (CMIP6 SSP5-8.5) estimate the mean maximum annual mixed layer depth (MLD) to reduce by ~20 m by the end of this century (Kwiatkowski *et al*., 2020). This increased stratification reduces nutrient input from the deep ocean to the euphotic zone and prolongs phytoplankton residence time in higher irradiances at the ocean surface (Cermeño *et al*., 2008; Gao *et al*., 2012). Major structural and chemical changes to the euphotic zone exert a strong influence on ocean productivity through their effect on phototrophic phytoplankton (Roxy *et al*., 2016). Effects of shallowing MLD have been shown to decrease net primary productivity, due to increased competition for resources and photoinhibition (Gao *et al.,* 2012; Roxy *et al*., 2016; Gao *et al*., 2019). While the magnitude of decline in productivity depends on the light and temperature limits of individual phytoplankton, as well as top-down effects from grazing, shifts in ocean productivity are expected as oceans warm.

One of the greatest contributors to ocean primary productivity and marine biomineralisation are phytoplankton from the group known as diatoms (Bacillariophyta). They are responsible for over 40% of ocean primary production and because of their

silica-based cell wall, are key players in marine silicon (Si) cycling. Furthermore, their dense, silica-based shell, known as a frustule, aids in their sinking, making them important for ocean carbon sequestration (Tréguer *et al*., 2018). Silicification (the biomineralisation process leading to the formation of the silica frustule) by diatoms has been shown to vary with environmental condition — decreasing under iron limitation (Durkin et al. 2012), elevated temperatures (Baker *et al*. 2016; Sheehan et al 2020) and acidification (Milligan & Morel, 2002; Petrou et al., 2019). However, gaps in our understanding of potential synergistic environmental effects from climate change on diatom silicification remain.

A key ecological trait in diatoms, largely responsible for their wide-spread success, is their capacity for buoyancy regulation to optimise growth, where individual cells regulate their position in the water column, undertaking photosynthesis and cell division at the surface and carrying out repair to damaged photosystems (Gao et al., 2018) and other biochemical adjustment processes (pigment and protein production) at depth (Petrucciani *et al.,* 2023). In the context of ocean warming, increased shoaling of the mixed layer from thermal stratification has the potential to restrict diatom migration, decreasing repair time (e.g. turnover of D1 proteins of photosystem II) in deeper waters, and exposing cells to prolonged UV radiation, which can be deleterious to cellular components (Ganapathy et al., 2017) and lower rates of photosynthesis (García-Gómez et al. 2016). Additionally, ocean acidification combined with high irradiance has been shown to work synergistically to damage the photosynthetic health of diatoms (Gao *et al.,* 2012_a, 2012_b). In contrast, the diatoms confined to deeper waters, while possibly less affected by acidification due to lower light levels (Gao *et al.,* 2012_a, 2012_b) or nutrient limitation (Cermeño *et al*., 2008), may be unable to monopolise on the nutrient rich

environment, as light will be limiting. These changes to ocean mixing may alter diatom C:Si stoichiometry with consequent impacts for elemental fluxes. Understanding how diatom productivity and rate of silica deposition change in response to light under increasing ocean acidification, is important for solving the complex puzzle on how diatoms will fare under projected future conditions.

Here, we investigated diatom growth, morphology, silicification and biomolecular composition in two commonly used model diatoms: the pennate diatom, *Phaeodactylum tricornutum* and centric diatom *Thalassiosira weissflogii*. We measured physiological responses in cells grown under high (surface MLD) and low (deep MLD) light at current and future pCO_2 concentrations, simulating conditions expected from climate change-induced ocean shoaling.

Methods

Experimental design

Cultures of *Phaeodactylum tricornutum*, strain CCAP1055/1 (Bigelow National Center of Marine Algae and Microbiota collection) and *Thalassiosira weissflogii,* strain CS871 (CSIRO) were grown in filtered (0.2 µm) seawater (FSW) collected from about 7km off the coast of south Sydney (-34.117583, 151.21815) and enriched with F/20 medium (Guillard & Ryther, 1962). Media was filter sterilised to avoid affecting the natural buffering capacity of the seawater and potentially stripping low concentration alkalinity ions that can happen with autoclaving (Kremling *et al*., 1999). Cultures were grown under two light intensities (200 and 20 µmol photons m^{-2} s^{-1}), represented as high light (HL) and low light (LL) and two pH conditions (approx. 8.1 and 7.8, total scale), represented as +C for the low pH. All treatments were grown in replicate (n=5). Cultures were incubated at 20 °C in

a temperature and light controlled incubator on a 12:12h light:dark cycle. To minimise gas exchange and equilibration with air, cultures were grown in 275 mL polycarbonate tissue culture flasks and filled to the bottom of the narrow neck, reducing headspace to less than 5 mL.

To ensure stable carbonate chemistry, batch cultures were grown semi-continuously and cell density maintained below 150,000 and 35,000 cells mL^{-1} for *P. tricornutum* and *T. weissflogii,* respectively, to limit consumption of dissolved inorganic carbon (DIC) to less than 5% of total (European Commission. Directorate-General for Research, 2011). Cell counts, total alkalinity (TA) and pH measurements were carried out daily. Any volume of culture removed for analyses was replaced with pH adjusted media for each treatment, respectively. When cultures reached their cell concentration threshold, they were re-cultured at 1000 cells mL^{-1} in new pH-adjusted media (see section on CO_2 *perturbation* below). Cultures were acclimated to the four conditions for a minimum of four weeks (five-day growth cycle duration, equivalent to 30-40 generations, calculated from growth rate) and were sampled during exponential growth phase for physiological parameters.

Growth rates and cell volume

To obtain growth rates, cultures were sub-sampled daily. Cells were counted using flow cytometry; briefly 250 µL of each culture replicate (in technical triplicate) were placed in a 96-well plate and run on a CytoFlex S Coulter flow cytometer (CytoFlex S Coulter, Beckman, USA) for one minute using consistent gating. For morphological parameters, cells were imaged using light microscopy on a Neubauer counting chamber. Images

were analysed using ImageJ (Schneider *et al.*, 2012) and cell measurements used to calculate cell size, volume and surface area, according to Hillebrand *et al.*, (1999).

CO_2 perturbations and seawater carbonate chemistry

The carbonate chemistry of each culture was maintained daily; 40 mL of culture was analysed using potentiometric titration on a Metrohm Titrino Plus, to obtain the Total Alkalinity (TA) and pH (total scale) of each culture flask. Samples were gently filtered (0.2µm) before titration to remove cells and debris, which could affect TA and/or DIC measurements (Dickson, 2010). The pH probe was calibrated daily with (pH 4, 7, 10; chem supply laboratory reagent, 500M) and TA values calibrated to certified reference material (Batch #196, Dickson, 2010). Carbonate chemistry parameters (Table 1) were calculated in an R script utilising the R package "seacarb" based on CO2SYS (Lewis & Wallace, 1998) with known salinity (PSU), temperature (°C) and nutrient concentrations (Total P and S µmol/kg). For K1 and K2 constants, Mehrbach *et al.,* 1973 refit by A. G. Dickson & Millero (1987), were used, and for KSO_4 and B_I constants, A. G. Dickson (1990) and Uppstrom (1974) were used, respectively. One molar hydrochloric acid (HCl), sodium hydroxide (NaOH) and sodium carbonate (Na_2CO_3) were used to adjust TA and pH (Gattuso *et al.,* 2010). Acid/base additions were calculated to the volume remaining in the flask (230 mL) with the remainder refilled with pH-adjusted F/20 media (~40 mL).

Photophysiology

Once growth rates for each respective treatment were stable (four weeks), cells from each treatment were assessed for photophysiological health. A steady state light curve, using a Pulse Amplitude Modulation (PAM) fluorometer (Water PAM; Walz Effeltreich, Germany) was performed, with measurements collected using Win-Control 3 software.

Aliquots (2 mL) were low-light adapted (<2 µmol photons m^{-2} s^{-1}) for 15 min prior to being exposed to a saturating pulse of light (width=0.8s, intensity=8) followed by an eight-step light curve of five minutes at each light intensity (163, 240, 360, 540, 767, 1050, 1690, and 2450 µmol photons m^{-2} s^{-1}). Minimum and maximum fluorescence were recorded to obtain maximum and effective quantum yield of photosystem two (PSII). Light curves were fitted according to the equation of Ralph and Gademann (2005) to obtain the following parameters: light utilisation efficiency (α), minimum saturating irradiance (E_K), maximum electron transport rate (*rETRmax*), maximum saturating irradiance (*Em*) and photoinhibition irradiance (*Eb*).

Chlorophyll a and c measurement

For pigment determination, 50mL of sample were filtered onto a 47mm glass fibre filter (Nucleopore, Whatman), snap frozen in liquid nitrogen and stored at -80°C. For analysis, filters were placed in 3mL of 90% acetone, left for 16 hours overnight, and then centrifuged at 3214 RCF for 5 minutes. Chlorophyll *a* and *c* content were measured using a Spectrophotometer (Shimadzu, UV-1280) at 630 mm and 664 mm, and calculated according to Ritchie (2006).

Silicification rates and biogenic silica (bSi) content

Biogenic silica (BSi) and silica incorporation rate (silicification) were measured following the methods described in McNair *et al*., (2015). Incorporation rate of silica into the frustule was assessed by incubating cells with the fluorescent dye 2-(4-pyridyl)-5-((4-(2-dimethylaminoethylaminocarbamoyl) methoxy) phenyl) oxazole (PDMPO), which binds to newly deposited silica. Polycarbonate flasks were filled with 170mL of pH adjusted

(respective to treatment) filtered seawater media (F/20) and inoculated with cells to an initial concentration of 20,000 and 10,000 cells mL^{-1} for *P. tricornutum* and *T. weissflogii,* respectively. All replicates were spiked with Lysosensor Yellow/Blue DND-160 (PDMPO, ThermoFisher Scientific, Australia) to a final concentration of 0.125 µM PDMPO. After 24 h, 50 mL of sample was filtered through a 47 mm, 0.4 µm polycarbonate filter (Nucleopore, Whatman). Unbound PDMPO was washed off with an initial 0.2 µm filtered seawater rinse after which the filter was covered with 2 mL of 10% HCl and left for two minutes to lyse cells and disrupt cellular membranes to remove unbound intracellular PDMPO (Leblanc & Hutchins, 2005). A further MiliQ rinse (1 mL, three times) ensured that any extracellular PDMPO, cellular components and HCl was removed. Rinsed filters were then placed in cryovials, snap frozen in liquid nitrogen and stored at -80 °C until further analysis.

Silicification rate and bSi determination

To determine PDMPO incorporation and bSi content, samples were thawed, and diatom frustules were initially solubilised via a hot-alkaline-digest (in 0.2M NaOH at 95ºC for 3h) to release frustule-bound PDMPO, according to Leblanc & Hutchins (2005). Samples were subsequently measured using a fluorescence plate reader (Tecan Infinite M1000; Switzerland) set to excite at 375 nm and compared against a PDMPO standard curve (0, 5, 10, 25, 50, 100 µM Si, $R^2 = 0.995$) prepared using the digestion (NaOH + HCl) solution. BSi production was then calculated from quantitative PDMPO incorporation using the ratio of 2916 mol bSi per mol PDMPO (McNair *et al.,* 2015). Using a separate aliquot of the alkaline-digest, colorimetric analysis of reactive silicate was conducted following the methodology of Strickland and Parsons (1972), modified by Nelson *et al.,* (1989).

Absorbance was measured at 810 nm (Cary Eclipse, Agilent Technologies, U.S.A.) and compared against a standard curve (R^2 = 0.997) made with sodium metasilicate stock solution (0, 5, 25, 50, 100, 200 µM Si). Data were normalised to both cell count and surface area.

Biomolecular content by synchrotron-based FTIR

The biomolecular composition of *P. tricornutum* and *T. weissiflogii* was determined using synchrotron-based FTIR microspectroscopy. Spectral analyses were performed on formalin-fixed (5% v/v final concentration) cells. To ensure consistency across cells, all cells measured were single cells and not dividing. The spectral data of individual cells (5-10 cells per replicate per treatment) were obtained on the Infrared (IR) Beamline at the Australian Synchrotron, Victoria (within 6 months of samples being fixed and refrigerated). Samples were loaded directly into a micro-compression cell between two 13 mm diameter, 0.5 mm thick BaF_2 windows. Spectra were acquired over the measurement range 4000 – 800 cm^{-1} with a Vertex 80v FTIR spectrometer (Bruker Optic, Ettlingen, Germany), with an IR microscope (Hyperion 3000, Bruker) fitted with a narrow-band mercury cadmium telluride detector cooled with liquid nitrogen. The measurements were performed on hydrated cells which has been shown to limit light scattering effects (Bambery et al, 2012). Co-added interferograms (sample n = 64, background n = 64) were collected at a wavenumber resolution of 4 cm^{-1}. All measurements were made in transmission mode, using a measuring aperture diameter of 11.1 µm (area = 96.77 µm). All cells were measured once, and the aperture was sufficient to capture the entire cell in the measurement. Opus 8.0 software (Bruker) was used for both spectral acquisition and instrument control.

Data analysis

To determine significant effects of increasing light and pCO_2 on diatom physiology and morphology, two-factor Analysis of Variance (ANOVA) was used with Tukey's multiple comparison test at alpha <0.05. All data were tested for homogeneity of variance and normality *a priori,* in cases where assumptions weren't met, non-parametric Kruskal Wallace test was used. When determining the significance differences between carbonate chemistry treatments, a linear mixed-effect model on the pooled data (all days together) with sample as random factor to control for repeated measures was used. Statistical analyses were performed using GraphPad Prism, version 10.0.2 (GraphPad Software, Boston, Massachusetts USA) and RStudio Team (2019) RStudio: Integrated Development for R. RStudio, Inc., Boston, MA. Photophysiological data from the steady state light curves were analysed in SigmaPlot* (V 14.5, Systat Software Inc., CA, USA) using a custom-made macro according to the curve-fitting protocol of Ralph & Gademann (2005). From the macro we were able to obtain *alpha* (light utilisation efficiency), *Ek* (minimum light saturating irradiance), *Em* (maximum light saturating irradiance), *Eb* (initial photoinhibition irradiance), and maximum relative electron transport rate (*rETRmax*) (Table 2). Infra-red spectra were analysed using R (R Development Core Team 2018). The major biological bands detected in regions of 3050-2800, 1770-1100 cm^{-1} (Table 3), were selected for analysis. Spectral data were then smoothed (4 pts either side) and second derivative (3rd order polynomial) transformed using the Savitzky-Golay algorithm from the prospectr package (Stevens and Ramirez-Lopez, 2022) and normalised using the method of Single Normal Variate (SNV). Biomolecular content was estimated based on integrating the area under each assigned

peak (Table 3), providing metabolite content according to the Beer-Lambert Law, which assumes a direct relationship between absorbance and relative analyte concentration (Wagner et al., 2010).

Results

Carbonate chemistry

Cultures were maintained within ~5% of target DIC for the duration of the experiments (**Figure 2.1**). Average pH for the low pCO_2 treatments ranged from 8.11-8.16, while the high pCO_2 treatments ranged from 7.79-7.87 (**Table 2.1; Figure 2.1**). Greatest pH drift during growth was observed in the high light, low pH (HL+C) cultures (**Figure 2.1**), however, there was no overlap in the pH of low and high pCO_2 treatments at any stage of the experiment.

Growth rates, cell volume and pigment content

Growth rates were significantly affected by light treatment in both species (p <0.0001), with ~25% slower growth in *P. tricornutum* (**Figure 2.2A**) and ~50% slower growth in *T. weissflogii* (**Figure 2.2B**) under low light conditions. Growth was unaffected by pCO_2 in either species (**Figure 2.2**). *P. tricornutum* cells grown under low light were significantly smaller (~25%, P <0.0001) than those grown under high light (**Figure 2.2C**), with no effect of pCO_2 on cell size. In contrast, for *T. weissflogii,* cells grown at low light and low pCO_2 were significantly larger, roughly ~20%, ($F_{(3, 12)}$ = 22.49, P <0.0001; **Figure 2.2D**) than cells from all other growth conditions. Chlorophyll *a* and *c* content per cell did not change with treatment in *P. tricornutum* (**Figure 2.3**). There were, however, significant differences in both chlorophyll *a* and *c* content in *T. weissflogii* ($F_{(3, 12)}$ = 20.86 and 23.71 respectively, P

<0.0001; **Figure 2.3B and 2.3D**), with significantly higher chlorophyll *a* and *c* content in cells grown under low light (P <0.0001). We also saw a supressing effect of pCO_2 on chlorophyll *a* content at low light and chlorophyll *c* content at high light (P <0.0001, **Figure 2.3B and 2.3D, respectively**).

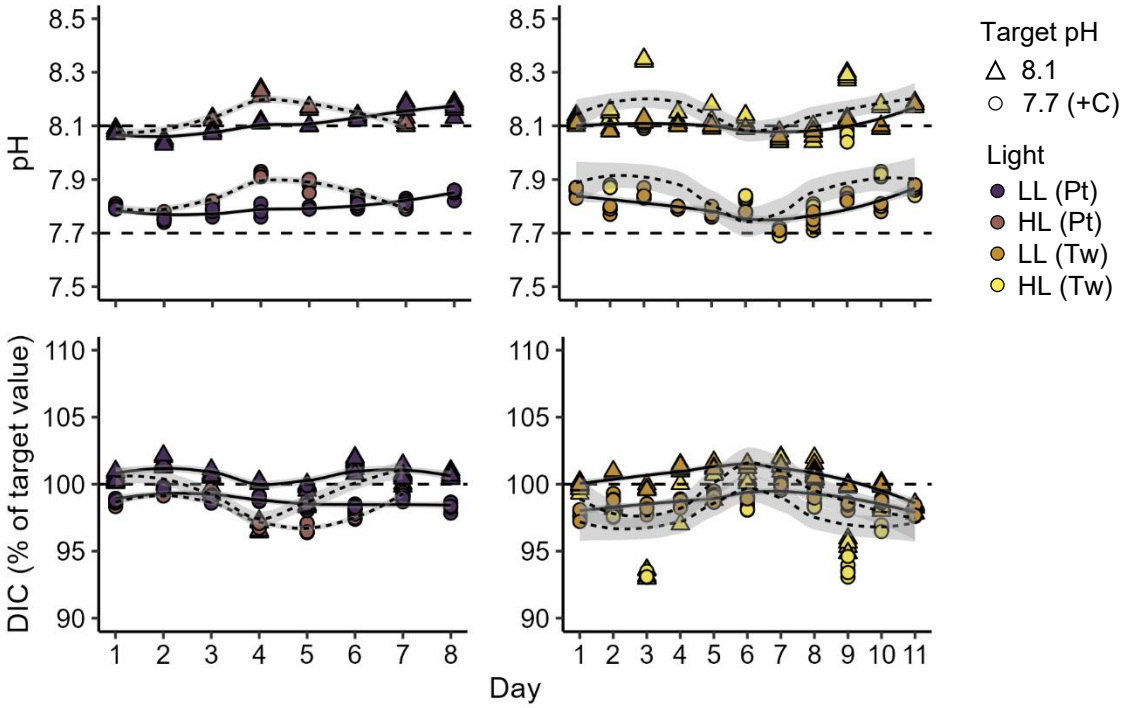

Figure 2. 1 pH and % DIC over time in cultures of *Phaeodactylum tricornutum* (left) and *Thalassiosira weissflogii* (right). Cultures were grown under control (~350 µatm, 8.1 pH) and projected future (~800 µatm; +C) pCO_2 concentrations with at low (20 µmol photons m^{-2} s^{-1}; LL) and high (200 µmol photons m^{-2} s^{-1}; HL) light. Data represent the mean ± shaded 95% CI, n=5. Dashed horizontal line indicates target values.

Table 2. 1 Seawater carbonate chemistry for *Phaeodactylum tricornutum* and *Thalassiosira weissflogii* grown under control (~350 µatm, 8.1 pH) and projected future (+C, ~800 µatm, 7.8 pH) pCO_2 concentrations at low (20 µmol photons m^{-2} s^{-1}) and high (200 µmol photons m^{-2} s^{-1}) light. Total Alkalinity and pH were measured using potentiometric titration on a Metrohm Titrino Plus. Remaining carbonate chemistry parameters (total inorganic carbon (DIC), pCO_2, carbonate and bicarbonate concentrations) were calculated using software CO2SYS. Culture carbonate chemistry was measured daily over a minimum of five weeks. Data represent the mean values of pre-adjusted media over time (5 weeks) ± SD. Treatment replication, n=5.

Species	Treatment	pCO_2	$pH_{(total)}$	DIC	HCO_3^-	CO_3^{2-}	CO_2	TA
Phaeodactylum	HL	335 ± 48	8.13 ± 0.05	2093 ± 34	1855 ± 51	226 ± 22	10.8 ± 1.6	2413 ± 21
tricornutum	HL+C	748 ± 97	7.83 ± 0.05	2239 ± 24	2086 ± 34	128 ± 13	24.2 ± 3.1	2403 ± 10
	LL	354 ± 42	8.11 ± 0.05	2113 ± 15	1882 ± 27	219 ± 21	11.4 ± 1.4	2423 ± 31
	LL+C	809 ± 66	7.79 ± 0.03	2252 ± 13	2106 ± 17	112 ± 8.4	26.1 ± 2.1	2403 ± 12
Thalassiosira	HL	309 ± 66	8.16 ± 0.08	2072 ± 53	1820 ± 86	241 ± 37	10.0 ± 2.1	2415 ± 16
weissflogii	HL+C	695 ± 188	7.87 ± 0.12	2220 ± 47	2056 ± 77	141 ± 36	22.5 ± 6.1	2406 ± 11
	LL	356 ± 29	8.11 ± 0.03	2107 ± 19	1879 ± 29	216 ± 13	11.5 ± 0.9	2413 ± 12
	LL+C	805 ± 91	7.80 ± 0.04	2250 ± 15	2104 ± 23	120 ± 11	26.0 ± 2.9	2402 ± 7

Table 2. 2 Photophysiological parameters from light curves of *Phaeodactylum tricornutum* and *Thalssiossira weissflogii*. Cultures were grown under control (~350 µatm, 8.1 pH) and projected future (+C, ~800 µatm, 7.8 pH) pCO_2 concentrations at low (20 µmol photons m^{-2} s^{-1}) and high (200 µmol photons m^{-2} s^{-1}) light. Maximum rate of electron transport (rETRmax), light utilisation efficiency (a), minimum and maximum saturating irradiance (Ek and Em respectively) and initial photoinhibiting irradiance (Eb). Parameters were obtained from the light curve according to Ralph & Gademann (2005). Data are the means ± SD, n=5, except HL *T. weissflogii* n=3. Superscript letters indicate significant differences between treatment groups using Tukey's post hoc multiple comparisons, α = 0.05.

Species	*Treatment*	*rETRmax*	*α*	*Ek*	*Em*	*Eb*
Phaeodactylum	HL	152±4.3^{a}	0.307±0.008	496±11.9^{a}	1347±32^{a}	1358±33^{a}
tricornutum	HL+C	161±4.2^{b}	0.318±0.011	507±30.6^{a}	1378±83^{a}	1389±85^{a}
	LL	126±2.9^{c}	0.305±0.004	411±5.9^{b}	1118±16^{b}	1125±16^{b}
	LL+C	130±1.5^{c}	0.309±0.004	421±4.2^{b}	1145±11^{b}	1152±11^{b}
Thalassiosira	HL	169±6.6^{a}	0.301±0.001^{a}	562±22.6^{a}	1529±61^{a}	1541±59^{a}
weissflogii	HL+C	177±5.4^{b}	0.324±0.007^{b}	545±9.1^{a}	1483±24^{a}	1494±23^{a}
	LL	153±3.9^{cd}	0.328±0.005^{b}	465±9.5^{b}	1265±26^{b}	1274±25^{b}
	LL+C	156±1.3^{d}	0.330±0.005^{b}	473±8.3^{b}	1287±23^{b}	1295±22^{b}

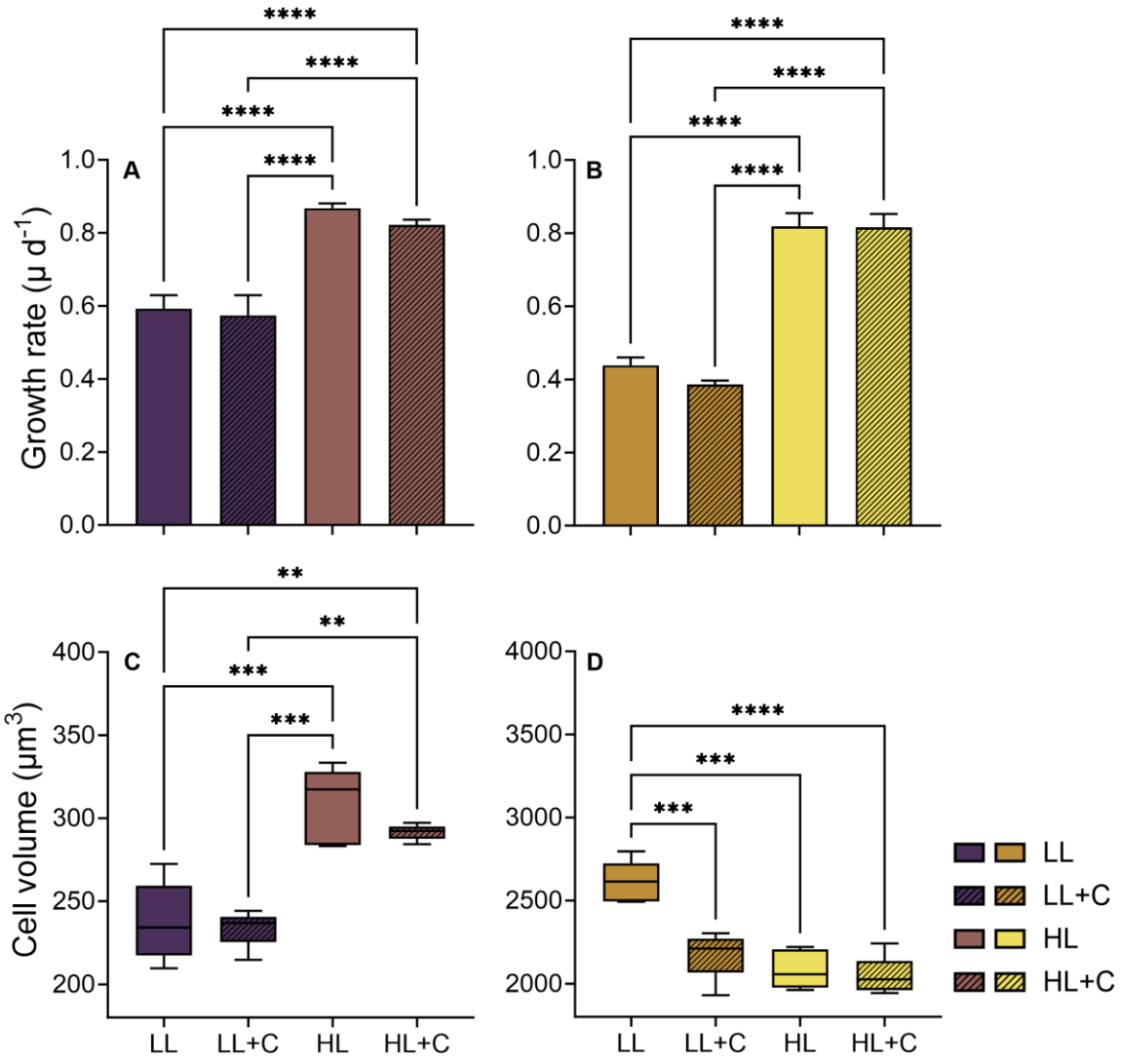

Figure 2. 2 Growth rates and cell volume of *Phaeodactylum tricornutum* (left) and *Thalassiosira weissflogii* (right). Cultures were grown under control (~350 µatm, 8.1 pH) and projected future (~800 µatm; +C) pCO_2 concentrations with at low (20 µmol photons m^{-2} s^{-1}; LL) and high (200 µmol photons m^{-2} s^{-1}; HL) light. Data represent the mean ± SD, n=5. Data were analysed for significance using a two-way ANOVA. Asterisks indicate significance (* p <0.05, ** p <0.01, *** p <0.001, **** p <0.0001).

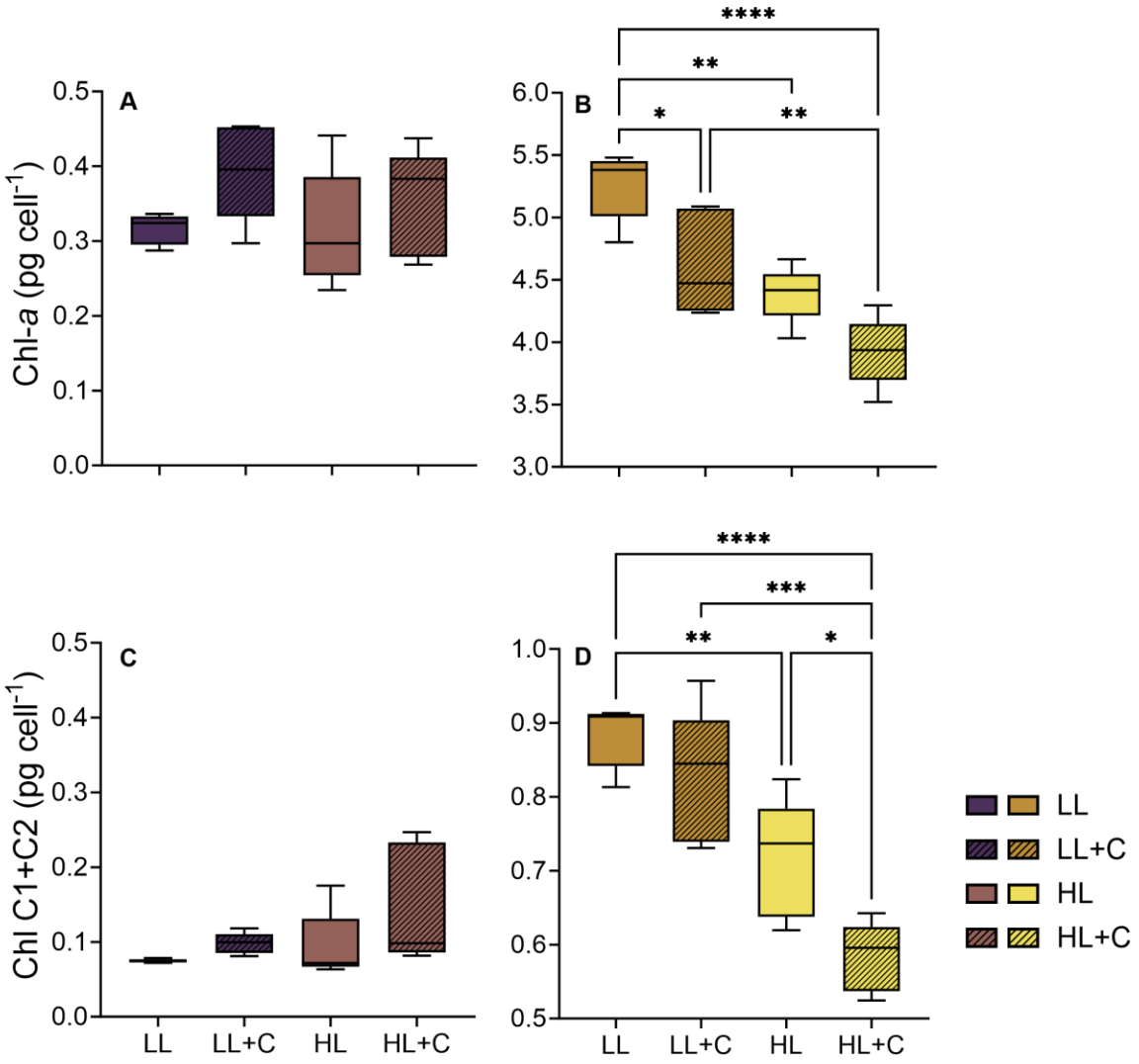

Figure 2. 3 Chlorophyll *a* and *c* of *Phaeodactylum tricornutum* (left) and *Thalassiosira weissflogii* (right). Cultures were grown under control (~350 µatm, 8.1 pH) and projected future (~800 µatm; +C) pCO_2 concentrations with at low (20 µmol photons m^{-2} s^{-1}; LL) and high (200 µmol photons m^{-2} s^{-1}; HL) light. Data represent the mean ± SD, n=5. Data were analysed for significance using a two-way ANOVA. Asterisks indicate significance (* p <0.05, ** p <0.01, *** p <0.001, **** p <0.0001).

Photophysiological effect of pCO_2 at low and high irradiance

Both species displayed higher relative electron transport rates (rETR) when grown in high light (HL) compared to low light (LL) conditions (**Figure 2.4A-B**). High pCO_2 resulted in a 2-6% increase in rETRmax for both *P. tricornutum* ($F_{(3, 12)}$ = 121.8, P <0.0001) and *T. weissflogii* ($F_{(3, 10)}$ = 54.66, P <0.0001 with the highest mean rETRmax of 176 µmol photons m^{-2} s^{-1} recorded in high light adapted, high pCO_2 *T. weissflogii* (**Table 2.2**). There was no measurable effect of pCO_2 on maximum quantum yield of PSII (F_V/F_M) in either species (**Figure 2.4**), however, there was an effect of light on the F_V/F_M of *T. weissflogii* grown at low light ($F_{(3,10)}$ = 11.85, P = 0.0012; **Figure 2.4D**). Saturating irradiances (*Ek, Em*) were higher (approx. 100-250 µmol photons $m^{-2}s^{-1}$) for cultures grown in high light and photoinhibition (*Eb*) was induced earlier under low light conditions in both species compared to those grown in high light (**Table 2.2; Figure 2.4**).

Biogenic silica (BSi) and silicification rates in response to light and pCO_2

Biogenic silica (BSi) quotas for *P. tricornutum* were extremely low (<0.08 fmol μm^2) with no measurable effect of treatment on bSi content (data not shown). For *T. weissflogii*, bSi per surface area was highest in the LL+C treatment and lowest in the LL treatment ($F_{(3,12)}$ = 74.66, P<0.001; **Figure 2.5A**). Silicification rates determined via PDMPO were below the detection limit for *P. tricornutum* (data not shown). Together with the low bSi quota, these data suggest minimally silicified *P. tricornutum* cells. Silica incorporation rates for *T. weissflogii* however, were highest at high light in low pCO_2 cultures (P = 0.001; **Figure 2.5B**). This was not the case for high light cultures at high pCO_2, which instead showed similar rates to the cells grown at low light (**Figure 2.5B**). Isolating the effect of pCO_2 on cell silica dynamics, we observed that bSi quota and growth rates showed inverse

relationships with pCO_2 condition (**Figure 2.5C**). Cells were more silicified with high pCO_2 at low light, but showed similar levels of bSi content at high light, irrespective of pCO_2 condition. We found that low pCO_2 cultures increased their silica content with increased irradiance (R^2 = 0.88, P <0.0001), but high pCO_2 cultures showed lower silica per surface area (R^2 = 0.83, P = 0.0002), despite growth rates doubling. Similarly, for cultures grown at low pCO_2 we saw a positive significant relationship between growth and silicification rates (R^2 = 0.87, P <0.0001; **Figure 2.5D**). However, under high pCO_2 conditions this relationship was lost, highlighting an interaction between light and pCO_2. To further support the role of light, we found strong relationships between silica production and maximum quantum yield of PSII (F_V/F_M) (**Figure 2.5E**). Biogenic silica content showed a significant negative relationship with F_V/F_M (R^2 = 0.77, P = 0.004) that became positive under high pCO_2 conditions (R^2 = 0.48, P = 0.025, **Figure 2.5E**). Similar relationships were found with PDMPO-derived silicification rates where we saw a strong correlation between silicification rate and F_V/F_M (R^2 = 0.81, P = 0.002; **Figure 2.5F**), but only under low pCO_2 conditions.

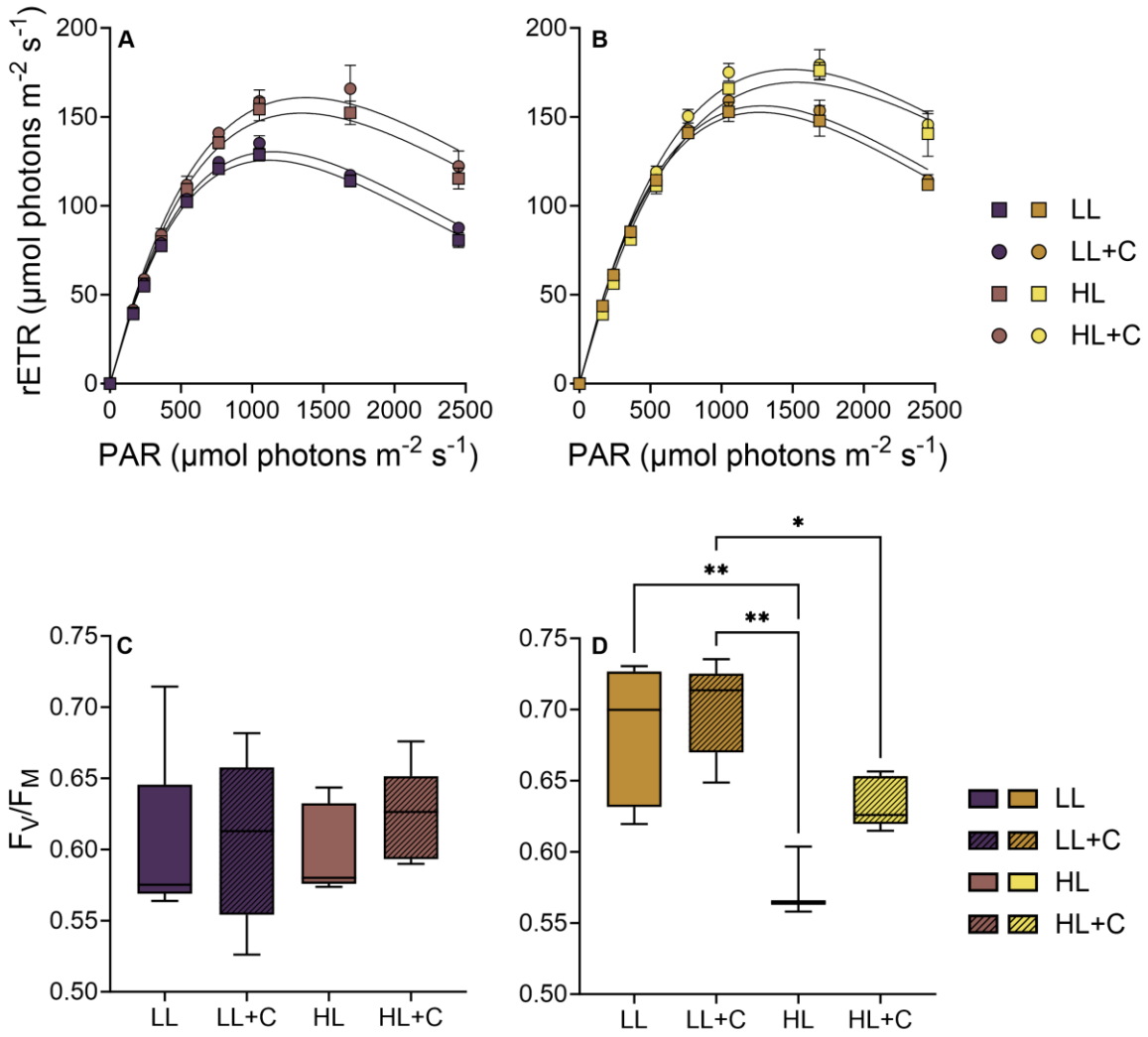

Figure 2. 4 Photophysiological parameters; steady-state light curves (A-B) and maximum quantum yield of PSII (F_V/F_M; C-D) of *Phaeodactylum tricornutum* (left) and *Thalassiosira weissflogii* (right) grown under control (~350 µatm, 8.1 pH) and projected future (~800 µatm; +C) pCO_2 concentrations with at low (20 µmol photons m^{-2} s^{-1}; LL) and high (200 µmol photons m^{-2} s^{-1}; HL) light. Data represent mean ± SD, n=5. Data were analysed for significance using a two-way ANOVA. Asterisks indicate significance (* p <0.05, ** p <0.01, *** p <0.001, **** p <0.0001).

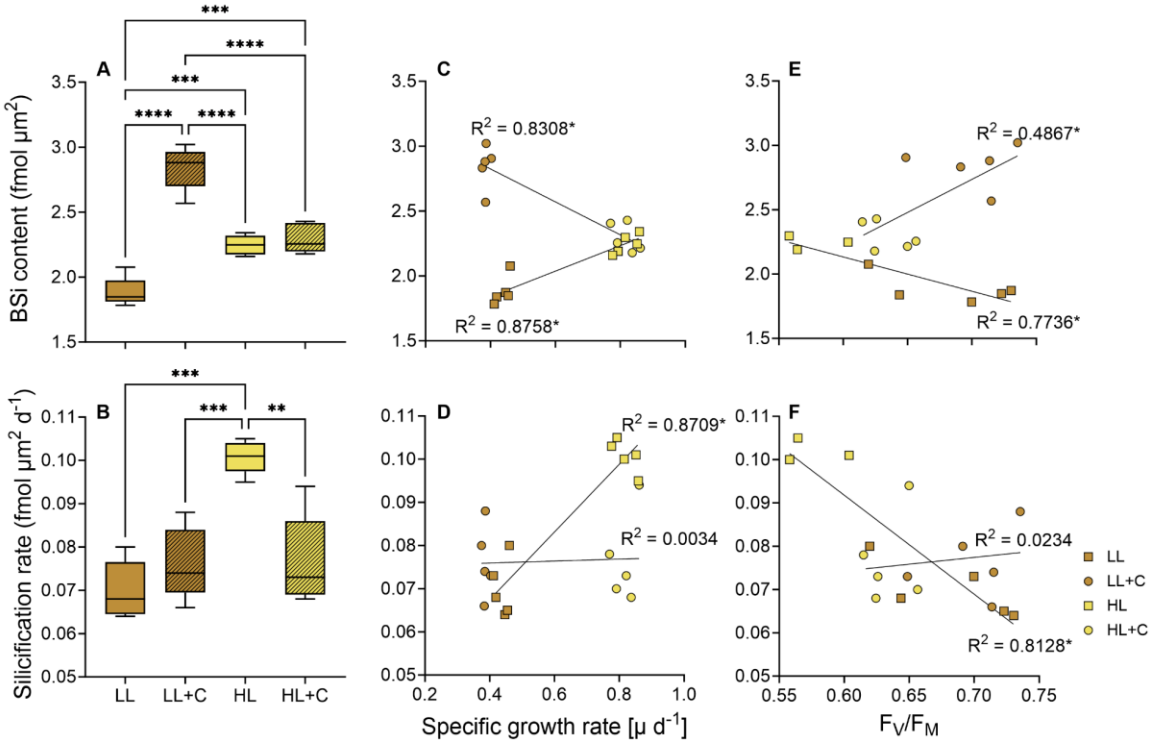

Figure 2. 5 Biogenic silica content (A), silicification rate (B), relationships between bSi content as a function of growth rate (C) and F_V/F_M (E), and relationships between silicification rates as a function of growth rate (D) and F_V/F_M (F) for *Thalassiosira weissflogii* grown under control (~350 µatm, 8.1 pH) and projected future (~800 µatm; +C) pCO_2 concentrations with at low (20 µmol photons m^{-2} s^{-1}; LL) and high (200 µmol photons m^{-2} s^{-1}; HL) light. Box plots represent mean ± SD, n=5 and data analysed using a two-way ANOVA, with asterisks indicate significance (* p <0.05, ** p <0.01, *** p <0.001, **** p <0.0001). Relationships were tested using linear regression, asterisk on the R^2 value indicates regression was significant at $P < 0.05$.

Effect of light and pCO2 on biomolecular composition

Changes in light and pCO_2 were found to alter the biomolecular profiles (**Figures 2.6 and 2.7**). In *P. tricornutum*, we saw significant increases in both lipid (saturated lipids ($F_{(3,109)} = 8.324$, $P < 0.0001$), ester carbonyl ($F_{(3,104)} = 4.985$, $P < 0.0029$)) and protein (amide II, $F_{(3,108)} = 10.8$, $P < 0.0001$) content, with high pCO_2 and high light, but no effect at low light. Growth irradiance had a significant influence on unsaturated fatty acid ($F_{(3,94)} = 4.245$, $P = 0.0074$), base pairs of nucleic acids ($F_{(3,90)} = 9.883$, $P < 0.0001$) and protein ($F_{(3,108)}$ $P < 0.0001$) content, with higher concentrations observed at low light, independent of pCO_2 (**Figure 2.6A**). Principal component analysis (PCA) confirmed the strong pCO_2 effect, with PC1 explaining 40.2% of the variation. PC2 was more closely associated with the light effect, which explained 19% of the variation (**Figure 2.6B**). The most pronounced response to pCO_2 was an increase in lipid and fatty acid content at high pCO_2, whereas proteins, unsaturated fatty acids and nucleic acid content were differentiated along PC2, with higher concentrations at low light (**Figure 2.6B**). For *T. weissflogii*, we saw a strong light effect (**Figure 2.7A**), with an increase in lipid (ester carbonyl ($F_{(3,108)} = 16.83$, $P < 0.0001$), and saturated lipid ($F_{(3,112)} = 26.48$, $p < 0.0001$)), and a decrease in protein ($F_{(3,112)} = 5.054$, $P < 0.0025$) content. The only pCO_2 effect evident in the biomolecular profile of *T. weissfloggi* was in saturated lipid content under high light conditions, where high pCO_2 resulted in significantly lower saturated lipid content (**Figure 2.7A**). The scores plot from the PCA confirmed the strong light effect, with PC1 explaining 35.1% of the variation, whereas PC2, associated pCO_2 explained 21% of the variation (**Figure 2.7B**).

Table 2. 3 Infrared (IR) band assignments and corresponding wavenumber for s-FTIR microspectroscopy used in this study.

Wave number (cm^{-1})	Band Assignment
~3011	ν(CH) – from unsaturated fatty acids[a]
~2852	ν_s(C−H) from methylene (−CH_2) from saturated lipids (CH-Stretch IV) [a]
~2921	ν_{as}(C−H) from methylene (−CH_2) from saturated fatty acids[a]
~1744	ν (C=O) ester carbonyl group from lipid triglycerides and fatty acids[a]
~1720	ν_s (C=O) – from base pairs of nucleic acids
~1549	Protein (Amide II mode); mainly δ(N−H) of amides[b]

[a]Vongsvivut et al. 2013; [b]Heraud et al., 2007

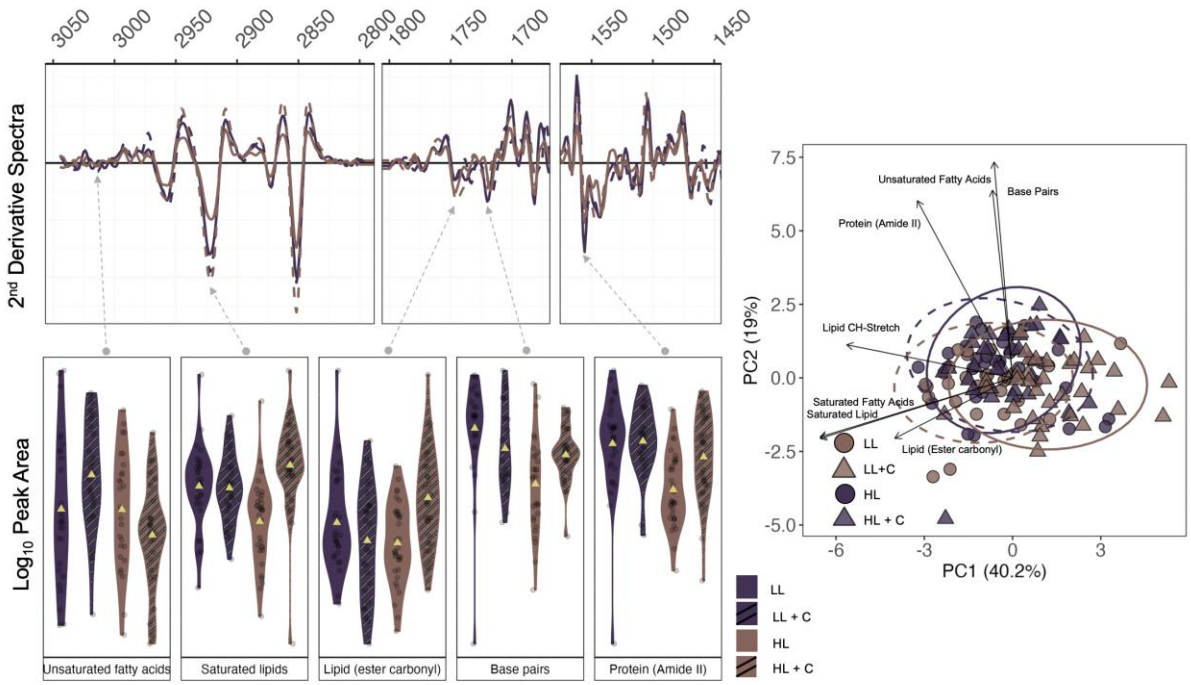

Figure 2. 6 Normalised 2nd derivitive spectra and violin plots of integrated peak area of selected biomolecules (A) and principal component analysis (PCA) scores plot with vectors of biologically relavent peaks (B) for *P. tricornutum* grown under control (~350 µatm, 8.1 pH) and projected future (~800 µatm; +C) pCO_2 concentrations with at low (20 µmol photons m^{-2} s^{-1}; LL) and high (200 µmol photons m^{-2} s^{-1}; HL) light. Spectra show averages of cells from each treatment, violin plots show distribution of peak areas for individual cells from within each treatment, with the mean indicated by the yellow diamond. Ellipses on the scores plot denote the 95% confidence interval.

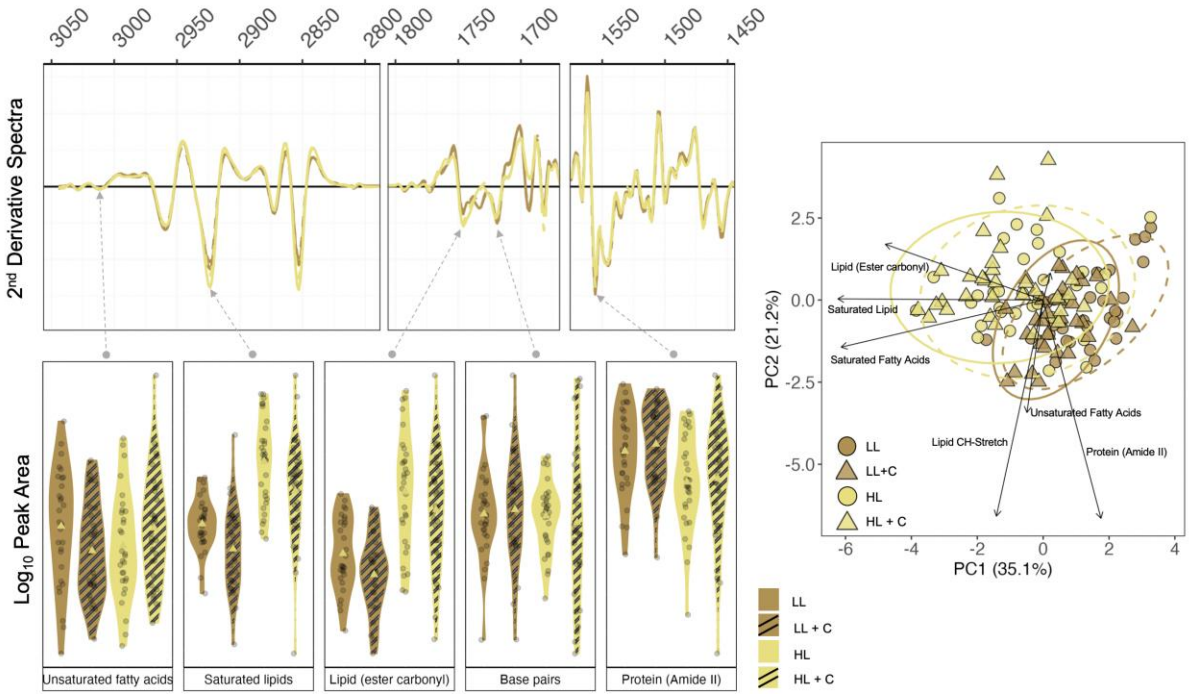

Figure 2. 7 Normalised 2nd derivitive spectra and violin plots of integrated peak area of selected biomolecules (A) and principal component analysis (PCA) scores plot with vectors of biologically relavent peaks (B) for *T. weissflogii* grown under control (~350 µatm, 8.1 pH) and projected future (~800 µatm; +C) pCO2 concentrations with at low (20 µmol photons m−2 s−1; LL) and high (200 µmol photons m−2 s−1; HL) light. Spectra show averages of cells from each treatment, violin plots show distribution of peak areas for individual cells from within each treatment, with the mean indicated by the yellow diamond. Ellipses on the scores plot denote the 95% confidence interval.

Discussion

In this study, we used an orthogonal design of pH and light for simulating shoaling of the mixed layer depth under a predicted future ocean scenario to elucidate the effect on diatom physiology, looking beyond growth rate and productivity as sole indicators for response. We measured and compared morphological, physiological and metabolic responses to high and low irradiance at two pH levels (representing contemporary and projected future ocean conditions) in two diatom species, *Phaeodactylum tricornutum* and *Thalassiosira weissflogii*. Although a commonly used model species, *P. tricornutum* is unlike most diatoms. It is a facultative silicifier (De Martino *et al.*, 2007) with pleiomorphic abilities, allowing it to change its shape in response to environmental conditions. These inimitable characteristics are interesting to explore, as they may prove to be important traits for responding to rapid environmental change, but are atypical of most diatom species. As an obligate silicifier, *T. weissflogii* represents a more typical diatom for investigating general metabolic and physiological changes in response to ocean acidification (lowered pH) and shoaling (high light), offering potential insight into ecological implications for diatoms in future ocean conditions. Consistent across both species were significant changes in growth and photophysiology in response to irradiance, but little to no effect on these traits with changes in pCO_2. Growth rates increased under high light, whilst light-adaptation properties, such as F_V/F_M, chlorophyll *a* and *c* quotas, were greater under sub-saturating conditions, congruent with previous studies (Li *et al.*, 2014; Heiden *et al.*, 2016).

A key aspect to this study, was interrogating the influence of high light and high pCO_2 on diatom silica production and biomolecular content, as significant changes to their carbon and silica allocation has the potential to modify pelagic food webs and revise

budgets of silicon and carbon fluxes (Tréguer *et al.*, 2018). In *P. tricornutum*, we found no significant production of silicate, suggesting that silica incorporation was not advantageous in its current growth form, nor under the tested conditions. Given its ability to grow without silicate (De Martino *et al.*, 2007), this result was perhaps to be expected. The absence of a frustule suggests that using *P. tricornutum* as a 'model' diatom species obviates uncovering important details when wanting to understand broad scale ecological shifts or fine scale mechanistic adaptations, such as frustule morphogenesis, to ocean change. Unlike *P. tricornutum,* acidification significantly affected silicification rates in *T. weissflogii*, a finding consistent with an earlier study on Antarctic diatoms (Petrou *et al.,* 2019). We found a decrease in the rate of new silica deposition under high pCO_2, but only at high irradiance. This decline was independent of many other physiological, metabolic and morphological changes, including bSi content and growth rate, explaining how previous studies may have overlooked this effect of pH and suggesting a potentially unique effect of acidification on diatom biomineralisation and its regulation. In contrast to previous work that found a negative correlation between bSi content and growth rate in *T. weissflogii* grown at a range of pCO_2 concentrations (Li *et al.*, 2019), a negative correlation between growth rate and bSi was only evident at high pCO_2 in this study, implicating differences in culture nutrient availability and growth irradiance as potential factors in determining pCO_2 sensitivity.

Evidence exists for the role of the frustule in photo-regulation (Noyes *et al.*, 2008; Ellegaard *et al.*, 2016). We saw that under low pCO_2 conditions, high light resulted in lowered photosynthetic capacity, yet higher silica quota and silicification rates in *T. weissflogii*, supporting the idea that the frustule may filter incoming light, aiding photophysiological resilience (Ellegaard et al., 2016; Goessling *et al.*, 2018). Assuming a

photoprotective role of the frustule, it is possible that when light levels increase, energy is shuttled from photosynthesis to frustule formation, assisting in protecting the cell from photoinhibition. Under high pCO_2 this relationship was lost, possibly due to the increase in carbon availability, enabling enhanced photosynthetic capacity, thereby reducing the cells reliance on the photoprotective role of the silica frustule, a hypothesis supported by the low chl *c* content measured in the high light, high pCO_2 cultures. These data support previous studies, that highlight an important interplay between light and pCO_2 on diatom growth (Gao *et al.*, 2012_a), but add new evidence of the important role of the frustule, whereby the effects observed here link growth, photosynthesis and silica dynamics in an intricate web of energy exchange to optimise cell homeostasis.

Although *P. tricornutum* showed no variation in silica content, its nutritional state was affected by both light and pCO_2. Our results showed that pCO_2 significantly increased lipid production at high irradiance, in line with previous studies (Wu *et al.*, 2019; Duncan *et al.*, 2022). An increase in lipids were also measured in *T. weissflogii*, but only in response to increased light. Common to both species was a reduction in cellular protein content at higher irradiance. If the increased lipid and decreased protein content under high light is found to be a general trait of diatoms, greater residence time in surface waters predicted under ocean warming, could drive a long-term decline in diatom protein:lipid content, affecting energy transfer throughout the food web (Ullah *et al.*, 2018).

There is no doubt that ocean acidification combined with shoaling will bring about broad ecological changes to diatoms in the photic zone, through the restriction of nutrient input, prolonged exposure to high light and UV radiation, and higher grazing and remineralisation rates (Gao *et al.*, 2012_a, 2012_b; Ganapathy *et al.*, 2017; Gao *et al.*, 2019).

Using current knowledge and the data presented here, we can start to build a portrait of present and future diatom ecophysiological processes. Under contemporary ocean conditions (low-pCO_2) diatom silicification was enhanced by increasing irradiance, likely due to greater energy availability, greater need for photoprotection, and faster growth. Ecologically, this could represent a trait to help regulate ballast (Arrieta *et al*., 2020), whereby cells in sunlit surface waters silicify more, becoming negatively buoyant and sinking down more readily through the water column (Raven & Waite, 2004). However, the increase in light energy has also been shown to increase floating capacity (Petrucciani *et al*., 2023), which could be driven by greater lipid production, such as was seen here, potentially countering any increased ballast. Under projected future ocean conditions (high- pCO_2), however, silicification rate did not increase with increased irradiance, possibly due to changes in CCM activity (relief from carbon limitation) and reduced photoinhibition. These conditions also elicited lower saturated lipid content. Together, these light and pCO_2-induced cellular adjustments mean a change in diatom C:Si stoichiometry, potentially influencing trophic energy transfer efficiency, vertical migration and elemental flux. Independent of the mechanisms at play, changes to diatom biomolecular content and frustule nanostructure are important, with scalable impacts, from the sub-cellular to regional biogeochemistry. Therefore, the role of growth conditions in regulating diatom energy partitioning and frustule formation needs to be fully resolved to complete our understanding of the function of marine diatoms in a future ocean.

Acknowledgements

BF-L, RJD and AMT are supported by an Australian Government Research Training Program Scholarship. RJD has also receives support from the Australian Institute of Nuclear Science and Engineering (AINSE Ltd.) Postgraduate Research Award (PGRA). This research was supported by an Australian Research Council grant DP210101360 awarded to KP. Part of this work was funded by the Australian Synchrotron through merit-based beamtime awarded on the Infrared Microscopy (IRM) beamline at the Australian Synchrotron, part of the Australian Nuclear Science and Technology Organisation (ANSTO) (AS233/IRM/20349) awarded to KP and DAN. The authors would like to thank the IRM beamline scientists at the Australian Synchrotron.

Chapter 3: Disentangling species-specific physiological and morphological responses to ocean acidification in a coastal diatom community

Abstract

Ocean acidification (OA) is a pervading global threat to marine ecosystems, impacting all trophic levels, including phytoplankton. How these microorganisms will fare in changing ocean conditions is still unclear, with positive, neutral and negative responses being reported. Oftentimes however, these results stem from either single strain culture work (negating within, across and multi species interactions) or bulk assessments (potentially masking outliers in phenotypic response and/or taxonomic variability). Here, we combine community level responses with single cell analysis to investigate the impact of OA on diatom silicification, taking a close look at the individual contributions of each species to the overall response. We measured and compared physiological responses of phytoplankton communities exposed to two pH levels (representing current and projected future ocean conditions). To tease apart species-specific responses, we focussed on ten diatom taxa, *Asterionellopsis glacialis*, *Chaetoceros didymus*, *Cylindrotheca closterium*, *Eucampia zodiacus*, *Leptocylindrus danicus*, *Navicula* sp., *Pseudo-nitzschia* spp.*, Rhizosolenia setigera, Thalassiosira* spp. >20 µm and *Thalassiosira* spp. <20 µm. Our study found that OA reduced total diatom biomass by 33% and species diversity by 25% in the natural community. We saw a measurable negative effect of OA on community silica incorporation, but when analysed at a species level, we found that two species increased cell-specific silicification at low pH, with no effect detected in the other species. These data suggest that the influence of OA on community silica production is a result of negative effects on growth rather than directly altering silicon incorporation rates. Furthermore, in taking a single-celled approach, we revealed that not all diatoms are equal, with variability in response to lowered pH, level of phenotypic plasticity, and physiological strategy of adjustment. The findings from this

study extend the geographic range of our current knowledge on diatom silicification responses to OA and highlight the potential impacts of diatom loss from OA for the sustainability of food webs and biogeochemical cycling.

Introduction

One of the most pervasive threats to marine communities globally is ocean acidification (OA); a process whereby increasing anthropogenic carbon emissions are absorbed by oceans, causing a decrease in seawater pH (Orr *et al*., 2005). With atmospheric pCO_2 concentrations predicted to rise beyond 1000 ppmv by 2150, ocean pH could decline by as much as 0.5 units (Haugen & Drange, 1996; Hofmann and Schellnhuber, 2010; Gattuso *et al*., 2015). Concurrent with increasing atmospheric and oceanic pCO_2, is global warming; whereby the greenhouse effect is warming oceans (Sarmiento *et al*., 2004). While these effects will be felt across all oceans, some areas are experiencing faster declines in pH and increases in sea surface temperature (SST) than the global average. These regions are referred to as 'ocean hotspots' (Wernberg *et al*., 2011; Hobday & Pecl, 2014). Nearshore, coastal habitats, such as those along Australia's eastern seaboard and around the Tasman Sea, are such areas, as they are projected to feel the effects of warming sooner than most other parts of the global ocean.

Although data on long-term trends in ocean acidification around Australia are sparse, records from the National Reference Station Port Hacking (NRS PH), a long-standing oceanographic time series mooring close to Sydney, reveal that the region is experiencing pH levels below the global mean (Lenton *et al*., 2015, 2016) and continued warming SST anomalies over the last few decades (**Figure 3.1**). As a region of clashing water bodies, the area is oceanographically dynamic; The East Australia Current (EAC)

moves down along the coast from the Coral Sea, bringing with it warm, low nutrient waters from the South Pacific Gyre (**Figure 3.1**). Once these waters reach New South Wales, however, they encounter some resistance from the Tasman Sea, and start to form warm and/or cold core eddies (Suthers *et al*., 2011; Macdonald *et al*., 2016). Whilst the warm core eddies generally drag low nutrient waters downward, and are commonly perceived as features of low productivity, several phytoplankton taxa have been shown to monopolise on these conditions and are able to proliferate in these eddies (Firme *et al*., 2023). In contrast, the cold core eddies are typically known to be highly productive, as they promote vertical mixing with deeper ocean waters and pull nutrients up to the surface, stimulating high biomass and generally favouring bloom-forming phytoplankton (Thompson *et al*., 2011 Marchesiello & Middleton, 2000) (**Figure 3.1**). This dualism means that phytoplankton, both tropical species brought down in the EAC and local temperate species, have opportunity to thrive in these waters, increasing overall biodiversity. However, with predicted changes to ocean temperature, mixing and pH, the balance of these communities may shift and for these species to continue thriving, they will have to draw on their plasticity to adapt at such short time scales.

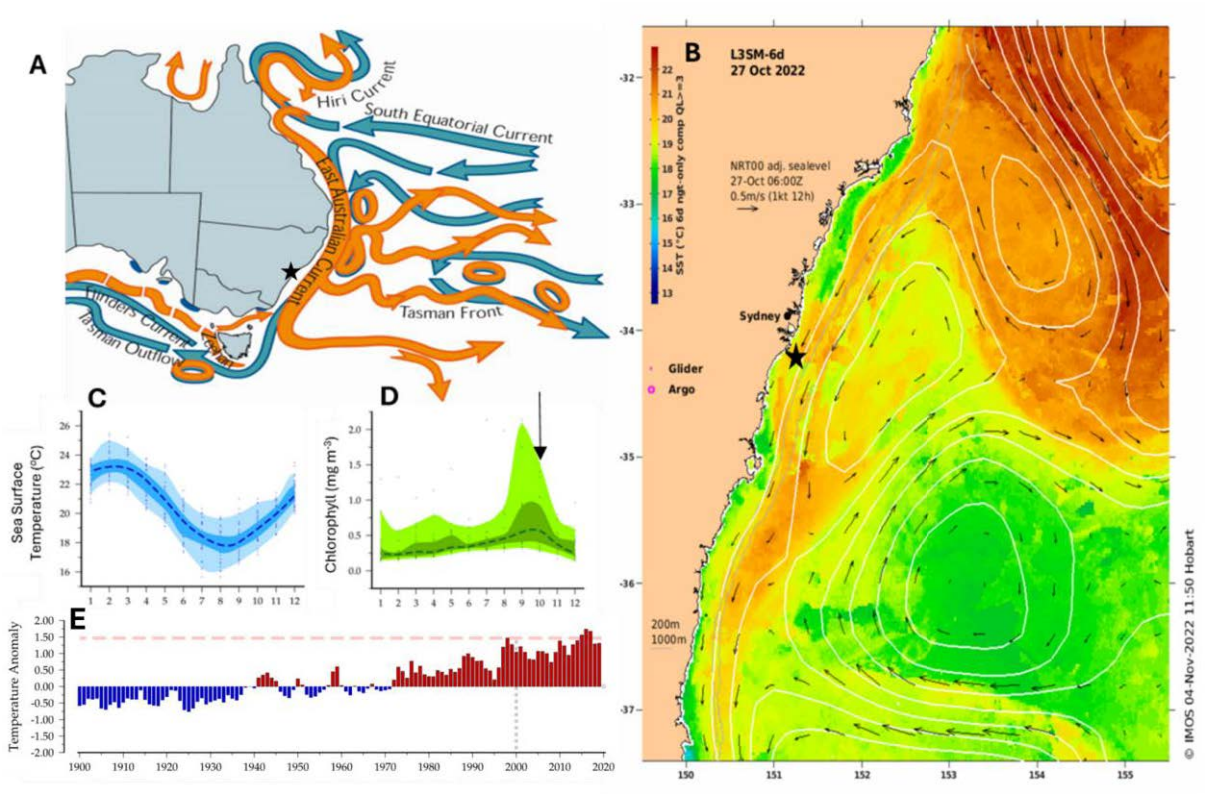

Figure 3. 1 (A) Schematic showing the inflow of the South Equatorial Current into the Coral Sea from the South Pacific Gyre. The East Australian Current flows south from the Coral Sea towards Hobart, Tasmania. Subsurface currents are shown in blue whilst surface currents are in orange (Ridgeway & Hill, 2009). (B) shows the 6-Day Sea Surface Temperature (SST) of the New South Wales, Australian coastline on 27th of October 2022 with the position of the National reference station (NRS) Port Hacking, indicated as a black star (-34.117583, 151.21815) Data were sourced from Australia's Integrated Marine Observing System (IMOS) – IMOS is enabled by the National Collaborative Research Infrastructure Strategy (NCRIS)**.** (C-D) show mean sea surface temperature (SST) and chlorophyll a (mg m^{-3}) respectively throughout the year (2022) at Port Hacking time series, sampling time indicated by black arrow. Wintertime (June - August) deep-water mixing stimulates nutrient upwelling, confirmed by maximum chlorophyll *a* in September. (E) shows yearly temperature anomaly increasing since 1900, with last 50 years showing only positive anomalies. Data taken from COPEPODITE (O'Brien & Oakes, 2020).

Understanding how phytoplankton communities interact and respond to change can be challenging. We are currently constrained in our understanding of how OA will affect ocean biogeochemistry by the complexity of individual physiologies and the biological interactions within their communities. Bulk assessments offer snapshots into how the whole community might fare under a given condition but are unable to provide information on, or account for, outliers in phenotypic responses, nor do they expose important taxonomic changes (Lima-Mendez *et al.,* 2015; Lomas *et al*., 2021; Aubert *et al*., 2022). On the other hand, using single strain culture experiments to extrapolate how

other phytoplankton might respond is fraught with limitations, both within species and across species, as well as being insufficient in understanding the potential role of multi-species interactions (Cottingham *et al*., 2005; Riebesell & Gattuso, 2015; Kreyling *et al*., 2018). Several studies have shown that within and between species responses differ under environmental change (Nicotra *et al*., 2010; Franks & Hoffmann, 2012; Ajani *et al*., 2021), therefore this high variability necessitates assessing individual taxonomic responses within a natural community, in an ecologically relevant environmental setting (Havenhand *et al*., 2010), if we are to elucidate potential floristic shifts and identify 'winners and losers' of climate change in our marine systems.

Diatoms (Bacillariophyta) are a ubiquitous and diverse group of marine phytoplankton, responsible for 40% of ocean primary productivity (Nelson *et al*., 1995). Diatoms are unique amongst the phytoplankton in that they are dependent on silicic acid to produce silica cell walls (frustules). This regulation of silicon in their metabolism makes them important in biogeochemical cycling of marine silicon (Yool & Tyrell, 2003; Struyf *et al*., 2009). Furthermore, the deposition of silica into their frustule increases their ballast, which aids sinking, and when combined with their productivity, makes them important for ocean carbon sequestration (Buesseler, 1998; Smetacek, 1999; Tréguer *et al*., 2018). It is through this complex interplay of silica content, growth and productivity that determines the export potential of a given diatom species (Smetacek, 1999; Baines *et al*., 2010; Tréguer *et al*., 2018). Therefore, alterations in any of these traits has the potential to influence export, which in turn, can affect the biological carbon pump; the process by which carbon dioxide (CO_2) is utilised in photosynthesis, converted to organic carbon and sequestered to the deep ocean via sinking particles.

As with growth, the rate at which diatoms deposit silica to their frustule (silicification) has been shown to vary with environmental conditions (Baines *et al.*, 2010; Javaheri *et al.*, 2015), however our understanding of the relationship between ocean acidification and diatom silicification is still in its infancy. Previous studies have looked at the mechanistic relationship of pH and silica biomineralisation (Milligan & Morel., 2002), synergistic effects of irradiance and CO_2 on silicification (FitzGerald-Lowry *et al* (**Chapter 2**, under review)) and environmental pH shift on silicification (Hervé *et al.*, 2012). Notably, Petrou *et al.*, (2019) conducted mesocosm experiments on a nearshore Antarctic community (1km offshore from Davis Station, 68° 35' S, 77° 58' E), an area important for carbon uptake and sequestration (Marinov *et al.*, 2006; Landschützer *et al.*, 2015). They exposed the community to increasing levels of CO_2 and found that silicification rates of the diatom community strongly diminished, declining more than 60% in extreme future prediction conditions (Petrou *et al.*, 2019). Whether this response is regionally specific, affecting only polar species or representative of multiple coastal habitats is yet to be validated. Importantly, through single-cell analyses they were also able to show that different diatom species responded to differing degrees (Petrou *et al.,* 2019), highlighting the importance of including taxon-specific resolution in mixed community experiments. From these data it is evident that to complete our understanding of diatom responses to OA, we need to probe, in fine-scale detail, diatom community dynamics across a broad latitudinal range of ecosystems.

Here we investigated species specific silicification rates within a natural coastal phytoplankton community following a 7-day exposure to modern and future predicted ocean pH. While we were unable to completely avoid bottle effects, the inclusion of the whole microbial community (phytoplankton, bacteria and viruses) provided reasonable

representation of among and between trophic level responses, thereby affording a better predictive ability when extrapolating to natural systems (Cottingham *et al*., 2005; Kreyling *et al*., 2018). By matching community-level responses with individual single-cell analysis, we start to see the direct effect ocean acidification plays on diatom silicification and delineate each species contributions to the overall response.

Methods

Experimental design

Seawater was collected from the National Reference Station (NRS) oceanographic site, Port Hacking, 7 km off South Sydney coast (-34.117583, 151.21815) and filtered through a 210 µm mesh to remove larger zooplankton and debris into two, 20 L carboys. Seawater was then left overnight (12 h), ready for sub-sampling the next day. The morning of experimental setup, alkalinity and pH of the carboys were measured after being well mixed. Two litre Schott bottles (microcosms) were filled with filtered seawater to the base of the neck, reducing headspace to less than 5 mL to minimise gas exchange and equilibration with air (Riebesell *et al*., 2011). Microcosms were then enriched with F/200 medium according to Guillard & Ryther (1962), acid/base adjusted to target treatment conditions (Schulz *et al*., 2009; Gattuso *et al.,* 2010) and well mixed. The coastal communities were incubated at 18 °C in temperature and light controlled water baths, with light supplied at 100 µmol photons m^{-2} s^{-1} on a 12:12h light:dark cycle. Conditions included two pH levels (five replicates per treatment), representing current and future (year 2140) pH scenarios (pH 8.1 and 7.62, total scale). Total Alkalinity, pH, nutrient concentration and photosynthetic capacity were measured daily to ascertain cell health and maintain treatment conditions. Any water removed from the sampling was replaced

with pH adjusted filtered seawater for each treatment respectively. Phytoplankton communities were exposed to their respective conditions for seven days before analyses.

CO_2 perturbations and seawater chemistry

Microcosm carbonate chemistry was maintained daily to limit dissolved inorganic carbon (DIC) consumption to less than five percent of total (Riebesell *et al*., 2011), stabilise parameters and negate treatment overlap. Fifty mL were removed for analysis (carboys and/or microcosm bottle) and analysed though potentiometric titration using a Metrohm Titrino Plus, to obtain the Total Alkalinity (TA) and pH (total scale). To maintain an accurate TA and/ or DIC value, samples were gently filtered (0.2µm) to remove cells due to potentially altering TA/DIC measurements (Gattuso *et al*., 2010). The pH probe was three-point calibrated daily (pH 4, 7, 10; chem supply laboratory reagent, 500M) and TA values calibrated to certified reference material (Batch #196, Dickson, 2010). R package "seacarb" was used to calculate remaining carbonate chemistry parameters based on CO2SYS (Lewis & Wallace, 1998) with known nutrient concentrations (Total P and S µmol/kgSW), salinity (PSU) and temperature (°C). A. G. Dickson (1990) KSO_4 and Uppstrom (1974) B_l constants were used with Mehrbach *et al.,* 1973 refit by A. G. Dickson & Millero (1987) for K1 and K2 constants. Acid/base adjustments were calculated to microcosm volume (2280 mL) and adjusted using one molar hydrochloric acid (HCl), sodium carbonate (Na_2CO_3) and sodium hydroxide (NaOH) (Gattuso *et al.,* 2010). The remaining volume was refilled with pH-adjusted F/200 media (50mL).

Phytoplankton growth and photophysiology

Phytoplankton community growth and health was assessed daily through measuring photosynthetic health and nutrient concentration. For photosynthetic health, 2 mL aliquots were low light adapted (<2 µmol photons m^{-2} s^{-1}) for 15 min prior to exposure of a saturating pulse of light (width=0.8s, intensity=8). Maximum fluorescence (Fv/Fm) was calculated from minimum (F*o*) and maximum (F*m*) fluorescence ((F*m*-F*o*)/F*m*) using a Pulse Amplitude Modulated (PAM) fluorometer (Water PAM; Walz Effeltreich, Germany). For assessment of nutrient concentrations and thereby community growth as a function of nutrient removal, colorimetric analyses of nitrate/nitrite and silicate concentrations were performed following the methods of Schnetger *et al.*, (2014) and Ringuet *et al.*, (2011) respectively. Briefly, for nitrate/nitrite assays, 180 µL of sample (in triplicate) were placed into a 96-well microplate. A reducing agent (120 µL) was added and incubated at 45 °C for 60 min before being analysed. The microplate was gently shaken (60 rpm) to remove air bubbles before absorbance measured at 540 nm. Silicate assay samples (200 µL) were placed in a 96-well microplate (in triplicate) and 20 µL of acidified ammonium paramolybdate added and gently shaken for 30 min. Oxalic acid (20 µL) and ascorbic acid (10 µL) were then added and shaken for a further 30 min before absorbance was measured at 810 nm. Both assays were run on a TECAN Spark ® Multimode Microplate Reader (Spark Control version 3.1).

Chlorophyll a and c measurements

To determine pigment content, 100 mL of sample was filtered onto a 47 mm glass fibre filter (Whatman), snap frozen in liquid nitrogen and stored at -80°C. For analysis, filters were placed in 3 mL of 90% acetone for 16 h, centrifuged at 3214 RCF for five minutes.

Chlorophyll *a* and *c* absorbance was measured in a Shimadzu (UV-1280) spectrophotometer using the wavelengths of 630 and 664 nm and calculated according to Ritchie (2006).

Silicification and biogenic silica (bSi) content

Bulk biogenic silica content (biologically produced silica) and silicification rate were measured following the methods detailed in McNair *et al.*, (2015), whereby the fluorescent dye PDMPO (2-(4-pyridyl)-5-((4-(2-dimethylaminoethylaminocarbamoyl) methoxy) phenyl) oxazole) was added to a 24-h incubation. This fluorophore binds to newly deposited silica in the frustule and therefore can be used to measure the rate of newly deposited silica. Incubations were carried out initially on pre-treated seawater to ascertain in-situ biogenic silica and after eight days of incubation in the microcosms, to assess treatment effect.

Polycarbonate flasks were filled with 170 mL of pH adjusted seawater amended with F/200 nutrients (N=5 per treatment) and spiked with Lysosensor Yellow/Blue DND-160 (PDMPO, ThermoFisher Scientific, Australia) to a final concentration of 0.125 µM PDMPO. At the end of the incubation, samples were filtered onto polycarbonate filter paper (47 mm, 0.4 µm, Nucleopore, Whatman). Three washing steps were then carried out; an initial 0.2 µm filtered seawater rinse to remove extracellular PDMPO, followed by covering the filter with 2 mL 10% HCl for two minutes to lyse cells, disrupt cellular membranes and to remove unbound intracellular dye, and lastly a MilliQ rinse to remove any HCl, cellular components and fluorophore residue. Washed filters were snap frozen in cryovials using liquid nitrogen and stored at -80 °C. The same method was used for the initial community, however with unadjusted seawater before the incubation.

PDMPO and bSi determination

To determine bSi content and silica incorporation rates, diatom frustules were solubilised via a hot-alkaline-digest (boiling in 0.2M NaOH for 3h) according to Leblanc & Hutchins (2005). Fluorometric analysis was performed using a Tecan Infinite M1000 spectrofluorometer (Company, Switzerland), at excitation of 375 nm and data were compared against a PDMPO standard curve (0, 5, 10, 25, 50, 100 µM Si, R^2 = 0.9991) prepared using the digestion (NaOH-HCl) matrix. Following the methods of Strickland and Parsons (1968), modified by Nelson *et al.*, (1989), an aliquot of the alkaline-digest and was used to measure reactive silicate. Briefly, an ammonium paramolybdate solution (1 mL) was added to the supernatant of digested cells, vortexed and let stand for 10 min. A reducing agent (1.5 mL) was then added, vortexed again and left for three hours to react. Samples were then aliquoted into a 96-well plate (in triplicate) and absorbance set to excite at 810 nm (Cary Eclipse, Agilent Technologies, USA). Data was compared against a sodium metasilicate stock solution (0, 5, 25, 50, 100, 200 µM Si, R^2 = 0.990) with quantitative PDMPO incorporation converted to biogenic silica incorporation using the ratio of 912.6 mol $bSiO_2$ per mol PDMPO when Si concentration was < 3 µmol (McNair *et al.,* 2015).

Particulate organic carbon and nitrogen

Preparation of particulate organic carbon and nitrogen (POC/PON) sampling was carried out by filtering 100 mL onto pre-combusted (450 °C for 5 hours) 0.7 µm, glass microfiber filters (Whatman) and stored in pre-combusted aluminium foil at -80 °C. Three replicates per initial carboy (n=6), one per biological replicate at time final (n=10) and six blanks (100 mL filtered seawater amended with F/200) were filtered. For processing, sample

)filters were thawed, acidified with 10% HCl until saturated to remove carbonates, and dried for 24 hours at 60 °C. Filters were folded, wrapped and pelletised into 9 mm tin cups (Elemental Microanalysis, UK) and sent to the Biogeochemical Stable Isotope Facility (University of Hawaii at Mānoa). Carbon and nitrogen values were determined using an elemental analyser (Cos - tech ECS 4010 Elemental Combustion System using a Zero Blank Autosampler) and mass spectrometer (Thermo-Delta V Advantage).

Taxonomy and microscopy

For taxonomic identification and quantification, in-situ community composition and cell counts were collected from the open access Australian Ocean Data Network (AODN) for the 27th October 2022 (day of water collection). For microcosms post experiment, 50 mL aliquots of each microcosm were sampled on day seven and fixed with Lugol's solution. Samples were left to settle for two days before being concentrated via aspiration of the supernatant. Concentrated cells were then identified and enumerated via light microscopy using a Sedgwick Rafter chamber until more than 400 cells were recorded. For cell specific silicification, a 2 mL fixed sample (2% glutaraldehyde) was centrifuged for 10 min at 3000 RCF and the supernatant removed. Pellets were then incubated in pure ethanol at 80°C for three hours to degrade chlorophyll and minimise autofluorescence. This method was adapted from McNair *et al*., (2015) after trials with methanol for degradation of autofluoresence (4°C for 24 hours) were unsuccessful. A 1mL aliquot of MilliQ water was added upon incubation completion to dissolve any remaining precipitated salts before being centrifuged at 3000 RCF for an additional 10 minutes. Cleaned cells were resuspended in 50 µL of MilliQ water and dropped onto poly-l-lysine coated microscope slides and placed in a drying oven at 30°C to evaporate for 1.5 h.

Antifade was added (15 µL) to help reduce photobleaching of the fluorescence signal, a glass coverslip applied and sealed with clear nail varnish. A fluorescence microscope (Nikon Eclipse Ni, Japan) was used at 20x magnification, set to run an 8x8 field of view, large scan collecting images using a custom filter to detect PDMPO stained cells (535 nm) and autofluorescence (852 nm, chlorophyll-a (mCherry)). The grid was also imaged in a 30 µm Z-stack (2.5 µm increments, 13 layers) to collect data across a greater field of view. Post processing deconvolution was applied using the Richardson-Lucy iterative algorithm (20 iterations, 12 SNR) within NIS-Elements software, to increase image sharpness and reduce blur (Ingaramo *et al.*, 2014). Incorporation of PDMPO into individual diatom frustules over a 24-h period was used to quantify relative amounts of newly precipitated silica frustule per cell. This was then compared against the relative newly precipitated silica in each species per treatment.

Custom made macros in ImageJ software (Schneider *et al.*, 2012) were used to analyse PDMPO fluorescence of each cell following the methods of Nielsen *et al.*, (2018) A total of 1472 cells were analysed to ensure statistical power of analyses. However, it must be noted that the number of cells measured were not equal amongst species due to variable abundance within samples. Cells were aligned vertically or horizontally to be cropped with minimal background. Any interfering fluorescence was then removed manually, and remaining area set to zero-pixel intensity. Background fluorescence was measured in the four corners of the image with the average background +1 standard deviation subtracted from the total image to remove background fluorescence. Total fluorescence could then be calculated from total pixel intensity. When two or more cells were closely positioned (e.g. chain forming species) and difficult to separate, the number of cells were recorded,

and total fluorescence divided by the number of cells to give fluorescence per cell was used.

Statistical analysis

To determine significant effects of ocean acidification on diatom morphology, one-way Analysis of Variance (ANOVA) was used with Tukey's multiple comparison test at alpha <0.05. All data were tested for homogeneity of variance and normality *a priori,* in cases where assumptions weren't met, non-parametric Kruskal Wallace test was used. Unpaired t-tests were also used to assess treatment effect on diatoms compared to ambient conditions. If assumptions were violated, Wilcoxon signed-rank test was used. Statistical analysis was performed using GraphPad Prism, version 10.0.2 (GraphPad Software, Boston, Massachusetts USA) and R. Core Team (2021).

Results

Microcosm maintenance, nutrients and carbonate chemistry

Initial seawater nutrient concentrations (AODN supplied) were heavily depleted at the surface, with nitrate and silicate both below detection, whilst phosphate concentrations were 0.07 µmol L^{-1}. Seawater carbonate chemistry showed relatively low DIC, high pH and TA concentrations (Table 3.1). Additions of F/200 nutrients were added to microcosms on days 1, 4 and 6 (black arrows), inoculating each time NOx concentrations reached below detection, to ensure initial and continued growth (**Figure 3.2A**). Daily adjustment of carbonate chemistry ensured that the microcosms were maintained within ~5% of target DIC for the duration of the experiment (Table 3.1), where average pH in the 8.1 pH microcosms ranged from 8.0-8.15, whilst 7.62 pH microcosms ranged from

7.63-7.72. Greatest pH drift was observed in the 8.1 pH microcosms, however there was no overlap in pH shift at any stage of the experiment (**Figure 3.2B**).

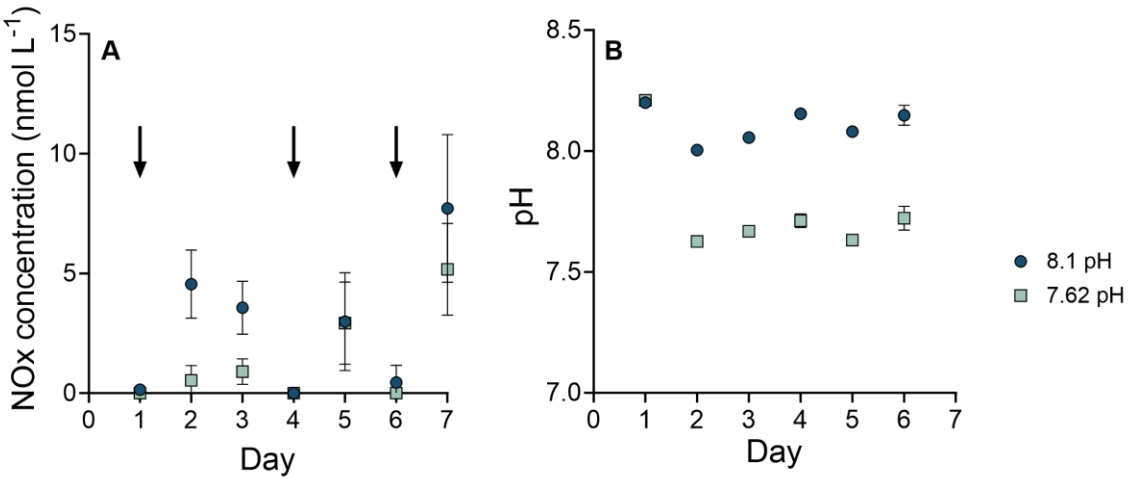

Figure 3. 2 Nitrate + nitrite (NOx) concentrations (nmol L^{-1}) (A) and pH (total scale) (B) across two conditions (modern day 8.1 pH and future predictions 7.62 pH) over the 7-day experiment. Data points are mean ± SD, n=5.

Table 3. 1 Carbonate chemistry parameters under modern (8.1) and projected future (7.62) pH conditions. Salinity, temperature, nutrient concentrations, pH and alkalinity were used to derive all other parameters using CO_2SYS software (Lewis & Wallace, 1998). Data are means ± SD (N=25).

Microcosm	pCO_2	$pH_{(total)}$	DIC	HCO_3^-	CO_3^{2-}	CO_2	TA
Initial	255±2.5	8.2	1985±2.4	1739±1.5	235±2	8.7±0.1	2322±50
8.1 pH	359±59	8.09±0.1	2034±29	1832±47	189±2	12.3±2.0	2302±13
7.62 pH	1066±114	7.67±0.05	2215±13	2096±12	83±9	36.4±3.9	2302±23

Photophysiological effect of pCO_2

Daily measurements of maximum quantum yield of PSII (F_V/F_M) showed no measurable effect of pCO_2, with both conditions increasing from initial values of ~0.5 (before amendment with nutrients) to above 0.6 once placed into their respective conditions until the end of the experiment (**Figure 3.3A**). Chlorophyll *a* and *c* concentrations showed no effect of treatment by day 7 (**Figure 3.3B-C**).

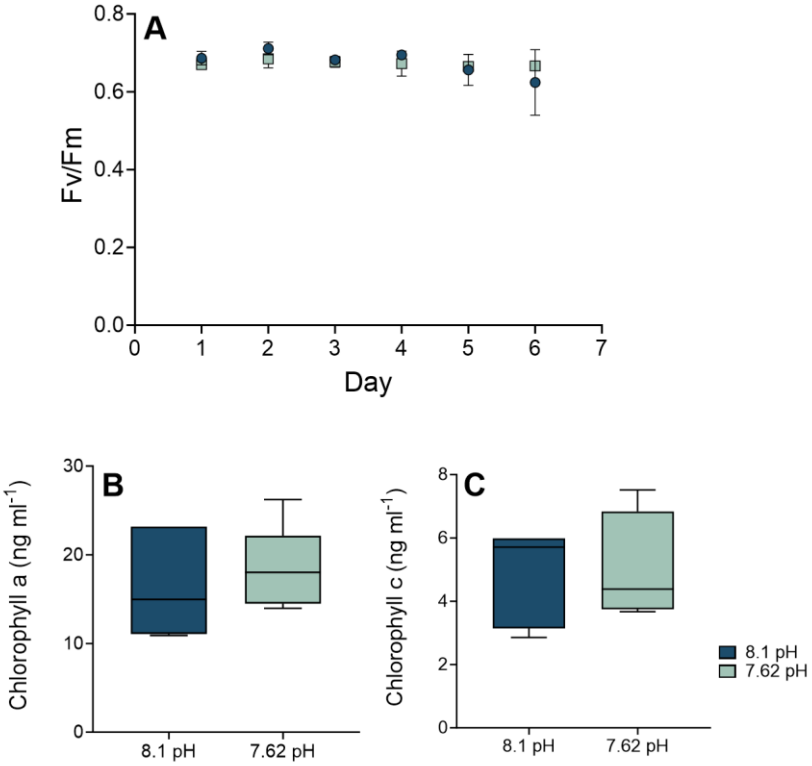

Figure 3. 3 Daily maximum quantum yield of photosystem II (A). Mean total chlorophyll *a* (B) and *c* (C) across microcosms under modern (8.1) and predicted future (7.62) pH conditions after 7-days exposure.

Community composition

Initial phytoplankton community composition was found to consist of ~72% diatoms, ~27% dinoflagellates and the remaining 1% comprised of ciliates and other taxa, including zooplankton, cryophytes, foraminifera and brown algae (**Appendix Table 3.1**; **Figure 3.4A**). Taxonomic diversity diminished during incubations from 35 taxa in the whole water, to only 24 and 18 taxa in the control and treatment, respectively, by day 7 (**Figure 3.4A-C**). Initial filtration would have potentially excluded some of the larger taxa and micrograzers from our incubations, but there were also losses in flagellates and other smaller taxa. By the end of the experiment, cell counts from the microcosms showed increased diatom counts, with diatoms in both the control and treatment making

up ~98% of the community (**Figure 3.4B-C**). When looking at the diatom portion, both 8.1 pH and 7.62 pH total cell counts increased compared to initial values however, cells growth was significantly suppressed (36.5% less) by increased pCO_2 in comparison to contemporary conditions (**Figure 3.4D**, $F_{(2, 8)} = 9.443$, $P = 0.0078$). Further breakdown of the community into species specific counts revealed significantly lower cell numbers in five diatom species under increased pCO_2 compared to control microcosms (*Chaetoceros didymus* ($F_{(4, 4)} = 23.56$, $P = 0.0029$), *Cylindrotheca closterium* ($F_{(4, 4)} = 4.856$, $P = 0.0045$), *Navicula* sp. ($F_{(4, 4)} = 43.79$, $P = 0.0007$), *Pseuod-nitzschia* spp. ($F_{(4, 4)} = 37.25$, $P = 0.01$) and *Thalassiosira* spp. >20 µm ($F_{(4, 4)} = 24.47$, $P = 0.0042$)), whilst the other species measured (*Asterionellopsis glacialis*, *Eucampia Zodiacus, Leptocylindrus danicus, Rhizosolenia setigera* and *Thalassiosira* spp. <20 µm) had approx. the same mean cell densities (**Figure 3.4E**).

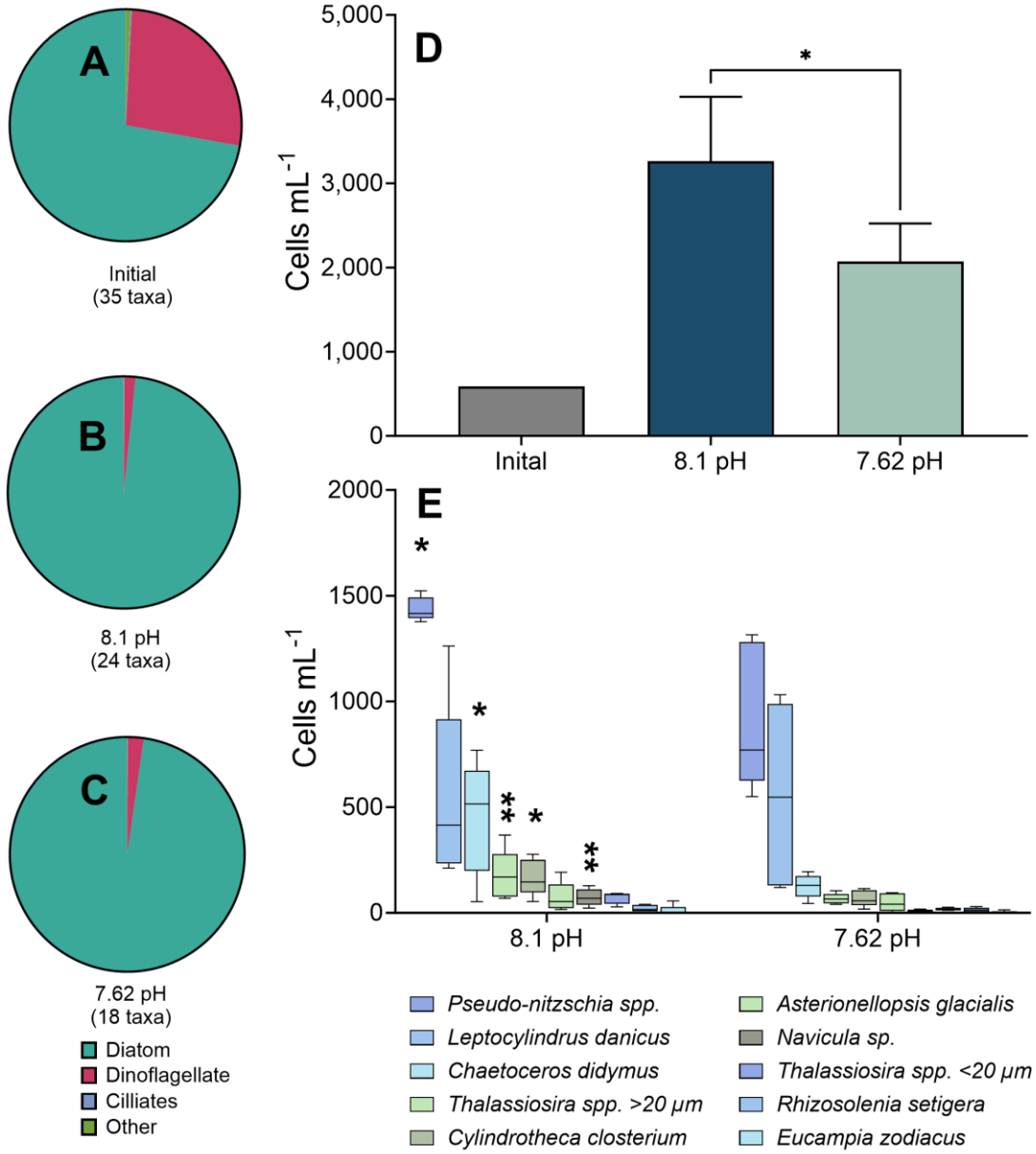

Figure 3. 4 (A-C) show the community composition distribution amongst phytoplankton groups (diatoms, dinoflagellates, ciliates and other, consisting of zooplankton, cryophytes, foraminifera and brown algae, number of tax present in parenthesis). (D) shows total cells initially and post 7-day experiment (8.1pH and 7.62 pH), (E) shows the abundance on day 7 of all diatom taxa included in the single-cell analyses within each treatment. Asterisks indicate significance (* P <0.05, ** P <0.01).

Biogenic silica (BSi) and silicification rates in response to pCO_2

Bulk biogenic silica (BSi) increased significantly over the 7-day experimental period in both the control and treatment when compared to the initial ($F_{(2, 12)} = 56.23$, P = <0.0001),

however no significant difference was detected between conditions on day 7 (**Figure 3.5A**). Bulk PDMPO incorporation, was lower under increased pCO_2 ($F_{(3, 4)} = 36.16$, P = 0.0238, **Figure 3.5B**). There was no measurable effect of pCO_2 on total carbon and nitrogen within microcosms (**Figure 3.5C-D**) and elemental stoichiometry, C:N (mol:mol), were consistent with Redfield ratios (7.1±1.3 and 8.3±0.9 SD control and treatment, respectively). Similar ratios of C:Si and N:Si were measured across conditions (**Figure 3.5F-G**).

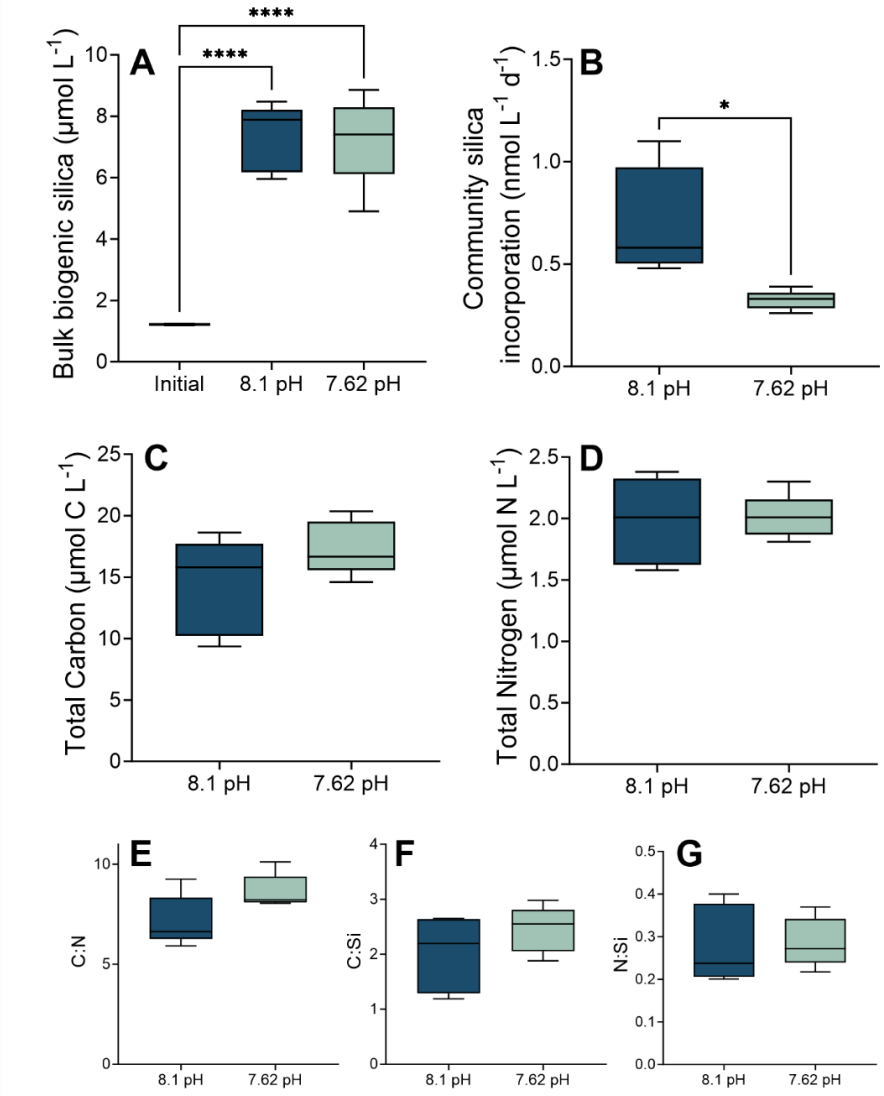

Figure 3. 5 Initial bulk biogenic silica against treatment concentrations at the end of the experiment (A), community silica incorporation (µmol L^{-1}) across conditions on day 7 (B). Total mean carbon and nitrogen (µmol L^{-1}) on day 7 (C and D). Elemental ratios - C:N, C:Si, N:Si (E-G). Vertical bars are mean ± SD, N=5. Asterisks indicate significance (* P <0.05, **** P <0.0001).

Silica incorporation within ten key diatom taxa

Initial inspection of the fluorescence images revealed a direct relationship between the mCherry and PDMPO channels (**Figure 3.6A; Appendix Figure 3.1**). Given the lack of overlap in excitation and emission, these data suggest some background fluorescence was being detected in both channels. To account for this bleed over, we used the residuals from the regression, eliminating the 1:1 relationship between the channels (**Figure 3.6B; Appendix Figure 3.2**). In plotting the PDMPO residuals improved delineation of the fluorescence per cell data (**Figure 3.6C-D**). As such, all PDMPO data are presented as the residuals.

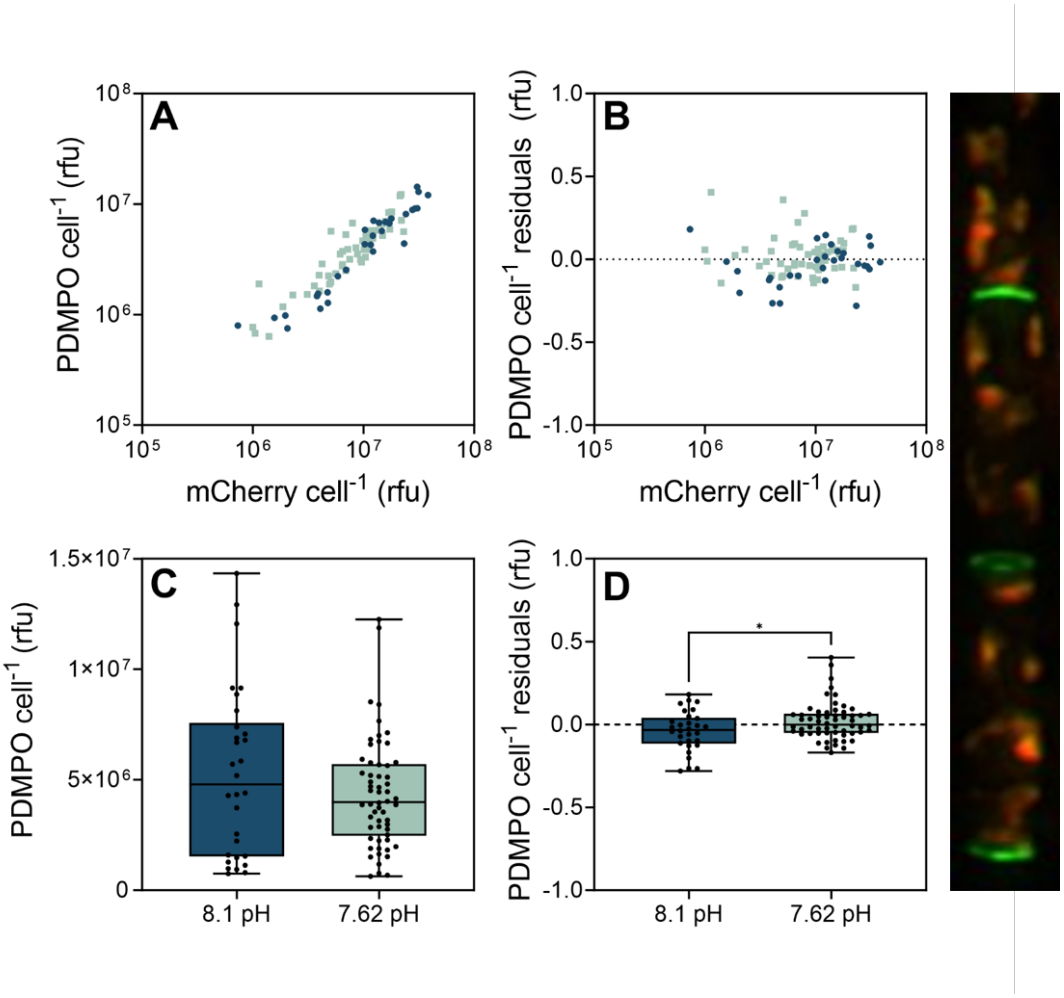

Figure 3. 6 Composite of *Leptocylindrus danicus* silica incorporation. Near 1:1 relationship between mCherry and PDMPO channels (A). This relationship is lost when plotting mCherry against PDMPO per cell residuals (B). Cell specific PDMPO and PDMPO residuals are plotted to demonstrate the removal of this bleed over on the per cell data (C-D). Asterisks indicate significance (* P <0.05). Bar on the right shows three *Leptocylindrus danicus* cells. Cellular

components are highlighted in red by autofluorescence whilst newly precipitated silica is highlighted in green by PDMPO staining.

We found that silica incorporation per cell differentially affected diatom species (**Figure 3.7**), with higher pCO_2 significantly increasing rates in four taxa (*Chaetoceros didymus* ($F_{(77, 62)} = 1.15$, $P = 0.0043$), *Leptocylindrus danicus* ($F_{(29, 57)} = 1.15$, $P = 0.0224$), Other Centric ($F_{(23, 17)} = 1.727$, $P = 0.0018$), and *Pseudo-nitzschia* spp. ($F_{(143, 124)} = 1.338$, $P = 0.0002$)). When normalised to cell area, which differed across species and treatment (**Appendix Figure 3.3**), only two of the taxa (*Leptocylindrus danicus* ($F_{(29, 57)} = 1.061$, $P = 0.0071$) and *Pseudo-nitzschia* spp. ($F_{(143, 124)} = 1.487$, $P = 0.0015$)) showed significant increases in silicification rates under high pCO_2 (**Figure 3.8**).

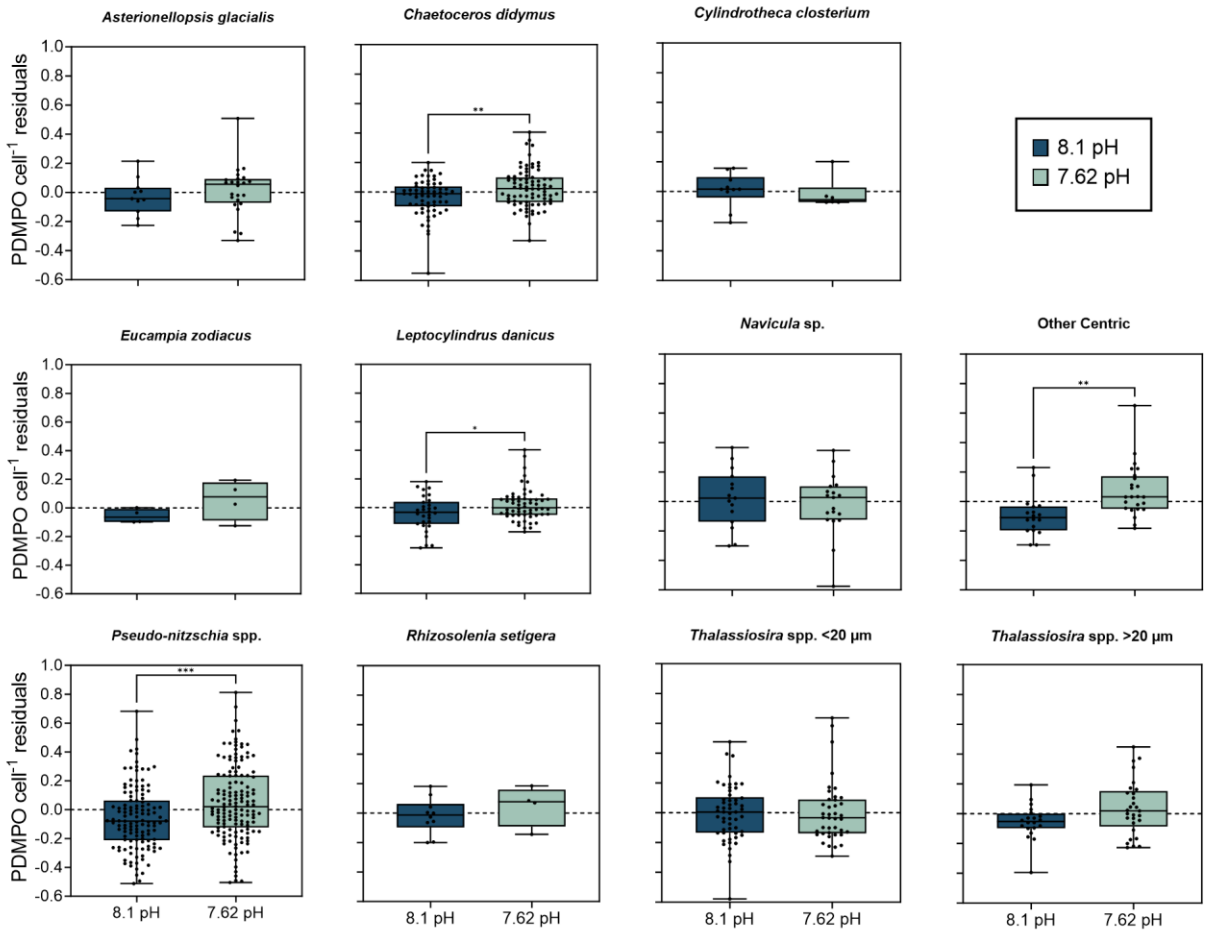

Figure 3. 7 Silica incorporation measured as residuals of cell PDMPO fluorescence in *Asterionellopsis glacialis*, *Chaetoceros didymus*, *Cylindrotheca closterium*, *Eucampia zodiacus*, *Leptocylindrus danicus*, *Navicula* sp., Other centrics, *Pseudo-nitzschia* spp., *Rhizosolenia setigera*, *Thalassiosira* spp. <20 µm and <20 µm. Data are visualised as box plots with overlain black dots showing the individual PDMPO fluorescence residual of individual cells after 24h PDMPO incubations. Asterisks indicate significance (* p = <0.05, ** p = <0.01, *** p = <0.001).

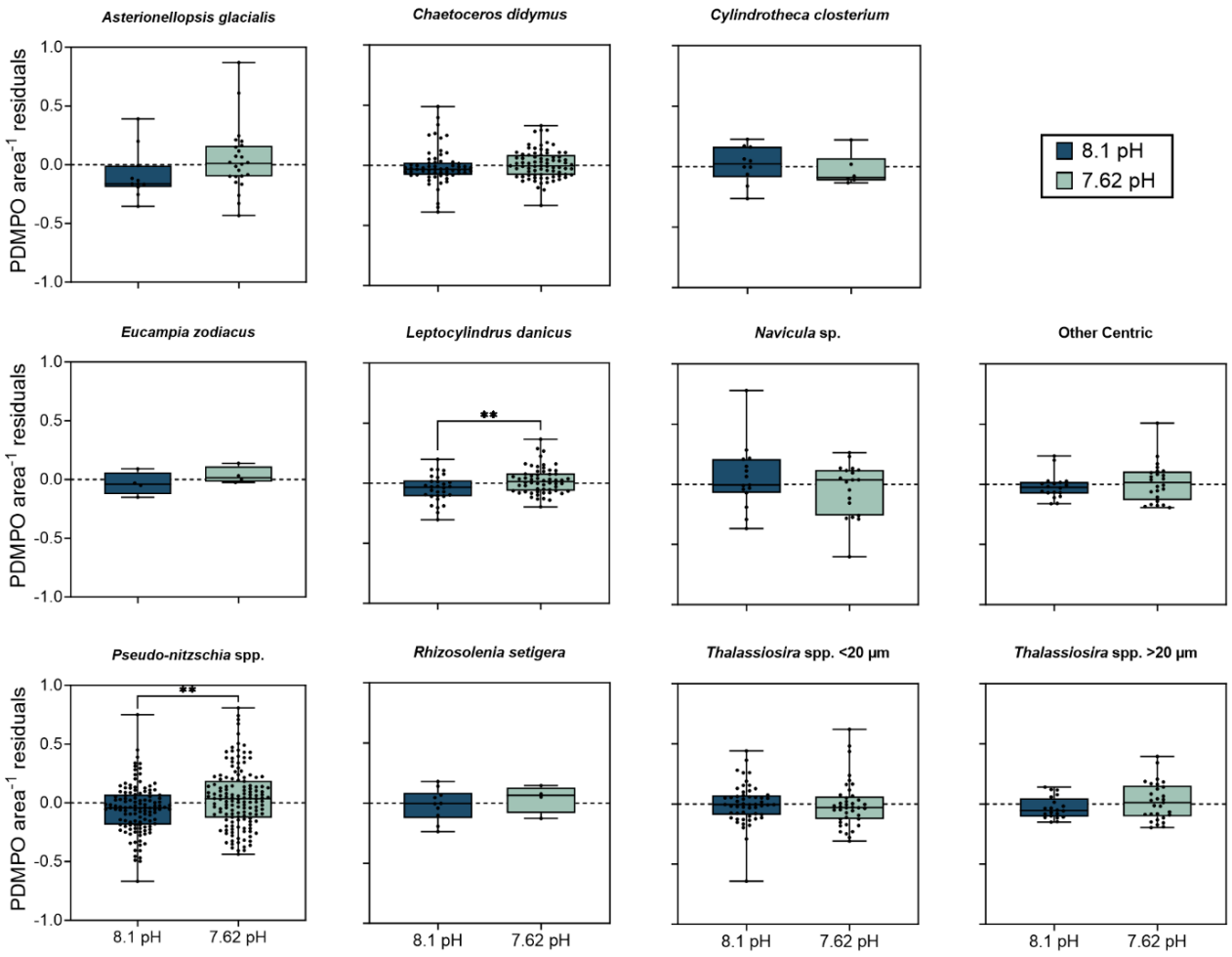

Figure 3. 8 Silica incorporation displayed as total residuals of PDMPO fluorescence per cell area in *Asterionellopsis glacialis*, *Chaetoceros didymus*, *Cylindrotheca closterium*, *Eucampia zodiacus*, *Leptocylindrus danicus*, *Navicula* sp., Other centrics, *Pseudo-nitzschia* spp., *Rhizosolenia setigera*, *Thalassiosira* spp. <20 µm and <20 µm. Data are visualised as box plots with overlain black dots showing the individual PDMPO fluorescence per cell area residual of individual cells after 24h PDMPO incubations. Asterisks indicate significance (** p = <0.01).

Discussion

In this study, we exposed nearshore phytoplankton communities to contemporary and predicted future ocean carbonate chemistry conditions to elucidate the effect of lowered pH on diatom physiology. By investigating individual cells from within the community, we aimed to look beyond bulk analyses, in which the distribution used to calculate the mean often masks fine scale details, and instead, uncover taxon-specific responses and the intra-specific variability amongst diatoms within a community when exposed to ocean acidification.

The low nutrient concentrations, high total alkalinity and pH combined with lowered DIC measured in the initial seawater, suggests samples were collected late or post bloom conditions (Engel *et al*., 2002; Zhai *et al*., 2014). This would match the timing of the sampling occurring post maximum annual chlorophyll *a* peak (**Figure 3.1D**). The effect of sampling in late bloom phase in unquantifiable, however, given the community was provided with nutrient supplementation and carbonate chemistry regulated throughout the experiment, it is likely that the incubations represented an otherwise healthy community. This assumption is supported by the marked growth and high photosynthetic yields measured throughout the study. Taxonomic diversity, however, did decline from the initial community to the end of our experiment. This can likely be attributed to bottle effects and competition, as well as some loss of larger taxa from the initial filtration to remove micrograzers. Despite some species losses, the overall diatom diversity remained high in both conditions by day 7.

Increased pCO_2 had no measurable effect on diatom photophysiology or pigment content, consistent with previous studies that showed despite high pCO_2 stimulating growth, it does not always translate to increased photosynthesis or pigment

concentrations, such as chlorophyll *a* or carotenoid production (Wu *et al.*, 2010; Boelen *et al.*, 2011; Li *et al.*, 2012; Wu *et al.*, 2014; Li *et al.*, 2017). The increase in available CO_2 at low pH likely countered any potential negative effect on electron transport through PSII (Gao *et al.*, 2012), with previous works finding RUBISCO production was promoted when CO_2 stimulated (McCarthy *et al.*, 2012). The lack of effect on pigment content at a community level corroborates the high F_V/F_M measured in both conditions. However, accounting for the significantly lower cell abundance at low pH (7.62), we can assume that there was greater chlorophyll *a* quotas in cells under high CO_2. This counters our finding in **Chapter 2**, where increased pCO_2 lowered chlorophyll *a* per cell in *T. weissflogii*. One plausible explanation for this discrepancy would be taxon-specific differences in response to these conditions, whereby the bulk data, which represents a mean, does not account for within community per/cell quota differences. Future work should consider the effect of light intensities in conjunction with pCO_2/pH on species-specific chlorophyll *a* quotas to provide better resolution for responses to climate change.

We found significant changes to the community structure and diatom abundance, including a decline in overall diversity by day 7, a common effect of bottle experiments (Zobell & Anderson, 1936; Nogueira *et al.*, 2014). However, abundance and diatom dominance increased under both conditions, but with high pCO_2 suppressing growth of many diatom taxa over the seven days, resulting in two-thirds of the ambient pCO_2 microcosm's cell density. This finding aligns with both Gao *et al.*, (2012) and Feng *et al.*, (2021), who found that although diatoms dominated phytoplankton assemblages, their abundance declined under higher pCO_2. Furthermore, although higher pCO_2 is often considered beneficial to diatoms, due to RUBISCO's affinity for CO_2 (Roberts *et al.*, 2007;

Young *et al.*, 2016), it has been suggested that photosynthesis for many species may already be saturated at ambient CO_2 conditions (Burkhardt *et al.*, 2001; Rost *et al.*, 2003) and therefore may not be advantageous.

To reconcile differences in the effect of high pCO_2 on bulk biogenic silica, elemental stoichiometry and gross silicification rate, we interrogated individual species' abundances and silica incorporation rates. We found four of the five most abundant species declined in abundance under high pCO_2 (*Psuedo-nitzschia* spp., *C. didymus, C. closterium* and *Thaslassiosira* spp >20 µm). This would indicate that for some of the taxa, cell size, carbon content, and/or silica density would have to be greater than their counterparts grown under ambient pCO_2, to account for the same amount of bulk BSi, C and N. Looking at size changes, we found that cell area indeed differed with pCO_2, significantly declining in *L. danicus*, and *R. setigera,* while increasing in 'other centric' (**Appendix Figure 3.3**). These data are incongruent with findings that suggest larger diatoms benefit from CO_2 stimulation (Bach & Taucher, 2019), as the largest cells in our study either showed either diminished growth and smaller cell size or no change in either trait.

To better understand how the lower bulk rates of silicification reflected individual species' rates and disentangle the lower diatom abundance from changes in actual silicon incorporation rates, we quantified cell specific silicification rates for 10 of the diatom taxa in the community. Contrary to expectation and the bulk data, four highly abundant taxa (*Chaetoceros didymus, Pseudo-nitzschia* spp., *Leptocylindrus danicus,* and *Thalassiosira* spp >20 µm) showed higher rates of silica incorporation per cell under high pCO_2. It is well documented that diatoms decrease in size with each division, whereby a daughter cell is smaller than its parent (Hense & Beckmann, 2015), therefore

observed differences in growth over the 7 days between pCO_2 conditions may have accounted for differences in mean cell area and thus per cell silica incorporation. To check for the potential influence of cell size, we normalised PDMPO fluorescence to cell area and found silicification rates were only greater in 2 of the 10 taxa (*L. danicus* and *Pseudo-nitzschia* spp.) under high pCO_2 reducing the overall effect of high pCO_2 on diatom silica production rates. These results present two very different physiological and ecological scenarios. In one instance, we see cell specific silicification rates increasing (in some diatom taxa) under higher pCO_2, which would suggest a greater uptake of silicon and no negative impact of OA on frustule development. However, at a bulk community level, we see a reduction in overall silicon incorporation, due to reduced growth and lower cell numbers, which in an ecological setting would mean overall lower biomineralisation and slower turnover of diatom biomass. A reduction in biomineralisation can have significant implications for marine ecosystems and global biogeochemical cycling. Lower diatom biomass can lead to a decrease in gross primary production (Gao *et al.*, 2012; Tréguer *et al.*, 2018) and destabilise trophic webs (Gattuso and Hansson, 2011), whilst also reducing nutrient cycling of major elements such as N, P, Si and C (Riebesell & Tortell, 2011; Sun *et al.*, 2011; Taucher *et al.*, 2022). Thus, the changes seen in this study raise some concern over the productivity and efficient cycling of nutrients in future temperate coastal systems.

In the two species whose silicification was enhanced under high pCO_2, each showed slightly different physiological strategies; *Pseudo-nitzschia* spp., the most numerically abundant diatom in the community, experienced diminished growth without change to mean cell area. Whereas for *L. danicus,* there was no change in growth rate (equal cell densities by day 7), but a decline in mean cell area with high pCO_2. In both cases

silicification rates were higher for both per cell and per area compared to the control, suggesting a potential thickening of the frustule. Together, these species could account for a large proportion of the bulk BSi measured in the high pCO_2 treatment, helping to explain these data. Additionally, despite experiencing the same conditions, the two species responded differently in their growth and morphology, highlighting the dynamic and diverse nature of physiological plasticity and adaptation strategies and providing support for the varied (positive, neutral and negative) results in OA experiments (Wu *et al.*, 2014; Dutkiewicz *et al.*, 2015; Sala *et al.*, 2016).

The ecological cause and consequence of species-dependent responses to ocean acidification are vast. When looking at causes, if we compare these data with those reported by Petrou *et al.*, (2019), we see no direct effect of OA on cell-specific silica production (however cellular abundance declined in five species), whereas they found severe reductions in silica production in six of the seven taxa they measured, but no major changes in growth rate. These differences represent potentially different trade-off strategies that may be attributed to the environment in which the diatoms persist. Temperate ocean systems are highly variable, with dramatic fluctuations in temperature (Hemming *et al.*, 2023), seasonal nutrient depletion (Ridgway & Hill, 2009; van Beusekom *et al.*, 2009) and rapid shifts between sub/super-saturating irradiances (Scott, 1978; 1983; Falkowski & Oliver, 2007). This variability demands a physiological flexibility often not required by taxa from more stable environments (Hinga, 2002; Leterme *et al.*, 2013; Clark *et al.*, 2018; Yamaguchi & Suga, 2019). Equally, temperature alone may play a key role in the difference in the response of diatoms to OA. Supra-optimal temperature has been found to reduce silicification albeit enlarging cell volume (Sheehan *et al.*, 2020). It was suggested these cells may incur a trade-off whereby large cell size and possibly a

greater nutrient demand (Wu *et al*., 2014) results in lower growth rates and reduced photosynthesis to respiration ratios. Climate change induced shoaling would place further stress on diatoms with reduced nutrient entrainment into the photic zone causing demand for resources to exceed supply (Sheehan *et al*., 2020).

When looking at multi stressor expression, increasing temperature and pCO_2 have been shown to synergistically reduce growth and carbon fixation (Li *et al*., 2018) only further challenging these cells. Furthermore, in this study we used light levels that were relatively low and potentially sub-saturating for many of the species, which could account for minimal negative impact. Previous research has shown that increasing light or CO_2 independently of each other imparts positive effects to diatoms (Riebesell & Tortell, 2011; Gao & Campbell, 2014), however when combined, saturating light levels and high pCO_2 concentrations work synergistically in reducing diatom fitness (Gao *et al*., 2012) and silicification (**Chapter 2**). This combination is a more likely scenario going forwards, with climate change inducing greater stratification, and consequently reducing the mixed layer depth, therefore exposing diatoms to greater mean irradiance and residence time at the surface (Cermeño *et al*., 2008; Gao *et al*., 2012).

Considering the potential ecological consequences of our findings, OA conditions are likely to influence temperate diatom community composition and growth. This in and of itself has implications for higher tropic levels (Rossoll *et* al., 2012; Friedland *et al*., 2020). Reduced abundance of primary producers consequently diminishes food availability and diversity for higher species which in turn could destabilise food webs and fisheries (Bermúdez *et al*., 2016; Hancock *et al*., 2018). Coupled with disadvantageous changes to macromolecular partitioning as a response to OA could also alter energy transfer through higher trophic levels (Duncan *et al*., 2022). We were able to demonstrate taxon-

specific changes in silica incorporation rates, whereby the cells' ability to produce frustule was not hindered under future ocean conditions. Our single celled analyses also highlighted the broad ranges in phenotypic plasticity across individual cells within populations. From the diatoms explored in this study, several could be considered generalist species (Casteleyn *et al*., 2008; Park *et al*., 2016; De Luca *et al*., 2019; Ajani *et al*., 2021), with broad temporal and spatial ecological niches. Such species may have an advantage over narrower niche taxa, when exposed to novel conditions. That said, ocean acidification and warming are likely to persist without abatement, which questions whether the phenotypic plasticity of a given diatom are sufficient to acclimate and prosper under new conditions in a timeframe concurrent with climate change.

Our study aimed to broaden current understanding of OA effects on diatom physiology and biomineralisation rates. By undertaking bulk and individual cell analyses we revealed negative effects of lowered pH on diatom growth and some positive effects of silica incorporation rates. Importantly, our work showed that these responses were taxon specific. This work contributes new knowledge on the potential implications of OA in a temperate coastal diatom community, expanding the geographic range of diatom responses beyond polar regions. It also highlights the need for future work to include light and temperature as key variables and incorporate single-cell phenotyping of species within natural communities, to elucidate the plasticity and thereby adaptive potential of diatoms and their role in ocean productivity, biomineralisation and carbon export.

Acknowledgements

Thank you to the IMOS sampling team for your continued monitoring and allowing me to collect these data and Nahschon for assisting in water collection. Thank you to the Microbial Imaging Facility (MIF), particularly Amy Bottomley, at UTS for helping me collate and process my data.

Appendix

Appendix Table 3. 1 Cell counts (L^{-1}) for in-situ (Initial), control (8.1 pH) and Treatment (7.62 pH). Initial counts were collected from Port Hacking (PHB). -34.1192, 151.2267, trip code PHB20221026, taken from AODN. Diatoms were identified to species level, when possible, otherwise grouped to genus or functional group.

Species	Initial (cells L^{-1})	Control (cells L^{-1})	Treatment (cells L^{-1})
Diatoms			
Asterionellopsis glacialis	233435	73695±70288	48990±42252
Cerataulina pelagica	734	3200±7155	5353±5480
Chaetoceros spp.	123935	451928±269473	126674±55327
Cylindrotheca closterium	550	168414±85478	68967±38754
Ditylum brightwellii < 40 µm width	183	6215±10042	0
Eucampia spp. <100 µm cell length	367	0	0
Eucampia zodiacus	3303	1120±25044	3000±6708
Guinardia delicatula	917	1600±3578	0
Lauderia annulata < 70 µm length	3303	16922±33705	13454±18964
Leptocylindrus danicus	25484	542763±425821	556746±430368
Navicula cf. 20-40 µm length	183	73652±39819	9105±6027
Pennate diatom 25 - 50 µm	183	0	0
Pseudo-nitzschia delicatissima complex <3 µm	3303	0	0
Pseudo-nitzschia seriata complex >3 µm	19083	1437809±56331	916367±343049
Rhizosolenia fallax	367	7692±10878	0
Rhizosolenia setigera	734	21212±15417	14276±10817
Skeletonema spp.	3853	73167±88090	7058±15783
Thalassiosira spp. 10-20 µm	2752	175858±119176	66483±24994
Thalassiosira spp. 20-40 µm	2018	60404±39065	17413±6006
Thalassionema spp.	0	4615±6880	0
Dinoflagellates			
Flagellate <10 µm fusiform	13761	0	0
Flagellate <10 µm round	142966	0	0
Prorocentrum spp.	367	4738±7122	3000±6708
Scrippsiella spp.	183	0	0
Small Protoperidinium	0	80888±43384	174098±44551
Tripos candelabrum	18	0	0
Unid dinoflagellate 10-30 µm	917	3077±6880	5151±4858
Unid dinoflagellate < 10 µm	765	42080±34618	33653±38406
Cilliates			
Ciliate (Inc. tintinnid)	367	1600±3578	0
Favella ehrenbergii	28	0	0
Laboea spp.	183	0	0
Cryptophytes			
Cryptophyta < 10 µm length	3823	0	0

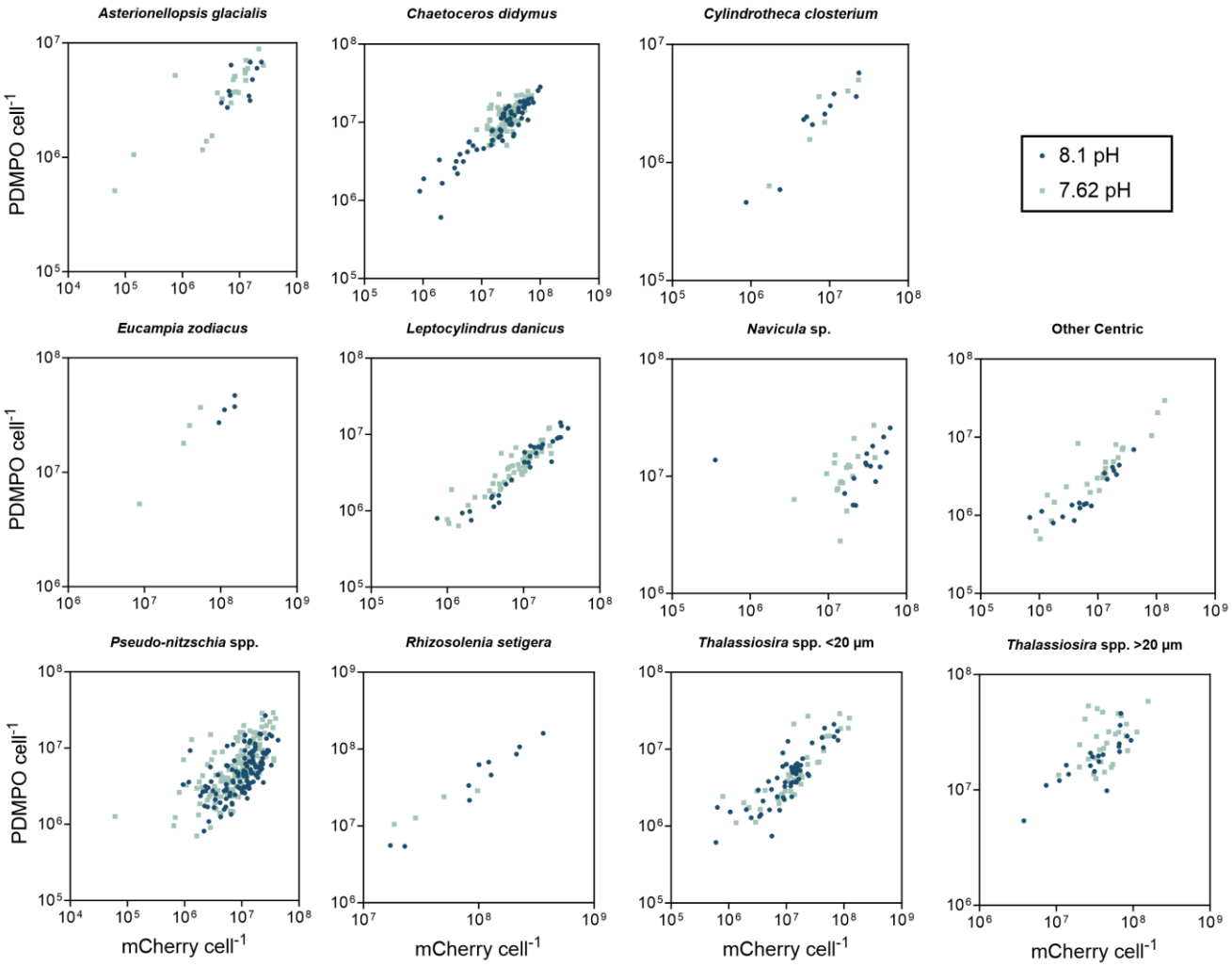

Appendix Figure 3. 1 Near 1:1 relationship between PDMPO and mCherry channels in *Asterionellopsis glacialis*, *Chaetoceros didymus*, *Cylindrotheca closterium*, *Eucampia zodiacus*, *Leptocylindrus danicus*, *Navicula* sp., Other centrics, *Pseudo-nitzschia* spp., *Rhizosolenia setigera*, *Thalassiosira* spp. <20 µm and <20 µm. Data are presented as scatter plots of individual cells after 24h PDMPO incubations.

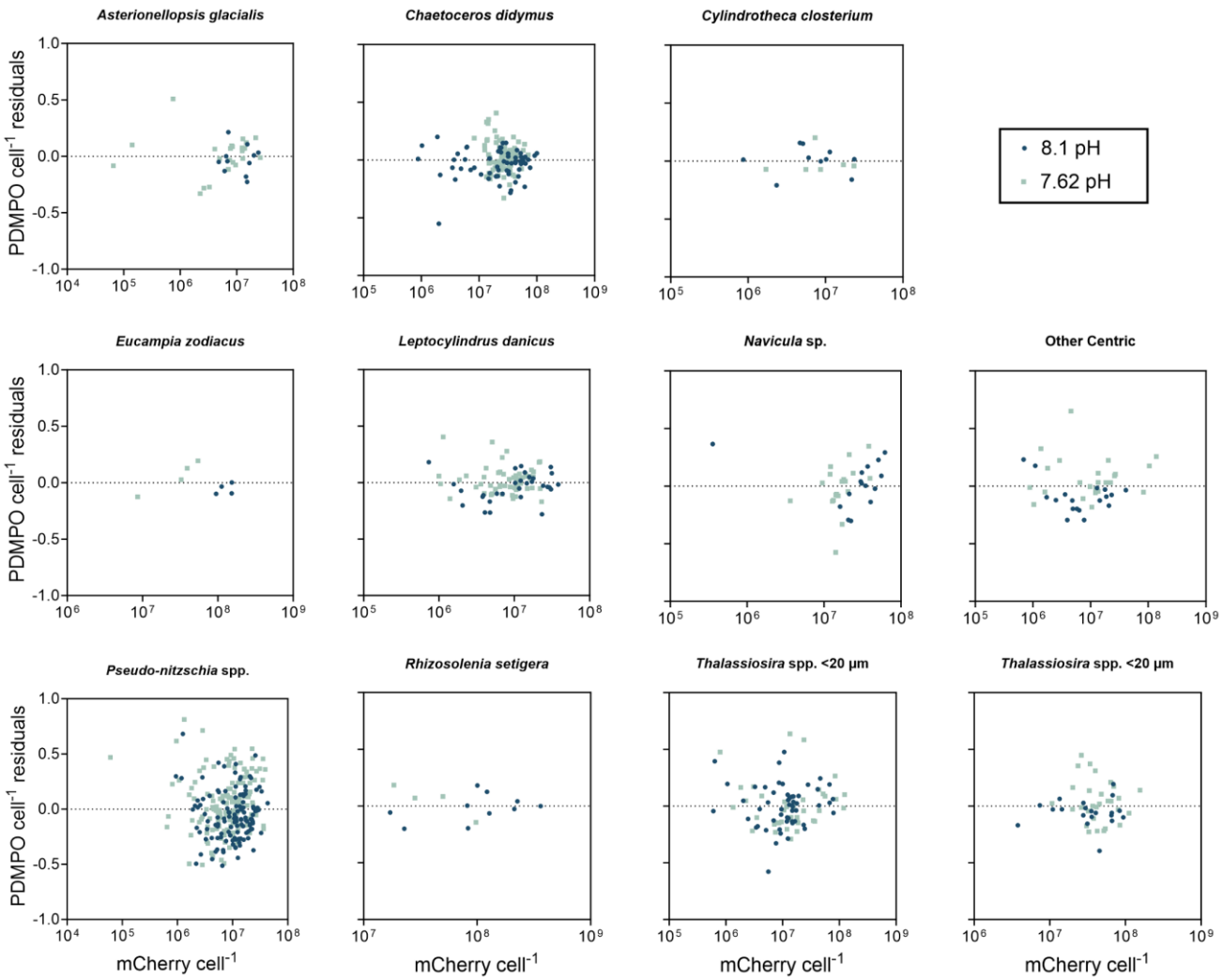

Appendix Figure 3. 2 Regression relationship between PDMPO and mCherry channels when PDMPO cell^{-1} residual is plotted against mCherry cell^{-1} in Asterionellopsis *glacialis*, *Chaetoceros didymus*, *Cylindrotheca closterium*, *Eucampia zodiacus*, *Leptocylindrus danicus*, *Navicula* sp., Other centrics, *Pseudo-nitzschia* spp., *Rhizosolenia setigera*, *Thalassiosira* spp. <20 µm and <20 µm. Data are presented as scatter plots of individual cells after 24h PDMPO incubations.

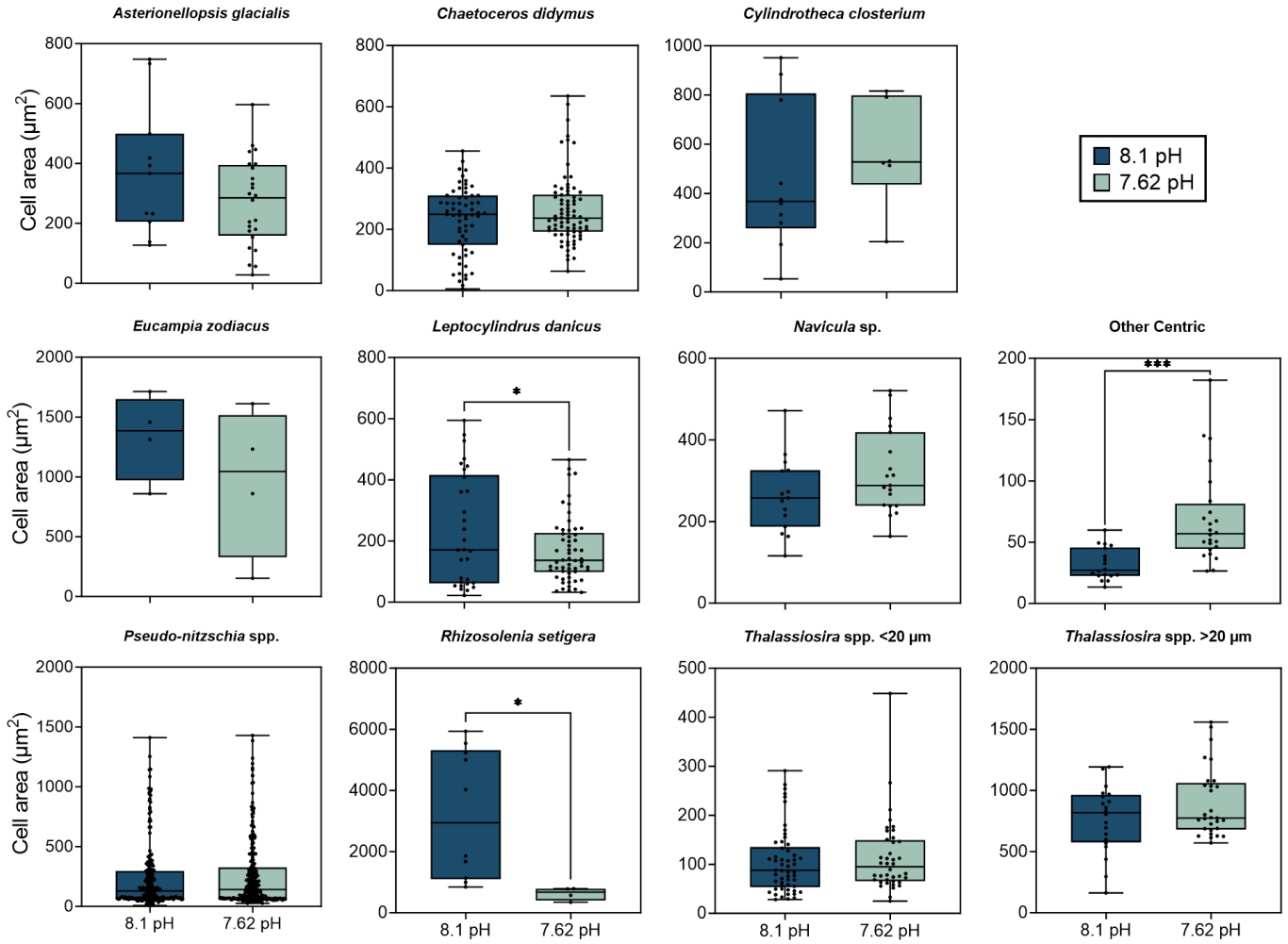

Appendix Figure 3. 3 Cell area of *Asterionellopsis glacialis*, *Chaetoceros didymus*, *Cylindrotheca closterium, Eucampia zodiacus*, *Leptocylindrus danicus*, *Navicula* sp., Other centrics, *Pseudo-nitzschia* spp., *Rhizosolenia setigera*, *Thalassiosira* spp. <20 µm and <20 µm. Data are visualised as box plots with overlain black dots showing the area of individual cells after 24h PDMPO incubations. Asterisks indicate significance (* p = <0.05, *** p = <0.001).

Chapter 4: Uncovering how light modulates diatom silicification in a Southern Ocean community

Abstract

The Southern Ocean Time Series (SOTS), situated in the Sub Antarctic Front, is considered a biologically unique region, when compared to the rest of the basin. Although chlorophyll accumulation is usually low, phytoplankton are often homogeneously present within the mixed layer instead of forming deep-/ chlorophyll maxima. This relative consistency across communities provides a good foundation from which to explore light-dependent diatom silicification. Here, we combined community level responses across three depths (at the surface, 40m and 150m) with single cell analysis thereby uncovering the how interactions of light and water column position impact diatom silicification. To address species-specific responses, we focussed on ten diatom taxa, *Cylindrotheca closterium*, *Dictyocha speculum*, *Fragilariopsis* spp., *Guinardia cylindrus*, *Leptocylindrus mediterraneus*, *Nitzschia bicapitata*, Other Pennate, *Pseudo-nitzschia seriata*, *Thalassiosira* spp. <20 µm and <20 µm. Our study found decreasing silicification under low irradiance in four of the 10 species measured (*C. closterium, N. bicapitata*, Other Pennates and small *Thalassiosira* spp. (>20 µm)) however responses were not uniform, suggesting potential light adaptation and energy capture potential differences amongst species which could be used to support silica incorporation. When resolved to cell area, we found silicification rates were consistent with per cell values for the four species, suggesting differences in silicification due to irradiance change is commensurate with cell size. We also found a significant decline in silicification per cell area from 100 to 27 µmol photons m^{-2} s^{-1} when pooling all area specific silicification data, but no change below 27 µmol photons m^{-2} s^{-} suggesting a minimal light requirement for net positive silicification. These findings together suggest that light modulates silicification in Sub-Antarctic phytoplankton communities under

non-depleted nutrient conditions. With predicted residence times in saturating irradiance increasing due to shoaling, light may provide energy for greater diatom silicification, however, when coupled with other factors (such as ocean acidification) it is unclear whether environmental change may work synergistically to reduce overall diatom fitness.

Introduction

Anthropogenic carbon emissions and consequent global warming are at an all-time high and show no sign of abating (Liu *et al.*, 2023). Global oceans are estimated to sequester ~30% of total carbon dioxide (CO_2) emissions each year (Gruber *et al.*, 2019), and hold up to 90% of the excess heat (Masson-Delmotte *et al.*, 2021). However, the magnitude and variability of carbon and heat uptake by our oceans are far from uniform with the Southern Ocean storing a disproportionate amount, as much as 50% of the CO_2 over the previous 125 years (Orr *et al.*, 2001; Gruber *et al.*, 2019; Le Quéré *et al.*, 2018) and ~70% of the additional heat (Stocker *et al.*, 2013; Frölicher *et al.*, 2015). This places the Southern Ocean on a pedestal in terms of sequestration capabilities, holding as much CO_2 and heat as the Atlantic, Indian, and Pacific oceans combined (Li *et al.*, 2023). For that reason, the Southern Ocean is known as a 'global change hotspot.' It is here also that dissolved inorganic carbon (DIC) and nutrient rich waters upwell from the Antarctic Circumpolar Current (Lumpkin & Speer, 2007; Marshall & Speer, 2012), providing a natural release of CO_2 via air-sea exchange whilst also promoting carbon drawdown via primary productivity (Gruber *et al.*, 2009). The net magnitude of carbon flux is highly variable over time (Takahashi *et al.*, 2012; Hauck *et al.*, 2013; Landschützer *et al.*, 2016) with a complex interplay of mechanisms driving this unpredictability; ocean circulation,

changes in temperature (Sallée, 2018; Williams *et al*., 2024), wind patterns (Keppler & Landschützer, 2019), upwelling intensities and primary productivity rates (Henley *et al*., 2020) all come together to influence carbon exchange, exacting a need for high accuracy, observation systems.

Observatories such as the Southern Ocean Time Series (SOTS) have been set up to monitor these varying timescale events, from day-night cycles to basin-wide decadal oscillations. Situated in the sub-Antarctic Front (SAZ, 47°S, 140°E, **Figure 4.1**), SOTS is at the meeting point of the eastward Antarctic Circumpolar Current and the weaker, westward flowing Tasman Sea (Herraiz-Borreguero & Rintoul, 2011). It also marks the origin of two important water masses, the Sub-Antarctic Mode Water (SAMW) and Antarctic Intermediate waters (AAIW). These water masses are formed from deep convective mixing which subducts under warmer, less dense tropical and sub-tropical masses (Li *et al*., 2022). With them, they carry excess heat and CO_2 from the surface ocean into the ocean interior, where it is sequestered for timescales relevant for anthropogenic climate change and mitigation (Langlais *et al*., 2017). This melting pot of water bodies makes the SOTS site uncharacteristic compared to the rest of the high nutrient, low chlorophyll (HNLC) Southern Ocean; the climate is temperate, with mixed layer depth temperatures ranging from 9-13 °C seasonally (Rintoul & Trull, 2001), relatively high nitrate and phosphate, with seasonal depletion of silicic acid (Lourey & Trull, 2001) affording low to moderate chlorophyll *a* concentration (Shadwick *et al*., 2023). These prevailing dynamic conditions therefore allows phytoplankton to prosper, with consequent seasonal drawdown strongly influencing surface water CO_2 concentrations and subsequent carbon export (Shadwick *et al*., 2015).

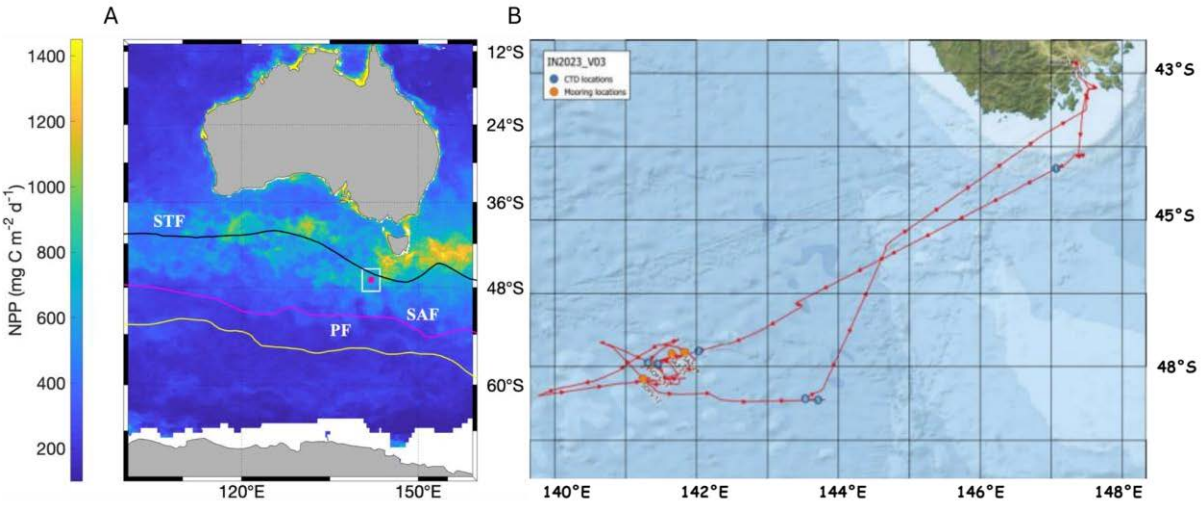

Figure 4. 1 Showing the position of the Southern Ocean Time Series (SOTS) as a red star, with climatological positions of the Subtropical Front (STF) Subantarctic Front (SAF) and Polar Front (PF) (Wynn-Edwards et al., 2020 following Orsi et al., 1995) and 1B showing voyage route taken by the RV Investigator during IN2023_VO3 (12-25th May, 2023).

Research into Southern Ocean phytoplankton is extensive, investigating carbon export potential (Tréguer *et al.*, 2018) physiology (Boyd *et al.*, 2019; Petrou *et al.*, 2016), distribution (Burckle, 1984; Rigual-Hernández *et al.*, 2015; Malviya *et al.*, 2016) nutrient limitation responses (Hoffmann *et al.*, 2008; Smetacek *et al.*, 2012; Boyd, 2019) and much more. Oftentimes however, these are bulk analyses detailing gross outputs, thereby dampening species specificity, taxonomic variability or phenotypic plasticity. Phytoplankton comprise a vast number of species, distributed amongst eight major functional groups. One of the most ecologically successful of these groups are the diatoms (Bacillariophyta), a diverse, polyphyletic group of photosynthetic protists, known for their ability to produce opal (SiO_2) cell walls from seawater silicic acid (De Tommasi *et al.*, 2017). Responsible for ~40% of ocean primary productivity (Nelson *et al.*, 1995), diatoms are major contributors to ocean productivity and biomineralisation in our oceans (Smetacek, 1999; Assmy *et al.,* 2013). Diatom cell volumes span nine orders of magnitude across all species (Litchman *et al.*, 2019) making surface area highly variable too, coupled with selective pressures and environmental change altering species silica

production (Baines *et al*., 2010; Javaheri *et al*., 2015) makes bulk assessments even more convoluted to untangle. One example is Petrou *et al*, (2019), who found that 6 out of 7 Southern Ocean taxa silicified less under ocean acidification, however cell-specific contributions highlighted that a single species was responsible for >80% of the new silica precipitation, whilst the most abundant species contributed the third lowest. These details can easily be lost when providing mean overall responses and therefore acquisition of species-specific data can provide finer resolution on understanding export potential or contributions to the biological pump.

Within previous chapters, we observed the synergistic effect of light and pCO_2 on silicification using two 'model' diatoms (**Chapter 2**), and how pCO_2 independently affected nearshore diatom communities and their silica deposition rates (**Chapter 3**). Here, we aimed to assess how light influences pelagic diatom silicification across a depth profile. Global predications suggest the mixed layer depth (MLD) to shoal by up to 20 metres (Kwiatkowski *et al*., 2020), increasing residence time in high irradiance (Cermeño *et al*., 2008; Gao *et al*., 2012) with many implications thereafter (Bopp *et al*., 2001; Cermeño *et al*., 2008, Chen *et al*., 2012; Sigman & Hain, 2012; Segschneider & Bendtsen, 2013; Fu *et al*., 2016; Gao *et al*., 2019,). Although time series data observed at the SOTS location shows little change to the MLD over the past decade (Shadwick *et al*., 2023), this affords us a baseline measurement for depth-dependent diatom silicification in Sub-Antarctic Front communities. The area is also biologically distinct; whilst chlorophyll accumulation is generally low (Trull *et al*., 2019) and less seasonally dependent than other Southern Ocean regions (Shadwick *et al*., 2015), it is often homogenously distributed within the mixed layer and without a distinct chlorophyll maximum (Trull *et al*., 2019). This therefore makes it interesting to see if the homogeneity

results in the same assemblages and physiologies or different ecotypes at the different depths. Furthermore, by uncovering how light and water column position impacts diatom silicification at the single cell level, we aim to provide individual contributions to the silica pool whilst potentially uncovering the species that make the area a net sequestration zone (Shadwick *et al.*, 2015; Shadwick *et al.*, 2023).

Methods

Water collection and experimental set up

Seawater was collected aboard the *RV* Investigator, during the SOTS_IN2023_V03 voyage to the Southern Ocean Time Series (-46.9649, 141.3512). A CTD rosette (conductivity, temperature and depth) was dropped into the ocean and Niskin bottles were fired at five depths; 5m, 40m, 70m, 100m and 150m. Surface (5m), chlorophyll maxima (40m) and deep chlorophyll maxima (150m) were used in 24h incubations, whilst additional samples from 70m and 100m were included in the assessment of phytoplankton photophysiological health. Forty litres of seawater from each depth were initially sampled through a 210 µm mesh into carboys to remove zooplankton and debris. Seawater was then gently vacuum filtered through a 2.0 µm PTCE filter. Before all liquid had passed through the filter, cells were resuspended into solution with a bulbous 5 mL pipette. Concentrated cell filtrate was then removed and stored in a 2L Schott bottle to be used as inoculum. This was completed for each depth, concentrating 40L down to 1.5 litres to be used in incubations. Polycarbonate flasks (170 mL) were filled to the brim without headspace with concentrated seawater (n=5) and grown at light levels corresponding to cast depth PAR values determined from an earlier CTD cast (~100, 27 and 0.7 µmol photons $m^{-2}\,s^{-1}$ PAR for surface, 40m and 150m respectively). All

incubations were carried out in a temperature-controlled room, matching in-situ seawater temperature (11 °C) in light-controlled water-bath incubators on a 12:12 light:dark cycle for 24 h.

Community photophysiological assessment

Upon collection of seawater from Niskin bottles, 100 mL from each depth were concentrated, following the above method, to 10mL for assessment of photophysiological health. Steady state light curves (n=3) using a Pulse Amplitude Modulated (PAM) fluorometer (Water PAM; Walz Effeltreich, Germany) were performed, with measurements collected using Win-Control 3 software. Aliquots (2 mL) were low-light adapted (<2 µmol photons m^{-2} s^{-1}) for 15 min prior to being exposed to a saturating pulse of light (width=0.8s, intensity=8) followed by a 12-step light curve of four minutes at each light intensity (32, 48. 92, 107, 163, 240, 360, 540, 767, 1050, 1690, and 2450 µmol photons m^{-2} s^{-1}). Minimum and maximum fluorescence were recorded for each light step to obtain the following parameters: maximum and effective quantum yield of photosystem two (PSII), and non-photochemical quenching (NPQ). Using a custom-made macro in SigmaPlot* (V 14.5, Systat Software Inc., CA, USA), all light curve data were fitted according to the curve-fitting protocol of Ralph & Gademann (2005) and maximum relative electron transport rate (rETRmax), light utilisation efficiency (α), minimum saturating irradiance (E_K) and maximum saturating irradiance (Em) were obtained.

Determination of silicification rates and biogenic silica (bSi) content

Silica incorporation rates were determined following the method of McNair *et al.*, (2015). All incubations were spiked with a fluorescent dye (PDMPO, 2-(4-pyridyl)-5-((4-(2-dimethylaminoethylaminocarbamoyl) methoxy) phenyl) oxazole) for 24-h to assess the incorporation of silica to the frustule. Lysosensor Yellow/Blue DND-160 (PDMPO, ThermoFisher Scientific, Australia) was added to a final concentration of 0.125 µM PDMPO. After 24 h, 100 mL of sample was filtered through a 47 mm, 0.4 µm polycarbonate filter (Nucleopore, Whatman), placed into cryovials and stored at -80 for later analysis.

Silica incorporation and bSi content

Biogenic silica content and silica incorporation were determined by hot-alkaline-digestion of diatom frustules (boiling in 0.2M NaOH for 3h) to release frustule-bound PDMPO, according to Leblanc & Hutchins (2005). To determine cellular silica content, colorimetric analysis of reactive silicate was conducted following the methodology of Strickland and Parsons (1972) and modified by Nelson *et al.,* (1989). Absorbance was measured at 810 nm (Cary Eclipse, Agilent Technologies, U.S.A.) and compared against a standard curve (R^2 = 0.999) made with sodium metasilicate stock solution (0, 5, 25, 50, 100, 200 µM Si). To determine silicification rate (rate of PMDPO incorporation), samples were measured using a fluorescence plate reader set to excite at 375nm (Tecan Infinite M1000; Switzerland) and compared against a PDMPO standard curve (0, 5, 10, 25, 50, 100 µM Si, R^2 = 0.989) prepared using the NaOH+HCl digestion solution. Quantitative PDMPO incorporation was then calculated from ambient silicate (1.5 µmol L^{-1}) using the ratio 912.6 mol bSi per mol PDMPO (McNair *et al.,* 2015).

Particulate organic carbon and nitrogen, HPLC pigments and nutrient analyses

Particulate organic carbon (POC) and nitrogen (PON) were sampled directly from Niskin bottles onto pre-combusted (450 °C for 5 hours) 13 mm quartz microfiber filters with e-Jet pumps and analysed following the methods described in Trull *et al.*, (2018). Collection of pigment samples followed the filter pad approach (Mitchell, 1990) and high-performance liquid chromatography used to quantify chlorophyll *a* and other photosynthetic pigment concentrations (fucoxanthin, chlorophyll *b,* c_2 and c_3). All analyses were conducted at the CSIRO analytical facility, Hobart, following the methods of Schallenberg *et al.*, (2020). In-situ macronutrient data (NO_x (sum of nitrate and nitrite) phosphate and silicate) were collected and analysed on-board *RV* Investigator during the cruise, following the methods of Rees *et al.*, (2019) using a segmented flow analyser (SFA); Seal Analytical Inc. AA3 HR Autoanalyser.

Single-cell silica production rates and community composition

For taxonomic identification and classification, in-situ community composition and cell counts were collected from the Australian Ocean Data Network (AODN) for SOTS_IN2023_V03 voyage. Sampling methodologies and laboratory analysis protocols are described in Eriksen *et al.,* (2019). Using the same slide preparation as in **Chapter 3**, cell specific silicification was analysed using fluorescence microscopy (Nikon Eclipse Ni, Japan) at the same magnification (20x). We use the field of view large scan (8x8 fields) and 30 µm Z-stacks (2.5 µm increments, 13 layers) as described in **Chapter 3**, however, this time we included differential interference contrast (DIC) to compliment the custom filter (535 nm) and autofluorescence (852 nm) imaging to aid in species identification.

The addition of DIC also helped to reduce potential bias in picking bright, high fluorescing cells in favour of dim, or non-fluorescing cells when using only fluorescence filters (custom and autofluorescence). Deconvolution using Richardson-Lucy iterative function was again used on all images to reduce blur and enhance image sharpness. PDMPO fluorescence of diatom frustules over a 24-h period were quantified per cell and later compared within species across light levels treatment.

To analyse PDMPO fluorescence of each cell, the same methods were used as described in **Chapter 3**, adapted from Nielsen *et al*., (2018), using ImageJ software (Schneider *et al*., 2012).

Statistical analysis

To determine significant effects of increased irradiance on diatom morphology, one-way Analysis of Variance (ANOVA) was used with Tukey's multiple comparison test at alpha <0.05. All data were tested for homogeneity of variance and normality *a priori,* in cases where assumptions weren't met, non-parametric Kruskal Wallace test was used. Statistical analyses were performed using GraphPad Prism, version 10.0.2 (GraphPad Software, Boston, Massachusetts USA).

Results

Southern Ocean Time Series depth profiles

In situ seawater temperature and salinity (**Figure 4.2A**), nutrient (**Figure 4.2B**) and pigment concentrations (**Figure 4.2C**) showed homogeneity over the sampled 150 metre depth profiles, indicating a well-mixed water mass. Although changes were only small, ammonia concentrations declined 0.01 μm L^{-1} between 40 and 100m and then remained

constant and Chlorophyll C_2 and C_3 also declined 0.011 µg L^{-1} between surface and 150m. Total chlorophyll *a* declined 0.23 µg L^{-1} over the same distance (**Figure 4.2C**).

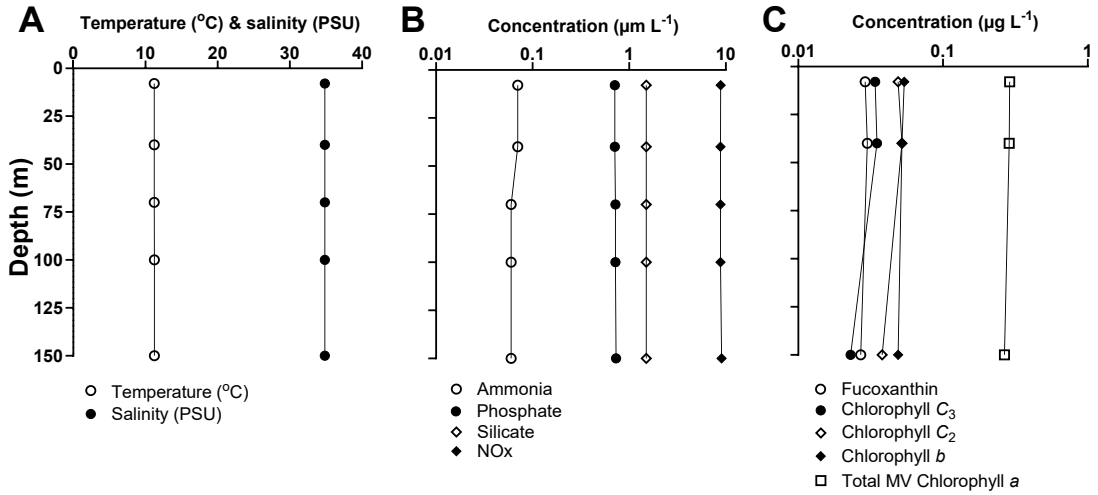

Figure 4. 2 Depth profiles of temperature and salinity (A) nutrient concentrations (B) and photosynthetic pigments (C) at the Southern Ocean Time Series (SOTS) aboard the RV Investigator, during the SOTS_IN2023_V03 voyage. CTD casts conducted at -46.9649, 141.3512. MV = mono vinyl.

Photophysiology of phytoplankton communities

Relative electron transport rates (rETR) did not show a depth-dependent response, however, deeper samples experienced photoinhibition post 1050 µmol photons m^{-2} s^{-1} in four depths (surface, 70m, 100m and 150m) compared with the 40 m community, where rETR started to decline at 764 µmol photons m^{-2} s^{-1} (**Figure 4.3A**). This was observed despite no variability in NPQ with depth (**Figure 4.3B**). Community Fv/Fm values ranged from 0.6 to 0.69 across all depths (**Figure 4.3C**), whereas the highest mean rETRmax were observed in the two lowest depths (100m and 150m, both 82 and 74 µmol photons m^{-2} s^{-1} respectively, **Figure 4.3D**). Light utilisation efficiency (α, **Figure 3E**) and minimum saturation irradiance (Ek, **Figure 4.3F**) were similar across depths (ranging from 0.23-0.29 and 244-332 µmol photons m^{-2} s^{-1}, respectively), however, there was weak evidence

of light adaptation within the communities, with higher rETR and Ek values at the lower depths (**Figure 4.3D and F**).

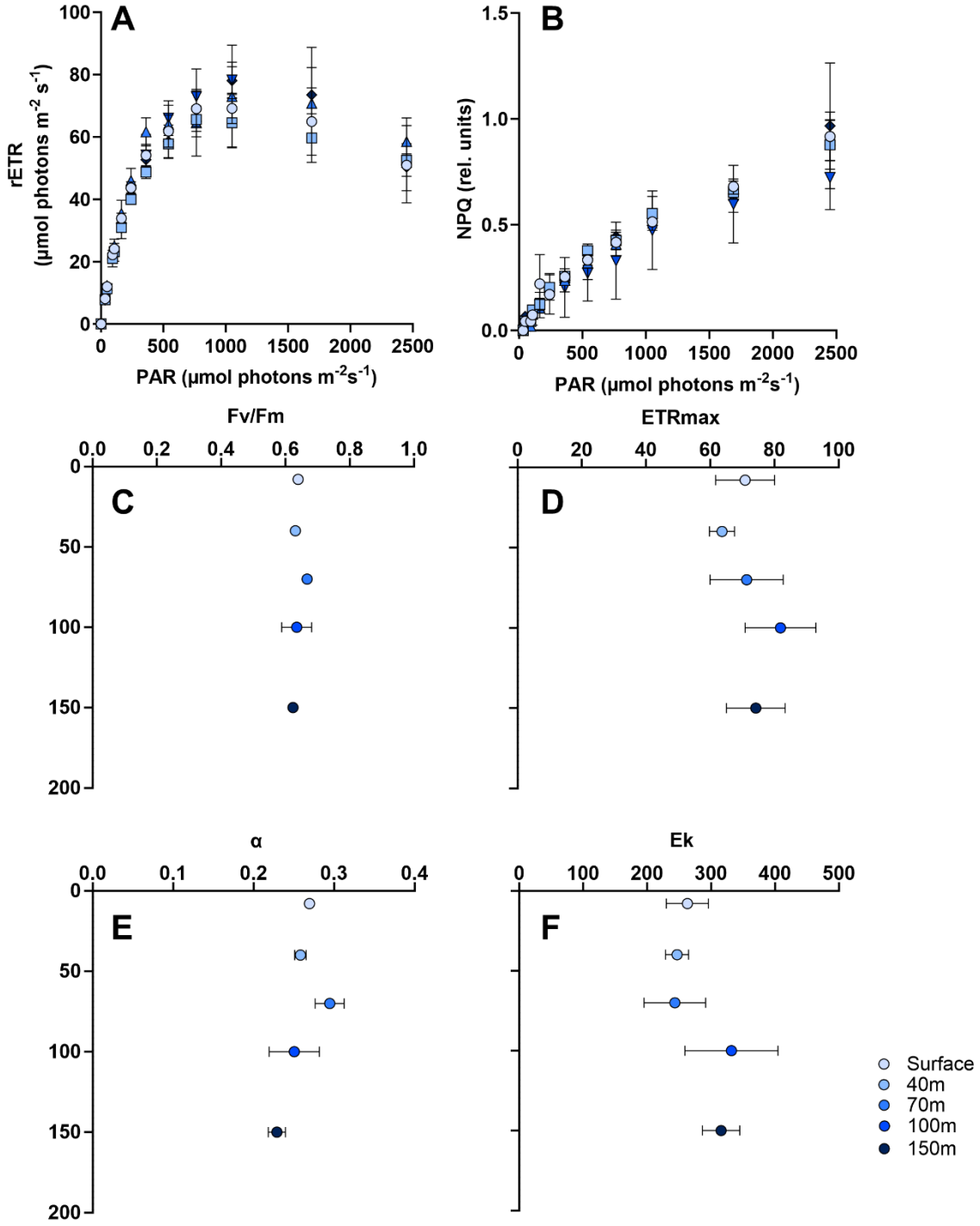

Figure 4. 3 Photosynthetic capacity of communities collected at five depths (surface, 40m, 70m, 100m and 150m) shown as: relative electron transport rate (A), non-photochemical quenching (B) maximum effective yield of PSII (C) maximum electron transport rate (D) light utilisation efficiency (E) and minimum saturating irradiance (F).

Species composition and cell counts

The phytoplankton communities across the three depths measured were highly diverse, with more than six major groups represented and over 95 taxa (**Figure 4.4A-D**). Total cell counts showed that surface and deep communities were highest in abundance, with 39,000 and 38,000 cells L^{-1}, whereas total cell abundance was lower at 40 m (28,000 cells L^{-1}, **Figure 4.4A**). Haptophytes dominated surface communities (41%), due to a surface *Phaeocystis* bloom. There was also a high proportion of haptophytes at 150 m depth (29%). Diatoms dominated the deeper water masses at 40 m and 150m, making up ~43% and 27.5% of total biomass, while dinoflagellate populations were found in high proportions at all three depths (approx. 24, 35 and 27% of the total community, in descending order). Looking at the main diatom species found at all depths, we can see a clear increase in abundance at 40 m with 12,000 diatom cells L^{-1} present compared to ~7500 and 10,500 at the surface and 150m, respectively. Further breakdown of the diatom community into species specific cell counts showed *Guinardia cylindrus* to dominate all three depths by an order of magnitude, followed by *Fragilariopsis* spp. (**Figure 4.4E-G**). High abundances of silicoflagellates were found at all three depths (**Figure 4.4B-D**). In particular, surface waters showed a high abundance of *Dictyocha speculum* (**Figure 4.4E**), which was subsequently included in our single-cell fluorescence analyses.

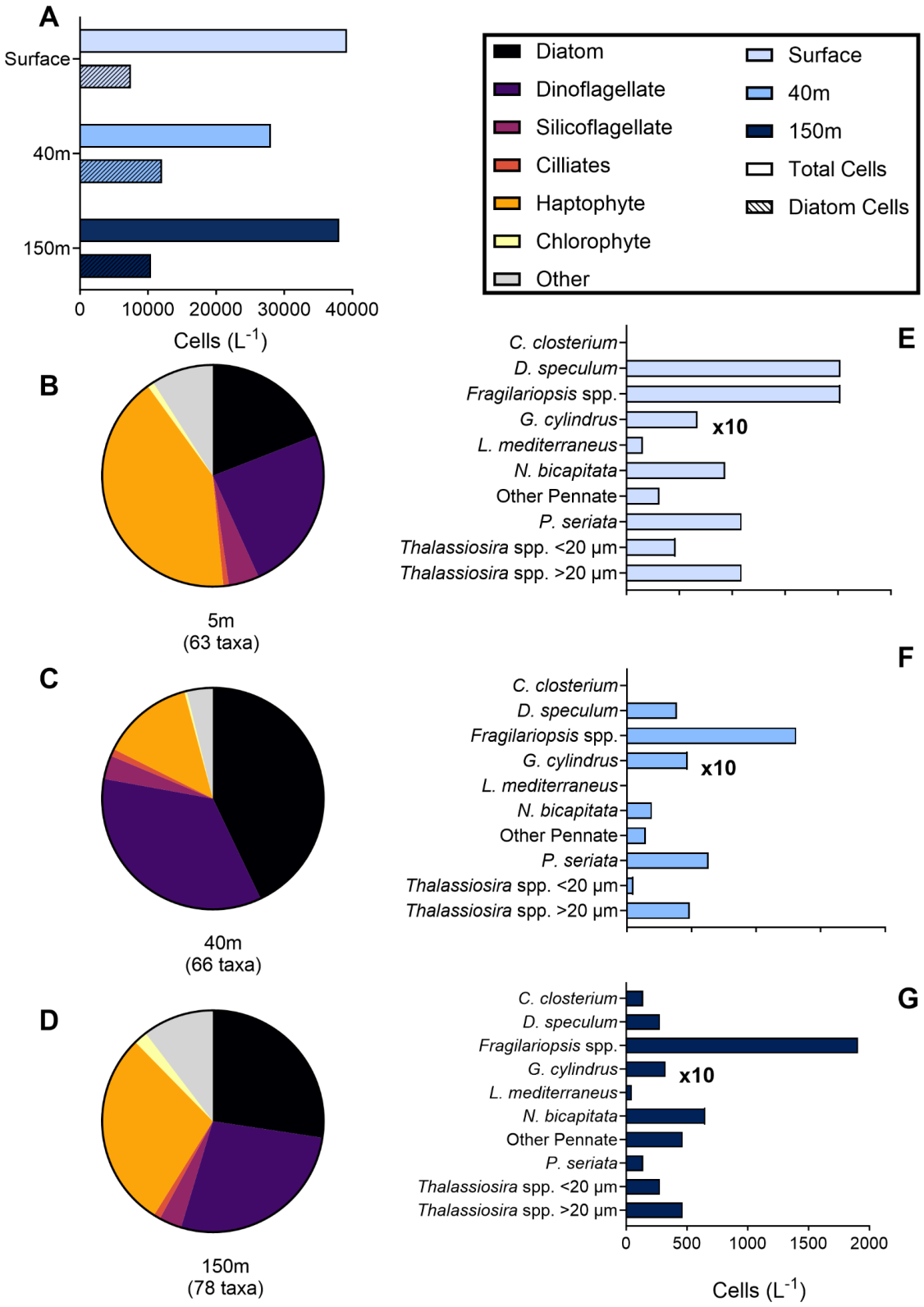

Figure 4. 4 (A) Total cell abundance at the surface, 40m and 150m (block colours, top) and the proportion of diatoms within (hashed lines, bottom). (B-D) Community composition distribution between phytoplankton groups - diatoms, dinoflagellates, silicoflagellates, ciliates, haptophytes, chlorophytes and other (zooplankton, cryptophytes, foraminifera). (E-G) Cell counts of 10 key diatom taxa from each depth. Note: *G.cylindrus* counts are 10x value depicted. Counts represent single 1L samples from each depth.

Biogenic silica, incorporated PDMPO and particulates

Biogenic silica (BSi) significantly declined in the 150 m treatment compared to the surface during the 24-h incubation ($F_{(2, 8)} = 4.905$, $P = 0.041$, **Figure 4.5A**) alongside a significant decline in silica incorporation ($F_{(2, 9)} = 6.558$, $P = 0.018$, **Figure 4.5B**). Due to the cells not being rinsed to remove unbound PDMPO, as described in the methods of McNair *et al.,* (2015), these numbers are likely an overestimation of gross silicification, however, the pattern is likely to be representative of the trend in total silica incorporation, as all samples were treated equally. Total carbon and nitrogen showed no change with depth, and elemental stoichiometry was consistent with Redfield ratios (6.5, 6.0 and 6.1 for surface, 40m and 150m respectively, **Figure 4.5B-C**). The C:Si and N:Si were similar across treatments, with the slight reduction in C:Si at 40 m, likely attributed to the reduced phytoplankton biomass at this depth (**Figure 4.5D-E**).

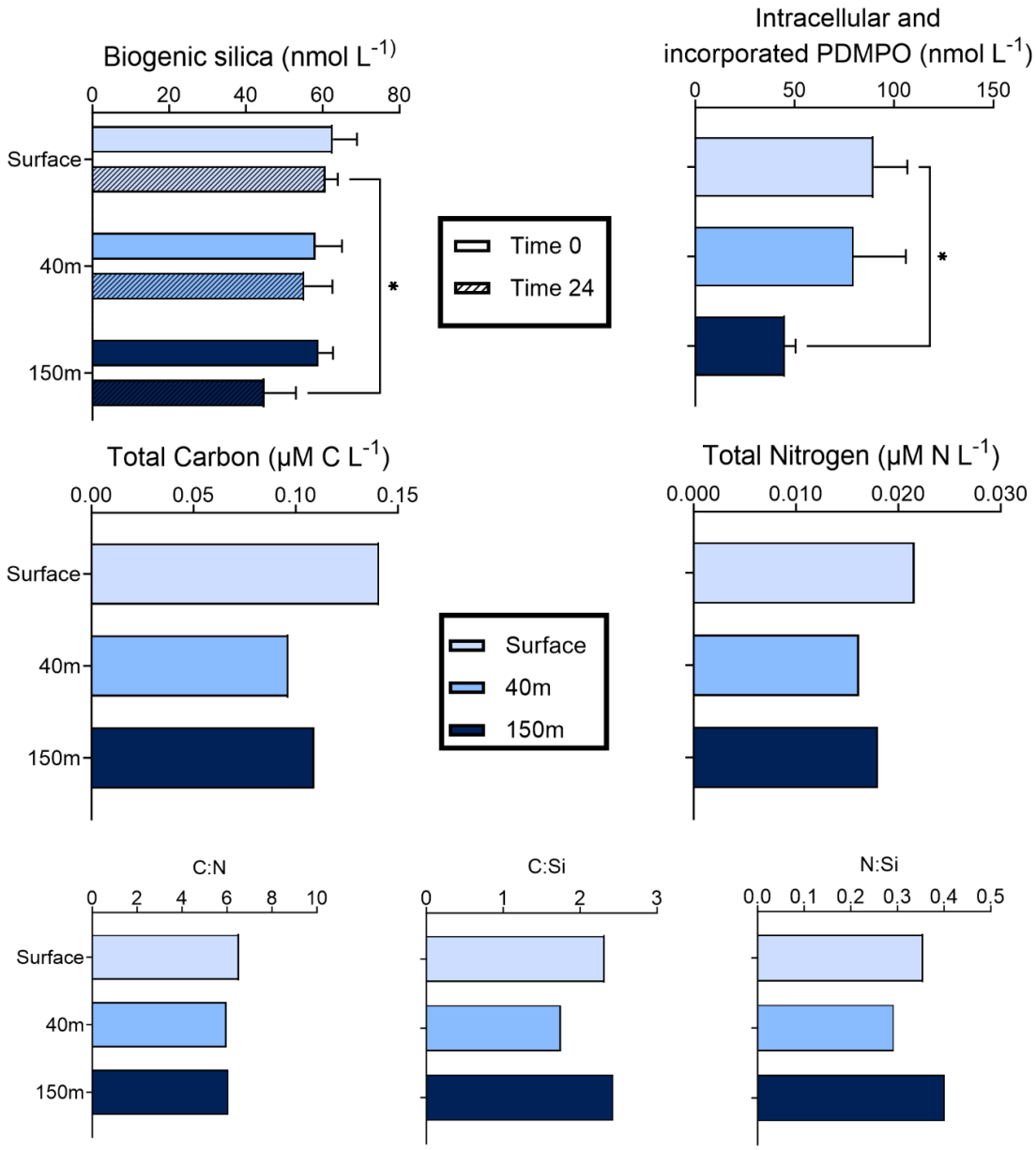

Figure 4. 5 Top row A-B: Comparison of initial bulk biogenic silica and gross PDMPO incorporation (nmol L^{-1}) at three irradiances, 100, 27 and 1 µmol photons m^{-2} s^{-1} (PAR values are comparable to CTD cast values at each depth) Middle row C-D: Total mean carbon and nitrogen at each depth (µM C L^{-1}) and bottom row E-G: elemental ratios - C:N, C:Si, N:Si. Asterisks indicate significance (* P <0.05) N=4 for top row, N=1 middle row.

We were able to obtain single-cell fluorescence measurements for 22 taxa (Appendix Table 4.2), however, to ensure statistically relevant representation across all depths, only 10 taxa were chosen for detailed analysis (**Figure 4.6**). Like **Chapter 2**, we found that cell specific silicification rates were differentially affected by irradiance, with differential response patterns across species (**Figure 4.6**). We found four taxa showed reduced silicification under low light conditions (*Cylindrotheca closterium* ($F_{(2, 38)} = 4.025$, $P = 0.026$), *Nitzschia bicapitata* ($F_{(2, 46)} = 9.205$, $P = 0.0004$), Other Pennate ($F_{(2, 57)} = 3.67$, $P = 0.032$) and *Thalassiosira* spp. <20 µm ($F_{(2, 136)} = 11.6$, $P = <0.0001$, **Figure 4.6**). We found a curious yet fairly consistent trend in cell area, whereby cells from the 40 m depth seemed to have smaller area than those from the other depths (**Appendix Figure 4.1**). Unlike in **Chapter 3**, when PDMPO fluorescence was normalised to cell area, all four species that showed a light-dependent rate per cell, maintained significant declines in silicification under low light conditions (*Cylindrotheca closterium* ($F_{(2, 38)} = 3.871$, $P = 0.0295$), *Nitzschia bicapitata* ($F_{(2, 46)} = 9.928$, $P = 0.0003$), Other Pennate ($F_{(2, 57)} = 4.155$, $P = 0.021$) and *Thalassiosira* spp. <20 µm ($F_{(2, 136)} = 12.58$, $P = <0.0001$, **Figure 4.7**). Because of the high variability in species' responses and the differences in number of measurements per taxa and therefore statistical power, we pooled all area specific silicification data from the cells measured and compared them against the incubation irradiance, representing each depth (100, 27 and 1 µmol photons m^{-2} s^{-1} for surface, 40 m and 150 m, respectively). We found a significant decline in silicification per cell area from 100 to 27 µmol photons m^{-2} s^{-1}, but no change below that irradiance (**Figure 4.8**).

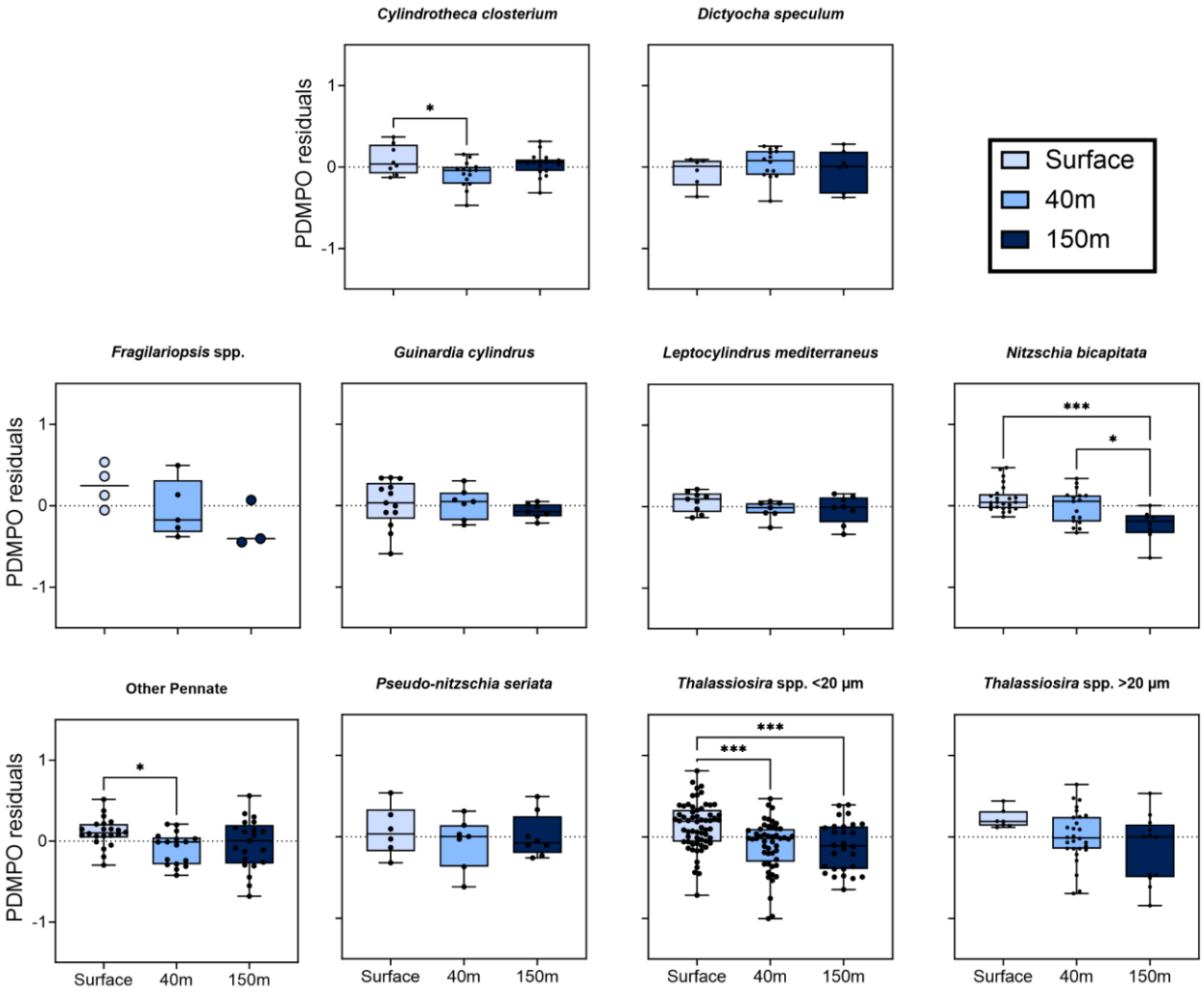

Figure 4. 6 Silica incorporation measured as total cell PDMPO fluorescence in *Cylindrotheca closterium*, *Dictyocha speculum*, *Fragilariopsis* spp., *Guinardia cylindrus*, *Leptocylindrus mediterraneus*, *Nitzschia bicapitata*, Other Pennate, *Pseudo-nitzschia seriata*, *Thalassiosira* spp. <20 µm and <20 µm. Data are visualised as box plots with overlain black dots showing the individual PDMPO fluorescence residual of individual cells after 24h PDMPO incubations. Asterisks indicate significance (* p <0.05, *** p <0.001).

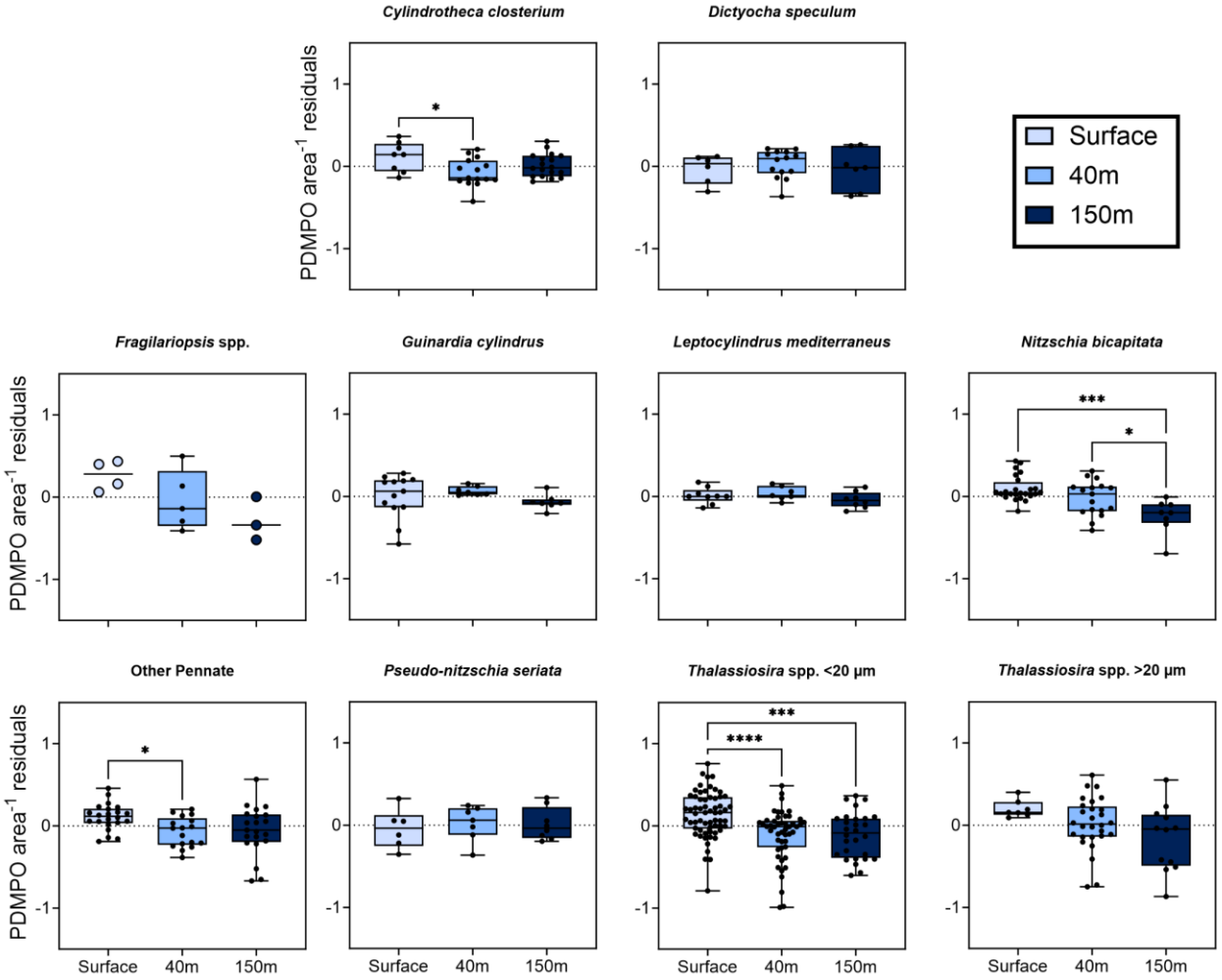

Figure 4. 7 Silica incorporation displayed as total PDMPO fluorescence per cell area in *Cylindrotheca closterium*, *Dictyocha speculum*, *Fragilariopsis* spp., *Guinardia cylindrus*, *Leptocylindrus mediterraneus*, *Nitzschia bicapitata*, Other Pennate, *Pseudo-nitzschia seriata*, *Thalassiosira* spp. <20 µm and <20 µm. Data are visualised as box plots with overlain black dots showing the individual PDMPO fluorescence per cell area residual of individual cells after 24h PDMPO incubations. Asterisks indicate significance (* p <0.05, *** p <0.001), **** p <0.0001).

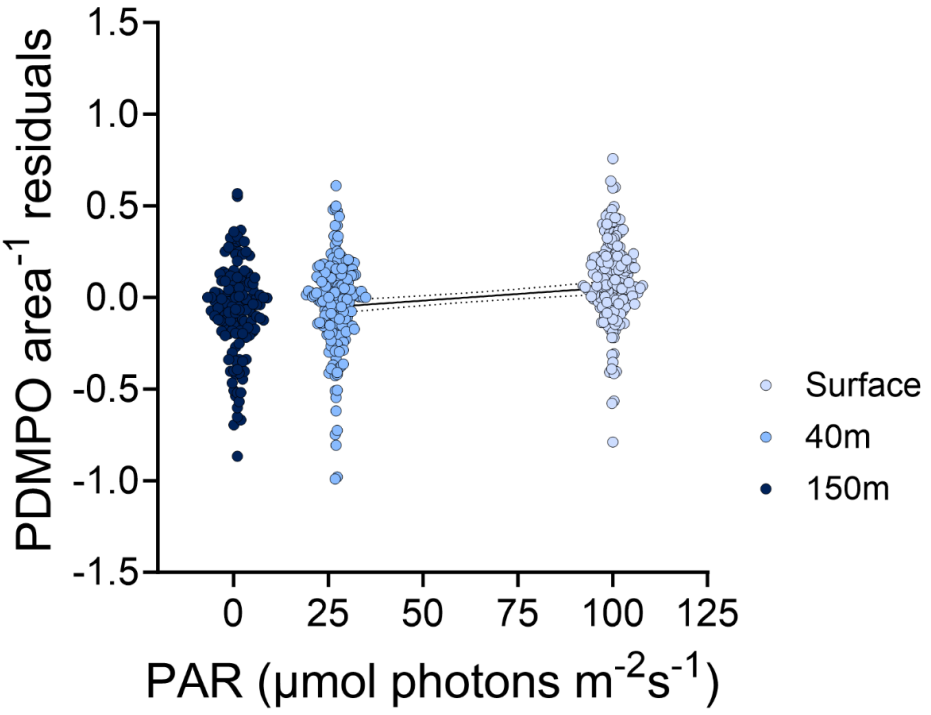

Figure 4. 8 Pooled area specific silicification compared against incubation (24 h) irradiance (100, 27 and 1 µmol photons m^{-2} s^{-1} for surface, 40 m and 150 m, respectively). Black link shows linear regression (R^2 = 0.044, $F_{(1, 361)}$ = 16.52, P = <0.0001). Dotted lines above and below show 95% confidence bands.

Discussion

In this study, we investigated how light affects diatom silicification in a Sub-Antarctic phytoplankton community. By assessing the community at a single cell level, we were able to ascertain light-dependent responses in individual species silicification rates, as well as reveal community composition shifts to different in-situ irradiances. The well mixed, homogeneous physicochemical properties of the water column meant that we were unable to detect any physiological differences in the phytoplankton communities sampled from each depth. Photosynthetic yields were high for communities from all depths, suggesting healthy phytoplankton populations. For natural samples, these relatively high F_V/F_M values would suggest the communities were not nutrient limited

(Geider *et al*., 1993; Beardall *et al*., 2001; Tan *et al*., 2019), further supported by the relatively high nitrate concentrations.

When assessing the diatom community, we saw structural and abundance shifts in the relative contribution of taxa to the phytoplankton communities at the surface, 40 m and 150 m, with haptophytes dominating the surface community and diatoms dominating the community found at 40 m. While acknowledging the potential loss of some of the larger or chain-forming species from the initial 210 µm mesh filtration, which may have biased some of our incubation results towards smaller cells, there were > 20 taxa present at all three depths. *Guinardia cylindrus* and *Fragilariopsis* spp., both commonly found in the Southern Ocean (Cornet-Barthaux *et al.,* 2007; Arrigo *et al.*, 2010; Liu *et al*., 2020) dominated all depths, whilst *Nitzschia bicapitata*, *Pseudo-nitzschia seriata* and *Thalassiosira* spp. were present in high numbers at all depths. *Cylindrotheca closterium*, usually abundant in Southern Ocean HNLC waters (Lafond *et al*., 2020) was found only at 150 m, whilst *Leptocylindrus mediterraneus* was present at the surface and 150 m, but not at 40 m. Silicoflagellates were well represented throughout the water column, with *Dictyocha speculum* being found in high abundance in surface waters but declining with depth. We did not detect a deep chlorophyll maximum (DCM), often present around 100-150 m range in the Southern Ocean (Parslow *et al*., 2001; Boyd *et al*., 2023). This could be due to the water being collected in austral autumn, meaning that although the mixed layer depth was beginning to deepen, nutrient entrainment from the deep ocean may not have occurred yet or long enough to support a larger deep community (Behrenfeld & Boss, 2018). Clarification of mechanisms controlling these communities is further complicated by the paucity of autumnal sampling within the literature of which those

available state that conditions for phytoplankton growth are deteriorating in autumn heading into winter in the Sub-Antarctic (Arteaga *et al*., 2020).

The relative consistency across communities and their physiologies provided a sound basis on which to explore light-dependent (depth-specific) diatom silicification. Both total biogenic silica and community-based silicification declined with decreasing light. This light-dependent response was not surprising, due to frustule morphogenesis being tied to energy production (Werner, 1977; Raven, 1983). When exposed to low or sub-saturating irradiances, diatoms have been seen to reduce nutrient uptake (Saito & Tsuda, 2003; Shi *et al*., 2015; Latour *et al*., 2024) and carbon fixation (Ye *et al*., 2023; Ryan-Keogh *et al*., 2018; Latour *et al*., 2024), and therefore biomolecular processes such as silica incorporation would also be reduced (Su *et al*., 2018), as was seen in **Chapter 2**. However, when looking at individual taxa, we observed highly variable responses. Silicification rates per cell only followed this trend in four of the ten species measured (*C. closterium, N. bicapitata*, Other Pennates and small *Thalassiosira* spp. (>20 µm)). Of these four species, responses were not uniform; *N. bicapitata* only showed a reduction in silicification under extremely low light (~1 µmol photons m^{-2} s^{-1}), whilst silicification was significantly reduced at 27 µmol photons m^{-2} s^{-1} in the other three species. This suggests a potential difference in their light adaptation capabilities and therefore energy capture (Heiden *et al*., 2016; Su *et al*., 2018), which could be used to support silica incorporation. Future work should consider using tools such as single-cell fluorometry to tease apart species' differences in light-dependent energy production.

In resolving taxon specific silicification rates on a per cell area basis, and probing whether silicification was dependent on size changes, we found that patterns in silicification rates were consistent with the per cell values measured (*C. closterium, N.*

bicapitata, Other Pennates and small *Thalassiosira* spp. (>20 µm)), indicating differences in cell area had no impact on silicification rate. This therefore would suggest that changes to silicification because of differences in light availability, is commensurate with cell size (Conley *et al.*, 1989). Whether the cell-specific declines measured in this study were sufficient to account for the total bulk response obtained is unclear; although we found surface irradiances able to support diatom silicification, and that this diminished with depth (low irradiance), we may have missed several key taxa that were either numerically significant or highly important with respect to silica production (Appendix Table 4.1) from our analyses. By not capturing the fluorescence data for all diatom taxa, there is the potential that we omitted key contributors to silicification (large or heavily silicified cells) such as *Corethron* spp., *Dactyliosolen* spp. or *Rhizosolenia* spp. (Appendix Table 4.2). It is known from sediment studies that different diatom taxa contribute differently to silica and carbon export (Assmy *et al.*, 2013). This decoupling is thought to occur due to frustule thickness and density; large, heavily silicified species are thought to persist at the surface for longer periods due to reduced grazing pressure (Smetacek *et al.*, 2004; Irigoien *et al.*, 2005) and therefore when they sink are often intact, resulting in a higher Si:C ratio (Smetacek *et al.*, 2004). Conversely, small, less silicified species aggregate upon mortality, sink to the deep ocean as clumps or marine snow, taking with them greater carbon per silicon (Assmy *et al.*, 2013). A higher rate of predation for small species also keeps this silica in the surface once excreted by zooplankton, effectively creating a silicon trap (Crosta *et al.*, 1997; Zielinski & Gersonde, 1997; Esper et al*.,* 2010). Therefore, to undertake a complete budget of silica production as a function of cell size and thereby identify the heavyweights of biomineralisation, greater taxonomic coverage spanning multiple size classes and genera is needed. This work should be

expanded to ensure that there is sufficient taxonomic coverage across a wider range of environments coupled with greater frequency in sampling within each depth profile.

Taxon specific measurements of cell area revealed populations of smaller cells at 40 m, for both small and large *Thalassiosira* spp. and the 'other pennate' group. The physiological and ecological explanation for such a size shift is unknown, as changes to this trait would depend on the mixing rate and direction of mixing (whether cells were on their way up or down). However, we could argue that the smaller cell sizes resulted from higher division rates (possibly from ample non-photoinhibiting light at this depth), as daughter cells are smaller than their parent cells (Hense & Beckmann, 2015). This is potentially supported by the higher abundance of diatoms observed at 40 m. It could, however, also be the result of preferential grazing on the larger cells, as overall community density was lower, and predation is likely to be highest here (Lampert, 1989). Although speculative, with the CTD cast being taken at night (8pm), diatoms may be attempting to get out of the surface waters and down to depths safe from zooplankton grazing (Raven & Waite, 2004; Arrieta *et al*., 2020). Although this does not explain the increasing of taxon-specific cell size at 150 m, it is plausible that light penetration at such a depth ensures that predation is minimal, thus allowing for cell size to grow larger and less silicified, as division rates are slowed. The four species seen to have the greatest change in cell size over the three depths were some of the smallest species measured in this study (Cornet-Barthaux *et al*., 2007). Their small surface area to volume ratio would increase nutrient affinity and diffusive flux into the cell (Grover, 1989; Irwin *et al*., 2006) which when reaching higher nutrient concentrations near the mixed layer depth (Williams & Follows, 2003; Rigby *et al*., 2020), could provide essential nutrients for cell size replenishment (Richardson *et al*., 1998).

In combining our single-celled data, we were able to confirm an energy threshold on silicification in diatoms and silicoflagellates, mediated by light. We found that with the light levels used in this study, loss in silica incorporation was significant at irradiance levels below 100 µmol photons m^{-2} s^{-1}, but not below 27 µmol photons m^{-2} s^{-1}, suggesting a minimal light requirement for net positive silicification. Physiologically, more energy results in faster growth, and frustule synthesis is a key component to diatom proliferation whereby newly deposited silica during cytokinesis forms one half of the new daughter cell (Sumper & Kröger, 2004). Other potentially important functions of the frustule are its light focussing and photoprotective properties (Noyes *et al*., 2008; Yamanaka *et al.,* 2008; Ellegaard *et al*., 2016) as described in **Chapter 2**. Cells in the surface waters exposed to higher irradiance may be able to utilise thicker frustules to aid in photo-regulation (Romann *et al*., 2015; Ellegaard et al., 2016; Goessling *et al*., 2018), whereas cells found deeper in the water column, free from photo-inhibition, may not need this protection, saving on energy. Ecologically, this change in silica incorporation could work to regulate ballast (Arrieta *et al*., 2020), whereby cells in deeper waters reduce frustule morphogenesis thereby avoiding sinking below the mixed layer (Moore & Villareal, 1996; Villareal *et al*., 2014). In contrast, cells in sunlit surface waters invest in frustule synthesis increasing their ballast and assisting them to sink to nutrient rich depths (Raven & Waite, 2004). Greater frustule strength is also hypothesised to be beneficial against grazing (Hamm *et al*., 2003), with recent research showing that varying light intensity can distort frustule nanostructure (Xu *et al*., 2021), altering mechanical strength on a per species level. Consideration of diatom frustule mechanical properties, not just its biogenic silica content (Xu *et al*., 2021), in future ocean scenarios may be an important factor if longer residence times in saturating light intensities becomes the norm (Cermeño *et al*., 2008).

Taken together, higher silica incorporation into frustule production when exposed to higher irradiance afford cells a suite of physiological and ecological advantages that may have contributed to diatom success in contemporary oceans (Malviya *et al*., 2016; Behrenfeld *et al*., 2021), what is yet to be ascertained whether these advantages will sustain diatom success under predicted future ocean scenarios (**Chapter 2** &**3**).

Our study has shown that silicification in a Sub-Antarctic phytoplankton community is a light-dependent process, with a minimum light threshold somewhere between 27-100 µmol photons m^{-2} s^{-1}. In undertaking single-celled analyses, we have highlighted that this effect can be species specific, emphasising the importance of understanding phenotypic and physiological variability in determining ecosystem responses. Current conditions at SOTS make the area a net annual carbon sink (Landschützer *et al*., 2016), through a complex interplay of biological and abiotic forcings, however it is unclear whether this region will continue to drawdown anthropogenic CO_2, with spatio-temporal effects of climate change observed already across the Sothern Ocean (Le Quéré *et al*., 2007; Constable *et al*., 2014; Petrou *et al*., 2016; Deppeler &Davidson, 2017; Petrou *et* al., 2019; Pan *et al*., 2023). Single variable experiments can often yield positive responses in diatoms (e.g. temperature, pCO_2, UV), however, environmental shifts due to climate change will not occur in isolation, and it has already been found that when measured in conjunction with one another, variables often work synergistically to reduce primary productivity and alter phytoplankton community structure (Gao *et al*., 2012). The effect of multiple stressors, coupled with their magnitude, timing and rate will almost certainly alter Southern Ocean phytoplankton community structure and individual species' physiologies, influencing the region's productivity and export potential in a future ocean.

Acknowledgements

Thank you very much to Elizabeth Shadwick and Ruth Eriksen for making data collection and further analysis possible. Thank you to the RV Investigator crew for providing an amazing experience to the Southern Ocean and to the hydrochemistry team onboard for assisting with analysis.

Appendix

Appendix Table 4. 1 Cell counts (mL^{-1}) taken from three different depths (surface, 40m and 150m) collected aboard the RV Investigator, during the SOTS_IN2023_V03 voyage to the Southern Ocean Time Series (-46.9649, 141.3512). Data obtained from the Australian Open Data Network (AODN), methods described in Eriksen *et al*., (2019).

Species	Surface (cells mL^{-1})	40m (cells mL^{-1})	150m (cells mL^{-1})	Total (cells mL^{-1})
Centric diatom 10-20 µm	0	97	0	97
Chaetoceros cf. *convolutus*	0	49	0	49
Chaetoceros dichaeta	62	0	233	295
Chaetoceros peruvianus	62	49	93	204
Chaetoceros spp. 10-20 µm	125	486	0	611
Chaetoceros spp. <10 µm cell width	0	49	0	49
Corethron pennatum	62	97	186	346
Cylindrotheca closterium	0	0	140	140
Dactyliosolen antarcticus	0	146	186	332
Dactyliosolen fragilissimus	125	0	93	218
Dactyliosolen fragilissimus <150 µm length	0	243	0	243
Dictyocha fibula	935	535	884	2354
Dictyocha speculum	686	389	279	1354
Dictyocysta elegans	0	49	93	142
Dictyocysta mitra	125	0	0	125
Fragilariopsis cf. *doliolus*	62	0	326	388
Fragilariopsis cf. *rhombica*	62	97	47	206
Fragilariopsis kerguelensis	0	97	279	376
Fragilariopsis spp.	0	389	140	528
Fragilariopsis spp. 10-20 µm	561	194	931	1686
Fragilariopsis spp. 5-10 µm	125	535	186	845
Guinardia cylindrus	2618	4616	3072	10306
Leptocylindrus danicus	0	0	47	47
Leptocylindrus mediterraneus	62	0	47	109
Nanoneis hasleae	935	1409	791	3135
Nitzschia bicapitata	374	194	652	1220
Nitzschia cf. longissima	0	97	47	144
Nitzschia spp.	62	0	47	109
Pennate diatom 25 - 50 µm	62	49	140	251
Pennate diatom 50 - 75 µm	62	97	233	392
Pennate diatom 75 - 100 µm	0	0	93	93
Planktoniella sol	0	194	279	474
Proboscia alata	436	583	233	1252
Pseudo-nitzschia delicatissima group <3 µm	312	777	47	1136
Pseudo-nitzschia seriata group >3 µm	436	632	140	1208
Rhizosolenia antennata f. semispina	125	97	605	827
Thalassiosira lentiginosa	62	49	233	344
Thalassiosira spp. 20-40 µm	436	486	465	1388
Thalassiosira spp. <10 µm	187	49	279	515
Thalassiothrix antarctica	62	146	140	348
Trichotoxon reinboldii	0	49	0	49

Appendix Table 4. 2 Species cell counts for single-cell silica production rates

Species	Number of cells measured for fluorescence
Chaetoceros dichaeta	1
Chaetoceros peruvianus	5
Chaetoceros spp [other]	4
Cylindrotheca closterium	41
Dactyliosolen antarcticus	2
Dictyocha fibula	5
Dictyocha speculum	27
Dictyocysta other	3
Fragilariopsis spp.	12
Guinardia cylindrus	27
Leptocylindrus mediterraneus	24
Nanoneis hasleae	4
Nitzschia bicapitata	49
Pennate [other]	60
Planktoniella sol	7
Proboscia alata	1
Pseudo-nitzschia delicatissima group <3 µm	6
Pseudo-nitzschia seriata group >3 µm	21
Rhizosolenia antennata f semispina	5
Thalassiosira spp 20-40 µm	47
Thalassiosira spp <10 µm	139
Thalassiothrix antarctica	6

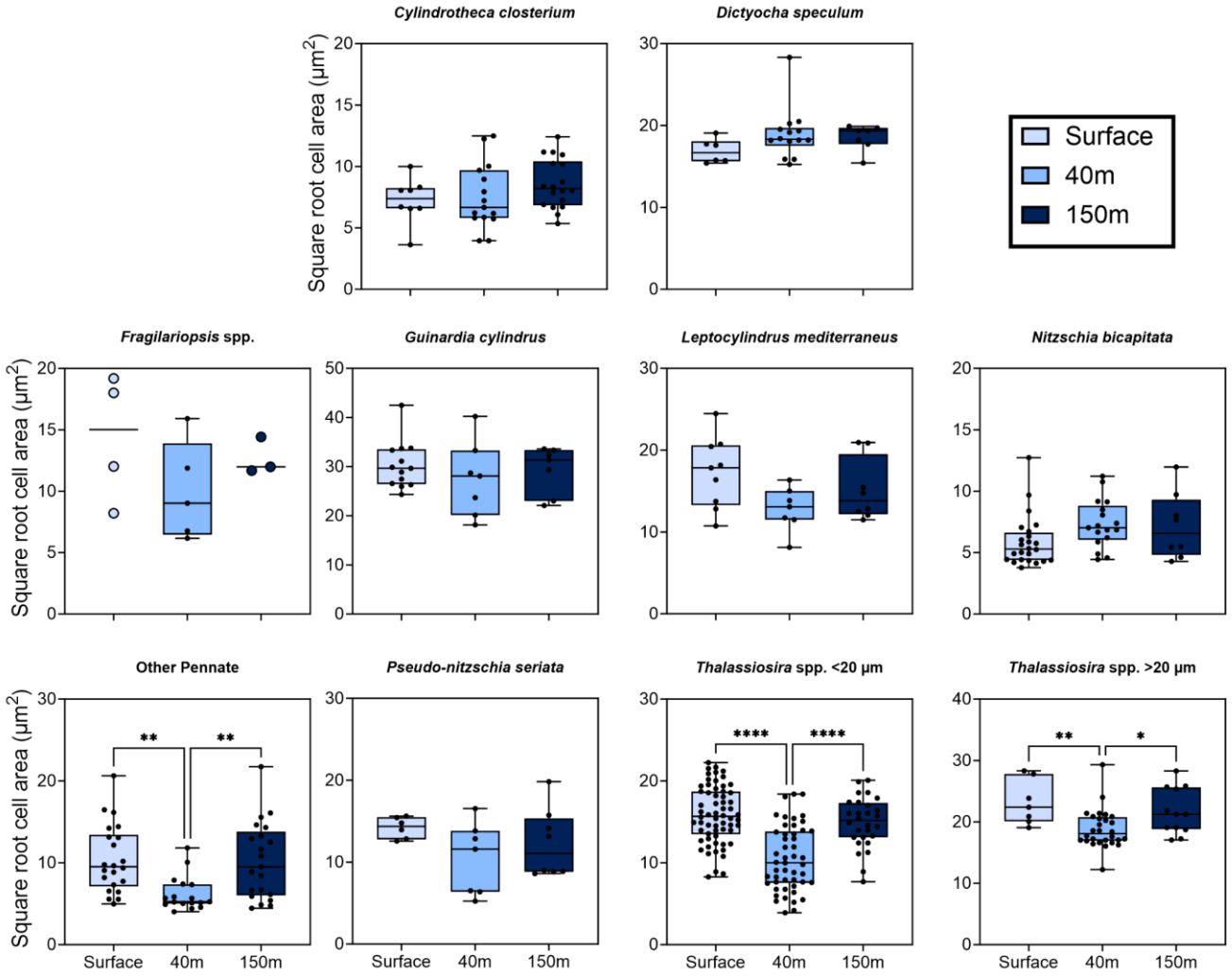

Appendix Figure 4. 1 Square root of cell area of *Cylindrotheca closterium, Dictyocha speculum*, *Fragilariopsis* spp., *Guinardia cylindrus*, *Leptocylindrus mediterraneus*, *Nitzschia bicapitata*, Other Pennate, *Pseudo-nitzschia seriata, Thalassiosira* spp. <20 µm and <20 µm. Data are visualised as box plots with overlain black dots showing individual cells after 24h PDMPO incubations. Asterisks indicate significance (* p = <0.05, ** p = <0.01, **** p = <0.0001).

Chapter 5: General discussion, future directions and conclusions

General discussion

Phytoplankton are essential for marine life to prosper. These organisms form the base of marine pelagic food webs, provide energy and essential nutrient transfer to higher trophic levels and play an important role in the biogeochemical cycling of elements (Struyf *et al.*, 2009; Benoiston *et al.*, 2017; Vance *et al.*, 2017). One group, the diatoms, are unique from their counterparts due to their production of silica frustules. This silica-based architecture provides grazing resistance and photo selective/protective functions whilst also placing them on a pedestal with respect to carbon and silica sequestration (Tréguer *et al.*, 2018). The work in this thesis has demonstrated that ocean acidification (OA) and light intensity affects silicification rates, community structure and the biomolecular composition of diatoms, highlighting some of the ways in which climate change may impact the functioning of marine ecosystems.

This research was motivated by my desire to better understand how diatom silicification will be impacted by climate change induced perturbations, both at the single cell and whole community levels. Through single strain culture experiments and field experiments, I wanted to look at how changes in environmental conditions might induce species specific silicification responses and capture any potential community compositional shifts. The bigger picture driver for these investigations was the understanding that any changes to morphology, physiology, metabolic and biomolecular function in diatoms will likely have consequences for diatom fitness, which in turn can influence trophic web dynamics and biogeochemical cycling.

My first investigation involved undertaking a laboratory study using two diatom species, *Phaeodactylum tricornutum* and *Thalassiosira weissflogii*, which have been used in culture work for decades. These 'model' diatoms were used to assess the cumulative effects of light and pH under deep and shallow mixing, to simulate potential expected conditions from climate induced ocean shoaling on diatom growth, morphology, silicification and biomolecular composition (**Chapter 2**). Although observing no change to silicification and biogenic silica quotas in the facultative silicifier *P. tricornutum,* we observed OA significantly reduced silica production under high irradiance in the obligate silicifier *T. weissflogii*. We found this response linked with photochemical efficiency, in isolation of other traits, suggesting a unique effect on silica production with CO_2. These findings led us to speculate about a potential energy balance mechanism whereby silicification plays a role in photosynthesis and photoprotection under the strong interactive effects of light and pCO_2. The different responses observed in each species highlights the inherent variability and plasticity of diatoms. Understanding the two very different strategies (facultative and obligate silicification) may uncover potential mechanisms for survival in future ocean scenarios. If our data is true for other species, whereby saturating light and pCO_2 synergistically reduce silicification, is it possible that *P. tricornutum* possess coping strategies (due to possessing little to no frustule) that other diatoms may need to employ in the future. That said, our findings demonstrate that direct comparison and/or extrapolation from one genera to another may not be suitable when predicting climate change influencesand that easy to culture strains with full genome mapping may not be the best requisites for labelling a species as 'model'.

This species' discrepancy in responses led us to investigate how multiple diatom species are impacted by OA, focussing on a natural community from a coastal marine

environment (**Chapter 3**). By combining community level response with single cell analyses, we found total diatom biomass declined by 33% and species diversity by 25% under future OA conditions. Contrary to expectation, we also showed that two species within the diatom community (*Leptocylindrus danicus* and *Pseudo-nitzschia* spp.) increased their silica incorporation under OA conditions, with large intra-specific variability in silicification rates. These findings detail the phenotypic plasticity within species and how individual diatom taxa are differentially affected by OA. Not all diatoms are equal, their differential contributions to the silica pool highlight the need for further single-cell phenotyping across a greater range of habitats to fully comprehend widescale changes and responses to single and multi-stressor climate change. Our inability to find a negative OA effect on these coastal taxa, (such as **Chapter 2**), while surprising, could be attributed to non-supersaturating light levels used in the study. If we were to replicate the experiment, but utilising saturating irradiances with high pCO_2 we may obtain similar results to **Chapter 2**. Despite this, our study revealed a gross decline of diatom biomass and species richness under OA conditions, which could have far-reaching impacts for trophic structure and elemental cycling in temperate coastal communities. Whether this is exacerbated by lowered silicification when exposed to saturating irradiance, or even temperature increase, is still to be uncovered.

In the final chapter, we had the opportunity to explore how light intensity modulates diatom silicification in a Sub Antarctic Front (SAF) diatom community at the Southern Ocean Time Series (SOTS). Community composition and physiology was relatively consistent with depth down to 150m suggesting a well-mixed assemblage, which gave us a sound basis on which to explore light-dependent (depth-specific) diatom silicification. Following incubations at three different light levels, representative of

depth-related irradiance, we found non-uniform lowered silicification in four species (*Cylindrotheca closterium, Nitzschia bicapitata*, Other Pennates and small *Thalassiosira* spp. (>20 µm)) under low irradiance, suggesting potentially different light adaptation and energy capture strategies amongst species. Pooling the depth dependent, area specific silicification data of all ten species, we found a significant decline in silicification per cell area from 100 to 27 µmol photons m^{-2} s^{-1} but no change below 27 µmol photons m^{-2} s^{-1}, suggesting a minimal light requirement for net positive silicification. Future work should consider a transplant style experiment, taking deep communities and incubating them at higher intensities and vice versa to test for inherent or acclimated light-driven silicification. Similarly, it would be good to repeat these experiments on communities in more stratified waters to see how deep chlorophyll maxima (DCM) vs surface communities respond. This work revealed light-dependent silicification rates in diatoms from the SAF, suggesting that increasing irradiance in future predicted ocean conditions may provide energy for greater diatom silicification. However, the addition of other stressors, such as OA, could act synergistically to become detrimental to diatom productivity. Going further and assessing co-limitation, it would be informative to conduct these experiments at contemporary and future predicted pCO_2 conditions and see whether future conditions promote or disperse these distinct communities.

Taken together, the findings presented in this thesis provide new insights into diatom silicification in response to climate change induced perturbations, specifically pCO_2 and light. The species-specific responses and high level of phenotypic plasticity measured throughout, confirm the importance of conducting single cell analyses alongside bulk assessments to gain a clearer understanding of pronounced changes and more nuanced shifts. The variability in silicification responses presented here, indicate a level of

adaptability in diatom response to changing environmental conditions, although the rate of change necessary for survival is yet to be determined. A synthesis of major findings is presented below, with future directions offered within this final chapter.

Ocean acidification differentially influences diatom silicification

Our current understanding of how ocean acidification will affect marine phytoplankton has shown positive, neutral and negative outcomes for various groups of phytoplankton. Diatom specific responses are more limited, with focus directed towards growth, productivity and community composition (Tatters *et* al., 2013; Davidson *et* al., 2016; Schulz *et al*., 2017; Deppeler *et al*., 2018; Bach *et al*., 2019). How OA will affect the ability for diatoms to silicify however, is only just beginning to be explored. Other environmental factors such as light and temperature have been considered, although pH effect on frustule synthesis and the potential for synergistic or antagonist mechanisms of multiple stressors is poorly understood. My research aimed to fill some of the gaps surrounding the potential effects of climate change on biomineralisation by diatoms, adding to the thin body of knowledge surrounding diatom silicification in response to ocean perturbations (**Chapters 2**, **3** & **4**). My initial investigations found that when comparing two commonly used species, *P. tricornutum* and *T. weissflogii*, there was an interactive effect of OA and silicification in *T. weissflogii,* but not in *P. tricornutum* (**Chapter 2**). The fact that *P. tricornutum* is a facultative silicifier, raises questions of its suitability as a model diatom for any physiological investigations, much less those aiming to understand environmental change and the potential influence on ocean ecology and biogeochemistry. For *T. weissflogii*, we observed that when exposed to high irradiance and acidified conditions, silica deposition was reduced to the same rate as its low light counterparts. The synergistic effect of light saturation and ocean acidification have

already been shown to reduce diatom productivity (Gao *et al*., 2012) and now we have shown that silicification rates are also impacted. We speculated that this interactive effect was the result of a shift in energy appropriation whereby cells are able to monopolise on higher light and carbon availability to enhance photosynthetic capacity thereby negating the potentially photodamaging excess light energy which allows cells to reduce their reliance on new frustule formation as a photoprotective mechanism. This however, is yet to be confirmed experimentally.

The difference in responses between these two species highlights the inherent complexity of biology, and the individualism of response expected when exposed to environmental change. We therefore set about elucidating the responses of a nearshore diatom community to OA, aiming to assess whether individual diatom taxa within the community are differentially affected and how their silicification rates are impacted (**Chapter 3**). Contrary to expectation, and in contrast to our findings in **Chapter 2**, we found two species increased their silicification rate under OA (*L. danicus* and *Psuedo-nitszchia* spp.). On its own, this would suggest greater uptake of silica and no negative impact of OA on frustule synthesis, however total diatom biomass, gross silica incorporation of the community and species richness all declined under OA conditions. These findings suggest that generalist species with broad temporal and spatial ecological niches, such as *L. danicus* and *Psuedo-nitszchia* spp., may hold an advantage over narrower niche taxa in response to OA, but that overall, we are seeing a decline in community fitness, which can play a huge role in trophic web dynamics and localised sequestration. Interestingly, the two species less impeded by OA with respect to silicification were chain forming species, questioning whether morphology and growth strategy affords greater resilience to environmental change. *Chaetoceros didymus*,

another chain forming species, followed a similar pattern to *Psuedo-nitszchia* spp. whereby its overall abundance significantly declined whilst its silicification per cell increased (not significant when normalised to cell area). It is possible for chain forming species to alter microenvironments around themselves (Musielak *et al*., 2009; Ramos *et al*., 2014; Bergkvist *et al*., 2018), which may afford them an ability to better control external environmental perturbations. Future work should include exploring the role of chain formation in resilience to OA and to distil whether a species phenotypic plasticity affords them rapid, acute responses or an evolutionary advantage through genetic adjustments.

Potential questions surrounding grazing pressure and carbon export arise when considering less silicified cells in future ocean scenarios; if survival is the ultimate outcome of an organism, is it better to rapidly proliferate, with less protection (frustule) per cell? Or does longevity arise from greater grazing protection and reproduction of fortified, hard to graze cells, akin to *r* and *k* selection? (Kemp & Villereal, 2018). Due to its laboratory setting, it is likely that we are missing some vital information. There is research suggesting the presence of grazer exudates increases silicification in natural environments (Pondaven *et al.,* 2007), therefore it would be good in future studies to include this treatment to see if it counters or exacerbate OA impacts on silica production. While the answers to these questions may provide information about the immediate survival of diatoms, thinner frustules could also have broader ecological effects on the biogeochemical cycling of elements like silicon and carbon. Reduced ballast could make sinking more difficult, increasing retention in the upper ocean and encouraging recycling of elements rather than export (Bopp *et al.,* 2005; Segschneider & Bendtsen, 2013), and with the release of carbon emissions showing no sign of

abatement, reduced carbon sequestration could turn our oceans from net carbon sinks to sources.

Elucidating contributors to carbon sink environments is integral to our understanding of climate change responses. Locations such as the SOTS drawdown more carbon than they release due to primary productivity in the region (**Chapter 4**). We observed a light modulating response on silicification, showing declining silica incorporation with decreasing irradiance, similar to **Chapter 2** in contemporary oceans, corroborating results of both datasets. We do not however know how the community at SOTS will fair under OA. Records at the time series show a decline in ocean pH decoupled from inter-annular variability (Shadwick *et al*., 2023) therefore future research should be directed towards a combination of environmental factors (OA and irradiance change), utilising the framework of **Chapter 2**, in a community setting.

Light plays a key role in diatom silicification – what is its influence in the context of a shoaling ocean?

Ocean acidification is not occurring in isolation. Ocean warming, increasing stratification of density layers reducing the mixed layer depth and reduced nutrient entrainment to the mixed layer are all expected to alter marine environments, especially in the euphotic zone (Cermeño *et al*., 2008; Yamaguchi & Suga, 2019; Li *et al*., 2020). It is therefore plausible that combinations of stressors that in isolation positively affect diatoms, could combine to negatively affect them. The minimal negative impact of OA in **Chapter 3** could suggest that light levels used were potentially sub-saturating for the community (100 µmol photons m^{-2} s^{-1}). Previous research has shown that increasing CO_2 and increasing light independent of each other can impart a positive effect on diatoms,

however when combined—saturating light (200 µmol photons m^{-2} s^{-1}) and high pCO_2 levels—they work synergistically to decrease diatom fitness (Gao *et al.*, 2012) and silicification (**Chapter 2**). Discovery of a minimal light requirement for net positive silicification in a Sub Antarctic Front diatom community (**Chapter 4**) confirms a bottom threshold for net positive silicification, it follows then, that an upper threshold could also be possible, mediated by carbon availability (**Chapter 2**). Utilisation of greater light regimes (at the very least saturating irradiance) in conjunction with OA will likely reveal more relevant results than single stressors as deterministic responses to environmental change. Whether the 200 µmol photons m^{-2} s^{-1} saturation irradiance found in Gao *et* al., (2012) and Chapter 2 is the point at which silica deposition is down regulated is unclear, and likely to again be species specific, with individual taxa having different light utilisation efficiencies (**Chapter 2** & **Chapter 4**). Furthermore, variation of light regimes could uncover diel-variation of frustule synthesis or whether silicification can happen as a rapid response to increasing and/or super saturating irradiance. Further work is needed to untangle the role of irradiance in silica production and better understand how multiple stressors (OA, temperature, nutrients) interact or are influenced by light.

Light also plays an important role on the buoyancy of a cell (Falciatore *et al.*, 2000). Diatoms are thought to silicify in high light surface waters due to greater energy availability, an increased demand for photoprotection and faster growth. This could be suggestive of a mechanistic trait for altering buoyancy (Moore & Villareal, 1996; Su *et al.*, 2018; Lavoire & Raven, 2020), whereby cells silicify more in high irradiance, becoming negatively buoyant and are able to sink more readily through the water column (Raven & Waite, 2004). The increasing light availability has also been found to stimulate lipid production (**Chapter 2**) which may counter the increase in density from frustule

synthesis and increase floating capacity (Petrucciani *et al*., 2023). Conversely, when cells were in a low light environment, we found lower silicification rates (**Chapter 2** & **4**) coupled with an increase in cell volume. This reduction in ballasting could enable ascension through the water column (Moore & Villareal, 1996; Villareal *et al*., 2014). Taken together, while not perfect, these processes could be indicative of a buoyancy regulatory mechanism, as the two processes are complementary and likely able to be used to regulate cell position in the water column by controlling vertical movement (Arrieta *et al*., 2020).

When considering these changes in the presence of OA in future scenarios, we observed two outcomes; When diatoms are under ample sub-saturating irradiance, the stimulation of pCO_2 enabled greater silica deposition in two species and no effect in eight species, although the overall community health declined (**Chapter 3**). When light was increased to saturating irradiances, silicification declined in one species and no change in another (**Chapter 2**). This highlights strong species-specific differences in their tolerances to environmental change. By going further than single deterministic response experiments, only looking at growth rate and productivity as sole indicators for response, we were able to identify physiological responses which are crucial to diatom form and function. It is unclear however which is the driving factor in silicification change; Does the increase in pCO_2 mediate the increase in otherwise photo-inhibiting irradiances, promoting greater photosynthetic rates to account for excess light energy, or does the increasing light enable the cell to utilise the excess CO_2, enabling energy production to be used in processes that can counter the simultaneous pH decline. Increasing light has been shown to increase cellular silica content (Su *et al*., 2018) whilst OA has been shown to decrease silicification (Petrou *et al*., 2019). As diatom frustules have been found to

mediate internal pH, afford protection of pH-dependent process such as cell proliferation, maintenance of the silica deposition vesicle and cell cycle progression (Brzezinski *et al.,* 1990; Hervé *et al*., 2012; Hildebrand *et al*., 2018; de Haan *et al*., 2023), it would therefore be interesting for further research to investigate whether the increased energy availability under future conditions is able to fulfil the role of the frustule in internal regulation of homeostasis. These findings would be of particular importance to Southern Ocean (SO) (**Chapter 4**) and polar species, with a generally lower mean irradiance annually and cooler, well mixed waters enabling greater intrusion of CO_2. If light mitigates OA, then species in higher latitudes maybe be at greater risk of the detrimental effects of OA (Petrou *et al.*, 2019) than temperate or tropical species (Ajani *et al*., 2021).

Untangling the response of the community from the contributions of the individual

A combination of single strain culture work, bulk assessment of communities and single cell analysis of the individual species contributions within them has provided novel insight into how diatom silicification will be affected in changing ocean conditions. Through culture work (**Chapter 2**), we were able to uncover the potential mechanisms at play when considering OA and increasing irradiance effects on frustule synthesis, affording us a healthy starting point before moving to whole community responses (**Chapter 3** & **4**). By interrogating two commonly used species, we could make comparisons with previous literature on the physiological responses of these species to environmental change. With both species labelled as 'model' diatoms, there was potential for extrapolation to other taxa should the responses of both species share commonality. This was not the case, instead, we saw highly varied responses to OA and light across the measured variables between the two species. Species specific

differences were further highlighted in **Chapters 3** & **4**. These findings therefore prompt future studies to use a greater range of species, preferably whole communities, which invariably include multiple strains of the same species, to gain a greater understand of diatom responses and plasticity in ecologically relevant scenarios.

Large scale experiments come with their own challenges but afford us greater insight and provide a more nuanced understanding of the potential 'winers and losers' in future ocean scenarios. By using single cell analyses within a mixed community study (Chapter 3 &4) we were able to uncover how these mechanism work at the fine scale and link that to the bigger picture. Our community analyses uncovered OA-induced changes to diatom community diversity, biomass, and bulk silicification rate, which all declined at high *p*CO2. However, our fine-scale approach revealed that some species reacted positively, with increasing pCO_2 stimulating silicification in two of the ten species measured (**Chapter 3**). We also showed that increasing light non-uniformly stimulated silicification in four species from the SO (**Chapter 4**). If we had hand-picked the most abundant or easiest to grow species, we may have missed these subtleties. Through combining community-level response with individual single-cell analysis, we have shown the individual contributions to the silica pool, species specific phenotypic response to environmental change and taxonomic shifts when exposed to novel conditions. By allowing within, across and multi-species interactions, we can also assume that results are a better representation of future ocean scenarios, compared to artificial conditions often associated with laboratory experiments.

Despite our best efforts, we still observed species richness decline, potentially due to bottle effects, accidental exclusion of larger species, or lossof species due to death from the imposed conditions. This therefore could mean we omitted key contributors to

silicification (large, heavily silicified cells), rare species within the community or interactions not yet observed from the current results. To undertake a complete budget of silica production under environmental change, greater taxonomic coverage, spanning multiple size classes and all genera is needed. In understanding interspecific and intraspecific variability, we can better classify the potential 'winners and losers' of climate change, with highly plastic taxa able to adjust at the rate of change required and those more rigid, may fall away. What implications this will have on community structure, nutrient cycling, carbon export and higher trophic web dynamics is still to be uncovered.

A snapshot of potential change in our future ocean surface waters: a diatom perspective

Environmental perturbations from climate change will likely impact the health and success of diatoms in a future ocean. While a comprehensive understanding of diatom silicification in response to climate change is still beyond our reach, my research has provided new insight into several changes that may be expected in a future, high *p*CO2, warmer ocean, in which diatoms are constrained to the upper, high irradiance, low nutrient surface waters (**Figure 5.1**). Summarising my key findings in **Figure 5.1**, I suggest that we may see a transition from highly diverse diatom communities to less diverse (**Chapter 3**), less silicified populations of lower overall biomass (**Chapter 2**). While evidence herein suggested that increased irradiance alone may increase silicification in diatoms and influence buoyancy regulation (**Chapters 4**), the cumulative effects show a decline in silicification when combined with OA (**Chapter 2**). We also may see a shift towards chain-forming diatom dominance (**Chapter 3**) with these species potentially

able to mitigate the detrimental effects of climate change, better than single cells, by altering their surrounding microenvironment. Reduced mixing depth and subsequent nutrient entrainment into surface waters due to ocean warming causing greater stratification of ocean layers (Capotondi *et al*., 2012) will result in increased residence times for diatoms in high irradiance, low nutrient conditions. This increases the multiplicity of stresses on diatoms in surface waters, with warmer, high pCO_2, high irradiance conditions further exacerbated by potentially nutrient limited conditions. This lack of mixing is set to alter contemporary oceans, from the well-mixed, high carbon export systems of today, into superficial nutrient recycling zones, with minimal export in the future.

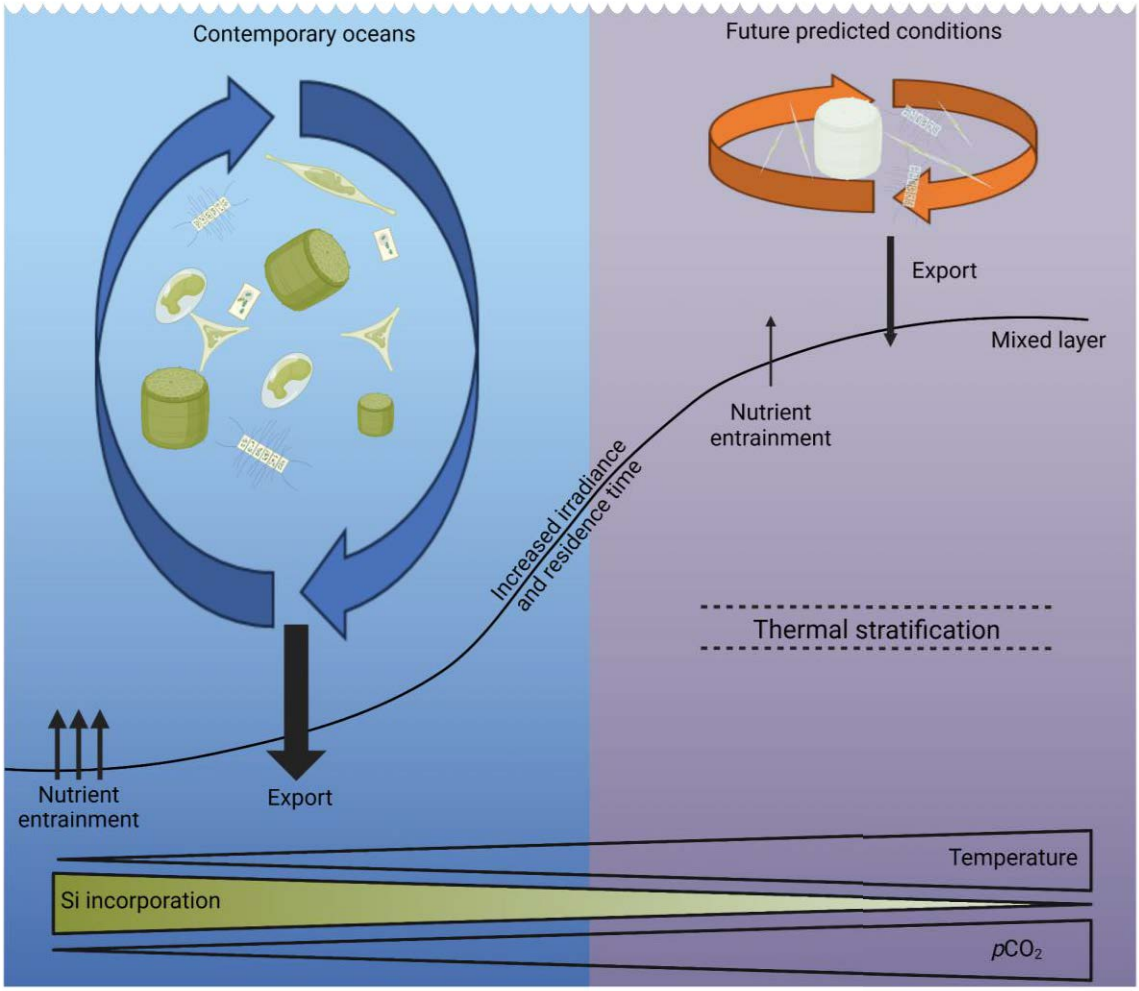

Figure 5. 1 Conceptual model of contemporary (left) and future predicted ocean conditions (right). Blue arrows depict vertical mixing of diatoms and nutrients producing large export from the euphotic zone. Orange arrows depict greater recycling of nutrients compared to contemporary oceans, reducing export and mixing under greater stratification. Mixed layer shallowing concurrently increases mean residence time of diatoms in saturating light in more stratified, future ocean conditions. Climate change induced temperature and pCO_2 could reduce silica incorporation of diatoms when exposed to multiple stressors (bottom arrows).

Future Directions

In undertaking the studies presented herein, my journey to answer my key research questions has invariably led to more questions. Here I present a few key areas that I feel are a natural extension to my work, the answers to which would provide a more comprehensive view of how ocean change is likely to influence diatom silicification. It is by no means meant as an exhaustive list of knowledge gaps and future research, rather a glimpse into some of the research questions I would have liked to include, had time permitted.

Role of nutrients and potential co-limitation in diatom silicification

Low silicic acid concentrations have been shown to reduce diatom silicification (Durkin *et al.*, 2013; Kranzler *et al.*, 2019), yet our understanding of other macronutrients co-limiting or promoting frustule synthesis is still constrained. Diatoms under nitrogen stress have been shown to increase lipid production (Levitan *et al.*, 2015) potentially partitioning workload when nutrient depletion arises, posing the idea that limitation of another essential nutrient could promote or limit silicification. If that is possible, the results in **Chapter 2** could be an underestimation of silicification decline in *T. weissflogii* due to the addition of artificially high nutrient concentrations (F/20) dampening the effect of high pCO_2. Similarly, nutrients (F/200) were added every few days during the coastal community incubations to avoid nutrient starvation (**Chapter 3**). Again, this could have masked potential co-limiting effects of OA on diatom silicification. When making comparison to the only other community study assessing diatom silicification response to OA, Petrou *et al.*, (2019) did not amend their mesocosms with macronutrients, instead sampling diatom response at the end of the exponential growth phase, allowing for nutrient exhaustion. They observed that in 7 out of 8 species silicification rates declined with increasing acidity. It would therefore be insightful to address how interactive effects of nutrient enrichment affect diatom silicification under OA. As any reduction in nutrient availability will likely make protection against the detrimental effects of OA, other climate change inducted perturbations and maintenance of cell homeostasis more difficult (Flynn *et al.*, 2012; Shi *et al.*, 2019; Zhong *et al.*, 2021).

Consideration should also be given to the role of micronutrients and trace metals in cellular function under environmental change. For example; It has been shown that silica

incorporation can be affected by iron (Fe) (Durkin *et al.*, 2012) which is already a limiting element for diatom photosynthetic activity in the SO, with seasonal and temporal variability (Boyd, 2002). It follows then, that if additions of artificial nutrients are part of experimental design when looking at SO species silicification rates, or any trait analysis, results may underestimate the effect on diatoms. Furthermore, if iron depletion is impactful on silicification in all diatoms, species in temperate and tropical regions with higher iron input may fare better in changing ocean. This leaves a big gap in knowledge and fertile ground for future work to explore the role of macro and micronutrient limitation and co-limitation on diatom silicification and taken further, how that interacts with OA.

Inter-organism interactions influence on silicification

Whilst we expand our knowledge of internal regulation of diatom silicification, further work is also needed on the inter-organism interactions, or external influences. Underpinning diatom success is their ability to secrete dissolved organic matter (Helliwell *et al.*, 2022) which attracts a wide variety of heterotrophic bacteria (Azam & Malfatti, 2007; Buchan *et al.*, 2014). These heterotrophs in return supply nutrients and cofactors forging symbiotic relationships essential for diatom survival (Amin *et al.*, 2015; Seymour *et* al., 2017; Shibl *et al.*, 2020; Le Reun *et al.*, 2023). Exchange of these extracellular products occurs in the thin boundary layer surrounding the diatom known as the phycosphere (Bell & Mitchell, 1972). These relationships already show strong seasonal and spatial variability (Ajani *et al.*, 2018; Le Reun *et al.*, 2022), and the provision of various molecules is often species specific (Amin *et al.*, 2015; Behringer *et al.*, 2018; Bramucci *et al.*, 2018). With respect to the SO particularly, metal chelation and iron rich

ligand formation from the microbiome and its influence on silicification are poorly understood. It would therefore benefit our understanding to assess the effect of microbiome composition and metabolite production on diatom silicification in natural communities, which might be overlooked in laboratory settings. Any change to microbial community, metabolite provider or production under projected environmental stressors could see the balance of exchange shift, impacting both diatoms and their associated microbial partners.

As there are beneficial interactions, there are also detrimental interactions. It has been shown that low silica concentrations result in greater viral attack on diatoms (Kranzler *et al.*, 2019) presumably due to less biogenic silica available for frustule production, yet diatoms found in iron limited regions have been found to escape viral lysis (Kranzler *et al.*, 2021). Whether these two responses are suggestive of a silica-iron link in relation to viral impact is unclear, prompting the need for further research to understand the interplay of elemental availability, frustule synthesis capability and viral susceptibility. Furthermore, future ocean perturbations such as temperature and OA could further alter these interactions, with acidic stress shown to exacerbate viral attacks (Häder & Gao, 2023), reduce photosynthetic performance in the presence of high viral load (Chen *et al.*, 2015) and increase the abundance of viruses and heterotrophic bacteria (Huang *et al.*, 2021) suggesting both direct and indirect influence on diatom-virus-bacteria interactions. As the greatest agents of mortality in the marine environment, understanding how viral infection rates may change under future conditions is key to addressing gaps in understanding future predictions of diatom productivity and biogeochemical cycling.

Protection against attack is an important trait for diatom proliferation and success in the open ocean. Studies have shown increased silicification in diatoms exposed to grazer exudates (Pondaven *et al.,* 2007) and changes to diatom production of cytotoxic compounds (Ianora & Miralto, 2010), both of which are strategies thought to increase resilience. These toxic compounds are not only thought to deter herbivorous feeding but also act as allelopathic agents against other species thereby effecting growth of diatom community competitors (Pouvreau *et* al., 2007; Xu *et al*., 2015) while retarding (teratogenic) growth in zooplankton eggs (Starr *et al*., 1999; Ianora *et al*., 2004). These findings question whether a reduction in silicification could incite toxin production in diatoms as defence mechanism against viral and grazer attack. In **Chapter 3** and **4**, we found the silicification rate of a known toxin producing diatom group, *Pseudo-nitszchia spp.,* (Ajani *et al*., 2013) to increase under OA conditions. If silicification is linked to toxin production, or independently OA induces toxin production regardless of biogenic silica metabolism, there could be cascading effects for marine food webs, with social implications for marine industries and aquaculture.

Morphology and molecular control

There is currently no comprehensive understanding of if and how environmental change will affect diatom morphology, or equally, how morphology influences resilience or susceptibility to environmental change. Although constrained to single species studies, salinity, light intensity/wavelength, pH and temperature have all been shown to influence frustule structure (Conley *et al*., 1989; Vrieling *et al*., 1999; Claquin *et al*., 2002; Hoogstraten *et al*., 2012), but nothing is known about synergistic effects or community level (broad scale) responses. When predicting future ocean scenarios, many of these

factors are expected to co-adjust, demanding further analysis at the community level with single cell inference to better understand the extent, magnitude and plasticity of diatom responses.

Questions surrounding centric and pennate adaptability due to shape morphology and the difference in chain formation versus single cell are just two of the many avenues still to be explored. While some work has been done on understanding shape and size with respect to silicon and carbon export (Smetacek, 1999; Assmy *et al.*, 2013), a mechanistic understanding of these two questions will aid further research into elucidating the 'winners and losers' of climate change.

Diatom success has been attributed to their evolution of carbon concentration mechanisms (CCMs). Enzymes such as carbonic acid (CA) augment carbon supply around RUBISCO, which catalyse bicarbonate (HCO_3^-) to carbon dioxide (CO_2) assisting in uptake for utilisation in photosynthetic carbon fixation. Milligan and Morel (2002) proposed that diatom frustules could be used as a proton donator for the dehydration of HCO_3^-. When exposed to increased pCO_2 in future conditions, energy expensive CCMs may be downregulated and a reduced dependency on frustule deposition (and proton donation) may be possible. The mechanism behind the proton donation, and whether silica dissolution occurs to offer the proton are yet to be uncovered. A mass balance of silicic acid under OA suggested that despite no change to influx rates, silica incorporation to the frustule was reduced and efflux rates were higher in cells stimulated by pCO_2 (Milligan *et al.*, 2004). Disentangling how these regulatory processes interlink and how environmental changes alter these processes will provide a better mechanistic understanding of silicification and dissolution of diatom frustules.

By answering 'how,' we can also look to answering 'when' do these processes take place. Diel activity is known to be a strong regulator of molecular processes (Ashworth *et al.*, 2013) and inextricably involved in photosynthesis (Owens *et al.*, 1980; Harding *et al.*, 1981; Putt & Prézelin, 1988) and photo-repair (Li *et* al., 2014; Li *et al.*, 2016; Gao *et al.*, 2018) however, little is known about the diel regulation of silicification. Whether diatoms can rapidly silicify in response to an immediate stressor or if it is linked to a day-night cycle mechanism is still unanswered. Both short and long (hours to days) exposure experiments would help explore the variations in silicification rates and whether climate change perturbations such as increased residence time in high light alter these processes. Genetic expression through transcriptomics, already showing diatoms transition between four states with different up/down gene regulation cycles (dawn, dusk, exponential growth and stationary phase, Ashworth *et al.*, 2013) could provide a foundational basis from which to assess silicification. These experiments are important, as energy for silicification is said to be provided by aerobic respiration (Lewin, 1955) rather than photosynthesis (Sullivan, 1976), suggesting OA effect on respiration may uncover more answers about the mechanism behind frustule synthesis. Silica uptake, incorporation and division can be uncoupled from photosynthesis and is highly species specific (references within Martin-Jézéquel *et al.*, 2000) suggesting great value in uncovering whether environmental perturbations change these processes.

Role of multiple drivers and potential synergisms

With increased residence time in high irradiance surface waters, photoinhibition becomes a greater threat to diatoms. We found interactive effects of light and CO_2 yet more detail on light specific responses is needed if we are to tease apart the range of effects from multiple stressors. Single-cell fluorescence can be utilised to ascertain

species differences in light-dependent energy production, and how multiplicity of factors may differentially affect light utilisation.

Light and OA are not the only environmental factors that influence diatom metabolism. Temperature, which is rapidly increasing across global biomes, is a major driver of metabolism, yet our knowledge of interactive effects with OA and light on diatom physiology, especially silicification, is still poorly understood. Elucidating the effects of temperature, OA and light on the amplification or amelioration of silica production will be complicated, expensive and take time if we are to collect meaningful results, yet imperative in filling gaping holes in our knowledge. Without assessing multiple drivers and potential synergisms (positive or negative) at the same time, we may miss out on mitigation or exacerbation of negative effects by one or multiple perturbations. These changes will affect diatoms spatially, temporally and latitudinally. Potential synergism between temperature and OA could see location specific changes. Areas such as ocean hotspots and the SO, due to its disproportionate heat and CO_2 absorption (Hobday & Pecl, 2014), should be prioritised for investigation.

Diversity and plasticity

Diversity can come in many forms; genetic, phenotypic, morphological or bioregional. In the case of diatoms, they exhibit high levels of diversity in all areas. Of particular importance with respect to rapid climate change is phenotypic diversity, which is a measure of species plasticity (Barrett & Schluter, 2008; Cox, 2014; Godhe & Rynearson, 2017). This diversity plays a critical role in determining how species can adapt to changing environmental conditions. We have seen throughout this thesis that within and across species variability can be quite high necessitating further research into how this

variability relates to adaptability on a regional or global scale within the relevant climate change pace. It would therefore be beneficial to look at strain variability within species (Ajani *et al*., 2021) and assess whether greater strain diversity affords improved survivability/adaptability. Furthermore, how phenotypic variability differs between generalist and specialist species with respect to silicification could be an important comparison to make, particularly for ecologically or commercially important species.

Undertaking a study on silicification in a cosmopolitan species, such as *Cylindrotheca closterium,* across a large transect may reveal subtle intra-species variability with respect to location. In contrast, a species that inhabits a more specialised niche may show a lack of plasticity in responding to environmental change. These sorts of in-depth latitudinal or bioregional studies could provide valuable insight into the adaptive mechanisms and evolutionary strategies that different species employ to cope with varying environmental conditions. By analysing the extent of silicification in the cosmopolitan species across diverse geographic regions, we could identify patterns of morphological or physiological adjustments that are driven by local environmental factors such as temperature, salinity, nutrient availability, or light intensity. These insights could also enhance our understanding of how these globally dispersed species maintain their wide distribution by adapting to local conditions, and equally, elucidate how niche species may be more vulnerable to environmental shifts.

Alongside species or latitudinal variability, it may also be important to look at diatoms from other environments, such as brackish and estuarine systems. Species inhabiting these waters are generally exposed to greater variability of conditions on a regular basis (Shirokawa *et al*., 2012; Hevia-Orube *et al*., 2016; Kamakura *et al*., 2022) and could therefore, hold some answers to physiological plasticity and the genetic coding or

mechanistic strategies involved in rapid acclimation. It would be informative to ascertain if successful traits to environmental change are present in these communities and whether they translate to marine species.

Concluding remarks

Through the body of work contained in this thesis, I have aimed to address some critical knowledge gaps, providing novel insight into diatom silicification under changing ocean conditions. By utilising a range of complexities from multi-factorial to multi-species studies, I have interrogated the phenotypic plasticity and physiological responses of diatoms to ocean acidification and variable light. By combining community level responses with single cell analyses, we have gained a better understanding of within, across and multi-species interactions affording a greater coverage of physiological and ecological responses. These results open a window into revealing some of the traits that may elucidate the potential winners and losers of climate change.

References

Abelmann, A., Gersonde, R., Cortese, G., Kuhn, G., & Smetacek, V. (2006). Extensive phytoplankton blooms in the Atlantic sector of the glacial Southern Ocean. *Paleoceanography*, *21*(1). https://doi.org/10.1029/2005PA001199

Abrantes, F., Cermeno, P., Lopes, C., Romero, O., Matos, L., Van Iperen, J., Rufino, M., & Magalhães, V. (2016). Diatoms Si uptake capacity drives carbon export in coastal upwelling systems. *Biogeosciences*, *13*(14), 4099–4109. https://doi.org/10.5194/bg-13-4099-2016

Ajani, P. A., Kahlke, T., Siboni, N., Carney, R., Murray, S. A., & Seymour, J. R. (2018). The Microbiome of the Cosmopolitan Diatom Leptocylindrus Reveals Significant Spatial and Temporal Variability. *Frontiers in Microbiology*, *9*. https://doi.org/10.3389/fmicb.2018.02758

Ajani, P. A., Petrou, K., Larsson, M. E., Nielsen, D. A., Burke, J., & Murray, S. A. (2021). Phenotypic trait variability as an indication of adaptive capacity in a cosmopolitan marine diatom. *Environmental Microbiology*, *23*(1), 207–223. https://doi.org/10.1111/1462-2920.15294

Ajani, P., Murray, S., Hallegraeff, G., Lundholm, N., Gillings, M., Brett, S., & Armand, L. (2013). The diatom genus Pseudo-nitzschia (Bacillariophyceae) in New South Wales, Australia: Morphotaxonomy, molecular phylogeny, toxicity, and distribution. *Journal of Phycology*, *49*, 765–785. https://doi.org/10.1111/jpy.12087

"Algae in glass houses": The art of arranging diatoms. (2019, March 14). *Muséum National d'histoire Naturelle*. https://vieetudiantemnhn.wordpress.com/2019/03/14/algae-in-glass-houses-the-art-of-arranging-diatoms/

Alldredge, A. L., & Gotschalk, C. C. (1989). Direct observations of the mass flocculation of diatom blooms: Characteristics, settling velocities and formation of diatom aggregates. *Deep Sea Research Part A. Oceanographic Research Papers*, *36*(2), 159–171. https://doi.org/10.1016/0198-0149(89)90131-3

Alldredge, A. L., Passow, U., & Haddock, H. D. (1998). The characteristics and transparent exopolymer particle (TEP) content of marine snow formed from thecate dinoflagellates. *Journal of Plankton Research*, *20*(3), 393–406. https://doi.org/10.1093/plankt/20.3.393

Allen, J. T., Brown, L., Sanders, R., Mark Moore, C., Mustard, A., Fielding, S., Lucas, M., Rixen, M., Savidge, G., Henson, S., & Mayor, D. (2005). Diatom carbon export enhanced by silicate upwelling in the northeast Atlantic. *Nature*, *437*(7059), 728–732. https://doi.org/10.1038/nature03948

Amin, S. A., Hmelo, L. R., van Tol, H. M., Durham, B. P., Carlson, L. T., Heal, K. R., Morales, R. L., Berthiaume, C. T., Parker, M. S., Djunaedi, B., Ingalls, A. E., Parsek, M. R., Moran, M. A., & Armbrust, E. V. (2015). Interaction and signalling between a cosmopolitan phytoplankton and associated bacteria. *Nature*, *522*(7554), 98–101. https://doi.org/10.1038/nature14488

Anderson, S. I., & Rynearson, T. A. (2020). Variability approaching the thermal limits can drive diatom community dynamics. *Limnology and Oceanography*, *65*(9), 1961–1973. https://doi.org/10.1002/lno.11430

Armbrust, E. V. (2009). The life of diatoms in the world's oceans. *Nature*, *459*(7244), Article 7244. https://doi.org/10.1038/nature08057

Armstrong McKay, D. I., Staal, A., Abrams, J. F., Winkelmann, R., Sakschewski, B., Loriani, S., Fetzer, I., Cornell, S. E., Rockström, J., & Lenton, T. M. (2022). Exceeding 1.5°C global warming could trigger multiple climate tipping points. *Science*, *377*(6611), eabn7950. https://doi.org/10.1126/science.abn7950

Arrieta, J., Jeanneret, R., Roig, P., & Tuval, I. (2020). On the fate of sinking diatoms: The transport of active buoyancy-regulating cells in the ocean. *Philosophical Transactions of the Royal Society A: Mathematical, Physical and Engineering Sciences*, *378*(2179), 20190529. https://doi.org/10.1098/rsta.2019.0529

Arrigo, K. R., Mills, M. M., Kropuenske, L. R., van Dijken, G. L., Alderkamp, A.-C., & Robinson, D. H. (2010). Photophysiology in Two Major Southern Ocean Phytoplankton Taxa: Photosynthesis and Growth of Phaeocystis antarctica and Fragilariopsis cylindrus under Different Irradiance Levels. *Integrative and Comparative Biology*, *50*(6), 950–966. https://doi.org/10.1093/icb/icq021

Arteaga, L. A., Boss, E., Behrenfeld, M. J., Westberry, T. K., & Sarmiento, J. L. (2020). Seasonal modulation of phytoplankton biomass in the Southern Ocean. *Nature Communications*, *11*, 5364. https://doi.org/10.1038/s41467-020-19157-2

Ashworth, J., Coesel, S., Lee, A., Armbrust, E. V., Orellana, M. V., & Baliga, N. S. (2013). Genome-wide diel growth state transitions in the diatom Thalassiosira pseudonana. *Proceedings of the National Academy of Sciences of the United States of America*, *110*(18), 7518–7523. https://doi.org/10.1073/pnas.1300962110

Assmy, P., Smetacek, V., Montresor, M., Klaas, C., Henjes, J., Strass, V. H., Arrieta, J. M., Bathmann, U., Berg, G. M., Breitbarth, E., Cisewski, B., Friedrichs, L., Fuchs, N., Herndl, G. J., Jansen, S., Krägefsky, S., Latasa, M., Peeken, I., Röttgers, R., … Wolf-Gladrow, D. (2013). Thick-shelled, grazer-protected diatoms decouple ocean carbon and silicon cycles in the iron-limited Antarctic Circumpolar Current. *Proceedings of the National Academy of Sciences*, *110*(51), 20633–20638. https://doi.org/10.1073/pnas.1309345110

Aubert, A., Beauchard, O., de Blok, R., Artigas, L. F., Sabbe, K., Vyverman, W., Martínez, L. A., Deneudt, K., Louchart, A., Mortelmans, J., Rijkeboer, M., & Debusschere, E. (2022). From Bacteria to Zooplankton: An Integrative Approach Revealing Regional Spatial Patterns During the Spring Phytoplankton Bloom in the Southern Bight of the North Sea. *Frontiers in Marine Science*, *9*. https://doi.org/10.3389/fmars.2022.863996

Azam, F., & Malfatti, F. (2007). Microbial structuring of marine ecosystems. *Nature Reviews Microbiology*, *5*(10), 782–791. https://doi.org/10.1038/nrmicro1747

Bach, L. T., Hernández-Hernández, N., Taucher, J., Spisla, C., Sforna, C., Riebesell, U., & Arístegui, J. (2019). Effects of Elevated CO2 on a Natural Diatom Community in the Subtropical NE Atlantic. *Frontiers in Marine Science*, *6*. https://doi.org/10.3389/fmars.2019.00075

Bach, L. T., & Taucher, J. (2019). CO_2 effects on diatoms: A synthesis of more than a decade of ocean acidification experiments with natural communities. *Ocean Science*, *15*(4), 1159–1175. https://doi.org/10.5194/os-15-1159-2019

Baines, S. B., Twining, B. S., Brzezinski, M. A., Nelson, D. M., & Fisher, N. S. (2010). Causes and biogeochemical implications of regional differences in silicification of marine diatoms. *Global Biogeochemical Cycles*, *24*(4). https://doi.org/10.1029/2010GB003856

Baker, K. G., Robinson, C. M., Radford, D. T., McInnes, A. S., Evenhuis, C., & Doblin, M. A. (2016). Thermal Performance Curves of Functional Traits Aid Understanding of Thermally

Induced Changes in Diatom-Mediated Biogeochemical Fluxes. *Frontiers in Marine Science*, *3*. https://doi.org/10.3389/fmars.2016.00044

Balch, W. M., Bates, N. R., Lam, P. J., Twining, B. S., Rosengard, S. Z., Bowler, B. C., Drapeau, D. T., Garley, R., Lubelczyk, L. C., Mitchell, C., & Rauschenberg, S. (2016). Factors regulating the Great Calcite Belt in the Southern Ocean and its biogeochemical significance. *Global Biogeochemical Cycles*, *30*(8), 1124–1144. https://doi.org/10.1002/2016GB005414

Balch, W. M., Drapeau, D. T., Bowler, B. C., Lyczkowski, E. R., Lubelczyk, L. C., Painter, S. C., & Poulton, A. J. (2014). Surface biological, chemical, and optical properties of the Patagonian Shelf coccolithophore bloom, the brightest waters of the Great Calcite Belt. *Limnology and Oceanography*, *59*(5), 1715–1732. https://doi.org/10.4319/lo.2014.59.5.1715

Bambery, K., Wood, B., & McNaughton, D. (2012). Resonant Mie scattering (RMieS) correction applied to FTIR images of biological tissue samples. *Analyst*, *137*(1), 126–132. https://doi.org/10.1039/C1AN15628D

Barrett, R. D. H., & Schluter, D. (2008). Adaptation from standing genetic variation. *Trends in Ecology & Evolution*, *23*(1), 38–44. https://doi.org/10.1016/j.tree.2007.09.008

Bartual, A., Gálvez, J. A., & Ojeda, F. (2008). *Phenotypic response of the diatom Phaeodactylum tricornutum Bohlin to experimental changes in the inorganic carbon system*. *51*(5), 350–359. https://doi.org/10.1515/BOT.2008.047

Bathmann, U. V., Scharek, R., Klaas, C., Dubischar, C. D., & Smetacek, V. (1997). Spring development of phytoplankton biomass and composition in major water masses of the Atlantic sector of the Southern Ocean. *Deep Sea Research Part II: Topical Studies in Oceanography*, *44*(1), 51–67. https://doi.org/10.1016/S0967-0645(96)00063-X

Beardall, J., Berman, T., Heraud, P., Omo Kadiri, M., Light, B. R., Patterson, G., Roberts, S., Sulzberger, B., Sahan, E., Uehlinger, U., & Wood, B. (2001). A comparison of methods for detection of phosphate limitation in microalgae. *Aquatic Sciences*, *63*(1), 107–121. https://doi.org/10.1007/PL00001342

Beardall, J., Young, E., & Roberts, S. (2001). Approaches for determining phytoplankton nutrient limitation. *Aquatic Sciences*, *63*(1), 44–69. https://doi.org/10.1007/PL00001344

Behrenfeld, M. J., & Boss, E. S. (2018). Student's tutorial on bloom hypotheses in the context of phytoplankton annual cycles. *Global Change Biology*, *24*(1), 55–77. https://doi.org/10.1111/gcb.13858

Behrenfeld, M. J., Halsey, K. H., Boss, E., Karp-Boss, L., Milligan, A. J., & Peers, G. (2021). Thoughts on the evolution and ecological niche of diatoms. *Ecological Monographs*, *91*(3), e01457. https://doi.org/10.1002/ecm.1457

Behringer, G., Ochsenkühn, M. A., Fei, C., Fanning, J., Koester, J. A., & Amin, S. A. (2018). Bacterial Communities of Diatoms Display Strong Conservation Across Strains and Time. *Frontiers in Microbiology*, *9*. https://doi.org/10.3389/fmicb.2018.00659

Bell, W., & Mitchell, R. (1972). Chemotactic and growth responses of marine bacteria to algal extracellular products. *The Biological Bulletin*, *143*(2), 265–277. https://doi.org/10.2307/1540052

Benoiston, A.-S., Ibarbalz Federico, M., Bittner, L., Guidi, L., Jahn, O., Dutkiewicz, S., & Bowler, C. (2017). The evolution of diatoms and their biogeochemical functions. *Philosophical Transactions of the Royal Society B: Biological Sciences*, *372*(1728), 20160397. https://doi.org/10.1098/rstb.2016.0397

Bergkvist, J., Klawonn, I., Whitehouse, M. J., Lavik, G., Brüchert, V., & Ploug, H. (2018). Turbulence simultaneously stimulates small- and large-scale CO2 sequestration by chain-forming diatoms in the sea. *Nature Communications*, *9*(1), 3046. https://doi.org/10.1038/s41467-018-05149-w

Bergmann, C. (1848). *Über die Verhältnisse der Wärmeökonomie der Thiere zu ihrer Größe*. https://data.europeana.eu/item/368/item_SZ3JTS6HNPWX35ZIWS5QLA7TA4LDAXDO

Bermúdez, J. R., Riebesell, U., Larsen, A., & Winder, M. (2016). Ocean acidification reduces transfer of essential biomolecules in a natural plankton community. *Scientific Reports*, *6*(1), 27749. https://doi.org/10.1038/srep27749

Bienfang, P. K., Harrison, P. J., & Quarmby, L. M. (1982). Sinking rate response to depletion of nitrate, phosphate and silicate in four marine diatoms. *Marine Biology*, *67*(3), 295–302. https://doi.org/10.1007/BF00397670

Boé, J., Hall, A., Colas, F., McWilliams, J. C., Qu, X., Kurian, J., & Kapnick, S. B. (2011). What shapes mesoscale wind anomalies in coastal upwelling zones? *Climate Dynamics*, *36*(11), 2037–2049. https://doi.org/10.1007/s00382-011-1058-5

Boelen, P., van de Poll, W. H., van der Strate, H. J., Neven, I. A., Beardall, J., & Buma, A. G. J. (2011). Neither elevated nor reduced CO2 affects the photophysiological performance of the marine Antarctic diatom *Chaetoceros brevis*. *Journal of Experimental Marine Biology and Ecology*, *406*(1), 38–45. https://doi.org/10.1016/j.jembe.2011.06.012

Bopp, L., Aumont, O., Cadule, P., Alvain, S., & Gehlen, M. (2005). Response of diatoms distribution to global warming and potential implications: A global model study. *Geophysical Research Letters*, *32*(19). https://doi.org/10.1029/2005GL023653

Bopp, L., Monfray, P., Aumont, O., Dufresne, J.-L., Le Treut, H., Madec, G., Terray, L., & Orr, J. C. (2001). Potential impact of climate change on marine export production. *Global Biogeochemical Cycles*, *15*(1), 81–99. https://doi.org/10.1029/1999GB001256

Boyd, P., Antoine, D., Baldry, K., Cornec, M., Ellwood, M., Halfter, S., Lacour, L., Latour, P., Strzepek, R., Trull, T., & Rohr, T. (2023). *Controls on Polar Southern Ocean Deep Chlorophyll Maxima: Viewpoints from Multiple Observational Platforms*. https://doi.org/10.22541/essoar.168677216.63458355/v1

Boyd, P. W. (2002). Environmental Factors Controlling Phytoplankton Processes in the Southern Ocean1. *Journal of Phycology*, *38*(5), 844–861. https://doi.org/10.1046/j.1529-8817.2002.t01-1-01203.x

Boyd, P. W. (2019). Physiology and iron modulate diverse responses of diatoms to a warming Southern Ocean. *Nature Climate Change*, *9*(2), 148–152. https://doi.org/10.1038/s41558-018-0389-1

Boyd, P. W., Ellwood, M. J., Tagliabue, A., & Twining, B. S. (2017). Biotic and abiotic retention, recycling and remineralization of metals in the ocean. *Nature Geoscience*, *10*(3), 167–173. https://doi.org/10.1038/ngeo2876

Boyd, P. W., Jickells, T., Law, C. S., Blain, S., Boyle, E. A., Buesseler, K. O., Coale, K. H., Cullen, J. J., De Baar, H. J., Follows, M., & others. (2007). Mesoscale iron enrichment experiments 1993-2005: Synthesis and future directions. *Science*, *315*(5812), 612–617.

Boyd, P. W., & Law, C. S. (2001). The Southern Ocean Iron RElease Experiment (SOIREE)—Introduction and summary. *Deep Sea Research Part II: Topical Studies in Oceanography*, *48*(11), 2425–2438. https://doi.org/10.1016/S0967-0645(01)00002-9

Boyd, P. W., Watson, A. J., Law, C. S., Abraham, E. R., Trull, T., Murdoch, R., Bakker, D. C. E., Bowie, A. R., Buesseler, K. O., Chang, H., Charette, M., Croot, P., Downing, K., Frew, R., Gall, M., Hadfield, M., Hall, J., Harvey, M., Jameson, G., … Zeldis, J. (2000). A mesoscale

phytoplankton bloom in the polar Southern Ocean stimulated by iron fertilization. *Nature*, *407*(6805), 695–702. https://doi.org/10.1038/35037500

Bramucci, A. R., Labeeuw, L., Orata, F. D., Ryan, E. M., Malmstrom, R. R., & Case, R. J. (2018). The Bacterial Symbiont Phaeobacter inhibens Shapes the Life History of Its Algal Host Emiliania huxleyi. *Frontiers in Marine Science*, *5*. https://doi.org/10.3389/fmars.2018.00188

Bravo, I., & Figueroa, R. I. (2014). Towards an Ecological Understanding of Dinoflagellate Cyst Functions. *Microorganisms*, *2*(1), Article 1. https://doi.org/10.3390/microorganisms2010011

Bréhélin, C., Kessler, F., & Wijk, K. J. van. (2007). Plastoglobules: Versatile lipoprotein particles in plastids. *Trends in Plant Science*, *12*(6), 260–266. https://doi.org/10.1016/j.tplants.2007.04.003

Brussaard, C. P. D., Noordeloos, A. a. M., Witte, H., Collenteur, M. C. J., Schulz, K., Ludwig, A., & Riebesell, U. (2013). Arctic microbial community dynamics influenced by elevated CO_2 levels. *Biogeosciences*, *10*(2), 719–731. https://doi.org/10.5194/bg-10-719-2013

Brzezinski, M. A., & Nelson, D. M. (1989). Seasonal changes in the silicon cycle within a Gulf Stream warm-core ring. *Deep Sea Research Part A. Oceanographic Research Papers*, *36*(7), 1009–1030. https://doi.org/10.1016/0198-0149(89)90075-7

Brzezinski, M. A., Nelson, D. M., Franck, V. M., & Sigmon, D. E. (2001). Silicon dynamics within an intense open-ocean diatom bloom in the Pacific sector of the Southern Ocean. *Deep Sea Research Part II: Topical Studies in Oceanography*, *48*(19), 3997–4018. https://doi.org/10.1016/S0967-0645(01)00078-9

Brzezinski, M. A., Olson, R. J., & Chisholm, S. W. (1990). Silicon availability and cell-cycle progression in marine diatoms. *Marine Ecology Progress Series*, *67*(1), 83–96.

Buchan, A., LeCleir, G. R., Gulvik, C. A., & González, J. M. (2014). Master recyclers: Features and functions of bacteria associated with phytoplankton blooms. *Nature Reviews. Microbiology*, *12*(10), 686–698. https://doi.org/10.1038/nrmicro3326

Buesseler, K. O. (1998). The decoupling of production and particulate export in the surface ocean. *Global Biogeochemical Cycles*, *12*(2), 297–310. https://doi.org/10.1029/97GB03366

Burckle, L. H. (1984). Diatom distribution and paleoceanographic reconstruction in the Southern Ocean—Present and last glacial maximum. *Marine Micropaleontology*, *9*(3), 241–261. https://doi.org/10.1016/0377-8398(84)90015-X

Burkhardt, S., Amoroso, G., Riebesell, U., & Sültemeyer, D. (2001). CO2 and HCO3 ⇵ uptake in marine diatoms acclimated to different CO2 concentrations. *Limnology and Oceanography*, *46*(6), 1378–1391. https://doi.org/10.4319/lo.2001.46.6.1378

Burkhardt, S., Riebesell, U., & Zondervan, I. (1999). Effects of growth rate, CO2 concentration, and cell size on the stable carbon isotope fractionation in marine phytoplankton. *Geochimica et Cosmochimica Acta*, *63*(22), 3729–3741. https://doi.org/10.1016/S0016-7037(99)00217-3

Capitani, L., de Araujo, J. N., Vieira, E. A., Angelini, R., & Longo, G. O. (2022). Ocean Warming Will Reduce Standing Biomass in a Tropical Western Atlantic Reef Ecosystem. *Ecosystems*, *25*(4), 843–857. https://doi.org/10.1007/s10021-021-00691-z

Capone, D. G., Burns, J. A., Montoya, J. P., Subramaniam, A., Mahaffey, C., Gunderson, T., Michaels, A. F., & Carpenter, E. J. (2005). Nitrogen fixation by Trichodesmium spp.: An important source of new nitrogen to the tropical and subtropical North Atlantic Ocean. *Global Biogeochemical Cycles*, *19*(2). https://doi.org/10.1029/2004GB002331

Capotondi, A., Alexander, M. A., Bond, N. A., Curchitser, E. N., & Scott, J. D. (2012). Enhanced upper ocean stratification with climate change in the CMIP3 models. *Journal of Geophysical Research: Oceans*, *117*(C4).

Carpenter, E. J., & Foster, R. A. (2002). Marine Cyanobacterial Symbioses. In A. N. Rai, B. Bergman, & U. Rasmussen (Eds.), *Cyanobacteria in Symbiosis* (pp. 11–17). Springer Netherlands. https://doi.org/10.1007/0-306-48005-0_2

Casteleyn, G., Chepurnov, V. A., Leliaert, F., Mann, D. G., Bates, S. S., Lundholm, N., Rhodes, L., Sabbe, K., & Vyverman, W. (2008). Pseudo-nitzschia pungens (Bacillariophyceae): A cosmopolitan diatom species? *Harmful Algae*, *7*(2), 241–257. https://doi.org/10.1016/j.hal.2007.08.004

Cermeño, P., Dutkiewicz, S., Harris, R. P., Follows, M., Schofield, O., & Falkowski, P. G. (2008). The role of nutricline depth in regulating the ocean carbon cycle. *Proceedings of the National Academy of Sciences*, *105*(51), 20344–20349. https://doi.org/10.1073/pnas.0811302106

Cermeño, P., Marañón, E., Harbour, D., & Harris, R. P. (2006). Invariant scaling of phytoplankton abundance and cell size in contrasting marine environments. *Ecology Letters*, *9*(11), 1210–1215. https://doi.org/10.1111/j.1461-0248.2006.00973.x

Chen, B., Landry, M. R., Huang, B., & Liu, H. (2012). Does warming enhance the effect of microzooplankton grazing on marine phytoplankton in the ocean? *Limnology and Oceanography*, *57*(2), 519–526. https://doi.org/10.4319/lo.2012.57.2.0519

Chen, S., & Gao, K. (2011). Solar ultraviolet radiation and CO2-induced ocean acidification interacts to influence the photosynthetic performance of the red tide alga Phaeocystis globosa (Prymnesiophyceae). *Hydrobiologia*, *675*(1), 105–117. https://doi.org/10.1007/s10750-011-0807-0

Chen, S., Gao, K., & Beardall, J. (2015). Viral attack exacerbates the susceptibility of a bloom-forming alga to ocean acidification. *Global Change Biology*, *21*(2), 629–636. https://doi.org/10.1111/gcb.12753

Chlorophyll. (2024, April 30). [Text.Article]. NASA Earth Observatory. https://earthobservatory.nasa.gov/global-maps/MY1DMM_CHLORA

Claquin, P., Martin-Jézéquel, V., Kromkamp, J. C., Veldhuis, M. J. W., & Kraay, G. W. (2002). Uncoupling of Silicon Compared with Carbon and Nitrogen Metabolisms and the Role of the Cell Cycle in Continuous Cultures of Thalassiosira Pseudonana (bacillariophyceae) Under Light, Nitrogen, and Phosphorus Control1. *Journal of Phycology*, *38*(5), 922–930. https://doi.org/10.1046/j.1529-8817.2002.t01-1-01220.x

Clark, J. S., Poore, A. G. B., & Doblin, M. A. (2018). Shaping up for stress: Physiological flexibility is key to survivorship in a habitat-forming macroalga. *Journal of Plant Physiology*, *231*, 346–355. https://doi.org/10.1016/j.jplph.2018.10.005

Closset, I., McNair, H. M., Brzezinski, M. A., Krause, J. W., Thamatrakoln, K., & Jones, J. L. (2021). Diatom response to alterations in upwelling and nutrient dynamics associated with climate forcing in the California Current System. *Limnology and Oceanography*, *66*(4), 1578–1593. https://doi.org/10.1002/lno.11705

Cohen, N. R., Mann, E., Stemple, B., Moreno, C. M., Rauschenberg, S., Jacquot, J. E., Sunda, W. G., Twining, B. S., & Marchetti, A. (2018). Iron storage capacities and associated ferritin gene expression among marine diatoms. *Limnology and Oceanography*, *63*(4), 1677–1691. https://doi.org/10.1002/lno.10800

Colman, B., & Rotatore, C. (1995). Photosynthetic inorganic carbon uptake and accumulation in two marine diatoms. *Plant, Cell & Environment*, *18*(8), 919–924. https://doi.org/10.1111/j.1365-3040.1995.tb00601.x

Conley, D. J., Kilham, S. S., & Theriot, E. (1989). Differences in silica content between marine and freshwater diatoms. *Limnology and Oceanography*, *34*(1), 205–212. https://doi.org/10.4319/lo.1989.34.1.0205

Constable, A. J., Melbourne-Thomas, J., Corney, S. P., Arrigo, K. R., Barbraud, C., Barnes, D. K. A., Bindoff, N. L., Boyd, P. W., Brandt, A., Costa, D. P., Davidson, A. T., Ducklow, H. W., Emmerson, L., Fukuchi, M., Gutt, J., Hindell, M. A., Hofmann, E. E., Hosie, G. W., Iida, T., … Ziegler, P. (2014). Climate change and Southern Ocean ecosystems I: How changes in physical habitats directly affect marine biota. *Global Change Biology*, *20*(10), 3004–3025. https://doi.org/10.1111/gcb.12623

Cornet, V., Armand, L., & Quéguiner, B. (2007). Biovolume and biomass estimates of key diatoms in the Southern Ocean. *Aquatic Microbial Ecology - AQUAT MICROB ECOL*, *48*, 295–308. https://doi.org/10.3354/ame048295

Cottingham, K., Lennon, J., & Brown, B. (2005). Knowing When to Draw the Line: Designing More Informative Ecological Experiments. *Frontiers in Ecology and the Environment*, *3*, 145. https://doi.org/10.2307/3868542

Cox, E. J. (2014). Diatom identification in the face of changing species concepts and evidence of phenotypic plasticity. *Journal of Micropalaeontology*, *33*(2), 111–120. https://doi.org/10.1144/jmpaleo2014-014

Crosta, X., Pichon, J.-J., & Labracherie, M. (1997). Distribution of Chaetoceros resting spores in modern peri-Antarctic sediments. *Marine Micropaleontology*, *29*(3–4), 283–299. https://doi.org/10.1016/s0377-8398(96)00033-3

Davidson, A. T., McKinlay, J., Westwood, K., Thomson, P. G., Enden, R. van den, Salas, M. de, Wright, S., Johnson, R., & Berry, K. (2016). Enhanced CO2 concentrations change the structure of Antarctic marine microbial communities. *Marine Ecology Progress Series*, *552*, 93–113. https://doi.org/10.3354/meps11742

de Haan, D., Aram, L., Peled-Zehavi, H., Addadi, Y., Ben-Joseph, O., Rotkopf, R., Elad, N., Rechav, K., & Gal, A. (2023). Exocytosis of the silicified cell wall of diatoms involves extensive membrane disintegration. *Nature Communications*, *14*, 480. https://doi.org/10.1038/s41467-023-36112-z

De Luca, D. D., Kooistra, W. H. C. F., Sarno, D., Gaonkar, C. C., & Piredda, R. (2019). Global distribution and diversity of Chaetoceros (Bacillariophyta, Mediophyceae): Integration of classical and novel strategies. *PeerJ*, *7*, e7410. https://doi.org/10.7717/peerj.7410

De Martino, A., Meichenin, A., Shi, J., Pan, K., & Bowler, C. (2007). Genetic and phenotypic characterization of Phaeodactylum tricornutum (Bacillariophyceae) accessions1. *Journal of Phycology*, *43*(5), 992–1009. https://doi.org/10.1111/j.1529-8817.2007.00384.x

De Tommasi, E., Gielis, J., & Rogato, A. (2017). Diatom Frustule Morphogenesis and Function: A Multidisciplinary Survey. *Marine Genomics*, *35*, 1–18. https://doi.org/10.1016/j.margen.2017.07.001

Dell'Aquila, G., Ferrante, M. I., Gherardi, M., Cosentino Lagomarsino, M., Ribera d'Alcalà, M., Iudicone, D., & Amato, A. (2017). Nutrient consumption and chain tuning in diatoms exposed to storm-like turbulence. *Scientific Reports*, *7*(1), 1828. https://doi.org/10.1038/s41598-017-02084-6

Deppeler, S. L., & Davidson, A. T. (2017). Southern Ocean Phytoplankton in a Changing Climate. *Frontiers in Marine Science*, *4*. https://doi.org/10.3389/fmars.2017.00040

Deppeler, S., Petrou, K., Schulz, K. G., Westwood, K., Pearce, I., McKinlay, J., & Davidson, A. (2018). Ocean acidification of a coastal Antarctic marine microbial community reveals a critical threshold for CO₂ tolerance in phytoplankton productivity. *Biogeosciences*, *15*(1), 209–231. https://doi.org/10.5194/bg-15-209-2018

DeVries, T. (2014). The oceanic anthropogenic CO2 sink: Storage, air-sea fluxes, and transports over the industrial era. *Global Biogeochemical Cycles*, *28*(7), 631–647. https://doi.org/10.1002/2013GB004739

Dickson, A. (2010). Standards for Ocean Measurements. *Oceanography*, *23*(3), 34–47. https://doi.org/10.5670/oceanog.2010.22

Dickson, A. G. (1990). Thermodynamics of the dissociation of boric acid in potassium chloride solutions from 273.15 to 318.15 K. *Journal of Chemical & Engineering Data*, *35*(3), 253–257. https://doi.org/10.1021/je00061a009

Dickson, A. G., & Millero, F. J. (1987). A comparison of the equilibrium constants for the dissociation of carbonic acid in seawater media. *Deep-Sea Research, Part A: Oceanographic Research Papers*, *34*(10), 1733–1743. https://doi.org/10.1016/0198-0149(87)90021-5

Dugdale, R. C., & Wilkerson, F. P. (1998). Silicate regulation of new production in the equatorial Pacific upwelling. *Nature*, *391*(6664), 270–273. https://doi.org/10.1038/34630

Duncan, R. J., Nielsen, D. A., Sheehan, C. E., Deppeler, S., Hancock, A. M., Schulz, K. G., Davidson, A. T., & Petrou, K. (2022). Ocean acidification alters the nutritional value of Antarctic diatoms. *New Phytologist*, *233*(4), 1813–1827. https://doi.org/10.1111/nph.17868

Duncan, R. J., Nielsen, D., Søreide, J. E., Varpe, Ø., Tobin, M. J., Pitusi, V., Heraud, P., & Petrou, K. (2024). Biomolecular profiles of Arctic sea-ice diatoms highlight the role of under-ice light in cellular energy allocation. *ISME Communications*, *4*(1), ycad010. https://doi.org/10.1093/ismeco/ycad010

Durkin, C. A., Bender, S. J., Chan, K. Y. K., Gaessner, K., Grünbaum, D., & Armbrust, E. V. (2013). Silicic acid supplied to coastal diatom communities influences cellular silicification and the potential export of carbon. *Limnology and Oceanography*, *58*(5), 1707–1726. https://doi.org/10.4319/lo.2013.58.5.1707

Durkin, C. A., Marchetti, A., Bender, S. J., Truong, T., Morales, R., Mock, T., & Armbrust, E. V. (2012). Frustule-related gene transcription and the influence of diatom community composition on silica precipitation in an iron-limited environment. *Limnology and Oceanography*, *57*(6), 1619–1633. https://doi.org/10.4319/lo.2012.57.6.1619

Dutkiewicz, S., Morris, J. J., Follows, M. J., Scott, J., Levitan, O., Dyhrman, S. T., & Berman-Frank, I. (2015). Impact of ocean acidification on the structure of future phytoplankton communities. *Nature Climate Change*, *5*(11), Article 11. https://doi.org/10.1038/nclimate2722

Edwards, K. F., Thomas, M. K., Klausmeier, C. A., & Litchman, E. (2016). Phytoplankton growth and the interaction of light and temperature: A synthesis at the species and community level. *Limnology and Oceanography*, *61*(4), 1232–1244. https://doi.org/10.1002/lno.10282

Edwards, M., & Richardson, A. J. (2004). Impact of climate change on marine pelagic phenology and trophic mismatch. *Nature*, *430*(7002), Article 7002. https://doi.org/10.1038/nature02808

Ellegaard, M., Lenau, T., Lundholm, N., Maibohm, C., Friis, S. M. M., Rottwitt, K., & Su, Y. (2016). The fascinating diatom frustule—Can it play a role for attenuation of UV radiation? *Journal of Applied Phycology*, *28*(6), 3295–3306. https://doi.org/10.1007/s10811-016-0893-5

Engel, A., Goldthwait, S., Passow, U., & Alldredge, A. (2002). Temporal decoupling of carbon and nitrogen dynamics in a mesocosm diatom bloom. *Limnology and Oceanography*, *47*(3), 753–761. https://doi.org/10.4319/lo.2002.47.3.0753

Eriksen, R., Davies, C. H., Bonham, P., Coman, F. E., Edgar, S., FR McEnnulty, McLeod, D., Miller, M. J., Rochester, W., Slotwinski, A., Tonks, M. L., Uribe-Palomino, J., & Richardson, A. J. (2019). *Australia's long-term plankton observations: The Integrated Marine Observing System National Reference Station Network*. https://figshare.utas.edu.au/articles/journal_contribution/Australia_s_long-term_plankton_observations_the_Integrated_Marine_Observing_System_National_Reference_Station_Network/23008904/1

Esper, O., Gersonde, R., & Kadagies, N. (2010). Diatom distribution in southeastern Pacific surface sediments and their relationship to modern environmental variables. *Palaeogeography, Palaeoclimatology, Palaeoecology*, *287*(1), Article 1. https://doi.org/10.1016/j.palaeo.2009.12.006

European Commission. Directorate-General for Research. (2011). *Guide to best practices for ocean acidification research and data reporting*. Publications Office. https://data.europa.eu/doi/10.2777/66906

Falciatore, A., d'Alcalà, M. R., Croot, P., & Bowler, C. (2000). Perception of Environmental Signals by a Marine Diatom. *Science*, *288*(5475), 2363–2366. https://doi.org/10.1126/science.288.5475.2363

Falkowski, P. G., Barber, R. T., & Smetacek, V. (1998). Biogeochemical Controls and Feedbacks on Ocean Primary Production. *Science*, *281*(5374), 200–206. https://doi.org/10.1126/science.281.5374.200

Falkowski, P. G., & Knoll, A. H. (2007). CHAPTER 1 - An Introduction to Primary Producers in the Sea: Who They Are, What They Do, and When They Evolved. In P. G. Falkowski & A. H. Knoll (Eds.), *Evolution of Primary Producers in the Sea* (pp. 1–6). Academic Press. https://doi.org/10.1016/B978-012370518-1/50002-3

Falkowski, P. G., & Oliver, M. J. (2007). Mix and match: How climate selects phytoplankton. *Nature Reviews Microbiology*, *5*(10), 813–819. https://doi.org/10.1038/nrmicro1751

Feng, Y., Chai, F., Wells, M. L., Liao, Y., Li, P., Cai, T., Zhao, T., Fu, F., & Hutchins, D. A. (2021). The Combined Effects of Increased pCO2 and Warming on a Coastal Phytoplankton Assemblage: From Species Composition to Sinking Rate. *Frontiers in Marine Science*, *8*. https://doi.org/10.3389/fmars.2021.622319

Feng, Y., Hare, C. E., Rose, J. M., Handy, S. M., DiTullio, G. R., Lee, P. A., Smith, W. O., Peloquin, J., Tozzi, S., Sun, J., Zhang, Y., Dunbar, R. B., Long, M. C., Sohst, B., Lohan, M., & Hutchins, D. A. (2010). Interactive effects of iron, irradiance and CO2 on Ross Sea phytoplankton. *Deep Sea Research Part I: Oceanographic Research Papers*, *57*(3), 368–383. https://doi.org/10.1016/j.dsr.2009.10.013

Field, C. B., Behrenfeld, M. J., Randerson, J. T., & Falkowski, P. (1998). Primary production of the biosphere: Integrating terrestrial and oceanic components. *Science (New York, N.Y.)*, *281*(5374), 237–240. https://doi.org/10.1126/science.281.5374.237

Finkel, Z. V., Beardall, J., Flynn, K. J., Quigg, A., Rees, T. A. V., & Raven, J. A. (2010). Phytoplankton in a changing world: Cell size and elemental stoichiometry. *Journal of Plankton Research*, *32*(1), 119–137. https://doi.org/10.1093/plankt/fbp098

Firme, G. F., Hughes, D. J., Laiolo, L., Roughan, M., Suthers, I. M., & Doblin, M. A. (2023). Contrasting phytoplankton composition and primary productivity in multiple mesoscale eddies along the East Australian coast. *Deep Sea Research Part I: Oceanographic Research Papers*, *193*, 103952. https://doi.org/10.1016/j.dsr.2022.103952

Flombaum, P., Gallegos, J. L., Gordillo, R. A., Rincón, J., Zabala, L. L., Jiao, N., Karl, D. M., Li, W. K. W., Lomas, M. W., Veneziano, D., Vera, C. S., Vrugt, J. A., & Martiny, A. C. (2013). Present and future global distributions of the marine Cyanobacteria Prochlorococcus and Synechococcus. *Proceedings of the National Academy of Sciences*, *110*(24), 9824–9829. https://doi.org/10.1073/pnas.1307701110

Flynn, K. J., Blackford, J. C., Baird, M. E., Raven, J. A., Clark, D. R., Beardall, J., Brownlee, C., Fabian, H., & Wheeler, G. L. (2012). Changes in pH at the exterior surface of plankton with ocean acidification. *Nature Climate Change*, *2*(7), 510–513. https://doi.org/10.1038/nclimate1489

Francius, G., Tesson, B., Dague, E., Martin-Jézéquel, V., & Dufrêne, Y. F. (2008). Nanostructure and nanomechanics of live Phaeodactylum tricornutum morphotypes. *Environmental Microbiology*, *10*(5), 1344–1356. https://doi.org/10.1111/j.1462-2920.2007.01551.x

Franks, S. J., & Hoffmann, A. A. (2012). Genetics of climate change adaptation. *Annual Review of Genetics*, *46*, 185–208. https://doi.org/10.1146/annurev-genet-110711-155511

Friedland, K. D., Morse, R. E., Shackell, N., Tam, J. C., Morano, J. L., Moisan, J. R., & Brady, D. C. (2020). Changing Physical Conditions and Lower and Upper Trophic Level Responses on the US Northeast Shelf. *Frontiers in Marine Science*, *7*. https://doi.org/10.3389/fmars.2020.567445

Frölicher, T. L., Sarmiento, J. L., Paynter, D. J., Dunne, J. P., Krasting, J. P., & Winton, M. (2015). *Dominance of the Southern Ocean in Anthropogenic Carbon and Heat Uptake in CMIP5 Models*. https://doi.org/10.1175/JCLI-D-14-00117.1

Fry, B., & Wainright, S. C. (1991). Diatom sources of 13 C-rich carbon in marine food webs. *Marine Ecology Progress Series*, *76*(2), 149–157. JSTOR.

Fu, W., Randerson, J. T., & Moore, J. K. (2016). Climate change impacts on net primary production (NPP) and export production (EP) regulated by increasing stratification and phytoplankton community structure in the CMIP5 models. *Biogeosciences*, *13*(18), 5151–5170. https://doi.org/10.5194/bg-13-5151-2016

Fuhrmann, T., Landwehr, S., El Rharbi-Kucki, M., & Sumper, M. (2004). Diatoms as living photonic crystals. *Applied Physics B*, *78*(3), 257–260. https://doi.org/10.1007/s00340-004-1419-4

Ganapathy, K., Chidambaram, K., Janarthanan, R., & Ramasamy, R. (2017). Effect of UV-B Radiation on Growth, Photosynthetic Activity andMetabolic Activities of Chlorella vulgaris. *Research and Reviews: Journal of Microbiology and Biotechnology*. https://www.semanticscholar.org/paper/Effect-of-UV-B-Radiation-on-Growth%2C-Photosynthetic-Ganapathy-Chidambaram/5220f933bf25f62ca02f8dc143b1f06b70917e57

Gao, G., Shi, Q., Xu, Z., Xu, J., Campbell, D. A., & Wu, H. (2018). Global warming interacts with ocean acidification to alter PSII function and protection in the diatom *Thalassiosira weissflogii*. *Environmental and Experimental Botany*, *147*, 95–103. https://doi.org/10.1016/j.envexpbot.2017.11.014

Gao, K., Beardall, J., Häder, D.-P., Hall-Spencer, J. M., Gao, G., & Hutchins, D. A. (2019). Effects of Ocean Acidification on Marine Photosynthetic Organisms Under the Concurrent Influences of Warming, UV Radiation, and Deoxygenation. *Frontiers in Marine Science*, *6*. https://www.frontiersin.org/articles/10.3389/fmars.2019.00322

Gao, K., & Campbell, D. A. (2014). Photophysiological responses of marine diatoms to elevated CO2 and decreased pH: A review. *Functional Plant Biology*, *41*(5), 449–459. https://doi.org/10.1071/FP13247

Gao, K., Helbling, E. W., Häder, D.-P., & Hutchins, D. A. (2012). Responses of marine primary producers to interactions between ocean acidification, solar radiation, and warming. *Marine Ecology Progress Series*, *470*, 167–189. https://doi.org/10.3354/meps10043

Gao, K., Wu, Y., Li, G., Wu, H., Villafañe, V. E., & Helbling, E. W. (2007). Solar UV Radiation Drives CO2 Fixation in Marine Phytoplankton: A Double-Edged Sword. *Plant Physiology*, *144*(1), 54–59. https://doi.org/10.1104/pp.107.098491

Gao, K., Xu, J., Gao, G., Li, Y., Hutchins, D. A., Huang, B., Wang, L., Zheng, Y., Jin, P., Cai, X., Häder, D.-P., Li, W., Xu, K., Liu, N., & Riebesell, U. (2012). Rising CO2 and increased light exposure synergistically reduce marine primary productivity. *Nature Climate Change*, *2*(7), Article 7. https://doi.org/10.1038/nclimate1507

Garcia, H. E., Antonov, J. I., Boyer, T. P., Levitus, S., & Locarnini, R. A. (2006). *World Ocean Atlas 2005. Volume 4: Nutrients (phosphate, Nitrate, Silicate)*. NOAA National Oceanographic Data Center.

García-Gómez, C., Mata, M. T., Breusegem, F. V., & Segovia, M. (2016). Low-steady-state metabolism induced by elevated CO2 increases resilience to UV radiation in the unicellular green-algae Dunaliella tertiolecta. *Environmental and Experimental Botany*, *132*, 163–174. https://doi.org/10.1016/j.envexpbot.2016.09.001

García-Reyes, M., & Largier, J. (2010). Observations of increased wind-driven coastal upwelling off central California. *Journal of Geophysical Research: Oceans*, *115*(C4). https://doi.org/10.1029/2009JC005576

Gattuso, J.-P., & Hansson, L. (2011). *Ocean Acidification*. OUP Oxford.

Gattuso, J.-P., Lee, K., Rost, B., & Schulz, K. (2010). Approaches and tools to manipulate the carbonate chemistry. In U. Riebesell, V. J. Fabry, L. Hansson, & J.-P. Gattuso (Eds.), *In: Guide to Best Practices for Ocean Acidification Research and Data Reporting. , Ed. By Riebesell, Ulf, Fabry, V. J., Hansson, L. and Gattuso, J.-P. Publications Office of the European Union, Luxembourg, Ch. 2.: Vol. Chapter 2* (p. Ch. 2). Publications Office of the European Union. https://doi.org/10/1/OA-Guide_Ch2_2010.pdf

Gattuso, J.-P., Magnan, A., Billé, R., Cheung, W. W. L., Howes, E. L., Joos, F., Allemand, D., Bopp, L., Cooley, S. R., Eakin, C. M., Hoegh-Guldberg, O., Kelly, R. P., Pörtner, H.-O., Rogers, A. D., Baxter, J. M., Laffoley, D., Osborn, D., Rankovic, A., Rochette, J., … Turley, C. (2015). Contrasting futures for ocean and society from different anthropogenic CO2 emissions scenarios. *Science*, *349*(6243), aac4722. https://doi.org/10.1126/science.aac4722

Geider, R. J., La Roche, J., Greene, R. M., & Olaizola, M. (1993). Response of the Photosynthetic Apparatus of Phaeodactylum Tricornutum (bacillariophyceae) to Nitrate,

Phosphate, or Iron Starvation. *Journal of Phycology*, *29*(6), 755–766. https://doi.org/10.1111/j.0022-3646.1993.00755.x

Gemmell, B. J., Oh, G., Buskey, E. J., & Villareal, T. A. (2016). Dynamic sinking behaviour in marine phytoplankton: Rapid changes in buoyancy may aid in nutrient uptake. *Proceedings of the Royal Society B: Biological Sciences*, *283*(1840), 20161126. https://doi.org/10.1098/rspb.2016.1126

Gleich, S. J., Plough, L. V., & Glibert, P. M. (2020). Photosynthetic efficiency and nutrient physiology of the diatom Thalassiosira pseudonana at three growth temperatures. *Marine Biology*, *167*(9), 124. https://doi.org/10.1007/s00227-020-03741-7

Godhe, A., & Rynearson, T. (2017). The role of intraspecific variation in the ecological and evolutionary success of diatoms in changing environments. *Philosophical Transactions of the Royal Society B: Biological Sciences*, *372*(1728), 20160399. https://doi.org/10.1098/rstb.2016.0399

Goessling, J. W., Su, Y., Cartaxana, P., Maibohm, C., Rickelt, L. F., Trampe, E. C. L., Walby, S. L., Wangpraseurt, D., Wu, X., Ellegaard, M., & Kühl, M. (2018). Structure-based optics of centric diatom frustules: Modulation of the in vivo light field for efficient diatom photosynthesis. *New Phytologist*, *219*(1), 122–134. https://doi.org/10.1111/nph.15149

Gómez, F. (2012). A checklist and classification of living dinoflagellates (Dinoflagellata, Alveolata). *CICIMAR Oceánides*, *27*(1), 65–140. https://doi.org/10.37543/oceanides.v27i1.111

Gordon, R., Losic, D., Tiffany, M. A., Nagy, S. S., & Sterrenburg, F. A. S. (2009). The Glass Menagerie: Diatoms for novel applications in nanotechnology. *Trends in Biotechnology*, *27*(2), 116–127. https://doi.org/10.1016/j.tibtech.2008.11.003

Grover, J. P. (1989). Influence of Cell Shape and Size on Algal Competitive Ability. *Journal of Phycology*, *25*(2), 402–405. https://doi.org/10.1111/j.1529-8817.1989.tb00138.x

Gruber, N., Clement, D., Carter, B. R., Feely, R. A., van Heuven, S., Hoppema, M., Ishii, M., Key, R. M., Kozyr, A., Lauvset, S. K., Lo Monaco, C., Mathis, J. T., Murata, A., Olsen, A., Perez, F. F., Sabine, C. L., Tanhua, T., & Wanninkhof, R. (2019). The oceanic sink for anthropogenic CO2 from 1994 to 2007. *Science*, *363*(6432), 1193–1199. https://doi.org/10.1126/science.aau5153

Gruber, N., Gloor, M., Mikaloff Fletcher, S. E., Doney, S. C., Dutkiewicz, S., Follows, M. J., Gerber, M., Jacobson, A. R., Joos, F., Lindsay, K., Menemenlis, D., Mouchet, A., Müller, S. A., Sarmiento, J. L., & Takahashi, T. (2009). Oceanic sources, sinks, and transport of atmospheric CO2. *Global Biogeochemical Cycles*, *23*(1). https://doi.org/10.1029/2008GB003349

Gruber, N., Landschützer, P., & Lovenduski, N. S. (2019). The Variable Southern Ocean Carbon Sink. *Annual Review of Marine Science*, *11*(Volume 11, 2019), 159–186. https://doi.org/10.1146/annurev-marine-121916-063407

Grzebyk, D., Denardou, A., Berland, B., & Pouchus, Y. F. (1997). Evidence of a new toxin in the red-tide dinoflagellate Prorocentrum minimum. *Journal of Plankton Research*, *19*(8), 1111–1124. https://doi.org/10.1093/plankt/19.8.1111

Guillard, R. R., & Ryther, J. H. (1962). Studies of marine planktonic diatoms. I. Cyclotella nana Hustedt, and Detonula confervacea (cleve) Gran. *Canadian Journal of Microbiology*, *8*, 229–239. https://doi.org/10.1139/m62-029

Häder, D.-P., & Gao, K. (2023). Aquatic Productivity under Multiple Stressors. *Water*, *15*(4), Article 4. https://doi.org/10.3390/w15040817

Hale, M. S., & Mitchell, J. G. (2001). Functional morphology of diatom frustule microstructures: Hydrodynamic control of Brownian particle diffusion and advection. *Aquatic Microbial Ecology*, *24*(3), 287–295. https://doi.org/10.3354/ame024287

Hamm, C. E., Merkel, R., Springer, O., Jurkojc, P., Maier, C., Prechtel, K., & Smetacek, V. (2003). Architecture and material properties of diatom shells provide effective mechanical protection. *Nature*, *421*(6925), Article 6925. https://doi.org/10.1038/nature01416

Hancock, A. M., Davidson, A. T., McKinlay, J., McMinn, A., Schulz, K. G., & van den Enden, R. L. (2018). Ocean acidification changes the structure of an Antarctic coastal protistan community. *Biogeosciences*, *15*(8), 2393–2410. https://doi.org/10.5194/bg-15-2393-2018

Harding, L. W., Meeson, B. W., Prézelin, B. B., & Sweeney, B. M. (1981). Diel periodicity of photosynthesis in marine phytoplankton. *Marine Biology*, *61*(2), 95–105. https://doi.org/10.1007/BF00386649

Hauck, J., Völker, C., Wang, T., Hoppema, M., Losch, M., & Wolf-Gladrow, D. A. (2013). Seasonally different carbon flux changes in the Southern Ocean in response to the southern annular mode. *Global Biogeochemical Cycles*, *27*(4), 1236–1245. https://doi.org/10.1002/2013GB004600

Haugan, P. M., & Drange, H. (1996). Effects of CO2 on the ocean environment. *Energy Conversion and Management*, *37*(6), 1019–1022. https://doi.org/10.1016/0196-8904(95)00292-8

Havenhand, J., Dupont, S., & Quinn, G. (2010). *Designing ocean acidification experiments to maximize inference*. Deakin University. https://dro.deakin.edu.au/articles/chapter/Designing_ocean_acidification_experiments_to_maximize_inference/21007063/1

Heiden, J. P., Bischof, K., & Trimborn, S. (2016). Light Intensity Modulates the Response of Two Antarctic Diatom Species to Ocean Acidification. *Frontiers in Marine Science*, *3*. https://doi.org/10.3389/fmars.2016.00260

Heil, C. A., Revilla, M., Glibert, P. M., & Murasko, S. (2007). Nutrient quality drives differential phytoplankton community composition on the southwest Florida shelf. *Limnology and Oceanography*, *52*(3), 1067–1078. https://doi.org/10.4319/lo.2007.52.3.1067

Helliwell, K. E., Shibl, A. A., & Amin, S. A. (2022). The Diatom Microbiome: New Perspectives for Diatom-Bacteria Symbioses. In A. Falciatore & T. Mock (Eds.), *The Molecular Life of Diatoms* (pp. 679–712). Springer International Publishing. https://doi.org/10.1007/978-3-030-92499-7_23

Hemming, M. P., Roughan, M., Malan, N., & Schaeffer, A. (2023). Observed multi-decadal trends in subsurface temperature adjacent to the East Australian Current. *Ocean Science*, *19*(4), 1145–1162. https://doi.org/10.5194/os-19-1145-2023

Henley, S. F., Cavan, E. L., Fawcett, S. E., Kerr, R., Monteiro, T., Sherrell, R. M., Bowie, A. R., Boyd, P. W., Barnes, D. K. A., Schloss, I. R., Marshall, T., Flynn, R., & Smith, S. (2020). Changing Biogeochemistry of the Southern Ocean and Its Ecosystem Implications. *Frontiers in Marine Science*, *7*. https://doi.org/10.3389/fmars.2020.00581

Hense, I., & Beckmann, A. (2015). A theoretical investigation of the diatom cell size reduction–restitution cycle. *Ecological Modelling*, *317*, 66–82. https://doi.org/10.1016/j.ecolmodel.2015.09.003

Heraud, P. R., Wood, B. R., Beardall, J., & McNaughton, D. (2007). Probing the influence of the environment on microalgae using infrared and Raman spectroscopy. In *New Approaches*

in Biomedical Spectroscopy (pp. 85–106). ACS Books. https://research.monash.edu/en/publications/probing-the-influence-of-the-environment-on-microalgae-using-infr

Herraiz-Borreguero, L., & Rintoul, S. R. (2011). Regional circulation and its impact on upper ocean variability south of Tasmania. *Deep Sea Research Part II: Topical Studies in Oceanography*, *58*(21), 2071–2081. https://doi.org/10.1016/j.dsr2.2011.05.022

Hervé, V., Derr, J., Douady, S., Quinet, M., Moisan, L., & Lopez, P. J. (2012). Multiparametric Analyses Reveal the pH-Dependence of Silicon Biomineralization in Diatoms. *PLOS ONE*, *7*(10), e46722. https://doi.org/10.1371/journal.pone.0046722

Hevia-Orube, J., Orive, E., David, H., Díez, A., Laza-Martínez, A., Miguel, I., & Seoane, S. (2016). Molecular and morphological analyses of solitary forms of brackish Thalassiosiroid diatoms (Coscinodiscophyceae), with emphasis on their phenotypic plasticity. *European Journal of Phycology*, *51*(1), 11–30. https://doi.org/10.1080/09670262.2015.1077394

Hildebrand, M., Lerch, S. J. L., & Shrestha, R. P. (2018). Understanding diatom cell wall silicification-moving forward. *Frontiers in Marine Science*, *5*(APR), Article APR. https://doi.org/10.3389/fmars.2018.00125

Hillebrand, H., Dürselen, C.-D., Kirschtel, D., Pollingher, U., & Zohary, T. (1999). Biovolume Calculation for Pelagic and Benthic Microalgae. *Journal of Phycology*, *35*(2), 403–424. https://doi.org/10.1046/j.1529-8817.1999.3520403.x

Hinga, K. R. (2002). Effects of pH on coastal marine phytoplankton. *Marine Ecology Progress Series*, *238*, 281–300. https://doi.org/10.3354/meps238281

Hobday, A. J., & Pecl, G. T. (2014). Identification of global marine hotspots: Sentinels for change and vanguards for adaptation action. *Reviews in Fish Biology and Fisheries*, *24*(2), 415–425. https://doi.org/10.1007/s11160-013-9326-6

Hoffmann, L. J., Peeken, I., & Lochte, K. (2008). Iron, silicate, and light co-limitation of three Southern Ocean diatom species. *Polar Biology*, *31*(9), 1067–1080. https://doi.org/10.1007/s00300-008-0448-6

Hofmann, M., & Schellnhuber, H. J. (2010). Ocean acidification: A millennial challenge. *Energy & Environmental Science*, *3*(12), 1883. https://doi.org/10.1039/c000820f

Hojjatoleslami, S. A., Avanaki, M. R. N., & Podoleanu, A. G. (2013). Image quality improvement in optical coherence tomography using Lucy-Richardson deconvolution algorithm. *Applied Optics*, *52*(23), 5663–5670. https://doi.org/10.1364/AO.52.005663

Hoogstraten, A., Timmermans, K. R., & de Baar, H. J. W. (2012). Morphological and Physiological Effects in Proboscia Alata (bacillariophyceae) Grown Under Different Light and Co2 Conditions of the Modern Southern Ocean. *Journal of Phycology*, *48*(3), 559–568. https://doi.org/10.1111/j.1529-8817.2012.01148.x

Huang, R., Sun, J., Yang, Y., Jiang, X., Wang, Z., Song, X., Wang, T., Zhang, D., Li, H., Yi, X., Chen, S., Bao, N., Qu, L., Zhang, R., Jiao, N., Gao, Y., Huang, B., Lin, X., Gao, G., & Gao, K. (2021). Elevated pCO2 Impedes Succession of Phytoplankton Community From Diatoms to Dinoflagellates Along With Increased Abundance of Viruses and Bacteria. *Frontiers in Marine Science*, *8*. https://doi.org/10.3389/fmars.2021.642208

Hutchins, D. A., & Bruland, K. W. (1998). Iron-limited diatom growth and Si:N uptake ratios in a coastal upwelling regime. *Nature*, *393*(6685), Article 6685. https://doi.org/10.1038/31203

Ianora, A., Bentley, M. G., Caldwell, G. S., Casotti, R., Cembella, A. D., Engström-Öst, J., Halsband, C., Sonnenschein, E., Legrand, C., Llewellyn, C. A., Paldavičienë, A.,

Pilkaityte, R., Pohnert, G., Razinkovas, A., Romano, G., Tillmann, U., & Vaiciute, D. (2011). The Relevance of Marine Chemical Ecology to Plankton and Ecosystem Function: An Emerging Field. *Marine Drugs*, *9*(9), Article 9. https://doi.org/10.3390/md9091625

Ianora, A., & Miralto, A. (2010). Toxigenic effects of diatoms on grazers, phytoplankton and other microbes: A review. *Ecotoxicology*, *19*(3), 493–511. https://doi.org/10.1007/s10646-009-0434-y

Ianora, A., Miralto, A., Poulet, S. A., Carotenuto, Y., Buttino, I., Romano, G., Casotti, R., Pohnert, G., Wichard, T., Colucci-D'Amato, L., Terrazzano, G., & Smetacek, V. (2004). Aldehyde suppression of copepod recruitment in blooms of a ubiquitous planktonic diatom. *Nature*, *429*(6990), 403–407. https://doi.org/10.1038/nature02526

Ingaramo, M., York, A. G., Hoogendoorn, E., Postma, M., Shroff, H., & Patterson, G. H. (2014). Richardson-Lucy deconvolution as a general tool for combining images with complementary strengths. *Chemphyschem : A European Journal of Chemical Physics and Physical Chemistry*, *15*(4), 794–800. https://doi.org/10.1002/cphc.201300831

Irigoien, X., Flynn, K. J., & Harris, R. P. (2005). Phytoplankton blooms: A 'loophole' in microzooplankton grazing impact? *Journal of Plankton Research*, *27*(4), 313–321. https://doi.org/10.1093/plankt/fbi011

Irwin, A. J., Finkel, Z. V., Schofield, O. M. E., & Falkowski, P. G. (2006). Scaling-up from nutrient physiology to the size-structure of phytoplankton communities. *Journal of Plankton Research*, *28*(5), 459–471. https://doi.org/10.1093/plankt/fbi148

Jabre, L. J., Allen, A. E., McCain, J. S. P., McCrow, J. P., Tenenbaum, N., Spackeen, J. L., Sipler, R. E., Green, B. R., Bronk, D. A., Hutchins, D. A., & Bertrand, E. M. (2021). Molecular underpinnings and biogeochemical consequences of enhanced diatom growth in a warming Southern Ocean. *Proceedings of the National Academy of Sciences*, *118*(30), e2107238118. https://doi.org/10.1073/pnas.2107238118

James, F. C. (1970). Geographic Size Variation in Birds and Its Relationship to Climate. *Ecology*, *51*(3), 365–390. https://doi.org/10.2307/1935374

Javaheri, N., Dries, R., Burson, A., Stal, L. J., Sloot, P. M. A., & Kaandorp, J. A. (2015). Temperature affects the silicate morphology in a diatom. *Scientific Reports*, *5*. https://doi.org/10.1038/srep11652

Jiang, L.-Q., Carter, B. R., Feely, R. A., Lauvset, S. K., & Olsen, A. (2019). Surface ocean pH and buffer capacity: Past, present and future. *Scientific Reports*, *9*(1), 18624. https://doi.org/10.1038/s41598-019-55039-4

Jiao, N., Yang, Y., Hong, N., Ma, Y., Harada, S., Koshikawa, H., & Watanabe, M. (2005). Dynamics of autotrophic picoplankton and heterotrophic bacteria in the East China Sea. *Continental Shelf Research*, *25*, 1265–1279. https://doi.org/10.1016/j.csr.2005.01.002

Johnson, Z. I., Zinser, E. R., Coe, A., McNulty, N. P., Woodward, E. M. S., & Chisholm, S. W. (2006). Niche partitioning among Prochlorococcus ecotypes along ocean-scale environmental gradients. *Science (New York, N.Y.)*, *311*(5768), 1737–1740. https://doi.org/10.1126/science.1118052

Kamakura, S., Ashworth, M. P., Yamada, K., Mikami, D., Kobayashi, A., Idei, M., & Sato, S. (2022). Morphological plasticity in response to salinity change in the euryhaline diatom Pleurosira laevis (Bacillariophyta). *Journal of Phycology*, *58*(5), 631–642. https://doi.org/10.1111/jpy.13277

Karlusich, J. J. P., Ibarbalz, F. M., & Bowler, C. (2020). Phytoplankton in the Tara Ocean. *Annual Review of Marine Science*, *12*(Volume 12, 2020), 233–265. https://doi.org/10.1146/annurev-marine-010419-010706

Karp-Boss, L., Boss, E., & Jumars, P. A. (1997). Nutrient fluxes to planktonic osmotrophs in the presence of fluid motion. *Oceanographic Literature Review*, *5*(44), 530.

Kemp, A. E. S., & Villareal, T. A. (2018). The case of the diatoms and the muddled mandalas: Time to recognize diatom adaptations to stratified waters. *Progress in Oceanography*, *167*, 138–149. https://doi.org/10.1016/j.pocean.2018.08.002

Keppler, L., & Landschützer, P. (2019). Regional Wind Variability Modulates the Southern Ocean Carbon Sink. *Scientific Reports*, *9*(1), 7384. https://doi.org/10.1038/s41598-019-43826-y

Kim, H.-C., Lee, K., & Choi, W. (2006). Contribution of phytoplankton and bacterial cells to the measured alkalinity of seawater. *Limnology and Oceanography - LIMNOL OCEANOGR*, *51*, 331–338. https://doi.org/10.4319/lo.2006.51.1.0331

Koester, J. A., Brawley, S. H., Karp-Boss, L., & Mann, D. G. (2007). Sexual reproduction in the marine centric diatom Ditylum brightwellii (Bacillariophyta). *European Journal of Phycology*, *42*(4), 351–366. https://doi.org/10.1080/09670260701562100

Kopanska, K. S., Tesson, B., Lin, H., Meredith, J. C., Hildebrand, M., & Davis, A. (2014). Morphological Factors Involved in Adhesion of Acid-Cleaned Diatom Silica. *Silicon*, *6*(2), 95–107. https://doi.org/10.1007/s12633-014-9178-2

Kopczyńska, E. E., Savoye, N., Dehairs, F., Cardinal, D., & Elskens, M. (2007). Spring phytoplankton assemblages in the Southern Ocean between Australia and Antarctica. *Polar Biology*, *31*(1), 77–88. https://doi.org/10.1007/s00300-007-0335-6

Kranzler, C. F., Brzezinski, M. A., Cohen, N. R., Lampe, R. H., Maniscalco, M., Till, C. P., Mack, J., Latham, J. R., Bruland, K. W., Twining, B. S., Marchetti, A., & Thamatrakoln, K. (2021). Impaired viral infection and reduced mortality of diatoms in iron-limited oceanic regions. *Nature Geoscience*, *14*(4), 231–237. https://doi.org/10.1038/s41561-021-00711-6

Kranzler, C. F., Krause, J. W., Brzezinski, M. A., Edwards, B. R., Biggs, W. P., Maniscalco, M., McCrow, J. P., Van Mooy, B. A. S., Bidle, K. D., Allen, A. E., & Thamatrakoln, K. (2019). Silicon limitation facilitates virus infection and mortality of marine diatoms. *Nature Microbiology*, *4*(11), 1790–1797. https://doi.org/10.1038/s41564-019-0502-x

Kremling, K., Andreae, M. O., Brügmann, L., van den Berg, C. m. g., Prange, A., Schirmacher, M., Koroleff, E., Kremling, K., & Kus, J. (1999). Determination of trace elements. In *Methods of Seawater Analysis* (pp. 253–364). John Wiley & Sons, Ltd. https://doi.org/10.1002/9783527613984.ch12

Kreyling, J., Schweiger, A. H., Bahn, M., Ineson, P., Migliavacca, M., Morel-Journel, T., Christiansen, J. R., Schtickzelle, N., & Larsen, K. S. (2018). To replicate, or not to replicate – that is the question: How to tackle nonlinear responses in ecological experiments. *Ecology Letters*, *21*(11), 1629–1638. https://doi.org/10.1111/ele.13134

Kustka, A. B., Allen, A. E., & Morel, F. M. M. (2007). Sequence Analysis and Transcriptional Regulation of Iron Acquisition Genes in Two Marine Diatoms. *Journal of Phycology*, *43*(4), 715–729. https://doi.org/10.1111/j.1529-8817.2007.00359.x

Kwiatkowski, L., Torres, O., Bopp, L., Aumont, O., Chamberlain, M., Christian, J., Dunne, J., Gehlen, M., Ilyina, T., John, J., Lenton, A., Li, H., Lovenduski, N., Orr, J., Palmiéri, J., Santana-Falcón, Y., Schwinger, J., Séférian, R., Stock, C., & Ziehn, T. (2020). Twenty-first century ocean warming, acidification, deoxygenation, and upper-ocean nutrient and primary production decline from CMIP6 model projections. *Biogeosciences*, *17*, 3439–3470. https://doi.org/10.5194/bg-17-3439-2020

Lafond, A., Leblanc, K., Legras, J., Cornet, V., & Quéguiner, B. (2020). The structure of diatom communities constrains biogeochemical properties in surface waters of the Southern

Ocean (Kerguelen Plateau). *Journal of Marine Systems*, *212*, 103458. https://doi.org/10.1016/j.jmarsys.2020.103458

Lampert, W. (1989). The Adaptive Significance of Diel Vertical Migration of Zooplankton. *Functional Ecology*, *3*(1), 21–27. https://doi.org/10.2307/2389671

Landschützer, P., Gruber, N., & Bakker, D. C. E. (2016). Decadal variations and trends of the global ocean carbon sink. *Global Biogeochemical Cycles*, *30*(10), 1396–1417. https://doi.org/10.1002/2015GB005359

Landschützer, P., Gruber, N., Haumann, F. A., Rödenbeck, C., Bakker, D. C. E., van Heuven, S., Hoppema, M., Metzl, N., Sweeney, C., Takahashi, T., Tilbrook, B., & Wanninkhof, R. (2015). The reinvigoration of the Southern Ocean carbon sink. *Science*, *349*(6253), 1221–1224. https://doi.org/10.1126/science.aab2620

Langlais, C. E., Lenton, A., Matear, R., Monselesan, D., Legresy, B., Cougnon, E., & Rintoul, S. (2017). Stationary Rossby waves dominate subduction of anthropogenic carbon in the Southern Ocean. *Scientific Reports*, *7*(1), 17076. https://doi.org/10.1038/s41598-017-17292-3

Lashof, D. A., & Ahuja, D. R. (1990). Relative contributions of greenhouse gas emissions to global warming. *Nature*, *344*(6266), 529–531. https://doi.org/10.1038/344529a0

Latour, P., Eggins, S., van der Merwe, P., Bach, L. T., Boyd, P. W., Ellwood, M. J., Bowie, A. R., Wuttig, K., & Strzepek, R. F. (2024). Characterization of a Southern Ocean deep chlorophyll maximum: Response of phytoplankton to light, iron, and manganese enrichment. *Limnology and Oceanography Letters*, *9*(2), 145–154. https://doi.org/10.1002/lol2.10366

Lavoie, M., & Raven, J. A. (2020). How can large-celled diatoms rapidly modulate sinking rates episodically? *Journal of Experimental Botany*, *71*(12), 3386–3389. https://doi.org/10.1093/jxb/eraa129

Le Quéré, C., Andrew, R. M., Friedlingstein, P., Sitch, S., Hauck, J., Pongratz, J., Pickers, P. A., Korsbakken, J. I., Peters, G. P., Canadell, J. G., Arneth, A., Arora, V. K., Barbero, L., Bastos, A., Bopp, L., Chevallier, F., Chini, L. P., Ciais, P., Doney, S. C., … Zheng, B. (2018). Global Carbon Budget 2018. *Earth System Science Data*, *10*(4), 2141–2194. https://doi.org/10.5194/essd-10-2141-2018

Le Quéré, C., Rödenbeck, C., Buitenhuis, E. T., Conway, T. J., Langenfelds, R., Gomez, A., Labuschagne, C., Ramonet, M., Nakazawa, T., Metzl, N., Gillett, N., & Heimann, M. (2007). Saturation of the Southern Ocean CO2 Sink Due to Recent Climate Change. *Science*, *316*(5832), 1735–1738. https://doi.org/10.1126/science.1136188

Le Reun, N., Bramucci, A., Ajani, P., Khalil, A., Raina, J.-B., & Seymour, J. R. (2023). Temporal variability in the growth-enhancing effects of different bacteria within the microbiome of the diatom Actinocyclus sp. *Frontiers in Microbiology*, *14*. https://doi.org/10.3389/fmicb.2023.1230349

Le Reun, N., Bramucci, A., O'Brien, J., Ostrowski, M., Brown, M. V., Van de Kamp, J., Bodrossy, L., Raina, J.-B., Ajani, P., & Seymour, J. (2022). Diatom Biogeography, Temporal Dynamics, and Links to Bacterioplankton across Seven Oceanographic Time-Series Sites Spanning the Australian Continent. *Microorganisms*, *10*(2), Article 2. https://doi.org/10.3390/microorganisms10020338

Leblanc, K., Cornet, V., Rimmelin-Maury, P., Grosso, O., Hélias-Nunige, S., Brunet, C., Claustre, H., Ras, J., Leblond, N., & Quéguiner, B. (2018). Silicon cycle in the tropical South Pacific: Contribution to the global Si cycle and evidence for an active pico-sized

siliceous plankton. *Biogeosciences*, *15*(18), 5595–5620. https://doi.org/10.5194/bg-15-5595-2018

Leblanc, K., & Hutchins, D. A. (2005). New applications of a biogenic silica deposition fluorophore in the study of oceanic diatoms. *Limnology and Oceanography: Methods*, *3*(10), 462–476. https://doi.org/10.4319/lom.2005.3.462

Lenton, A., McInnes, K., & O'Grady, J. (2015). *Marine Projections of Warming and Ocean Acidification in the Australasian Region*. https://doi.org/10.22499/2.6501.012

Lenton, A., Tilbrook, B., Matear, R. J., Sasse, T. P., & Nojiri, Y. (2016). Historical reconstruction of ocean acidification in the Australian region. *Biogeosciences*, *13*(6), 1753–1765. https://doi.org/10.5194/bg-13-1753-2016

Leterme, S. C., Prime, E., Mitchell, J., Brown, M. H., & Ellis, A. V. (2013). Diatom adaptability to environmental change: A case study of two Cocconeis species from high-salinity areas. *Diatom Research*, *28*(1), 29–35. https://doi.org/10.1080/0269249X.2012.734530

Levitan, O., Dinamarca, J., Zelzion, E., Lun, D. S., Guerra, L. T., Kim, M. K., Kim, J., Van Mooy, B. A. S., Bhattacharya, D., & Falkowski, P. G. (2015). Remodeling of intermediate metabolism in the diatom Phaeodactylum tricornutum under nitrogen stress. *Proceedings of the National Academy of Sciences*, *112*(2), 412–417. https://doi.org/10.1073/pnas.1419818112

Levitan, O., Rosenberg, G., Setlik, I., Setlikova, E., Grigel, J., Klepetar, J., Prasil, O., & Berman-Frank, I. (2007). Elevated CO2 enhances nitrogen fixation and growth in the marine cyanobacterium Trichodesmium. *Global Change Biology*, *13*(2), 531–538. https://doi.org/10.1111/j.1365-2486.2006.01314.x

Lewin, J. C. (1955). Silicon metabolism in diatoms. III. Respiration and silicon uptake in Navicula pelliculosa. *The Journal of General Physiology*, *39*(1), 1–10. https://doi.org/10.1085/jgp.39.1.1

Lewis, E. R., & Wallace, D. W. R. (1998). *Program Developed for CO2 System Calculations* (cdiac:CDIAC-105). Environmental System Science Data Infrastructure for a Virtual Ecosystem (ESS-DIVE) (United States). https://doi.org/10.15485/1464255

Li, F., Beardall, J., Collins, S., & Gao, K. (2017). Decreased photosynthesis and growth with reduced respiration in the model diatom Phaeodactylum tricornutum grown under elevated CO2 over 1800 generations. *Global Change Biology*, *23*(1), 127–137. https://doi.org/10.1111/gcb.13501

Li, F., Beardall, J., & Gao, K. (2018). Diatom performance in a future ocean: Interactions between nitrogen limitation, temperature, and CO2-induced seawater acidification. *ICES Journal of Marine Science*, *75*(4), 1451–1464. https://doi.org/10.1093/icesjms/fsx239

Li, G., Cheng, L., Zhu, J., Trenberth, K. E., Mann, M. E., & Abraham, J. P. (2020). Increasing ocean stratification over the past half-century. *Nature Climate Change*, *10*(12), Article 12. https://doi.org/10.1038/s41558-020-00918-2

Li, G., Woroch, A. D., Donaher, N. A., Cockshutt, A. M., & Campbell, D. A. (2016). A Hard Day's Night: Diatoms Continue Recycling Photosystem II in the Dark. *Frontiers in Marine Science*, *3*. https://doi.org/10.3389/fmars.2016.00218

Li, W., Gao, K., & Beardall, J. (2012). Interactive Effects of Ocean Acidification and Nitrogen-Limitation on the Diatom Phaeodactylum tricornutum. *PLOS ONE*, *7*(12), e51590. https://doi.org/10.1371/journal.pone.0051590

Li, Y., Gao, K., Villafañe, V. E., & Helbling, E. W. (2012). Ocean acidification mediates photosynthetic response to UV radiation and temperature increase in the diatom

Phaeodactylum tricornutum. *Biogeosciences*, *9*(10), 3931–3942. https://doi.org/10.5194/bg-9-3931-2012

Li, Y., Xu, J., & Gao, K. (2014). Light-Modulated Responses of Growth and Photosynthetic Performance to Ocean Acidification in the Model Diatom Phaeodactylum tricornutum. *PLOS ONE*, *9*(5), e96173. https://doi.org/10.1371/journal.pone.0096173

Li, Z., England, M. H., & Groeskamp, S. (2023). Recent acceleration in global ocean heat accumulation by mode and intermediate waters. *Nature Communications*, *14*(1), 6888. https://doi.org/10.1038/s41467-023-42468-z

Li, Z., Groeskamp, S., Cerovecki, I., & England, M. (2022). The Origin and Fate of Antarctic Intermediate Water in the Southern Ocean. *Journal of Physical Oceanography*, *52*. https://doi.org/10.1175/JPO-D-21-0221.1

Lima-Mendez, G., Faust, K., Henry, N., Decelle, J., Colin, S., Carcillo, F., Chaffron, S., Ignacio-Espinosa, J. C., Roux, S., Vincent, F., Bittner, L., Darzi, Y., Wang, J., Audic, S., Berline, L., Bontempi, G., Cabello, A. M., Coppola, L., Cornejo-Castillo, F. M., … Raes, J. (2015). Ocean plankton. Determinants of community structure in the global plankton interactome. *Science (New York, N.Y.)*, *348*(6237), 1262073. https://doi.org/10.1126/science.1262073

Lin, Y.-Y., Risk, M., Ray, S. M., Engen, D. V., Clardy, J., Golik, J., James, J. C., & Nakanishi, K. (2002, May 1). *Isolation and structure of brevetoxin B from the 'red tide' dinoflagellate Ptychodiscus brevis (Gymnodinium breve)* (world). ACS Publications; American Chemical Society. https://doi.org/10.1021/ja00412a053

Litchman, E., Klausmeier, C. A., Miller, J. R., Schofield, O. M., & Falkowski, P. G. (2006). Multi-nutrient, multi-group model of present and future oceanic phytoplankton communities. *Biogeosciences*, *3*(4), 585–606. https://doi.org/10.5194/bg-3-585-2006

Litchman, E., Klausmeier, C. A., & Yoshiyama, K. (2009). Contrasting size evolution in marine and freshwater diatoms. *Proceedings of the National Academy of Sciences*, *106*(8), 2665–2670. https://doi.org/10.1073/pnas.0810891106

Liu, Y., Blain, S., Crispi, O., Rembauville, M., & Obernosterer, I. (2020). Seasonal dynamics of prokaryotes and their associations with diatoms in the Southern Ocean as revealed by an autonomous sampler. *Environmental Microbiology*, *22*(9), 3968–3984. https://doi.org/10.1111/1462-2920.15184

Liu, Z., Deng, Z., Davis, S., & Ciais, P. (2023). Monitoring global carbon emissions in 2022. *Nature Reviews Earth & Environment*, *4*(4), 205–206. https://doi.org/10.1038/s43017-023-00406-z

Lomas, M. W., Baer, S. E., Mouginot, C., Terpis, K. X., Lomas, D. A., Altabet, M. A., & Martiny, A. C. (2021). Varying influence of phytoplankton biodiversity and stoichiometric plasticity on bulk particulate stoichiometry across ocean basins. *Communications Earth & Environment*, *2*(1), 1–10. https://doi.org/10.1038/s43247-021-00212-9

Losic, D., Rosengarten, G., Mitchell, J. G., & Voelcker, N. H. (2006). Pore Architecture of Diatom Frustules: Potential Nanostructured Membranes for Molecular and Particle Separations. *Journal of Nanoscience and Nanotechnology*, *6*(4), 982–989. https://doi.org/10.1166/jnn.2006.174

Lourey, M. J., & Trull, T. W. (2001). Seasonal nutrient depletion and carbon export in the Subantarctic and Polar Frontal zones of the Southern Ocean south of Australia. *Journal of Geophysical Research: Oceans*, *106*(C12), 31463–31487. https://doi.org/10.1029/2000JC000287

Lumpkin, R., & Speer, K. (2007). *Global Ocean Meridional Overturning*. https://doi.org/10.1175/JPO3130.1

Macdonald, H. S., Roughan, M., Baird, M. E., & Wilkin, J. (2016). The formation of a cold-core eddy in the East Australian Current. *Continental Shelf Research*, *114*, 72–84. https://doi.org/10.1016/j.csr.2016.01.002

Malan, N., Roughan, M., & Kerry, C. (2021). The Rate of Coastal Temperature Rise Adjacent to a Warming Western Boundary Current is Nonuniform with Latitude. *Geophysical Research Letters*, *48*(3), e2020GL090751. https://doi.org/10.1029/2020GL090751

Malviya, S., Scalco, E., Audic, S., Vincent, F., Veluchamy, A., Poulain, J., Wincker, P., Iudicone, D., de Vargas, C., Bittner, L., Zingone, A., & Bowler, C. (2016). Insights into global diatom distribution and diversity in the world's ocean. *Proceedings of the National Academy of Sciences*, *113*(11), E1516–E1525. https://doi.org/10.1073/pnas.1509523113

Mann, D. G. (1988). Why didn't Lund see sex in Asterionella? A discussion of the diatom life cycle in nature. *Algae and the Aquatic Environment.*, 384–412.

Mann, D. G. (2011). Size and Sex. In J. Seckbach & P. Kociolek (Eds.), *The Diatom World* (pp. 145–166). Springer Netherlands. https://doi.org/10.1007/978-94-007-1327-7_6

Mann, D. G., & Vanormelingen, P. (2013). An Inordinate Fondness? The Number, Distributions, and Origins of Diatom Species. *Journal of Eukaryotic Microbiology*, *60*(4), 414–420. https://doi.org/10.1111/jeu.12047

Mann, K. h., & Lazier, J. r. n. (2005). Vertical Structure of the Open Ocean: Biology of the Mixed Layer. In *Dynamics of Marine Ecosystems* (pp. 68–117). John Wiley & Sons, Ltd. https://doi.org/10.1002/9781118687901.ch3

Marchesiello, P., & Middleton, J. H. (2000). *Modeling the East Australian Current in the Western Tasman Sea*. https://journals.ametsoc.org/view/journals/phoc/30/11/1520-0485_2001_031_2956_mteaci_2.0.co_2.xml

Marchetti, A., Parker, M. S., Moccia, L. P., Lin, E. O., Arrieta, A. L., Ribalet, F., Murphy, M. E. P., Maldonado, M. T., & Armbrust, E. V. (2009). Ferritin is used for iron storage in bloom-forming marine pennate diatoms. *Nature*, *457*(7228), 467–470. https://doi.org/10.1038/nature07539

Margalef, R. (1978). Life-forms of phytoplankton as survival alternatives in an unstable environment. *Oceanologica Acta*. https://www.semanticscholar.org/paper/Life-forms-of-phytoplankton-as-survival-in-an-Margalef/1aa7aba56b3efc96f62c6d8278a5e171a44aa18e

Marinov, I., Gnanadesikan, A., Toggweiler, J. R., & Sarmiento, J. L. (2006). The Southern Ocean biogeochemical divide. *Nature*, *441*(7096), 964–967. https://doi.org/10.1038/nature04883

Marshall, J., & Speer, K. (2012). Closure of the meridional overturning circulation through Southern Ocean upwelling. *Nature Geoscience*, *5*(3), 171–180.

Martin, J. H., & Gordon, M. R. (1988). Northeast Pacific iron distributions in relation to phytoplankton productivity. *Deep Sea Research Part A. Oceanographic Research Papers*, *35*(2), 177–196. https://doi.org/10.1016/0198-0149(88)90035-0

Martin, J. H., Gordon, R. M., & Fitzwater, S. E. (1990). Iron in Antarctic waters. *Nature*, *345*(6271), Article 6271. https://doi.org/10.1038/345156a0

Martin-Jézéquel, V., Hildebrand, M., & Brzezinski, M. A. (2000). Silicon Metabolism in Diatoms: Implications for Growth. *Journal of Phycology*, *36*(5), 821–840. https://doi.org/10.1046/j.1529-8817.2000.00019.x

Masson-Delmotte, V., Zhai, P., Pirani, A., Connors, S. L., Péan, C., Berger, S., Caud, N., Chen, Y., Goldfarb, L., Gomis, M. I., Huang, M., Leitzell, K., Lonnoy, E., Matthews, J. B. R., Maycock, T. K., Waterfield, T., Yelekçi, Ö., Yu, R., & Zhou, B. (Eds.). (2021). *Climate Change 2021: The Physical Science Basis. Contribution of Working Group I to the Sixth Assessment Report of the Intergovernmental Panel on Climate Change*. Cambridge University Press. https://doi.org/10.1017/9781009157896

McCarthy, A., Rogers, S. P., Duffy, S. J., & Campbell, D. A. (2012). Elevated Carbon Dioxide Differentially Alters the Photophysiology of Thalassiosira Pseudonana (bacillariophyceae) and Emiliania Huxleyi (haptophyta). *Journal of Phycology*, *48*(3), 635–646. https://doi.org/10.1111/j.1529-8817.2012.01171.x

McNair, H. M., Brzezinski, M. A., & Krause, J. W. (2015). Quantifying diatom silicification with the fluorescent dye, PDMPO. *Limnology and Oceanography: Methods*, *13*(10), 587–599. https://doi.org/10.1002/lom3.10049

Mehrbach, C., Culberson, C. H., Hawley, J. E., & Pytkowicx, R. M. (1973). Measurement of the Apparent Dissociation Constants of Carbonic Acid in Seawater at Atmospheric Pressure1. *Limnology and Oceanography*, *18*(6), 897–907. https://doi.org/10.4319/lo.1973.18.6.0897

Meunier, C. L., Alvarez-Fernandez, S., Cunha-Dupont, A. Ö., Geisen, C., Malzahn, A. M., Boersma, M., & Wiltshire, K. H. (2018). The craving for phosphorus in heterotrophic dinoflagellates and its potential implications for biogeochemical cycles. *Limnology and Oceanography*, *63*(4), 1774–1784. https://doi.org/10.1002/lno.10807

Milligan, A. J., & Morel, F. M. M. (2002). A Proton Buffering Role for Silica in Diatoms. *Science*, *297*(5588), 1848–1850. https://doi.org/10.1126/science.1074958

Milligan, A. J., Varela, D. E., Brzezinski, M. A., & Morel, F. M. M. (2004). Dynamics of silicon metabolism and silicon isotopic discrimination in a marine diatomas a function of pCO_2. *Limnology and Oceanography*, *49*(2), 322–329. https://doi.org/10.4319/lo.2004.49.2.0322

Mitchell, B. G. (1990). *Algorithms for determining the absorption coefficient for aquatic particulates using the quantitative filter technique* (R. W. Spinrad, Ed.; p. 137). https://doi.org/10.1117/12.21440

Moore, J. K., & Villareal, T. A. (1996). Size-ascent rate relationships in positively buoyant marine diatoms. *Limnology and Oceanography*, *41*(7), 1514–1520. https://doi.org/10.4319/lo.1996.41.7.1514

Moore, J., & Villareal, T. (1996). Buoyancy and growth characteristics of three positively buoyant marine diatoms. *Marine Ecology Progress Series*, *132*, 203–213. https://doi.org/10.3354/meps132203

Moore, M., Mills, M., Arrigo, K., Berman-Frank, I., Bopp, L., Boyd, P., Galbraith, E., Geider, R., Guieu, C., Jaccard, S., Jickells, T., Laroche, J., Lenton, T., Mahowald, N., Maranon, E., Marinov, I., Moore, J., Nakatsuka, T., Oschlies, A., & Ulloa, O. (2013). Processes and patterns of oceanic nutrient limitation. *Nature Geoscience*, *6*, 701–710. https://doi.org/10.1038/NGEO1765

Morel, F. M. M., Cox, E. H., Kraepiel, A. M. L., Lane, T. W., Milligan, A. J., Schaperdoth, I., Reinfelder, J. R., & Tortell, P. D. (2002). Acquisition of inorganic carbon by the marine diatom Thalassiosira weissflogii. *Functional Plant Biology*, *29*(3), 301–308. https://doi.org/10.1071/pp01199

Musielak, M. M., Karp-Boss, L., Jumars, P. A., & Fauci, L. J. (2009). Nutrient transport and acquisition by diatom chains in a moving fluid. *Journal of Fluid Mechanics*, *638*, 401–421. https://doi.org/10.1017/S0022112009991108

Nakov, T., Beaulieu, J. M., & Alverson, A. J. (2019). Diatoms diversify and turn over faster in freshwater than marine environments*. *Evolution*, *73*(12), 2497–2511. https://doi.org/10.1111/evo.13832

Nelson, D. M., Smith, W. O., Muench, R. D., Gordon, L. I., Sullivan, C. W., & Husby, D. M. (1989). Particulate matter and nutrient distributions in the ice-edge zone of the Weddell Sea: Relationship to hydrography during late summer. *Deep Sea Research Part A. Oceanographic Research Papers*, *36*(2), 191–209. https://doi.org/10.1016/0198-0149(89)90133-7

Nelson, D. M., Tréguer, P., Brzezinski, M. A., Leynaert, A., & Quéguiner, B. (1995). Production and dissolution of biogenic silica in the ocean: Revised global estimates, comparison with regional data and relationship to biogenic sedimentation. *Global Biogeochemical Cycles*, *9*(3), 359–372. https://doi.org/10.1029/95GB01070

Nicotra, A. B., Atkin, O. K., Bonser, S. P., Davidson, A. M., Finnegan, E. J., Mathesius, U., Poot, P., Purugganan, M. D., Richards, C. L., Valladares, F., & van Kleunen, M. (2010). Plant phenotypic plasticity in a changing climate. *Trends in Plant Science*, *15*(12), 684–692. https://doi.org/10.1016/j.tplants.2010.09.008

Nielsen, D. A., Petrou, K., & Gates, R. D. (2018). Coral bleaching from a single cell perspective. *The ISME Journal*, *12*(6), 1558–1567. https://doi.org/10.1038/s41396-018-0080-6

Nogueira, P., Domingues, R. B., & Barbosa, A. B. (2014). Are microcosm volume and sample pre-filtration relevant to evaluate phytoplankton growth? *Journal of Experimental Marine Biology and Ecology*, *461*, 323–330. https://doi.org/10.1016/j.jembe.2014.09.006

Nowicki, M., DeVries, T., & Siegel, D. A. (2022). Quantifying the Carbon Export and Sequestration Pathways of the Ocean's Biological Carbon Pump. *Global Biogeochemical Cycles*, *36*(3), e2021GB007083. https://doi.org/10.1029/2021GB007083

Noyes, J., Sumper, M., & Vukusic, P. (2008). Light manipulation in a marine diatom. *Journal of Materials Research*, *23*(12), 3229–3235. https://doi.org/10.1557/JMR.2008.0381

O'Brien, T. D., & Oakes, S. A. (2020). Visualizing and Exploring Zooplankton Spatio-Temporal Variability. In *Zooplankton Ecology*. CRC Press.

Orr, J. C., Fabry, V. J., Aumont, O., Bopp, L., Doney, S. C., Feely, R. A., Gnanadesikan, A., Gruber, N., Ishida, A., Joos, F., Key, R. M., Lindsay, K., Maier-Reimer, E., Matear, R., Monfray, P., Mouchet, A., Najjar, R. G., Plattner, G.-K., Rodgers, K. B., … Yool, A. (2005). Anthropogenic ocean acidification over the twenty-first century and its impact on calcifying organisms. *Nature*, *437*(7059), 681–686. https://doi.org/10.1038/nature04095

Orr, J. C., Maier-Reimer, E., Mikolajewicz, U., Monfray, P., Sarmiento, J. L., Toggweiler, J. R., Taylor, N. K., Palmer, J., Gruber, N., Sabine, C. L., Le Quéré, C., Key, R. M., & Boutin, J. (2001). Estimates of anthropogenic carbon uptake from four three-dimensional global ocean models. *Global Biogeochemical Cycles*, *15*(1), 43–60. https://doi.org/10.1029/2000GB001273

Orsi, A. H., Whitworth, T., & Nowlin, W. D. (1995). On the meridional extent and fronts of the Antarctic Circumpolar Current. *Deep Sea Research Part I: Oceanographic Research Papers*, *42*(5), 641–673. https://doi.org/10.1016/0967-0637(95)00021-W

Owens, T. G., Falkowski, P. G., & Whitledge, T. E. (1980). Diel periodicity in cellular chlorophyll content in marine diatoms. *Marine Biology*, *59*(2), 71–77. https://doi.org/10.1007/BF00405456

Paerl, H. W., Otten, T. G., & Kudela, R. (2018). Mitigating the Expansion of Harmful Algal Blooms Across the Freshwater-to-Marine Continuum. *Environmental Science & Technology*, *52*(10), 5519–5529. https://doi.org/10.1021/acs.est.7b05950

Pan, X. L., Lai, X., Makabe, R., Hirano, D., & Watanabe, Y. W. (2023). Spatiotemporal high-resolution mapping of biological production in the Southern Ocean. *Communications Earth & Environment*, *4*(1), 1–8. https://doi.org/10.1038/s43247-023-01067-y

Park, J. S., Jung, S. W., Lee, S. D., Yun, S. M., & Lee, J. H. (2016). Species diversity of the genus Thalassiosira (Thalassiosirales, Bacillariophyta) in South Korea and its biogeographical distribution in the world. *Phycologia*, *55*(4), 403–423. https://doi.org/10.2216/15-66.1

Parslow, J. S., Boyd, P. W., Rintoul, S. R., & Griffiths, F. B. (2001). A persistent subsurface chlorophyll maximum in the Interpolar Frontal Zone south of Australia: Seasonal progression and implications for phytoplankton-light-nutrient interactions. *Journal of Geophysical Research: Oceans*, *106*(C12), 31543–31557. https://doi.org/10.1029/2000JC000322

Partensky, F., Blanchot, J., & Vaulot, D. (1999). *Differential distribution and ecology of Prochlorococcus and Synechococcus in oceanic waters: A review*. https://www.semanticscholar.org/paper/Differential-distribution-and-ecology-of-and-in-a-Partensky-Blanchot/5638b562e1c10b924d1303603a39ae3b8e6269a7

Partensky, F., Hess, W. R., & Vaulot, D. (1999). Prochlorococcus, a marine photosynthetic prokaryote of global significance. *Microbiology and Molecular Biology Reviews: MMBR*, *63*(1), 106–127.

Paul, V. J. (2008). Global warming and cyanobacterial harmful algal blooms. In H. K. Hudnell (Ed.), *Cyanobacterial Harmful Algal Blooms: State of the Science and Research Needs* (pp. 239–257). Springer. https://doi.org/10.1007/978-0-387-75865-7_11

Petrou, K., Baker, K. G., Nielsen, D. A., Hancock, A. M., Schulz, K. G., & Davidson, A. T. (2019). Acidification diminishes diatom silica production in the Southern Ocean. *Nature Climate Change*, *9*(10), Article 10. https://doi.org/10.1038/s41558-019-0557-y

Petrou, K., Kranz, S. A., Trimborn, S., Hassler, C. S., Ameijeiras, S. B., Sackett, O., Ralph, P. J., & Davidson, A. T. (2016). Southern Ocean phytoplankton physiology in a changing climate. *Journal of Plant Physiology*, *203*, 135–150. https://doi.org/10.1016/j.jplph.2016.05.004

Petrucciani, A., Moretti, P., Ortore, M. G., & Norici, A. (2023). Integrative effects of morphology, silicification, and light on diatom vertical movements. *Frontiers in Plant Science*, *14*. https://www.frontiersin.org/journals/plant-science/articles/10.3389/fpls.2023.1143998

Pickett-Heaps, J. (1990). The cell biology of diatom valve formation. *Progress in Phycological Research*, *7*, 1–101.

Piontek, F., Müller, C., Pugh, T. A. M., Clark, D. B., Deryng, D., Elliott, J., Colón González, F. de J., Flörke, M., Folberth, C., Franssen, W., Frieler, K., Friend, A. D., Gosling, S. N., Hemming, D., Khabarov, N., Kim, H., Lomas, M. R., Masaki, Y., Mengel, M., … Schellnhuber, H. J. (2014). Multisectoral climate impact hotspots in a warming world. *Proceedings of the National Academy of Sciences*, *111*(9), 3233–3238. https://doi.org/10.1073/pnas.1222471110

Pondaven, P., Gallinari, M., Chollet, S., Bucciarelli, E., Sarthou, G., Schultes, S., & Jean, F. (2007). Grazing-induced Changes in Cell Wall Silicification in a Marine Diatom. *Protist*, *158*(1), 21–28. https://doi.org/10.1016/j.protis.2006.09.002

Post, A. F., Dubinsky, Z., Wyman, K., & Falkowski, P. G. (1984). Kinetics of light-intensity adaptation in a marine planktonic diatom. *Marine Biology*, *83*(3), 231–238. https://doi.org/10.1007/BF00397454

Pouvreau, J.-B., Housson, E., Tallec, L. L., Morançais, M., Rincé, Y., Fleurence, J., & Pondaven, P. (2007). Growth inhibition of several marine diatom species induced by the shading effect and allelopathic activity of marennine, a blue-green polyphenolic pigment of the diatom *Haslea ostrearia* (Gaillon/Bory) Simonsen. *Journal of Experimental Marine Biology and Ecology*, *352*(1), 212–225. https://doi.org/10.1016/j.jembe.2007.07.011

Putt, M., & Prézelin, B. B. (1988). Diel Periodicity of Photosynthesis and Cell Division Compared in Thalassiosira Weissflogii (bacillariophyceae). *Journal of Phycology*, *24*(3), 315–324. https://doi.org/10.1111/j.1529-8817.1988.tb04472.x

R. Core Team. (2021). A language and environment for statistical computing. *(No Title)*. https://cir.nii.ac.jp/crid/1370298757441457025

Rajaneesh, K. M., Naik, R. K., Roy, R., & D'Costa, P. M. (2020). Chapter 3 - Cyanobacteria in tropical and subtropical marine environments: Bloom formation and ecological role. In P. K. Singh, A. Kumar, V. K. Singh, & A. K. Shrivastava (Eds.), *Advances in Cyanobacterial Biology* (pp. 35–46). Academic Press. https://doi.org/10.1016/B978-0-12-819311-2.00003-6

Ralph, P. J., & Gademann, R. (2005). Rapid light curves: A powerful tool to assess photosynthetic activity. *Aquatic Botany*, *82*(3), 222–237. https://doi.org/10.1016/j.aquabot.2005.02.006

Ramos, J. B. e, Schulz, K. G., Brownlee, C., Sett, S., & Azevedo, E. B. (2014). Effects of Increasing Seawater Carbon Dioxide Concentrations on Chain Formation of the Diatom Asterionellopsis glacialis. *PLOS ONE*, *9*(3), e90749. https://doi.org/10.1371/journal.pone.0090749

Raven, J. A. (1983). The Transport and Function of Silicon in Plants. *Biological Reviews*, *58*(2), 179–207. https://doi.org/10.1111/j.1469-185X.1983.tb00385.x

Raven, J. A., & Waite, A. M. (2004). The evolution of silicification in diatoms: Inescapable sinking and sinking as escape? *New Phytologist*, *162*(1), 45–61. https://doi.org/10.1111/j.1469-8137.2004.01022.x

Rees, C., Pender, L., Sherrin, K., Schwanger, C., Hughes, P., Tibben, S., Marouchos, A., & Rayner, M. (2019). Methods for reproducible shipboard SFA nutrient measurement using RMNS and automated data processing. *Limnology and Oceanography: Methods*, *17*(1), 25–41. https://doi.org/10.1002/lom3.10294

Reynolds, C. S. (2006). *The Ecology of Phytoplankton*. Cambridge University Press.

Richardson, T., & Cullen, J. (1995). Changes in buoyancy and chemical composition during growth of a coastal marine diatom: Ecological and biogeochemical consequences. *Marine Ecology Progress Series*, *128*, 77–90. https://doi.org/10.3354/meps128077

Richardson, T. L., Cullen, J. J., Kelley, D. E., & Lewis, M. R. (1998). Potential contributions of vertically migrating Rhizosolenia to nutrient cycling and new production in the open ocean. *Journal of Plankton Research*, *20*(2), 219–241. https://doi.org/10.1093/plankt/20.2.219

Ridgway, K., & Hill, K. (2009). The East Australian Current. *A Marine Climate Change Impacts and Adaptation Report Card for Australia 2009, NCCARF Publication*.

Riebesell, U. (1989). Comparison of sinking and sedimentation rate measurements in a diatom winter/ spring bloom. *Marine Ecology Progress Series*, *54*, 109–119.

Riebesell, U., & Gattuso, J.-P. (2015). Lessons learned from ocean acidification research. *Nature Climate Change*, *5*(1), Article 1. https://doi.org/10.1038/nclimate2456

Riebesell, U., Gattuso, J.-P., Thingstad, T. F., & Middelburg, J. J. (2013). Arctic ocean acidification: Pelagic ecosystem and biogeochemical responses during a mesocosm study. *Biogeosciences*, *10*, 5619–5626.

Riebesell, U., & Tortell, P. D. (2011). Effects of Ocean Acidification on Pelagic Organisms and Ecosystems. In J.-P. Gattuso & L. Hansson (Eds.), *Ocean Acidification* (p. 0). Oxford University Press. https://doi.org/10.1093/oso/9780199591091.003.0011

Rigby, S. J., Williams, R. G., Achterberg, E. P., & Tagliabue, A. (2020). Resource Availability and Entrainment Are Driven by Offsets Between Nutriclines and Winter Mixed-Layer Depth. *Global Biogeochemical Cycles*, *34*(7), e2019GB006497. https://doi.org/10.1029/2019GB006497

Rigual-Hernández, A. S., Trull, T. W., Bray, S. G., Cortina, A., & Armand, L. K. (2015). Latitudinal and temporal distributions of diatom populations in the pelagic waters of the Subantarctic and Polar Frontal zones of the Southern Ocean and their role in the biological pump. *Biogeosciences*, *12*(18), 5309–5337. https://doi.org/10.5194/bg-12-5309-2015

Ringuet, S., Sassano, L., & Johnson, Z. I. (2011). A suite of microplate reader-based colorimetric methods to quantify ammonium, nitrate, orthophosphate and silicate concentrations for aquatic nutrient monitoring. *Journal of Environmental Monitoring*, *13*(2), 370–376. https://doi.org/10.1039/C0EM00290A

Rintoul, S. R., & Trull, T. W. (2001). Seasonal evolution of the mixed layer in the Subantarctic zone south of Australia. *Journal of Geophysical Research: Oceans*, *106*(C12), 31447–31462. https://doi.org/10.1029/2000JC000329

Ritchie, G. A. (2006). Chlorophyll fluorescence: What is it and what do the numbers mean. *National Proceedings: Forest and Conservation Nursery Associations-2005*, 34–42.

Roberts, K., Granum, E., Leegood, R. C., & Raven, J. A. (2007). Carbon acquisition by diatoms. *Photosynthesis Research*, *93*(1), 79–88. https://doi.org/10.1007/s11120-007-9172-2

Rogato, A., & De Tommasi, E. (2020). Physical, Chemical, and Genetic Techniques for Diatom Frustule Modification: Applications in Nanotechnology. *Applied Sciences*, *10*(23), Article 23. https://doi.org/10.3390/app10238738

Rohde, R. A., & Hausfather, Z. (2020). The Berkeley Earth Land/Ocean Temperature Record. *Earth System Science Data*, *12*(4), 3469–3479. https://doi.org/10.5194/essd-12-3469-2020

Romann, J., Valmalette, J.-C., Røyset, A., & Einarsrud, M.-A. (2015). Optical properties of single diatom frustules revealed by confocal microspectroscopy. *Optics Letters*, *40*, 740. https://doi.org/10.1364/OL.40.000740

Rossoll, D., Bermúdez, R., Hauss, H., Schulz, K. G., Riebesell, U., Sommer, U., & Winder, M. (2012). Ocean Acidification-Induced Food Quality Deterioration Constrains Trophic Transfer. *PLoS ONE*, *7*(4), e34737. https://doi.org/10.1371/journal.pone.0034737

Rost, B., Riebesell, U., Burkhardt, S., & Sültemeyer, D. (2003). Carbon acquisition of bloom-forming marine phytoplankton. *Limnology and Oceanography*, *48*(1), 55–67. https://doi.org/10.4319/lo.2003.48.1.0055

Round, F. E., Crawford, R. M., & Mann, D. G. (1990). *Diatoms: Biology and Morphology of the Genera*. Cambridge University Press.

Roxy, M. K., Modi, A., Murtugudde, R., Valsala, V., Panickal, S., Prasanna Kumar, S., Ravichandran, M., Vichi, M., & Lévy, M. (2016). A reduction in marine primary productivity driven by rapid warming over the tropical Indian Ocean. *Geophysical Research Letters*, *43*(2), 826–833. https://doi.org/10.1002/2015GL066979

Rumyantseva, A., Henson, S., Martin, A., Thompson, A. F., Damerell, G. M., Kaiser, J., & Heywood, K. J. (2019). Phytoplankton spring bloom initiation: The impact of atmospheric forcing and light in the temperate North Atlantic Ocean. *Progress in Oceanography*, *178*, 102202. https://doi.org/10.1016/j.pocean.2019.102202

Ryabov, A., Kerimoglu, O., Litchman, E., Olenina, I., Roselli, L., Basset, A., Stanca, E., & Blasius, B. (2021). Shape matters: The relationship between cell geometry and diversity in phytoplankton. *Ecology Letters*, *24*(4), 847–861. https://doi.org/10.1111/ele.13680

Ryan-Keogh, T. J., Thomalla, S. J., Little, H., & Melanson, J.-R. (2018). Seasonal regulation of the coupling between photosynthetic electron transport and carbon fixation in the Southern Ocean. *Limnology and Oceanography*, *63*(5), 1856–1876. https://doi.org/10.1002/lno.10812

Saito, H., & Tsuda, A. (2003). Influence of light intensity on diatom physiology and nutrient dynamics in the Oyashio region. *Progress in Oceanography*, *57*(3), 251–263. https://doi.org/10.1016/S0079-6611(03)00100-9

Sala, M. M., Aparicio, F. L., Balagué, V., Boras, J. A., Borrull, E., Cardelús, C., Cros, L., Gomes, A., López-Sanz, A., Malits, A., Martínez, R. A., Mestre, M., Movilla, J., Sarmento, H., Vázquez-Domínguez, E., Vaqué, D., Pinhassi, J., Calbet, A., Calvo, E., … Marrasé, C. (2016). Contrasting effects of ocean acidification on the microbial food web under different trophic conditions. *ICES Journal of Marine Science*, *73*(3), 670–679. https://doi.org/10.1093/icesjms/fsv130

Sallée, J.-B. (2018). Southern Ocean Warming. *Oceanography*, *31*(2), 52–62.

Salter, I., Lampitt, R. S., Sanders, R., Poulton, A., Kemp, A. E. S., Boorman, B., Saw, K., & Pearce, R. (2007). Estimating carbon, silica and diatom export from a naturally fertilised phytoplankton bloom in the Southern Ocean using PELAGRA: A novel drifting sediment trap. *Deep Sea Research Part II: Topical Studies in Oceanography*, *54*(18), 2233–2259. https://doi.org/10.1016/j.dsr2.2007.06.008

Sanders, R., Henson, S. A., Koski, M., De La Rocha, C. L., Painter, S. C., Poulton, A. J., Riley, J., Salihoglu, B., Visser, A., Yool, A., Bellerby, R., & Martin, A. P. (2014). The Biological Carbon Pump in the North Atlantic. *Progress in Oceanography*, *129*, 200–218. https://doi.org/10.1016/j.pocean.2014.05.005

Sapriel, G., Quinet, M., Heijde, M., Jourdren, L., Tanty, V., Luo, G., Le Crom, S., & Lopez, P. J. (2009). Genome-Wide Transcriptome Analyses of Silicon Metabolism in Phaeodactylum tricornutum Reveal the Multilevel Regulation of Silicic Acid Transporters. *PLoS ONE*, *4*(10), e7458. https://doi.org/10.1371/journal.pone.0007458

Sarmiento, J. L., Slater, R., Barber, R., Bopp, L., Doney, S. C., Hirst, A. C., Kleypas, J., Matear, R., Mikolajewicz, U., Monfray, P., Soldatov, V., Spall, S. A., & Stouffer, R. (2004). Response of ocean ecosystems to climate warming. *Global Biogeochemical Cycles*, *18*(3). https://doi.org/10.1029/2003GB002134

Schallenberg, C., Strzepek, R. F., Schuback, N., Clementson, L. A., Boyd, P. W., & Trull, T. W. (2020). Diel quenching of Southern Ocean phytoplankton fluorescence is related to iron limitation. *Biogeosciences*, *17*(3), 793–812. https://doi.org/10.5194/bg-17-793-2020

Schaum, E., Rost, B., Millar, A. J., & Collins, S. (2013). Variation in plastic responses of a globally distributed picoplankton species to ocean acidification. *Nature Climate Change*, *3*(3), 298–302. https://doi.org/10.1038/nclimate1774

Schmittner, A. (2005). Decline of the marine ecosystem caused by a reduction in the Atlantic overturning circulation. *Nature*, *434*(7033), 628–633. https://doi.org/10.1038/nature03476

Schneider, C. A., Rasband, W. S., & Eliceiri, K. W. (2012). NIH Image to ImageJ: 25 years of image analysis. *Nature Methods*, *9*(7), 671–675. https://doi.org/10.1038/nmeth.2089

Schnetger, B., & Lehners, C. (2014). Determination of nitrate plus nitrite in small volume marine water samples using vanadium(III)chloride as a reduction agent. *Marine Chemistry*, *160*, 91–98. https://doi.org/10.1016/j.marchem.2014.01.010

Schulz, K. G., Bach, L. T., Bellerby, R. G. J., Bermúdez, R., Büdenbender, J., Boxhammer, T., Czerny, J., Engel, A., Ludwig, A., Meyerhöfer, M., Larsen, A., Paul, A. J., Sswat, M., & Riebesell, U. (2017). Phytoplankton Blooms at Increasing Levels of Atmospheric Carbon Dioxide: Experimental Evidence for Negative Effects on Prymnesiophytes and Positive on Small Picoeukaryotes. *Frontiers in Marine Science*, *4*. https://doi.org/10.3389/fmars.2017.00064

Schulz, K. G., Barcelos e Ramos, J., Zeebe, R. E., & Riebesell, U. (2009). CO_2 perturbation experiments: Similarities and differences between dissolved inorganic carbon and total alkalinity manipulations. *Biogeosciences*, *6*(10), 2145–2153. https://doi.org/10.5194/bg-6-2145-2009

Scott, B. D. (1978). Phytoplankton Distribution and Light Attenuation in Port Hacking Estuary. *Marine and Freshwater Research*, *29*(1), 31–44. https://doi.org/10.1071/mf9780031

Scott, B. D. (1983). Phytoplankton Distribution and Production in Port Hacking Estuary, and an Empirical Model for Estimating Daily Primary Production. In W. Cuff & M. Tomczak (Eds.), *Synthesis and Modelling of Intermittent Estuaries: A Case Study from Planning to Evaluation* (pp. 77–89). Springer. https://doi.org/10.1007/978-3-642-49991-3_6

Segschneider, J., & Bendtsen, J. (2013). Temperature-dependent remineralization in a warming ocean increases surface pCO2 through changes in marine ecosystem composition. *Global Biogeochemical Cycles*, *27*(4), 1214–1225. https://doi.org/10.1002/2013GB004684

Seymour, J. R., Amin, S. A., Raina, J.-B., & Stocker, R. (2017). Zooming in on the phycosphere: The ecological interface for phytoplankton–bacteria relationships. *Nature Microbiology*, *2*(7), 1–12. https://doi.org/10.1038/nmicrobiol.2017.65

Shadwick, E. H., Trull, T. W., Tilbrook, B., Sutton, A. J., Schulz, E., & Sabine, C. L. (2015). Seasonality of biological and physical controls on surface ocean CO2 from hourly observations at the Southern Ocean Time Series site south of Australia. *Global Biogeochemical Cycles*, *29*(2), 223–238. https://doi.org/10.1002/2014GB004906

Shadwick, E., Wynn-Edwards, C., Matear, R., Jansen, P., Schulz, E., & Sutton, A. (2023). Observed amplification of the seasonal CO2 cycle at the Southern Ocean Time Series. *Frontiers in Marine Science*, *10*. https://doi.org/10.3389/fmars.2023.1281854

Sheehan, C. E., Baker, K. G., Nielsen, D. A., & Petrou, K. (2020). *Temperatures above thermal optimum reduce cell growth and silica production while increasing cell volume and protein content in the diatom Thalassiosira pseudonana*. https://opus.lib.uts.edu.au/handle/10453/145942

Shi, D., Hong, H., Su, X., Liao, L., Chang, S., & Lin, W. (2019). The physiological response of marine diatoms to ocean acidification: Differential roles of seawater CO2 and pH. *Journal of Phycology*, *55*(3), 521–533. https://doi.org/10.1111/jpy.12855

Shi, P., Shen, H., Wang, W., Chen, W., & Xie, P. (2015). The relationship between light intensity and nutrient uptake kinetics in six freshwater diatoms. *Journal of Environmental Sciences*, *34*, 28–36. https://doi.org/10.1016/j.jes.2015.03.003

Shibl, A. A., Isaac, A., Ochsenkühn, M. A., Cárdenas, A., Fei, C., Behringer, G., Arnoux, M., Drou, N., Santos, M. P., Gunsalus, K. C., Voolstra, C. R., & Amin, S. A. (2020). Diatom modulation of select bacteria through use of two unique secondary metabolites. *Proceedings of the National Academy of Sciences*, *117*(44), 27445–27455. https://doi.org/10.1073/pnas.2012088117

Shirokawa, Y., Karino, K., & Mayama, S. (2012). Developmental plasticity and genotype–environment interactions influence valve morphology in the Cyclotella meneghiniana species complex (Bacillariophyceae). *European Journal of Phycology*, *47*(3), 245–253. https://doi.org/10.1080/09670262.2012.697580

Sigman, D., & Hain, M. (2012). The Biological Productivity of the Ocean. *Nature Education*, *3*, 1–16.

SigmaPlot (Version 14.5). (n.d.). [Computer software]. Systat Software, Inc.,. https://grafiti.com/

Smetacek, V. (1999). Diatoms and the Ocean Carbon Cycle. *Protist*, *150*(1), 25–32. https://doi.org/10.1016/S1434-4610(99)70006-4

Smetacek, V., Assmy, P., & Henjes, J. (2004). The role of grazing in structuring Southern Ocean pelagic ecosystems and biogeochemical cycles. *Antarctic Science*, *16*, 541–558. https://doi.org/10.1017/S0954102004002317

Smetacek, V., Klaas, C., Strass, V. H., Assmy, P., Montresor, M., Cisewski, B., Savoye, N., Webb, A., d'Ovidio, F., Arrieta, J. M., Bathmann, U., Bellerby, R., Berg, G. M., Croot, P., Gonzalez, S., Henjes, J., Herndl, G. J., Hoffmann, L. J., Leach, H., … Wolf-Gladrow, D. (2012). Deep carbon export from a Southern Ocean iron-fertilized diatom bloom. *Nature*, *487*(7407), Article 7407. https://doi.org/10.1038/nature11229

Smith, H. E. K., Poulton, A. J., Garley, R., Hopkins, J., Lubelczyk, L. C., Drapeau, D. T., Rauschenberg, S., Twining, B. S., Bates, N. R., & Balch, W. M. (2017). The influence of environmental variability on the biogeography of coccolithophores and diatoms in the Great Calcite Belt. *Biogeosciences*, *14*(21), 4905–4925. https://doi.org/10.5194/bg-14-4905-2017

Song, M., Pei, H., Hu, W., Han, F., Ji, Y., Ma, G., & Han, L. (2014). Growth and lipid accumulation properties of microalgal *Phaeodactylum tricornutum* under different gas liquid ratios. *Bioresource Technology*, *165*, 31–37. https://doi.org/10.1016/j.biortech.2014.03.070

Starr, M., Runge, J., & Therriault, J.-C. (1999). Effects of diatom diets on the reproduction of the planktonic copepod, Calanus finmarchicus. *Sarsia*, *84*, 378–389. https://doi.org/10.1080/00364827.1999.10807345

Stat, M., Morris, E., & Gates, R. D. (2008). Functional diversity in coral–dinoflagellate symbiosis. *Proceedings of the National Academy of Sciences*, *105*(27), 9256–9261. https://doi.org/10.1073/pnas.0801328105

Stevens, A., & Ramirez-Lopez, L. (2024). An introduction to the prospectr package. *R Package Vignette*.

https://www.researchgate.net/publication/255941339_An_introduction_to_the_prospectr_package

Stocker, T. F., Qin, D., Plattner, G.-K., Tignor, M. M. B., Allen, S. K., Boschung, J., Nauels, A., Xia, Y., Bex, V., Midgley, P. M., Alexander, L. V., Allen, S. K., Bindoff, N. L., Breon, F.-M., Church, J. A., Cubasch, U., Emori, S., Forster, P., Friedlingstein, P., … Wuebbles, D. (2013). *Climate Change 2013. The Physical Science Basis. Working Group I Contribution to the Fifth Assessment Report of the Intergovernmental Panel on Climate Change—Abstract for decision-makers; Changements climatiques 2013. Les elements scientifiques. Contribution du groupe de travail I au cinquieme rapport d'evaluation du groupe d'experts intergouvernemental sur l'evolution du CLIMAT - Resume a l'intention des decideurs*. https://www.osti.gov/etdeweb/biblio/22221318

Strickland, J. D. H., & Parsons, T. R. (1972). *A Practical Handbook of Seawater Analysis, 2nd edition*. https://doi.org/10.25607/OBP-1791

Struyf, E., Smis, A., Van Damme, S., Meire, P., & Conley, D. J. (2009). The Global Biogeochemical Silicon Cycle. *Silicon*, *1*(4), 207–213. https://doi.org/10.1007/s12633-010-9035-x

Su, Y., Lundholm, N., & Ellegaard, M. (2018). The effect of different light regimes on diatom frustule silicon concentration. *Algal Research*, *29*, 36–40. https://doi.org/10.1016/j.algal.2017.11.014

Sugie, K., & Yoshimura, T. (2016). Effects of high CO2 levels on the ecophysiology of the diatom Thalassiosira weissflogii differ depending on the iron nutritional status. *ICES Journal of Marine Science*, *73*(3), 680–692. https://doi.org/10.1093/icesjms/fsv259

Sullivan, C. W. (1976). DIATOM MINERALIZATION OK SILICIC ACID. I Si(OH)4 TRANSPORT CHARACTERISTICS IN NAVICULA PELLICULOSA. *Journal of Phycology*, *12*(4), 390–396. https://doi.org/10.1111/j.1529-8817.1976.tb02862.x

Sumper, M., & Brunner, E. (2008). Silica Biomineralisation in Diatoms: The Model Organism Thalassiosira pseudonana. *ChemBioChem*, *9*(8), 1187–1194. https://doi.org/10.1002/cbic.200700764

Sumper, M., & Kröger, N. (2004). Silica formation in diatoms: The function of long-chain polyamines and silaffins. *Journal of Materials Chemistry*, *14*(14), 2059–2065. https://doi.org/10.1039/B401028K

Sun, J., Hutchins, D. A., Feng, Y., Seubert, E. L., Caron, D. A., & Fu, F.-X. (2011). Effects of changing pCO2 and phosphate availability on domoic acid production and physiology of the marine harmful bloom diatom Pseudo-nitzschia multiseries. *Limnology and Oceanography*, *56*(3), 829–840. https://doi.org/10.4319/lo.2011.56.3.0829

Suthers, I. M., Young, J. W., Baird, M. E., Roughan, M., Everett, J. D., Brassington, G. B., Byrne, M., Condie, S. A., Hartog, J. R., Hassler, C. S., Hobday, A. J., Holbrook, N. J., Malcolm, H. A., Oke, P. R., Thompson, P. A., & Ridgway, K. (2011). The strengthening East Australian Current, its eddies and biological effects—An introduction and overview. *Deep Sea Research Part II: Topical Studies in Oceanography*, *58*(5), 538–546. https://doi.org/10.1016/j.dsr2.2010.09.029

Sverdrup, H. U. (1953). On Conditions for the Vernal Blooming of Phytoplankton. *ICES Journal of Marine Science*, *18*(3), 287–295. https://doi.org/10.1093/icesjms/18.3.287

Takahashi, T., Sweeney, C., Hales, B., Chipman, D. w, Newberger, T., Goddard, J. g, Iannuzzi, R. a, Sutherland, S. c, Hales, B., Chipman, D. w, Newberger, T., Goddard, J. g, Iannuzzi, R. a, & Sutherland, S. c. (2012). The changing carbon cycle in the Southern Ocean. *Oceanography*, *25*(3), 26–37. https://doi.org/10.5670/oceanog.2012.71

Tan, L., Xu, W., He, X., & Wang, J. (2019). The feasibility of Fv/Fm on judging nutrient limitation of marine algae through indoor simulation and *in situ* experiment. *Estuarine, Coastal and Shelf Science*, *229*, 106411. https://doi.org/10.1016/j.ecss.2019.106411

Tatters, A. O., Roleda, M. Y., Schnetzer, A., Fu, F., Hurd, C. L., Boyd, P. W., Caron, D. A., Lie, A. A. Y., Hoffmann, L. J., & Hutchins, D. A. (2013). Short- and long-term conditioning of a temperate marine diatom community to acidification and warming. *Philosophical Transactions of the Royal Society B: Biological Sciences*, *368*(1627), 20120437. https://doi.org/10.1098/rstb.2012.0437

Taucher, J., Bach, L. T., Prowe, A. E. F., Boxhammer, T., Kvale, K., & Riebesell, U. (2022). Enhanced silica export in a future ocean triggers global diatom decline. *Nature*, *605*(7911), 696–700. https://doi.org/10.1038/s41586-022-04687-0

Taucher, J., & Oschlies, A. (2011). Can we predict the direction of marine primary production change under global warming? *Geophysical Research Letters*, *38*(2). https://doi.org/10.1029/2010GL045934

Tesson, B., Gaillard, C., & Martin-Jezequel, V. (2009). Insights into the polymorphism of the diatom Phaeodactylum tricornutum Bohlin. *Botanica Marina - BOT MAR*, *52*, 104–116. https://doi.org/10.1515/BOT.2009.012

Thompson, P. A., Bonham, P., Waite, A. M., Clementson, L. A., Cherukuru, N., Hassler, C., & Doblin, M. A. (2011). Contrasting oceanographic conditions and phytoplankton communities on the east and west coasts of Australia. *Deep Sea Research Part II: Topical Studies in Oceanography*, *58*(5), 645–663. https://doi.org/10.1016/j.dsr2.2010.10.003

Timmermans, K. R., Gerringa, L. J. A., de Baar, H. J. W., van der Wagt, B., Veldhuis, M. J. W., de Jong, J. T. M., Croot, P. L., & Boye, M. (2001). Growth rates of large and small Southern Ocean diatoms in relation to availability o iron in natural seawater. *Limnology and Oceanography*, *46*(2), 260–266. https://doi.org/10.4319/lo.2001.46.2.0260

Tortell, P. D., DiTullio, G. R., Sigman, D. M., & Morel, F. M. M. (2002). CO2 effects on taxonomic composition and nutrient utilization in an Equatorial Pacific phytoplankton assemblage. *Marine Ecology Progress Series*, *236*, 37–43. https://doi.org/10.3354/meps236037

Tortell, P. D., Payne, C. D., Li, Y., Trimborn, S., Rost, B., Smith, W. O., Riesselman, C., Dunbar, R. B., Sedwick, P., & DiTullio, G. R. (2008). CO2 sensitivity of Southern Ocean phytoplankton. *Geophysical Research Letters*, *35*(4). https://doi.org/10.1029/2007GL032583

Tréguer, P., Bowler, C., Moriceau, B., Dutkiewicz, S., Gehlen, M., Aumont, O., Bittner, L., Dugdale, R., Finkel, Z., Iudicone, D., Jahn, O., Guidi, L., Lasbleiz, M., Leblanc, K., Levy, M., & Pondaven, P. (2018). Influence of diatom diversity on the ocean biological carbon pump. *Nature Geoscience*, *11*(1), 27. https://doi.org/10.1038/s41561-017-0028-x

Trimborn, S., Wolf-Gladrow, D., Richter, K.-U., & Rost, B. (2009). The effect of pCO2 on carbon acquisition and intracellular assimilation in four marine diatoms. *Journal of Experimental Marine Biology and Ecology*, *376*(1), 26–36. https://doi.org/10.1016/j.jembe.2009.05.017

Trull, T. W., Jansen, P., Schulz, E., Weeding, B., Davies, D. M., & Bray, S. G. (2019). Autonomous Multi-Trophic Observations of Productivity and Export at the Australian Southern Ocean Time Series (SOTS) Reveal Sequential Mechanisms of Physical-Biological Coupling. *Frontiers in Marine Science*, *6*. https://doi.org/10.3389/fmars.2019.00525

Trull, T. W., Passmore, A., Davies, D. M., Smit, T., Berry, K., & Tilbrook, B. (2018). Distribution of planktonic biogenic carbonate organisms in the Southern Ocean south of Australia: A

baseline for ocean acidification impact assessment. *Biogeosciences*, *15*(1), 31–49. https://doi.org/10.5194/bg-15-31-2018

Ullah, H., Nagelkerken, I., Goldenberg, S. U., & Fordham, D. A. (2018). Climate change could drive marine food web collapse through altered trophic flows and cyanobacterial proliferation. *PLoS Biology*, *16*(1), e2003446. https://doi.org/10.1371/journal.pbio.2003446

Uppstrom, L. R. (1974). The boron/chlorinity ratio of deep-sea water from the Pacific Ocean. *Deep Sea Res.*, *21*, 161–162. https://doi.org/10.1016/0011-7471(74)90074-6

Valiadi, M., & Iglesias-Rodriguez, D. (2013). Understanding Bioluminescence in Dinoflagellates—How Far Have We Come? *Microorganisms*, *1*(1), Article 1. https://doi.org/10.3390/microorganisms1010003

van Beusekom, J. E. E., Loebl, M., & Martens, P. (2009). Distant riverine nutrient supply and local temperature drive the long-term phytoplankton development in a temperate coastal basin. *Journal of Sea Research*, *61*(1), 26–33. https://doi.org/10.1016/j.seares.2008.06.005

Vance, D., Little, S. H., de Souza, G. F., Khatiwala, S., Lohan, M. C., & Middag, R. (2017). Silicon and zinc biogeochemical cycles coupled through the Southern Ocean. *Nature Geoscience*, *10*(3), 202–206. https://doi.org/10.1038/ngeo2890

Vergés, A., Steinberg, P. D., Hay, M. E., Poore, A. G. B., Campbell, A. H., Ballesteros, E., Heck, K. L., Booth, D. J., Coleman, M. A., Feary, D. A., Figueira, W., Langlois, T., Marzinelli, E. M., Mizerek, T., Mumby, P. J., Nakamura, Y., Roughan, M., van Sebille, E., Gupta, A. S., … Wilson, S. K. (2014). The tropicalization of temperate marine ecosystems: Climate-mediated changes in herbivory and community phase shifts. *Proceedings of the Royal Society B: Biological Sciences*, *281*(1789), 20140846. https://doi.org/10.1098/rspb.2014.0846

Villareal, T. A., Pilskaln, C. H., Montoya, J. P., & Dennett, M. (2014). Upward nitrate transport by phytoplankton in oceanic waters: Balancing nutrient budgets in oligotrophic seas. *PeerJ*, *2*, e302. https://doi.org/10.7717/peerj.302

Vongsvivut, J., Heraud, P., Gupta, A., Puri, M., McNaughton, D., & Barrow, C. (2013). FTIR microspectroscopy for rapid screening and monitoring of polyunsaturated fatty acid production in commercially valuable marine yeasts and protists. *Analyst*, *138*(20), 6016–6031. https://doi.org/10.1039/c3an00485f

Vrieling, E. G., Poort, L., Beelen, T. P. M., & Gieskes, W. W. C. (1999). Growth and silica content of the diatoms Thalassiosira weissflogii and Navicula salinarum at different salinities and enrichments with aluminium. *European Journal of Phycology*, *34*(3), 307–316. https://doi.org/10.1080/09670269910001736362

Wagner, H., Liu, Z., Langner, U., Stehfest, K., & Wilhelm, C. (2010). The use of FTIR spectroscopy to assess quantitative changes in the biochemical composition of microalgae. *Journal of Biophotonics*, *3*(8–9), 557–566. https://doi.org/10.1002/jbio.201000019

Wall, D., & Dale, B. (1968). Modern dinoflagellate cysts and evolution of the Peridiniales. *Micropaleontology*, *14*(3), 265–304.

Wernberg, T., Russell, B. D., Moore, P. J., Ling, S. D., Smale, D. A., Campbell, A., Coleman, M. A., Steinberg, P. D., Kendrick, G. A., & Connell, S. D. (2011). Impacts of climate change in a global hotspot for temperate marine biodiversity and ocean warming. *Journal of Experimental Marine Biology and Ecology*, *400*(1), 7–16. https://doi.org/10.1016/j.jembe.2011.02.021

Wernberg, T., Smale, D. A., Tuya, F., Thomsen, M. S., Langlois, T. J., de Bettignies, T., Bennett, S., & Rousseaux, C. S. (2013). An extreme climatic event alters marine ecosystem structure in a global biodiversity hotspot. *Nature Climate Change*, *3*(1), 78–82. https://doi.org/10.1038/nclimate1627

Werner, D. (1977). *The Biology of Diatoms*. University of California Press.

Williams, R. G., & Follows, M. J. (2003). Physical Transport of Nutrients and the Maintenance of Biological Production. In M. J. R. Fasham (Ed.), *Ocean Biogeochemistry: The Role of the Ocean Carbon Cycle in Global Change* (pp. 19–51). Springer. https://doi.org/10.1007/978-3-642-55844-3_3

Williams, R. G., Meijers, A. J. S., Roussenov, V. M., Katavouta, A., Ceppi, P., Rosser, J. P., & Salvi, P. (2024). Asymmetries in the Southern Ocean contribution to global heat and carbon uptake. *Nature Climate Change*, 1–9. https://doi.org/10.1038/s41558-024-02066-3

Winder, M., & Cloern, J. E. (2010). The annual cycles of phytoplankton biomass. *Philosophical Transactions of the Royal Society B: Biological Sciences*, *365*(1555), 3215–3226. https://doi.org/10.1098/rstb.2010.0125

Winter, A., Henderiks, J., Beaufort, L., Rickaby, R. E. M., & Brown, C. W. (2014). Poleward expansion of the coccolithophore Emiliania huxleyi. *Journal of Plankton Research*, *36*(2), 316–325. https://doi.org/10.1093/plankt/fbt110

Wu, L., Cai, W., Zhang, L., Nakamura, H., Timmermann, A., Joyce, T., McPhaden, M. J., Alexander, M., Qiu, B., Visbeck, M., Chang, P., & Giese, B. (2012). Enhanced warming over the global subtropical western boundary currents. *Nature Climate Change*, *2*(3), 161–166. https://doi.org/10.1038/nclimate1353

Wu, S., Gu, W., Huang, A., Li, Y., Kumar, M., Lim, P. E., Huan, L., Gao, S., & Wang, G. (2019). Elevated CO2 improves both lipid accumulation and growth rate in the glucose-6-phosphate dehydrogenase engineered Phaeodactylum tricornutum. *Microbial Cell Factories*, *18*(1), 161. https://doi.org/10.1186/s12934-019-1214-x

Wu, Y., Campbell, D. A., Irwin, A. J., Suggett, D. J., & Finkel, Z. V. (2014). Ocean acidification enhances the growth rate of larger diatoms. *Limnology and Oceanography*, *59*(3), 1027–1034. https://doi.org/10.4319/lo.2014.59.3.1027

Wu, Y., Gao, K., & Riebesell, U. (2010). CO_2-induced seawater acidification affects physiological performance of the marine diatom *Phaeodactylum tricornutum*. *Biogeosciences*, *7*(9), 2915–2923. https://doi.org/10.5194/bg-7-2915-2010

Wynn-Edwards, C. A., Shadwick, E. H., Davies, D. M., Bray, S. G., Jansen, P., Trinh, R., & Trull, T. W. (2020). Particle Fluxes at the Australian Southern Ocean Time Series (SOTS) Achieve Organic Carbon Sequestration at Rates Close to the Global Median, Are Dominated by Biogenic Carbonates, and Show No Temporal Trends Over 20-Years. *Frontiers in Earth Science*, *8*. https://doi.org/10.3389/feart.2020.00329

Xu, H., Shi, Z., Zhang, X., Pang, M., Pan, K., & Liu, H. (2021). Diatom frustules with different silica contents affect copepod grazing due to differences in the nanoscale mechanical properties. *Limnology and Oceanography*, *66*(9), 3408–3420. https://doi.org/10.1002/lno.11887

Xu, N., Tang, Y. Z., Qin, J., Duan, S., & Gobler, C. J. (2015). Ability of the marine diatoms Pseudo-nitzschia multiseries and P. pungens to inhibit the growth of co-occurring phytoplankton via allelopathy. *Aquatic Microbial Ecology*, *74*(1), 29–41. https://doi.org/10.3354/ame01724

Xue, T., Frenger, I., Oschlies, A., Stock, C. A., Koeve, W., John, J. G., & Prowe, A. E. F. (2022). Mixed Layer Depth Promotes Trophic Amplification on a Seasonal Scale. *Geophysical Research Letters*, *49*(12), e2022GL098720. https://doi.org/10.1029/2022GL098720

Yamaguchi, R., & Suga, T. (2019). Trend and Variability in Global Upper-Ocean Stratification Since the 1960s. *Journal of Geophysical Research: Oceans*, *124*(12), 8933–8948. https://doi.org/10.1029/2019JC015439

Yamamoto-Kawai, M., McLaughlin, F. A., Carmack, E. C., Nishino, S., & Shimada, K. (2009). Aragonite Undersaturation in the Arctic Ocean: Effects of Ocean Acidification and Sea Ice Melt. *Science*, *326*(5956), 1098–1100. https://doi.org/10.1126/science.1174190

Yamanaka, S., Yano, R., Usami, H., Hayashida, N., Ohguchi, M., Takeda, H., & Yoshino, K. (2008). Optical properties of diatom silica frustule with special reference to blue light. *Journal of Applied Physics*, *103*(7), 074701. https://doi.org/10.1063/1.2903342

Ye, Y., Sunda, W. G., Hong, H., & Shi, D. (2023). Interrelated influence of iron, light, and CO on carbon fixation in a Southern Ocean diatom. *Limnology and Oceanography*, *68*(7), 1504–1516. https://doi.org/10.1002/lno.12360

Yool, A., & Tyrrell, T. (2003). Role of diatoms in regulating the ocean's silicon cycle. *Global Biogeochemical Cycles*, *17*(4). https://doi.org/10.1029/2002GB002018

Young, J. N., Heureux, A. M. C., Sharwood, R. E., Rickaby, R. E. M., Morel, F. M. M., & Whitney, S. M. (2016). Large variation in the Rubisco kinetics of diatoms reveals diversity among their carbon-concentrating mechanisms. *Journal of Experimental Botany*, *67*(11), 3445–3456. https://doi.org/10.1093/jxb/erw163

Yuzaburo, I., Norihiro, H., Hirotaka, K., Atsushi, M., Satoshi, N., & Minoru, Y. (2000). A highly CO2-tolerant diatom, Thalassiosira weissflogii H1, enriched from coastal sea, and its fatty acid composition. *Fisheries Science*, *66*(4), 655–659. https://doi.org/10.1046/j.1444-2906.2000.00105.x

Zarzyczny, K. M., Rius, M., Williams, S. T., & Fenberg, P. B. (2024). The ecological and evolutionary consequences of tropicalisation. *Trends in Ecology & Evolution*, *39*(3), 267–279. https://doi.org/10.1016/j.tree.2023.10.006

Zepernick, B. N., Wilhelm, S. W., Bullerjahn, G. S., & Paerl, H. W. (2022). Climate change and the aquatic continuum: A cyanobacterial comeback story. *Environmental Microbiology Reports*, *15*(1), 3–12. https://doi.org/10.1111/1758-2229.13122

Zhai, W.-D., Chen, J.-F., Jin, H.-Y., Li, H.-L., Liu, J.-W., He, X.-Q., & Bai, Y. (2014). Spring carbonate chemistry dynamics of surface waters in the northern East China Sea: Water mixing, biological uptake of CO2, and chemical buffering capacity. *Journal of Geophysical Research: Oceans*, *119*(9), 5638–5653. https://doi.org/10.1002/2014JC009856

Zhong, J., Guo, Y., Liang, Z., Huang, Q., Lu, H., Pan, J., Li, P., Jin, P., & Xia, J. (2021). Adaptation of a marine diatom to ocean acidification and warming reveals constraints and trade-offs. *Science of The Total Environment*, *771*, 145167. https://doi.org/10.1016/j.scitotenv.2021.145167

Zielinski, U., & Gersonde, R. (1997). Diatom distribution in Southern Ocean surface sediments (Atlantic sector): Implications for paleoenvironmental reconstructions. *Palaeogeography, Palaeoclimatology, Palaeoecology*, *129*(3), 213–250. https://doi.org/10.1016/S0031-0182(96)00130-7

Zobell, C. E., & Anderson, D. Q. (1936). Observations on the multiplication of bacteria in different volumes of stored sea water and the influence of oxygen tension and solid surfaces. *The Biological Bulletin*, *71*(2), 324–342. https://doi.org/10.2307/1537438